ATTENTION: The Singapore Copyright Act applies to the use of this document. Nanyang Technological University Library

STUDY ON SURVIVAL MECHANISMS OF CIRCULATING TUMOR CELLS AND IDENTIFICATION OF METASTATIC BIOMARKERS FOR BREAST CANCER

FU AFU

SCHOOL OF CHEMICAL AND BIOMEDICAL ENGINEERING

2015

ATTENTION: The Singapore Copyright Act applies to the use of this document. Nanyang Technological University Library

STUDY ON SURVIVAL MECHANISMS OF CIRCULATING TUMOR CELLS AND IDENTIFICATION OF METASTATIC BIOMARKERS FOR BREAST CANCER

FU AFU

School of Chemical and Biomedical Engineering

A thesis submitted to the Nanyang Technological University

in fulfillment of the requirement for the degree of

Doctor of Philosophy

2015

ATTENTION: The Singapore Copyright Act applies to the use of this document. Nanyang Technological University Library

Acknowledgements

Foremost, I want to express my sincere gratitude and respect to my supervisor, Prof. Kathy Qian Luo, who has provided careful guidance and supports on my research work. Her scientific spirits always inspire me. Most importantly, her serious and meticulous attitude has given me very high standards in research and in life.

My sincere thanks also go to all people who have helped me on my research. I want to thank Mr. Zhang Xichen, Ms. Wei Na, Mr. Liu Xiaofeng, Mr. Ma Shijun, Ms. Chiew Giap Ying Geraldine, Ms. Luo Man and my FYP students Mr. Low Kar Perng, Mr. Ng Weida, Mr. Peh Yu Ming, Mr. Zhou Zhicai, Ms. Tan Xiao Xuan Blanche and Ms. Chrishella Fermi Budiarto, who have helped me during the experiments of this thesis. I want to acknowledge Dr. Zhu Xiaoming, Dr. Yu Ting, Ms. Padmaja Anand, Mr. Vivek Sheraton, Mr. Sagar Regmi, Dr. Wang Qi and Dr. Chen Yijun for their stimulating discussions, experimental support, and valuable comments on my thesis. I am also grateful to Ms. Chitra Devi D/O Subramaniam and other technical staffs for their guidance in using the equipment and purchasing the reagents.

I would like to thank all the collaborators in this study. I want to thank Prof. Christoph Wolfram Winkler and Dr. Martin Graf from National University of Singapore for proving the *fli1: EGFP* transgenic zebrafish. I am grateful to Prof. Mark Featherstone from School of Biological Sciences of NTU for facilitating the zebrafish experiments. I would like to thank Dr. Tan Ern Yu from Tan Tock Seng Hospital for providing clinical breast tumor samples, making suggestions on the clinical relevance, and editing the manuscript of my manuscript. I want to thank Prof. Newman Sze from

ATTENTION: The Singapore Copyright Act applies to the use of this document. Nanyang Technological University Library

School of Biological Sciences and Dr. Hongjin Huang from Applied Biomics Inc. in USA for conducting proteomics analysis in this thesis.

Last but not least, I would like to express my heartiest gratitude to my family and all my friends for their understanding and invaluable constant supports. A special appreciation goes to my wife, Dr. Wu Yue. She has provided me not only with living care and spiritual encouragement, but also with direct experimental support on my research.

I wish to dedicate this thesis to my beloved grandma, who passed away due to breast cancer.

ATTENTION: The Singapore Copyright Act applies to the use of this document. Nanyang Technological University Library

Publications

Journal articles

1. **Fu AF**, Wei N, Ngan WD, Peh YM and Luo KQ. Blocking PI3K/mTOR pathway in metastatic cancer cells suppress the cell survival and proliferation in a novel zebrafish cancer model. (*Manuscript in preparation*)
2. **Fu AF**, Ma SJ, Wei N, Tan BXX, Tan EY and Luo KQ. Targeting antioxidant enzyme MnSOD to sensitize circulating tumor cells to hemodynamic shear stress-induced apoptosis and adjuvant doxorubicin therapy. (*Manuscript arising from this thesis*, in submission)
3. Ma SJ, **Fu AF** and Luo KQ. Fluidic shear stress increases invasiveness of circulating tumor cells by elevating oxidative level. (Submitted to *Int. J. Cancer*).
4. Chiew GGY*, **Fu AF***, Low KP, Luo KQ. Physical supports from liver cancer cells are essential for differentiation and remodeling of endothelial cells in a HepG2-HUVEC co-culture model. *Scientific Reports* 2015, 5. (*, joint first author).
5. Anand P, **Fu AF**, Teoh SH, Luo KQ. Development of a fluorescent resonant energy transfer (FRET) sensor-based 3D breast tumor model for evaluating drug efficacy. *Biotechnology & Bioengineering* 2015, 112(8):1673-82.
6. Gao Y, Wang YQ, **Fu AF**, Shi W, Yeo D, Luo KQ, Ow H, Xu CJ. Tracking mesenchymal stem cell tumor-homing using fluorescent silica nanoparticles. *Journal of Materials Chemistry B. 2015,* 3 (7): 1245-1253.
7. Zhu XM, **Fu AF**, Luo KQ. A high-throughput fluorescence resonance energy transfer (FRET)-based endothelial cell apoptosis assay and its application for screening vascular disrupting agents. *Biochem. Biophys. Res. Commun*. 2012, 418 (4):641-646.

ATTENTION: The Singapore Copyright Act applies to the use of this document. Nanyang Technological University Library

Conference presentations

1. Chiew GGY, **Fu AF** and Luo KQ. The physical interaction between tumor and endothelial cells is a key inducer for liver cancer angiogenesis in a HepG2-HUVEC co-culture system. The 2015 American Society for Cell Biology Annual Meeting (ASCB 2015), December 12-16, 2015, San Diego, USA. (Microsymposium ePoster talk)
2. Ma SJ, **Fu AF** and Luo KQ. Hemodynamic shear stress stimulates the invasiveness of circulating tumor cells. The 2015 American Society for Cell Biology Annual Meeting (ASCB 2015), December 12-16, 2015, San Diego, USA. (Poster presentation)
3. Luo M, **Fu AF** and Luo KQ. Antioxidant Ability Mediates Metastasis-derived Doxorubicin Resistance of Breast Cancer Cells. The 2015 American Society for Cell Biology Annual Meeting (ASCB 2015), December 12-16, 2015, San Diego, USA. (Poster presentation)
4. Anand P, **Fu AF**, Teoh SH, Luo KQ. FRET-Based Analysis for Detection of Drug-Induced Apoptosis in A 3D Breast Tumor Model. The 2015 American Society for Cell Biology Annual Meeting (ASCB 2015), December 12-16, 2015, San Diego, USA. (Poster presentation)
5. Ma SJ, **Fu AF** and Luo KQ, Hemodynamic shear stress stimulates invasiveness of circulating tumor cells. Optofluidics 2015, July 26-29, 2015, Taipei, Taiwan. (**Best Conference Poster Award**)
6. Luo KQ and **Fu AF**. Using Integrative Approaches to Discover New Oncology Drugs and Study Metastasis. IUPHAR World Conference on the Pharmacology of Natural and Traditional Medicine 2015, July 22-24, 2015, Singapore. (Invited talk)

ATTENTION: The Singapore Copyright Act applies to the use of this document. Nanyang Technological University Library

7. Ma SJ, **Fu AF** and Luo KQ, Study of the effects of shear stress on tumor cell extravasation. 7th WACBE World Congress on Bioengineering, July 6-8, 2015, Singapore. (Poster presentation)
8. Chiew GGY, **Fu AF**, Low KP and Luo KQ, Physical supports from liver cancer cells are essential for differentiation and remodeling of endothelial cells in a HepG2-HUVEC co-culture model. 7th WACBE World Congress on Bioengineering, July 6-8, 2015, Singapore. (Poster presentation)
9. **Fu AF** and Luo KQ**.** Study the molecular mechanisms enabling metastatic breast cancer cells to survive in blood circulation and identify new metastatic markers. SCBE PhD symposium 2015, Nanyang Technological University, March 3-4 2015, Singapore. (Oral presentation, **Silver award**)
10. Liu XF, **Fu AF**, How YH and Luo KQ, Effects of hemodynamic shear stress on circulating tumor cells. The 15th International Conference on Miniaturized Systems for Chemistry and Life Sciences (MicroTAS 2014), October 26-30, 2014, San Antonio, USA. (Poster presentation)
11. Chiew GGY, **Fu AF** and Luo KQ, A FRET based co-culture system for monitoring angiogenesis in HepG2-DsRed and HUVEC-C3 cells. 7th Asia-Pacific Organization for Cell Biology (APOCB) Congress, February 24-27, 2014. (Poster presentation)
12. Luo KQ and **Fu AF**, Metastatic breast cancer cells survive better than non-metastatic cells to hemodynamic shear stress due to their higher anti-oxidant capacity. The 2013 American Society for Cell Biology Annual Meeting (ASCB 2013), December 14-18, 2013, New Orleans, USA. (Oral presentation in mini-symposium)

ATTENTION: The Singapore Copyright Act applies to the use of this document. Nanyang Technological University Library

13. **Fu AF** and Luo KQ, Application of a fluorescence resonance energy transfer (FRET)-based apoptosis sensor in zebrafish model for studying cancer metastasis and discovering new anti-cancer drugs. The 2013 American Society for Cell Biology Annual Meeting (ASCB 2013), December 14-18, 2013, New Orleans, USA. (Poster presentation, **Travel Award of ASCB**)
14. Liu XF, **Fu AF**, Luo KQ, Application of a FRET-based biosensor in studying shear stress-induced apoptosis in circulating tumor cells. The 15th International Conference on Biomedical Engineering (ICBME 2013), December 4-7, 2013, Singapore. (Oral presentation)
15. **Fu AF** and Luo KQ, Apply a GFP-based FRET apoptosis sensor in zebrafish model to study cancer metastasis and search for new anti-cancer drugs. The 15th International Conference on Biomedical Engineering (ICBME 2013), December 4-7, 2013, Singapore. (Oral presentation)

ATTENTION: The Singapore Copyright Act applies to the use of this document. Nanyang Technological University Library

List of Contents

ATTENTION: The Singapore Copyright Act applies to the use of this document. Nanyang Technological University Library

ATTENTION: The Singapore Copyright Act applies to the use of this document. Nanyang Technological University Library

ATTENTION: The Singapore Copyright Act applies to the use of this document. Nanyang Technological University Library

ATTENTION: The Singapore Copyright Act applies to the use of this document. Nanyang Technological University Library

ATTENTION: The Singapore Copyright Act applies to the use of this document. Nanyang Technological University Library

Summary

Breast cancer remains curable until the metastatic cancer cells disseminate beyond the regional lymph nodes. The 5-year relative survival rate of stage IV breast cancer is less than 22%. Therefore, strategies to prevent the dissemination of breast cancer cells into bloodstream, eliminate the circulating tumor cells (CTCs), or suppress the proliferation of disseminated tumor cells (DTCs), can potentially inhibit cancer progression and improve the survival of breast cancer patients. So far, the mechanisms of how hemodynamic shear force induces apoptosis of CTCs and how metastatic breast cancer cell manage to survive in blood circulation are still unclear. Therefore, this thesis focused on the survival mechanisms of CTCs and aims to identify functional biomarkers and develop therapeutic strategies for metastatic breast cancer.

First, I generated multiple apoptosis sensor cell lines and established several novel experimental models to facilitate the mechanism study and drug discovery targeting cancer metastasis. Using these integrative model systems, I revealed that hemodynamic shear stress induced the apoptosis of CTCs by affecting the normal function of mitochondrial and overproducing mitochondrial reactive oxygen species (ROS), which further cause mitochondrial dysfunction and activation of intrinsic apoptosis pathway. An inherent survival factor in metastatic breast cancer cells was identified to be the anti-oxidant enzyme manganese superoxide dismutase (MnSOD). MnSOD was able to rapidly eliminate excessive superoxide and reduce the oxidative stress. High level of MnSOD protected CTCs from ROS-mediated mitochondrial damage and conferred a survival advantage. Interestingly, the level of MnSOD in each individual cell was heterogeneous and only the cells with high levels of MnSOD were able to survive through circulation. The MnSOD levels were positively correlated with

ATTENTION: The Singapore Copyright Act applies to the use of this document. Nanyang Technological University Library

the survival ability of six human breast cancer cell lines during circulation. Moreover, in metastatic tumours as well as in lung metastases-derived cell lines, the overall levels of MnSOD were markedly elevated.

More importantly, high levels of MnSOD in the survived CTCs also facilitated chemotherapeutic resistance towards doxorubicin, which is a redox cycling agent. Down regulating MnSOD by siRNA has not only inhibited the survival of metastatic cells in circulation of nude mice, but has also sensitized them to doxorubicin treatment *in vitro*. These findings illustrate the potential clinical relevance of MnSOD, not only as a prognostic marker to guide treatment recommendations, but also as a novel therapeutic target. Therapies targeting MnSOD expression can potentially prevent the development of metastatic disease and reduce breast cancer specific mortality.

Furthermore, I also identified many other potential biomarkers for metastatic breast cancer by conducting comparative proteomics analysis in lung metastases derived cells versus their parental cells. Three subsets of biomarkers were identified to be related with the survival of CTCs, proliferation of DTCs, and the acquired drug resistance in metastatic tumor. These biomarkers can be validated and developed as prognostic markers or therapeutic targets in the future.

ATTENTION: The Singapore Copyright Act applies to the use of this document. Nanyang Technological University Library

List of Tables

ATTENTION: The Singapore Copyright Act applies to the use of this document. Nanyang Technological University Library

List of Figures

ATTENTION: The Singapore Copyright Act applies to the use of this document. Nanyang Technological University Library

ATTENTION: The Singapore Copyright Act applies to the use of this document. Nanyang Technological University Library

ATTENTION: The Singapore Copyright Act applies to the use of this document. Nanyang Technological University Library

ATTENTION: The Singapore Copyright Act applies to the use of this document. Nanyang Technological University Library

ATTENTION: The Singapore Copyright Act applies to the use of this document. Nanyang Technological University Library

ATTENTION: The Singapore Copyright Act applies to the use of this document. Nanyang Technological University Library

ATTENTION: The Singapore Copyright Act applies to the use of this document. Nanyang Technological University Library

List of Abbreviations

2D-DIGE	Two-dimensional differential in-gel electrophoresis
2-ME	2-Methoxyestradiol
ABC	ATP-binding cassette
AIA	Angiogenesis inhibiting agents
AIF	Apoptosis inducing factor
ATCC	American Type Culture Collection
BCRP	Breast cancer resistance protein
CA	Caudal artery
CFP	Cyan fluorescent protein
CSCs	Cancer stem cells
CTCs	Circulating tumor cells
CuZnSOD	Copper/zinc superoxide dismutase
DCF	Dichlorofluorescein
DCIS	Ductal carcinoma *in situ*
DIC	Differential interference contrast
DMSO	Dimethyl sulfoxide
DTC	Disseminated tumor cell
dpf	Days post fertilization
dpi	Days post injection
ECM	Extracellular matrix
EGFR	Epidermal growth factor receptor
EMT	Epithelial-mesenchymal transition

ATTENTION: The Singapore Copyright Act applies to the use of this document. Nanyang Technological University Library

ER	Estrogen receptor
FAK	Focal adhesion kinase
FBS	Fetal bovine serum
FFPE	Formalin fixed paraffin embedded
g	gram
GFP	Green fluorescent protein
GPX	Glutathione peroxidases
GI	Growth inhibition
GSH	Glutathione
GSSG	Glutathione disulfide
GST	Glutathione s-transferases
h	hour
HER2 or ERBB2	Human epidermal growth factor receptor 2
HIF	Hypoxia inducible factor
hpi	Hours post injection
IF	Immunofluorescence
IHC	Immunohistochemistry
IPA	Ingenuity pathway analysis
ISV	Intersegmental vessels
iTRAQ	Isobaric tags for relative and absolute quantification
JNK	C-Jun N-terminal kinases
kDa	Kilo Dalton
L	Litre
M	Molar

ATTENTION: The Singapore Copyright Act applies to the use of this document. Nanyang Technological University Library

mg	milligram
ml	millilitre
mM	millimolar
MAPK	Mitogen-activated protein kinase
MBC	Metastatic breast cancer
MDR1	Multi-drug resistance protein 1
min	minute
MMP	Mitochondrial membrane potential
MnSOD	Manganese superoxide dismutase
MPTP	Mitochondrial permeability transition pore
mtDNA	Mitochondrial DNA
MTT	3- 4, 5-dimethylthiazol-2-yl-2, 5-diphenyltetrazolium bromide
NBF	Neutral buffered formalin
NF-κB	Nuclear factor -κB
NOX	NADPH oxidase
PARP	Poly ADP-ribose polymerase
PBS	Phosphate buffered saline
PG	Propyl gallate
PgR	Progesterone receptor
RFP	Red fluorescent protein
ROCK	Rho-associated protein kinase
ROS	Reactive oxygen species
sensor C3	Caspase-3 biosensor

ATTENTION: The Singapore Copyright Act applies to the use of this document. Nanyang Technological University Library

SOD	Superoxide dismutase
STAT3	Signal transducer and activator of transcription 3
TNBC	Triple negative breast cancer
TNF	Tumor necrosis factor
TNFR	Tumor necrosis factor receptor
μg	microgram
μl	microliter
μM	micromolar
VDA	Vascular disrupting agents
YFP	Yellow fluorescent protein

ATTENTION: The Singapore Copyright Act applies to the use of this document. Nanyang Technological University Library

CHAPTER 1 Introduction

1.1 Curing Cancer is the Biggest Challenge

1.1.1 General Knowledge of Cancer

Cancer affects populations of all countries and regions, and is a leading cause of both disease and death worldwide [3]. In contrast to common perception, cancer is not the name of a single disease but the name of a group of related diseases. These diseases have common features of uncontrolled growth and spread to surrounding tissues as well as to distant organs. They can occur in almost anywhere in the human body and most cancers form solid tumors. Cancer cells are malignant, which means they can invade the surrounding tissues or spread to other parts of the body. In contrast to benign tumors, malignant tumors are much more dangerous because they usually relapse and undergo metastasis after surgery. Malignant tumors can be life threatening, whereas for benign tumors, only the brain tumors can be life threatening.

1.1.2 Worldwide Statistics of Cancer

Based on the statistical data of 2012 [3], about 14.1 million new cancer cases occurred all over the world. The most common types of cancer are lung cancer, female breast cancer, and colorectal and stomach cancers, which accounted for more than 40% of all cancer cases. In women, breast cancer is the most common cancer with a percentage of 25.2% in all new cases, followed by colorectum (9.2%), lung (8.7%), cervix (7.9%) and stomach cancer (4.8%). In men, lung cancer is the most common cancer (16.7% of the total), followed by prostate (15.0%), colorectum (10.0%), stomach (8.5%), and liver cancer (7.5%).

ATTENTION: The Singapore Copyright Act applies to the use of this document. Nanyang Technological University Library

Cancer alone caused 8.2 million deaths in 2012. Lung, stomach, liver, colorectal and female breast cancers are the leading cause of cancer related death and they constituted more than half of the death worldwide. Among women, breast cancer has the highest mortalities than any other cancers, with a proportion of 14.7% (521,817 over 3,547,898) in all cancer death; while in men, lung cancer contributes to 23.6% (1,098,606 over 4,653,132) of all cancer death.

1.2 Breast Cancer is a Leading Cause of Death in Women

Most of the studies in this thesis focused on breast cancer. Breast cancer is a cancer formed in tissues of the breast, such as in the lining of the milk ducts (ductal carcinoma) and in the lobules of the breast (lobular carcinoma) (Figure 1-1). Based on the histopathological characteristics, the most common types of breast cancers include invasive ductal carcinoma (55% of breast cancers), ductal carcinoma in situ (13%) and invasive lobular carcinoma (5%) [4].

1.2.1 Statistics of Breast Cancer

As introduced above, breast cancer has the second highest incidence in new cancer cases diagnosed in 2012 in the world and the highest incidence in women cancers. 25.2% of new women cancer cases were diagnosed in the breast in 2012. However, breast cancer has a relatively low fatality rate. Given its low mortality rate, if the 5-year prevalence rate is considered, the percentages of breast cancer in all populations and women alone are even higher. This means in reality breast cancer is the most common cancer in the world in women or in both sexes combined. Although it has the highest mortality rate than any other cancers in women, the mortality rate (14.7%) is

ATTENTION: The Singapore Copyright Act applies to the use of this document. Nanyang Technological University Library

less than its incidence rate of 25.2 % in women. This is because breast cancer patients have higher survival rates than any other cancers due to early diagnosis and improved treatments.

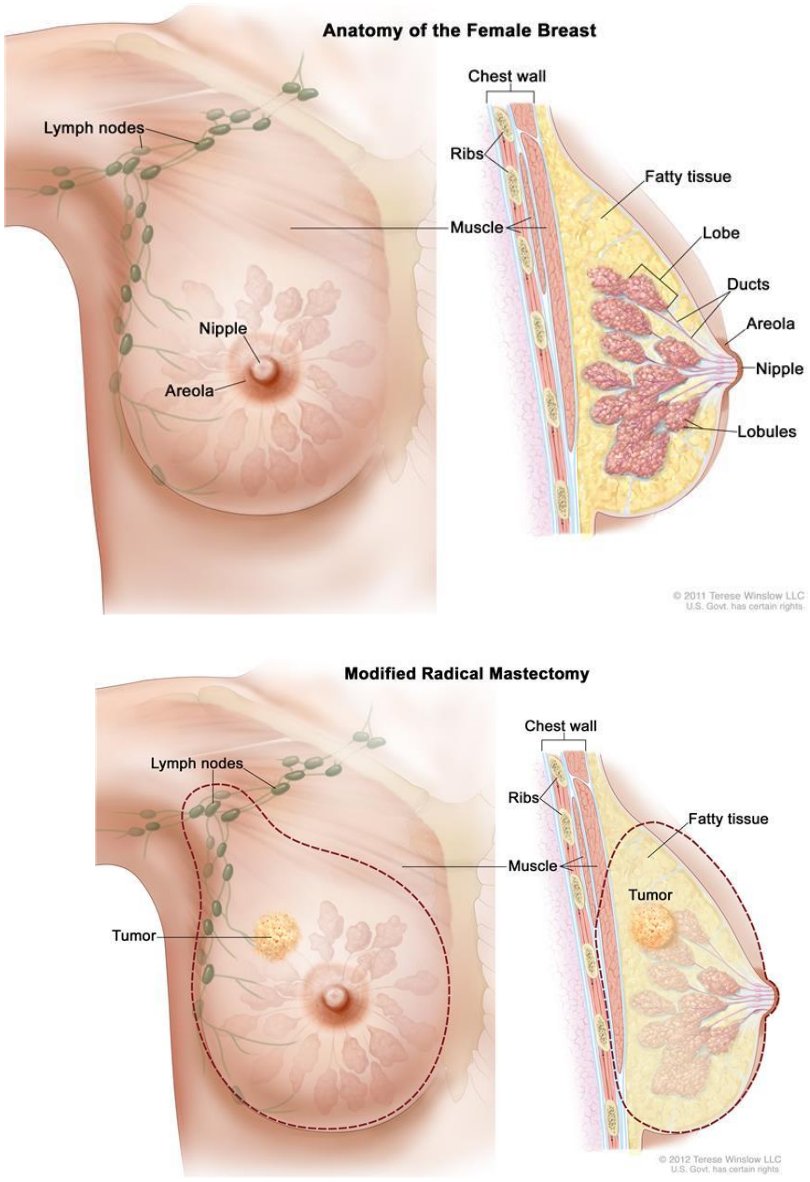

Figure 1-1. Anatomy of the normal female breast and breast tumor. Reprinted from National Cancer Institute [1, 2] with permission from Terese Winslow LLC.

ATTENTION: The Singapore Copyright Act applies to the use of this document. Nanyang Technological University Library

1.2.2 Breast Cancer in Singapore

Cancer is the top killer in Singapore, and it accounts for 29.3% of the total death in 2009. Based on the statistics from the Ministry of Health, 33 people are diagnosed with cancer in Singapore every day and 14 people die from cancer every day. Breast cancer is the most common cancer in women in Singapore. From 2006 to 2010, 29.3% of women cancer cases were diagnosed in the breast, with Singapore women having the highest breast cancer incidence rates in Asia. Breast cancer also caused 18% of cancer-related deaths in Singapore females from 2006 to 2010, which is higher than any other cancers. Moreover, there is an average of 3% increase in the number of new breast cancer cases every year in Singapore. This makes breast cancer a high risk disease for Singapore women, with 1 in 16 females developing breast cancer in their lifetime [5].

1.2.3 Risk Factors and Protective Factors of Breast Cancer

Breast cancer can be caused by multiple reasons including both endogenous factors and environmental factors [6]. Age is the first significant risk factor. The breast cancer incidence rates rise rapidly with increasing age [7]. Family history is also an important risk factor, which may be attributed by both genetic and environmental similarities among the family members [8]. 10-15% of breast cancers are associated with family history. Inherited genes such as BRCA1 and BRCA2 cause half of the family related breast cancer incidences [9]. Endogenous and exogenous hormones such as estrogens and progesterone, also increase the risks of breast cancer [10], which explain why breast cancer is seldom seen in men. Among the environmental factors, diet, especially the dietary fat is the most important risk factor [11]. Other environmental factors include alcohol consumption [12], smoking [13], and irradiation exposure [14].

ATTENTION: The Singapore Copyright Act applies to the use of this document. Nanyang Technological University Library

Protective factors and interventions that can reduce the risk of breast cancer of women include early pregnancy [15], breast feeding [16], estrogen usage [17], selective estrogen receptor modulators [18], aromatase inhibitors or inactivators [19], and risk-reducing mastectomy [20]. Exercising frequently can also reduce the risk of breast cancer in young women [21, 22]. In addition, food constituents from fruits, vegetables [13], and soy products have the potential to reduce the breast cancer risks, which are related to the lower incidence rates in Asian women [23].

1.2.4 Classification of Breast Cancer

Due to the diversity of carcinogenic factors, breast cancer is found to be highly heterogeneous. Breast cancer patients are diagnosed with distinct types of tumors, which exhibit variable histopathological and biological features, different clinical outcomes, and different responses to systemic therapies. To improve the diagnosis and treatment decision-making, breast cancers are classified into different subtypes based on the histopathological, biological, and molecular features.

Histopathological classification of breast cancers is based on the morphological feature of the tumors, from which 20 major tumor types and 18 minor subtypes of breast cancers are classified. Breast cancer can be broadly categorized into carcinoma in situ and invasive carcinoma. Breast carcinoma in situ is further sub-classified as either ductal or lobular carcinoma. Ductal carcinoma in situ (DCIS) and lobular carcinoma in situ (LCIS) can be distinguished by growth patterns and cytological features. Invasive carcinomas include infiltrating ductal, invasive lobular, ductal/lobular, mucinous (colloid), tubular, medullary and papillary carcinomas. Among these, invasive ductal carcinoma (IDC) is the most common subtype which

ATTENTION: The Singapore Copyright Act applies to the use of this document. Nanyang Technological University Library

account for 70-80% of all invasive lesions. IDC can be further sub-classified as either well-differentiated (grade 1), moderately differentiated (grade 2) or poorly differentiated (grade 3).

However, the histological classifications have minimal prognostic and predictive implications. The recent identification of the molecular subtypes of breast cancer has provided the guidance of systemic treatment and risk assessment in clinical use. These biological and molecular features of breast cancer cells including endocrine-responsive, human epidermal growth factor receptor 2 (HER2 or ERBB2) overexpression, and abnormal proliferation [24]. The most widely used molecular markers in the classification of breast cancers include estrogen receptor (ER), progesterone receptor (PgR), HER2, and Ki67. More recently, a new subtype classified as "claudin-low" has also been identified. These molecular subtypes of cancer can be identified by microassay-based gene expression analysis and unbiased hierarchical clustering. Based on these markers, breast cancer can be classified into the following subtypes (Table 1-1).

Table 1-1. Molecular subtypes of breast cancer and their gene expression level

	ER	**PR**	**HER2**	**Ki67**	**Outcome**
Luminal A	High	High	Low	Low	Good
Luminal B	High	Medium	Intermediate	High	Intermediate or poor
Basal-like	Low	Low	Low	High	Poor
HER2-enriched	Low	Low	High	High	Poor
Normal breast-like	Intermediate	Low	Low	Low/ Intermediate	Intermediate
Claudin-low	Low	Low	Low	Intermediate	Intermediate
Molecular apocrine	Negative	Negative	Positive/ Negative	High	Poor

ATTENTION: The Singapore Copyright Act applies to the use of this document. Nanyang Technological University Library

1.2.5 Triple Negative Breast Cancer

Breast tumors that are absent of ER, PR, and lack of HER2 expression are defined as triple negative breast cancer (TNBC). TNBC have many similarities with basal-like subtype of breast cancer. However, they are not the same. Although majority of TNBC are of basal-like phenotype and majority of tumors expressing basal type markers are triple-negative [25], 8-29% of TNBC did not show a basal-like subtype by gene expression profiling and 18-40% of basal-like breast cancers defined by expression profiling does not belong to the triple-negative phenotype [26]. Beside ER, PR and HER expression, basal-like breast cancers are also defined by some other biomarkers such as high-molecular-weight/basal cytokeratin (CK5/6, CK14, and CK17) and expression of epidermal growth factor receptor (EGFR) [27].

About 10-17% of all breast carcinomas are TNBC [28]. The main characteristics of TNBC are high risk and poor prognosis. TNBC more frequently occur in younger patients (<50 years) and are often present as interval cancers [29]. They are more aggressive than other breast tumor subtypes and the recurrence most frequently occur between the first and the third year. Most of TNBC-caused death occur in the first five years and patients with TNBC have a significantly shorter survival when the cells start to metastasis [30]. Moreover, lack of detection biomarkers and targeted therapies also limit the diagnosis and prognosis of TNBC [31]. Due to these features, TNBC remains a major challenge in the treatment of breast cancers [32].

1.2.6 Metastasis and Stages of Breast Cancer

The spread of breast cancer to other parts of the body is known as metastasis. There are three routes breast cancer cells can spread: invade into nearby tissues [33], enter

ATTENTION: The Singapore Copyright Act applies to the use of this document. Nanyang Technological University Library

the lymph system [34], and travel through the blood vessels [35]. Clinically, breast cancers are staged by determining the metastatic sites and the degree of breast cancer cells in other parts of the body. The determination methods include sentinel lymph node biopsy, chest X-ray, CT scan, bone scan, and positron emission tomography (PET) scan.

Using these methods, breast cancer is categorized into four stages based on various factors, including the size of the tumor (T), whether cells have spread into the nearby lymph nodes (N) and whether the tumor has spread to any other part of the body (metastasized: M) [36].

Stage 0: This stage is used to describe non-invasive breast cancers, in which abnormal cells are found in the lining of a breast duct (ductal carcinoma in situ, DCIS), in the lobules of the breast (lobular carcinoma in situ, LCIS), or in the nipple (Paget's disease of the nipple).

Stage I breast cancer is split into 2 stages:

Stage IA means the tumor has formed with a size of 2 cm or smaller. They have not spread out of the breast (Stage IA: T1N0M0).

Stage IB means that breast cancer cells have spread into the lymph nodes close to the breast with small clusters between 0.2 and 2mm. No tumor is found in the breast (T0N1M0) or the tumor size is 2 cm or smaller (T1N1M0).

Stage IIA: Tumor is small (<2 cm), but cancer cell has spread into axillary lymph nodes (T0N1M0) or in the lymph nodes near the breastbone (T1N1M0), or tumor is between 2-5 cm without spreading out (T2N0M0);

ATTENTION: The Singapore Copyright Act applies to the use of this document. Nanyang Technological University Library

Stage IIB: Tumor size is between 2-5 cm and has spread out to axillary lymph nodes (T2N0M0) or lymph nodes near the breast bone, or the tumor is larger than 5 cm without spreading out (T3N0M0).

Stage III breast cancer is divided into three groups:

Stage IIIA: although no cancer is detected in the breast, cancer cells have spread to multiple (4-9) axillary lymph nodes or lymph nodes near the breastbone (T0N2M0); or the cancer is between 2 to 5 cm and cancer cells have spread in 4-9 axillary lymph nodes or lymph nodes near the breastbone (T2N2M0); or the cancer is larger than 5 cm, and cancer cells have spread in 4-9 axillary lymph nodes or lymph nodes near the breastbone (T3N2M0).

Stage IIIB means the cancer cells has spread to the chest wall and/or the skin of the breast with no cells in the axillary lymph nodes (T4N0M0); or cancer cells has spread to the chest wall and/or the skin of the breast, with up to 9 the axillary lymph nodes (T4N1M0); or the lymph nodes near the breastbone are affected (T4N2M0).

Stage IIIC: The cancer can be any size and has spread to more than 10 axillary lymph nodes or lymph nodes above/below the collarbone and then spread to the skin of the breast (Any T, N3M0).

Stage IV: The cancer can be any size, the lymph nodes may or may not contain cancer cells but the cancer cells have spread to other organs of the body, most likely to the distant lymph nodes, lungs, bones, liver, or brain (Any T, Any N, M1).

ATTENTION: The Singapore Copyright Act applies to the use of this document. Nanyang Technological University Library

1.2.7 Metastatic Routes of Breast Cancer

Breast cancer in the advanced stage (stage IV, also called advanced breast cancer or metastatic breast cancer, MBC) causes 90% death of breast cancer patients [37]. In most cases, metastasis of breast cancer cells is initiated from the lymphatic route [38]. Lymphatic vessel invasion was found in most cases of breast cancer, while the prevalence of blood vessel invasion was particularly low. Meanwhile, lymphatic vessel invasion is a strong prognostic factor for breast cancer patients, while blood vessel invasion had no prognostic role for breast cancer [39]. As a portal for tumor cell dissemination, the lymphatic route has several advantages compared with blood vessels. First, the basement membrane is discontinuous and cell-cell junctions are loose for lymphatic vessels. Second, the lymphatic vessel has lower flow rate with minimized shear stress. Third, there is a much higher concentration of hyaluronic acid, which can protect breast cancer cells and increase their survival rate [34, 40].

However, lymph node metastases by themselves are not life threatening because they can be removed by surgery. The risk of lymphatic metastasis is that cancer cells located in the lymph nodes can continue their disseminations by draining into the blood circulation through the subclavian veins and metastasize to bone and visceral organs which can cause breast cancer patients to die [40]. Lung and bone are the most frequent metastasis sites of breast cancer. About 70% of patients with advanced breast cancer developed lung and bone metastases. Liver is the third common site and 60% of advanced breast cancer patients are diagnosed with liver metastasis. The next distant organ of breast cancer metastasis is brain, where metastases are detected in 20% of breast cancer patients. Breast cancer cells can also form metastases in multiple organs

ATTENTION: The Singapore Copyright Act applies to the use of this document. Nanyang Technological University Library

like spleen, pancreas, kidney, ovary, uterus, adrenal glands, heart and thyroid. However, the frequencies of metastasis in these organs are relatively lower [41].

The survival rates in patients diagnosed with different stages of breast cancer are very different. The survival rates are much higher when patients are diagnosed with breast carcinoma *in situ* or localized and regional metastasis compared to cancer patients with distant metastasis. The 5-year relative survival rates are listed below based on the statistics in the National Cancer Institute's Surveillance, Epidemiology, and End Results (SEER) database [42]:

Stage 0: 100%

Stage I: 100%

Stage II: 93%

Stage III: 72%

Stage IV: 22%

Because survival rates are obviously higher in the early stages of breast cancer, early diagnosis and treatment are thus crucial.

1.3 How Cancer Metastasis Happens

Cancer is life threatening mainly because of the metastasis of cancer cells to important visceral organs. Ninety percent of deaths from solid tumors are caused by metastasis [43]. Therefore, cancer metastasis has drawn many attentions and remains the biggest challenge in curing cancer. However, although the multi-step process of metastasis has been largely investigated and many gene signatures as well as specific mediators of metastasis have been identified, the anti-metastasis therapies are still not effective

ATTENTION: The Singapore Copyright Act applies to the use of this document. Nanyang Technological University Library

so far. This inspires people to make bigger efforts to understand the carcinogenesis, discover the metastatic traits, and identify anti-metastasis targets [44].

The formation of clinically detectable metastasis is a final result of a series of stochastic events that allow cancer cells to disperse and survive in secondary sites to grow as metastatic tumors [44]. These events include detachment from primary tumor, migration, local invasion, entry into the circulation and arrest at secondary sites, extravasation, and colonization (Figure 1-2).

The metastatic process of breast cancer also comprises of a series of sequential steps [45]. Metastasis of breast cancer cells starts with the local invasion in surrounding host tissue. Afterwards, the breast cancer cells invade into lymphatic vessels or blood vessels by intravasation [46, 47]. The local invasion and intravasation process require tumor cells to alter cell-to-cell adhesion and cell adhesion to the extracellular matrix (ECM). The epithelial to mesenchymal transition (EMT) plays a major role in assisting invasion and intravasion [48]. The tumor cells are further disseminated to distant organs via the lymphatic system and the blood circulation. In the distant organ, tumor cells adhere with the capillary beds and extravasate into the organ parenchyma. The microenvironment in the distant organ is critical to the survival and proliferation of disseminated tumor cells. It involves many different specialized cells, such as fibroblasts, immune cells, endothelial cells, mural cells of the blood and lymphatic vessels. These cells together with the ECM make up the microenvironment with influences the growth of metastatic tumor [49].

ATTENTION: The Singapore Copyright Act applies to the use of this document. Nanyang Technological University Library

1.3.1 Origins of Metastatic Traits

The classical view of tumor progression is the clonal evolutionary theory [50]. Based on this theory, most cancers arise from a single cell of origin. When the neoplastic cells start to proliferate, the expansion of tumor population produces genetic instability and gene mutations. Consequently, more aggressive sublines were sequentially selected during tumor progression, resulting in more advanced malignancies. Therefore, the metastatic ability of primary tumor cells is conferred by random mutations. These mutations are rare in the primary tumor, and are only selected and expanded in secondary organs after metastasis. This Darwinian view of the metastatic progression was supported by cancer cell transplantation in mice experiments [51] [52].

However, this clonal evolutionary has its conceptual inconsistency. The genes that enabled the step of metastasis would not confer increased proliferative benefit at the primary site. Therefore, these few cells with enhanced metastatic potential will remain rare in the primary tumor mass due to their low proliferative ability. Because the survival rate during metastasis is very low, the rare mutations in the primary tumor are hard to cause metastatic progression. Thus another mechanism was proposed that metastasis was driven by the same oncogenic forces that conferred selected replicative advantages at the early stage [53]. This view, however, was challenged by the clearly evolutionary features of cancer progression [54].

A complementary view was proposed by-revisiting the “seed and soil” hypothesis which suggests that cancer cells are able to become the seeds of metastasis when they reach a compatible tissue microenvironment [55]. According to this hypothesis, in the primary tumor, clonal heterogeneity provides abundant source for the selection of metastatic cancer cells. These cellular clones are genetically distinct and do not

ATTENTION: The Singapore Copyright Act applies to the use of this document. Nanyang Technological University Library

necessarily represent the majority of a primary tumor. Meanwhile, during metastatic process, these cells do not need to complete every step in the multiple processes of metastasis. Instead, every single mutation provides a slight selective advantage in one or several steps of the metastasis. The final metastatic cells result in a rare outcome which comes from extensive genomic and epigenomic alterations [44].

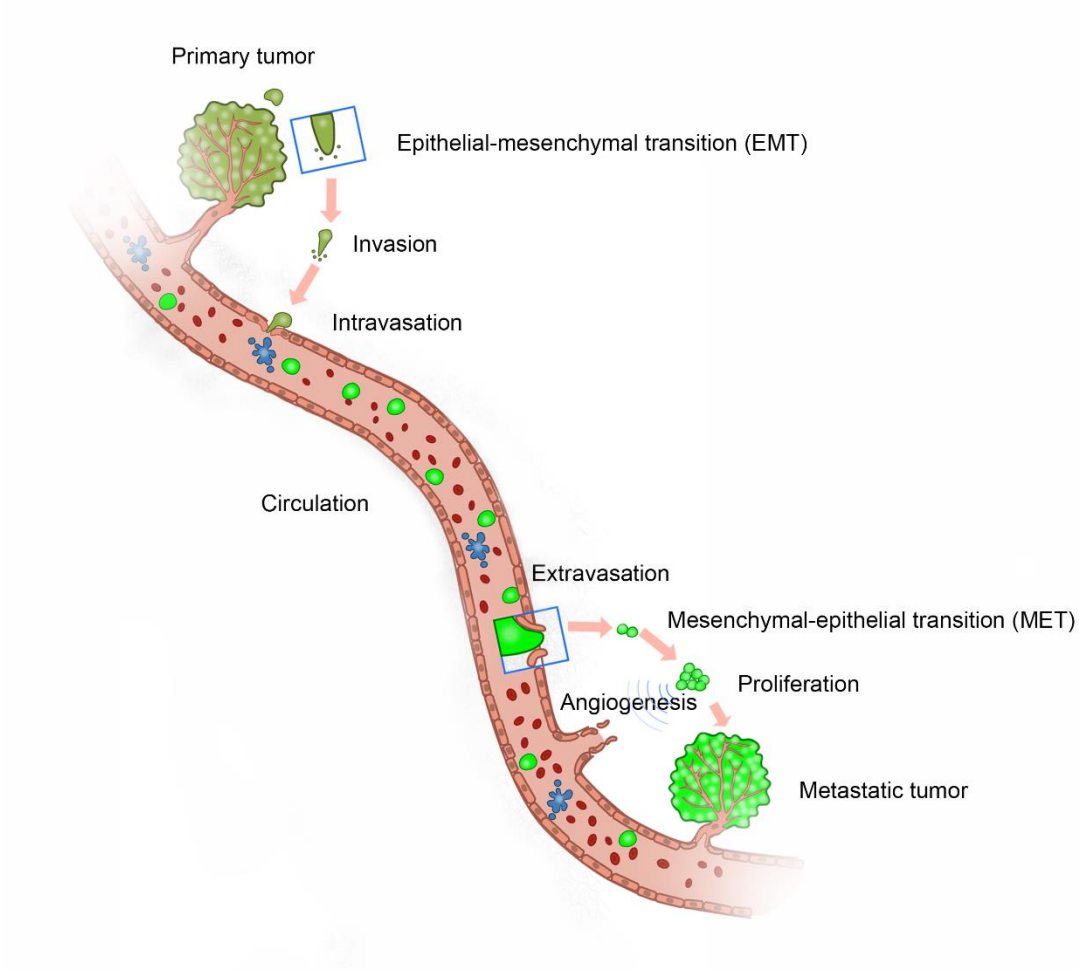

Figure 1-2. Multiple steps of cancer metastasis. Metastasis process of cancer cells involves epithelial to mesenchymal transition (EMT), local invasion, intravasation into lymphatic vessel or blood vessel, circulation within blood stream, extravasation from blood vessels, mesenchymal to epithelial transition (MET), proliferation in distant site and grow as a metastatic tumor.

ATTENTION: The Singapore Copyright Act applies to the use of this document. Nanyang Technological University Library

1.3.2 Cancer Stem Cells in Metastasis

Another model to explain the heterogeneity and inherent differences in tumor-regenerating capacity is the presence of cancer stem cells (CSCs) [56]. CSCs are a subpopulation of tumor cells that can self-renew and produce diverse cells in the tumor [57]. Therefore, these cells have 'stem-like' properties and ability to continually sustain tumorigenesis. CSCs have similar properties with normal tissue stem cells, including self-renewal and differentiation ability [56]. Different from clonal evolution model, cancer cells in CSC model are hierarchical and CSCs are on the top of the hierarchy. Meanwhile, CSCs also undergo clonal evolution [58]. In a primary tumor, not every cell is able to metastasize to other organs. Metastatic potential of cancer cells is determined by multiple factors governing cell growth, survival, angiogenesis, and invasion. CSCs are possibly the subpopulation in creating metastatic niches [59]. The advantage of CSCs in counteracting with metastatic pressure may be related to their direct linkage with epithelial-mesenchymal transition (EMT) [60].

1.3.3 Epithelial to Mesenchymal Transition

The initiation of cancer cell dissemination involves the dissociation of cancer cells from the primary tumor and the gain of invasiveness. Activation of an EMT program is a critical mechanism for the acquisition of malignant phenotypes of epithelial cancer cells [61]. An epithelium contains cells forming a thin sheet or layer due to mutually and extensively adherent laterally by cell-to-cell junctions. The molecular features of epithelium include cell-to-cell adhesion molecules (such as cadherin), extracellular matrix (ECM) adhesion sites (such as laminin), and polarized actin cytoskeleton as

ATTENTION: The Singapore Copyright Act applies to the use of this document. Nanyang Technological University Library

well as cytokeratin types of intermediate filaments [62]. Mesenchymal cells form relatively diffused tissue networks. They do not have complete cell layer, and cells only keep weak adhesion to their neighbours.

Mesenchymal cells have distinct molecular features. First, cell-cell adhesion involves different type of cadherin (such as N-cadherin). Second, adhesion sites to extracellular matrix (ECM) are widely distributed across all the surfaces instead of a polarized side. Third, the actin cytoskeleton is not apicobasally polarized and may form a cortical network and perhaps trans-cytoplasmic actin bundles. Cells thus align with a provisional "front-back" polarity [63]. Compared with endothelial cells, mesenchymal cells have much more relaxed organization, flexibility, individualism, and motile propensities. Thus, they are more likely to migrate out.

During EMT, several groups of molecules will change in their expression levels, distributions and functions. A typical event during EMT is the loss of E-cadherin, which maintains the stable junctions between cancer cells. Loss of E-cadherin is directly correlated with the loss of epithelial phenotype [64]. Down-regulation of E-cadherin during cancer progression occurs by transcriptional repression or gene mutation [61]. Snail protein was identified as the most important transcription repressor by strongly binding to the transcriptional start site of the E-cadherin gene [65]. In contrast, N-cadherin which mediates a weak intercellular adhesion is produced in EMT cells.

A summary of molecules which are changed during EMT (Figure 1-3) is listed below:

1. Growth factors: TGF-β, and wnts;
2. Transcription factors: snails, SMAD, LEF, and nuclear β-catenin;

ATTENTION: The Singapore Copyright Act applies to the use of this document. Nanyang Technological University Library

3. Cell-to-cell adhesion axis: cadherins, and catenins;
4. Cell-to-ECM adhesion axis: integrins, focal contact proteins, and ECM proteins;
5. Cytoskeletal modulators: Rho family;
6. Extracellular proteases: matrix metalloproteinases, and plasminogen activators;
7. Other molecular changes occurring after the initial behavioural change: e.g. replace cytokeratin intermediate filaments with other types, typically vimentin [62].

These molecules can be categorized into three groups based on their functionalities during EMT: EMT inducers, the extracellular cues that activate the EMT program; EMT core regulators, which are transcription factors that orchestrate the EMT program; and EMT effectors, which execute the EMT program [66]. Carcinoma cells are thought to undergo EMT in response to extracellular signals in the tumor microenvironment instead of triggering by genetic alterations. Many developmental signaling pathways, such as TGF-β, Wnt, Notch and growth factor receptor signaling cascades have been reported to inducing EMT program [66]. The EMT core regulators are important transcriptional regulators that regulate the gene expression related to cell adhesion, mesenchymal differentiation, cell migration and invasion. There are three group of core EMT regulators. The first group is the Snail zinc finger family, including Snail 1 and Snail 2. This family of transcription factors can directly bind to the E-boxes of the E-cadherin promoter to repress the transcription of E-cadherin. The second group is the distantly related zinc finger E-box-binding homeobox family proteins Zeb 1 and Zeb 2. Zeb 1/2 suppress E-cadherin transcription via a double-negative feedback loop [67]. Snail and Zeb families also repress the expression of other cell-cell adhesion

ATTENTION: The Singapore Copyright Act applies to the use of this document. Nanyang Technological University Library

proteins, such as claudins and ZO-1[68]. The third group of transcription factors include Twist1, Twist2, E12/E47. This group of transcription factors is the basic helix-loop-helix family. They can induce EMT alone or cooperatively with other transcription factors [66].

The EMT effectors are subcellular proteins that demarcate the epithelial or mesenchymal identity of tumor cells. The first type of effectors are various epithelial junction proteins, such as E-cadherin, α-catenin and γ-catenin. These proteins will be down-regulated at the mRNA and protein levels during EMT program. The second type of effectors are the intermediate filament molecules. During EMT, intermediate filaments are switched from cytokeratin to vimentin. The third type of EMT effectors are proteins that promote cell migration and invasion. These proteins include Fibronectin, PDGF/PDGF-receptor autocrine loop, N-cadherin, CD44 and integrin. With the modifications of these features during EMT program, carcinoma cells acquire the ability to break away from neighbouring cells and gain motilities to invade adjacent cell layers and start to disseminate from primary epithelial tumors to other parts of the body [69].

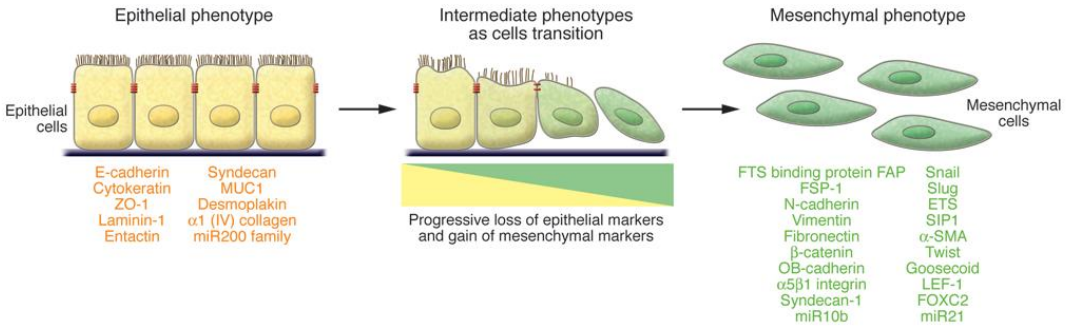

Figure 1-3. EMT program [70]. During EMT process, cancer cells lose their epithelial properties such as tight cell-cell adhesion, stiff intermediate filaments and gain mesenchymal molecular phenotype. Reprinted from ref [56] with permission from American Society for Clinical Investigation.

ATTENTION: The Singapore Copyright Act applies to the use of this document. Nanyang Technological University Library

1.3.4 Bottlenecks for Cancer Cell Metastasis

Aggressive tumors can release thousands of cancer cells into circulation each day, which can be correlated inferred from the numbers of circulating tumor cells (CTCs) present in the blood sample of cancer patients [35]. However, metastasis is still a highly inefficient process in which less than 0.01% of CTCs can eventually succeed to form secondary tumors [71]. The molecular mechanisms of cell invasion, motility and stromal interactions that allow cancer cells to enter the circulation and reach distant organs have been intensively investigated. Among those steps, leaving the primary tumor is the easiest part, while the main challenge for metastasis occur during the colonization at the distant organs [44]. Many circulating cancer cells die when they infiltrate distant organs [72]. They may die due to the inability to pass through endothelial barriers, lack of survival signals and missing supportive stroma in the host tissue [73, 74]. However, the biggest bottleneck of metastasis is actually during circulation. It has been reported that more than 99.9% of the CTCs were eliminated in the blood circulation [71]. The mechanisms on how CTCs die in circulation will be introduced separately in a later part of this chapter on circulating tumor cells. The other bottleneck is to find a suitable microenvironment after extravasation. Why cancer cells are so fragile at distant sites is still unknown, but this vulnerability serves as a major barrier to reduce the progression of metastatic cancers. Therefore, identifying the mechanisms that eliminate disseminated cancer cells will help to develop new therapeutic strategies to prevent cancer metastasis [44].

ATTENTION: The Singapore Copyright Act applies to the use of this document. Nanyang Technological University Library

1.3.5 Host-Tumor Cell Interactions and Microenvironment

Different cancers display different patterns of metastasis. Some mainly relapse in a particular organ, while others relapse in multiple organs. For example, prostate cancer most frequently relapses in bone; while breast cancer relapses in lung, liver, bone, and brain. Several factors can decide the metastatic patterns of cancer cells (Figure 1-4). The first factor is the blood circulation pattern which a cancer cell travels through. The preferred sites of metastasis for a certain type of cancer often include the first capillary beds downstream of the primary tumor [75]. For example, colon cancer cells always metastasize to the liver; while breast cancer cells frequently metastasize to the lungs. These tumor cells are mainly arrested by physical restriction in capillaries with small diameters (i.e. less than 5 μm) [73]. The second factor is the active adhesion of CTCs to the vasculature via specific proteins, such as selectin, integrin, and metadherin, which also contributes to the initial arrest [76]. The third factor is the extravasation process which enables the initial seeding in distant organs. Extravasation efficiency depends both on the tumor cell behaviour and host tissue characteristics. Related genes involved in the vascular and ECM remodelling include VEGF, COX2, MMP1, MMP-2, Twist, and TGF-β [77, 78].

Other than circulation pattern, adhesion with the vascular, and extravasation barriers, specific stromal components in a particular organ can serve as another important factor which can mediate organ specificity for metastasis. Furthermore, overt colonization critically depends on the capacity to interact with the host stroma cells [75]. The most typical example is how cancer cells exploit osteoclasts in the bone marrow for osteolytic metastasis [79].

ATTENTION: The Singapore Copyright Act applies to the use of this document. Nanyang Technological University Library

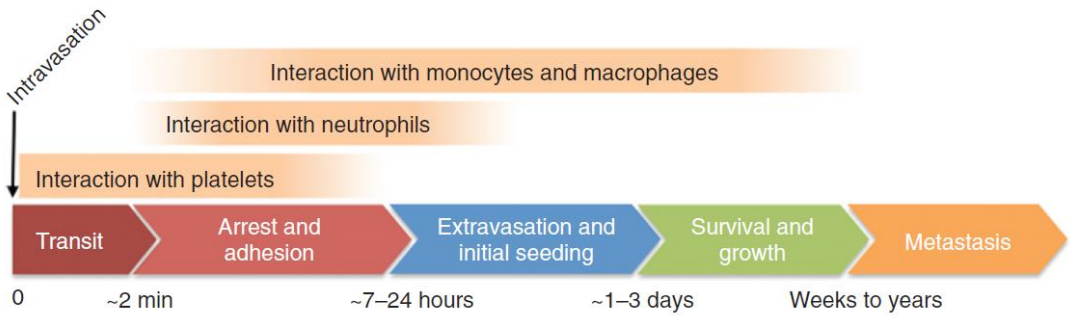

Figure 1-4. Dynamics of host-tumor cell interactions during metastasis [75]. Tumor cells interact with various host cells in blood circulation such as platelets, neutrophils, monocytes and macrophages in different stages during metastasis. Reprinted from ref [63] with permission from the American Association for Cancer Research.

1.4 Therapeutic Strategies of Metastatic Breast Cancer

1.4.1 Treatment of Breast Cancer

In breast cancer therapy, five types of standard treatments are used, including surgery, radiation therapy, chemotherapy, hormone therapy, and targeted therapy [80]. The standard treatments may cause side effects during the therapy or several months and years post treatment. Thus, new types of treatments are being tested in clinical trials such as high-dose chemotherapy with stem cell transplantation [81].

(1) Surgery

Most breast cancer patients receive surgery to remove the tumor [82]. Surgery may include:

1) Breast-conserving surgery (lumpectomy): to remove the tumor and some normal tissues around it, but not the breast itself.
2) Total mastectomy (simple mastectomy): to remove the entire breast that has the tumor.

ATTENTION: The Singapore Copyright Act applies to the use of this document. Nanyang Technological University Library

3) Modified radical mastectomy: to remove the whole breast that has a cancer, many of the lymph nodes under the arm, the lining over the chest muscles, and sometimes, part of the chest walls muscles.

Chemotherapy may be given before surgery (called neoadjuvant therapy) to shrink the tumor and reduce the amount of tissues to be removed. Radiation therapy, chemotherapy, or hormone therapy may also be given after the surgery and are known as adjuvant therapy. Adjuvant therapy is used to kill any cancer cells left after the surgery and to lower the risk of recurrence [82].

(2) Radiation therapy

High-energy X-rays or other types of radiation are used to kill breast cancer cells and prevent their proliferation [83]. Radiation therapy can be given to the body both externally and internally depending on the type and stage of the cancer [84].

(3) Chemotherapy

Breast cancer patients can receive chemotherapy by oral administration, intravenous injection, or through the cerebrospinal fluid. The type and stage of cancer also affect the pattern of chemotherapy used [85]. More than 60 anti-cancer drugs are used for treating breast cancer, including doxorubicin, fulvestrant, Herceptin, paclitaxel, tamoxifen, fluorouracil, and cyclophosphamide. Chemotherapy is often given with a combination of drugs, which works better than single drugs through different mechanisms [86, 87]. The combinations approved by FDA in treatment of breast cancer include AC, AC-T, CAF, CMF, FEC, and TAC [86].

1) AC: doxorubicin hydrochloride (Adriamycin) + cyclophosphamide

ATTENTION: The Singapore Copyright Act applies to the use of this document. Nanyang Technological University Library

2) AC-T: doxorubicin hydrochloride (Adriamycin) + cyclophosphamide + paclitaxel (Taxol)
3) CAF: cyclophosphamide + doxorubicin hydrochloride (Adriamycin) + fluorouracil
4) CMF: cyclophosphamide + methotrexate + fluorouracil
5) FEC: fluorouracil + epirubicin hydrochloride + cyclophosphamide
6) TAC: docetaxel + doxorubicin hydrochloride (Adriamycin) + cyclophosphamide.

(4) Hormone therapy

Hormones are substances made by the body glands and are circulated in the bloodstream. Some hormones can promote the growth of certain types of breast cancers. Therefore, hormone therapies by interference of the hormone or hormone receptors on the surface of breast cancer cells are widely used for women diagnosed with hormone receptor-positive breast cancer. The most important hormone that stimulates the growth of breast cancer is estrogen. Tamoxifen, an antagonist of the ER, can block the binding of estrogen with ER, and is widely used to treat ER positive breast cancer in adjuvant therapy [88, 89] or serves as a prevention agent [90]. Other hormone therapy drugs that block estrogen include toremifene (Fareston) and fulvestrant (Faslodex). Toremifene is similar to tamoxifen and is only approved to treat metastatic breast cancer [91]. However, this drug is not likely to work if tamoxifen has been used before or has stopped working. Fulvestrant can degrade ER thus eliminating its effect. It is also used to treat metastatic breast cancer, but often used after other hormone drugs like tamoxifen have failed [92]. Some drugs may also be used to reduce

ATTENTION: The Singapore Copyright Act applies to the use of this document. Nanyang Technological University Library

estrogen levels in cancer patients, such as aromatase inhibitor letrozole (Femara), anastrozole (Arimidex), and exemestane (Aromasin). Another strategy is to surgically remove the ovaries that are the main source of estrogen production.

(5) Targeted therapy

Targeted therapy of breast cancer normally uses monoclonal antibodies, tyrosine kinase inhibitors, and cyclin-dependent kinase inhibitors to identify and attack specific cancer cells without damaging normal cells.

Monoclonal antibody therapy includes the following types:

1) Trastuzumab (Herceptin): a monoclonal antibody that interferes with the HER2/neu receptor [93].
2) Pertuzumab: a monoclonal antibody that binds to HER2 and inhibits the dimerization of HER2 [94].
3) Ado-trastuzumab Emtansine: an antibody-drug conjugate consisting of the monoclonal antibody trastuzumab linked to the cytotoxic agent DM1 [95].

A tyrosine kinase inhibitor used to treat breast cancer is lapatinib which inhibits the phosphorylation of HER2 protein thus blocking the activation of EGFR pathways. It is used to treat HER2 positive breast cancer that has progressed after treatment with Herceptin [96].

A cyclin-dependent kinase inhibitor used to treat ER positive and HER2 negative breast cancer is palbociclib (PD-0332991) which is a selective inhibitor of the cyclin-dependent kinases CDK4 and CDK6 [97].

ATTENTION: The Singapore Copyright Act applies to the use of this document. Nanyang Technological University Library

1.4.2 Current Strategies to Treat Metastatic Breast Cancer

MBC is an incurable but treatable disease [98]. The median survival of MBC is about 18-24 months, although the range of survival spans from a few weeks to several years depending on the types of breast cancer [98]. There are treatment options available to extend a patient's life, delay the cancer progression, relieve cancer-related symptoms, and improve the quality of life. Treatments of MBC also include many of the same treatments as earlier stages of breast cancer as reviewed above, such as chemotherapy, radiation therapy, hormone therapy, targeted therapy, and breast surgery. All patients with MBC usually receive systemic therapy. Only in certain conditions, surgery or radiation therapy may be involved. MBC is more heterogonous compared with breast cancers in the early stages; thus, the choice of treatments depends on the tumor burden, patient symptoms, and the assessment of several predictive factors including ER, PR, and HER2.

In MBC diagnosed with hormone receptor or HER expression, systemic strategies with a combination of chemotherapy and endocrine therapy are most commonly used. Clinical studies have provided evidence that chemotherapy *per se* is associated with a survival benefit. But the randomized evidence does not support the use of high-dose chemotherapy with stem-cell support in advanced breast cancer [98]. Only 3.4% of MBC patients with systemic treatment were long-term survivors, with median survival time after diagnosis of metastatic breast cancer at 152 months [99]. A current study reported the efficacy of the drug combination in MBC treatment. In patients with HER-2 positive metastatic breast cancer, the addition of pertuzumab to trastuzumab and docetaxel can significantly improve the median overall survival to 56.5 months [100]. In cancer patients diagnosed with triple negative breast cancer, chemotherapy

ATTENTION: The Singapore Copyright Act applies to the use of this document. Nanyang Technological University Library

currently remains the only treatment option [101, 102]. If the hormone therapy is no longer working in hormone-positive cases, chemotherapy is also used. Moreover, chemotherapy drugs or combinations may be switched many times during the course of treatment of MBC, because metastases frequently develop drug resistance [103].

1.5 Circulating Tumor Cells (CTCs)

In breast cancer patients, the survival rates are relatively high (>70%) until cancer cells disseminate beyond the regional lymph nodes. In stage IV, metastatic breast cancer cells spread to distant organs such as lung, liver, bone, and brain via the blood circulation. Thus, it significantly reduces the survival rate of cancer patients (<22%) as well as their quality of life. Therefore, identification of detectable CTCs in peripheral blood of patients with solid tumors can provide an early alert for disseminated primary cancer cells through the vascular network [53, 104]. It has been demonstrated that CTCs can be used as independent prognostic markers to predict the overall survival rate of MBC patients [105-109]. Moreover, investigation of the biological properties of CTCs such as gene characteristics and protein expression profiles can also provide important information of the disease, such as cancer cell phenotype, stage and drug resistance [104, 110].

1.5.1 CTC Enrichment and Detection Approaches

CTCs were first observed early in the 1860s in a case of cancer patient where cells similar to those in tumors were seen in the blood after death [105]. Occurrence of cancer cells were then detected in the peripheral blood and venous blood draining the tumor area during operations [111]. CTCs were frequently reported in metastatic breast

ATTENTION: The Singapore Copyright Act applies to the use of this document. Nanyang Technological University Library

cancer patients as ‘carcinocythemia’ with a meaning of carcinoma cell leukemia [112-115]. However, the numbers of CTCs in the blood samples are very rare. Only recently, advancement in techniques facilitated the detection of rare CTCs from the peripheral blood of breast cancer patients [116-119].

Current approaches for CTCs detection and isolation include protein expression-based technologies and physical property-based technologies (Figure 1-5) [120]. Protein-based technologies detect CTCs by antibodies that target specific markers. An important mechanism is that epithelial markers are expressed on the surface of normal epithelia and epithelial tumors (carcinomas), but not expressed on the mesenchymal leukocytes. Therefore, these epithelial markers can be used for isolating CTCs from normal blood cells. EPCAM is the most frequently used surface markers for epithelial CTCs enrichment [121].

Physical properties are also used to distinguish CTCs from normal blood cells. The most important physical properties of CTCs are that they have larger sizes than normal blood cells. Based on this property, multiple methods have been developed, such as density gradient centrifugation and filtration through special filters. Some other methods were also established based on other physical properties including deformability and membrane properties [122].

After enrichment, the CTCs fraction still contains many leukocytes. Several methods are used to distinguish CTCs from normal blood cells. Antibodies to cytokeratin intermediate filaments of epithelial cells, are frequently used to detect CTCs. Immunofluorescence staining was used to detect these markers. Assays targeting specific mRNAs are also widely used for identifying CTCs. For breast cancer, mRNA of CK19 is the most frequently used in clinical studies [123]. Functional assays

ATTENTION: The Singapore Copyright Act applies to the use of this document. Nanyang Technological University Library

are also used to detect and characterize CTCs. The EPISPOT assay (Epithelial Immuno SPOT) is one of the functional assays used to detect specific proteins secreted by CTCs cultured *in vitro* [124]. Invasion assay to digest a fluorescently labelled cell adhesion matrix was also employed to examine the ability of CTCs [125].

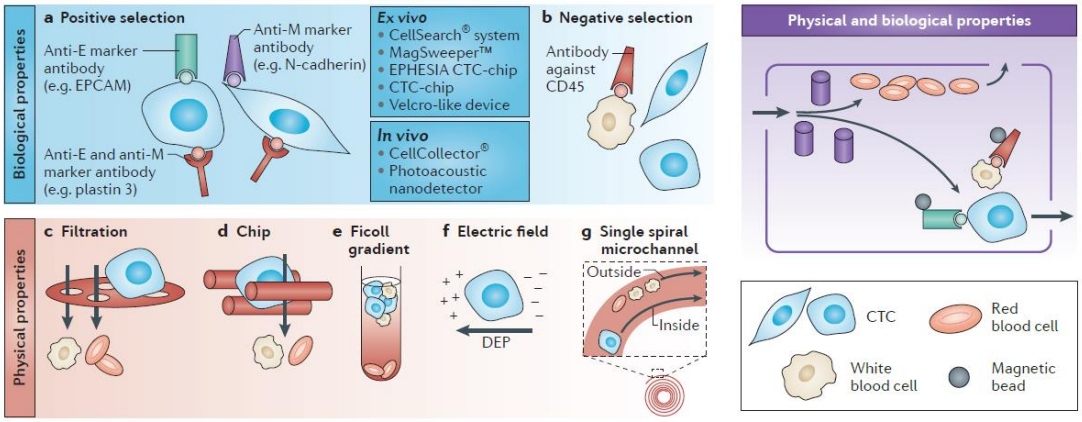

Figure 1-5. CTC enrichment methods [120]. Current CTC isolation methods are based on either biological properties or physical properties. Reprinted from ref [101] with permission from Nature Publishing Group.

1.5.2 The Clinical Utility of CTCs

Despite the increase in methodology and clinical validations, CTCs measurements have not been included into the clinical guidelines because their clinical usefulness is still unclear [120]. So far, CTCs measurements are unable to facilitate decisions to adopt or reject a therapeutic option. Some limitations still exist for the detection and the clinical relevance of CTCs. EMT is a potential challenge for CTCs detection. Cancer cells can maintain a balance between the EMT and MET during the metastatic cascade [126]. The current CTCs detection methods are based on either the physical or biological properties of CTCs. However, both methods are associated with the epithelial properties of CTCs, such as surface adhesion marker EpCAM, epithelial

ATTENTION: The Singapore Copyright Act applies to the use of this document. Nanyang Technological University Library

intermediate filament, and size. Therefore, mesenchymal-like cancer cells present in the bloodstream of cancer patients may be missed. Besides, existence of epithelial cells in patients with benign disease may lead to a false-positive diagnosis in CTCs testing [127]. Limited blood sample available from cancer patients is also another limitation of CTCs measurement. Normally, the number of CTCs in every 7.5 ml blood samples is about 5. Consequently, this may generate big variations in the detection.

1.5.3 Nature and Metastatic Relevance of CTCs

Although CTCs analysis is widely studied and suggested to be a real-time liquid biopsy to improve cancer detection and management [121], the nature of CTCs and their metastatic relevance still remains unclear. The question that must be answered is whether the characterization of CTCs can truly reveal their origin and/or their potential metastatic tumors. To understand this question, several facts need to be clarified. One is that CTCs can be released into the bloodstream from either the primary tumor or the metastatic tumor. Meanwhile, although most CTCs are isolated as single cells, clusters of CTCs (micro emboli) often occur in patients with advanced disease [128]. These clusters are most frequently missed in the current isolation methods. Therefore, the detected characteristics of CTCs may not reflect the true situation of primary tumors and the disease.

More importantly, the transition from CTCs to disseminated tumor cells (DTCs) and the fate of CTCs in blood stream are crucial, but have been least understood so far. DTCs are from the settlement of CTCs in secondary organs, such as lung, liver, bone, and brain [129]. The transition of CTCs to DTCs may depend on several factors including the survival fate of CTCs, EMT dynamics [130], chemo attraction of CTCs

ATTENTION: The Singapore Copyright Act applies to the use of this document. Nanyang Technological University Library

to particular organs [131], and homing of CTCs in distant organs [132]. In a clinical study of breast cancer patients, CTCs' numbers in the blood were counted before and after surgery. The half-life of CTCs was measured to be 1 to 2.4 h. After 24 h, the CTCs' number had reached its background level [128].

The half-life of CTCs tested in this study can reflect a possibility that primary tumor may refill the pool of CTCs continuously. But it is hard to conclude whether CTCs died or were arrested by other organs, which may result in distinct outcomes. The fate of CTCs in the circulation was associated with their resistance to anoikis, apoptosis, and necrosis. During the transit through the circulatory system, CTCs are subjected to hemodynamic forces, immunological stress, and collisions with host cells (blood and endothelial cells). Therefore, all these stresses may affect their survival fate [133]. These situations imply that current knowledge of CTCs is still limited, and detection of CTCs is not a matured method for cancer diagnosis. Better insights into the biology of CTCs will further improve the development of CTCs assay and the management of the disease.

1.5.4 Studies Regarding to the Survival of CTCs

Early in 1897, Goldmann first observed that the mere presence of CTCs is not synonymous with metastasis [134]. In 1915, Iwasaki demonstrated that many of CTCs were destroyed in circulation [135]. Many studies in animal models have revealed inefficiency of CTCs survival. In 1950s, quantitative studies of various phases of metastasis were completed. Their results indicated that most CTCs failed to form metastatic tumors and the number of metastases is dependent on the numbers of CTCs released into circulation [136]. In another study from the same group, CTCs were

ATTENTION: The Singapore Copyright Act applies to the use of this document. Nanyang Technological University Library

found to be able to pass through narrow vessels immediately or arrested by the vessels [137]. Following studies revealed that less than 0.1% of tumor cells survived for 24 h, and less than 0.01% of the cells formed metastases after intravenous injection [71]. In spontaneous metastasis models, naturally occurred metastasis was found to be even less efficient than experimental metastasis model following intravascular injection [138, 139]. In other metastasis routes such as liver metastasis via the portal vein, the metastatic efficiency were also found to be very low, in which 20% of the injected cells were detected after 15 min and only 0.68% of these cells retained morphological integrity after 48 h [140].

Although the efficiency of CTC survival is very low, the mechanisms of how hemodynamic shear stress damages CTCs and why metastatic CTCs are able to survive and become the true seeds of secondary tumor are still not investigated so far.

1.6 Cell Death and Apoptosis

Resisting cell death is the most important hallmark of cancer [141]. Programmed cell death by apoptosis serves as a natural barrier for cancer development and progression [142, 143]. In tumors that succeed in progressing with high-grade malignancy and resistance to therapy, apoptosis is often attenuated [144]. Therefore, detecting apoptosis in cancer cells and clarifying the apoptosis-resistant mechanism of cancer cells in each metastatic step is crucial to further understand the metastatic disease.

1.6.1 Definition of Apoptosis

Apoptosis is defined as a highly regulated and energy-dependent programmed cell death in which cells activate a signalling cascade that leads to cell death without

ATTENTION: The Singapore Copyright Act applies to the use of this document. Nanyang Technological University Library

triggering any inflammatory response [145]. Morphologically, it involves the rapid condensation and budding of cell body, followed by the formation of apoptotic bodies. These apoptotic bodies containing well-preserved organelles can be engulfed by neighbouring cells or white blood cells through phagocytosis [146]. The apoptotic process is responsible for maintaining tissue homeostasis as well as eliminating abnormal cells that are superfluous, diseased, or otherwise had served their useful purpose. Apoptosis can occur under normal cell condition or induced by chemotherapy drugs, radiation, or inhibition of growth factor signalling pathway [147]. Therefore, it makes apoptosis differ from another form of cell death called necrosis which is triggered by extreme physiological disturbance causing damage to the plasma membrane [145]. The impairment of cell's homeostasis with a huge influx of water and extracellular ions causes the swelling of cell body and results in cell lysis. The cytoplasmic organelles including lysosomes are released into extracellular fluid causing the digestion and lysis of neighbouring cells. Hence, necrosis is often associated with nearby cell death and inflammatory response [148].

1.6.2 Signaling Pathway of Apoptosis

Apoptosis is controlled by two major pathways, extrinsic pathway and intrinsic pathway. The extrinsic pathway is triggered after the ligation of cell surface death receptor with corresponding ligand. The intrinsic pathway is characterized by the leakage of cytochrome c from mitochondria [147]. Both pathways can activate caspase cascade and result in apoptosis as shown in Figure 1-6.

ATTENTION: The Singapore Copyright Act applies to the use of this document. Nanyang Technological University Library

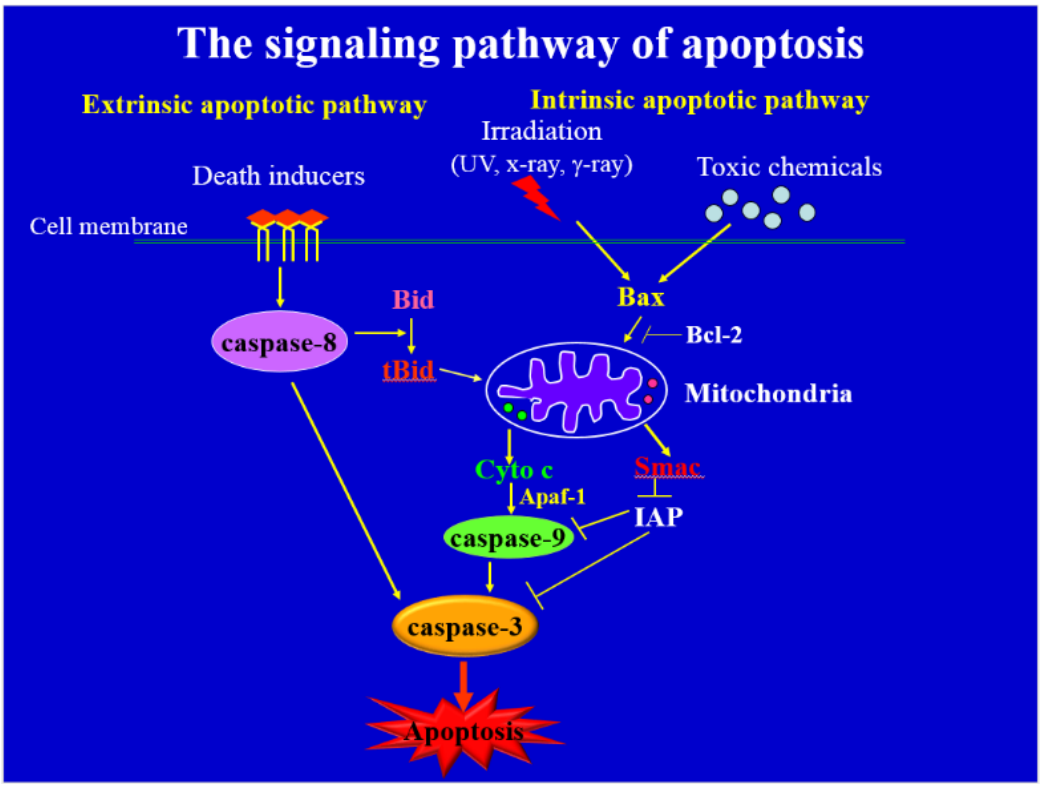

Figure 1-6. Extrinsic and intrinsic pathways of apoptosis. Both of extrinsic and intrinsic pathways involves the activation of caspase-3. This picture is provided by my supervisor Prof. Kathy Luo.

The extrinsic pathway, also known as death signal-induced, death receptor-mediated pathway, is regulated by the members of tumor necrosis factor (TNF) receptor (TNFR) super family, such as Fas and TNF-related apoptosis inducing ligand receptors. The binding of ligands like TNFα, Fas ligand, and TRAIL to the corresponding receptors result in receptor trimerization and clustering of receptor death domains. These domains will form a death inducing signaling complex (DISC) that links up with the adaptor molecule, Fas associated death domain (FADD), or the TNF receptor associated death domain (TRADD). The DISC binds to the initiator pro-caspase-8 and pro-caspase-10 through its death effector domains (DED), thereby causing the autocatalytic cleavage of pro-caspase-8 into activated caspase-8 and

ATTENTION: The Singapore Copyright Act applies to the use of this document. Nanyang Technological University Library

caspase-10. Both activated caspase-8 and caspase-10 will cause further activation of downstream executioner caspases including caspases-3, 6, and 7.

The intrinsic pathway, also known as stress-induced, mitochondrion-mediated pathway, is triggered by a wide range of apoptotic stimulus, such as withdrawal of growth factor, mild hypoxia, oxidative stress, irradiation, chemotherapy, and DNA damage. Upon triggering, pro-apoptotic members of the Bcl-2 super family, such as Bax and Bak, will bind on the mitochondrial surface and caused the formation of permeability transition pores (PT pores). In the normal condition, mitochondria are important power plants for the cells. But in the stress condition, mitochondria are potential gunpowder barrels in the cells. During apoptosis, the formation of PT pores on the mitochondrial membrane can cause the release of pro-apoptotic proteins such as cytochrome c, Smac/DIABLO, endonuclease G and apoptosis inducing factor (AIF) into cytosol. Cytochrome c can combine with Apaf-1 and procaspase-9 and ATP to form an apoptosome, which activates caspase-9 and subsequently, the activation of executioner caspases-3, -6, and -7 [149].

1.6.3 Caspase Family in Apoptosis

Caspases is a family of cysteine-aspartic acid-proteases. So far, 14 mammalian caspases have been identified. They are synthesized as inactive precursors, known as procaspases that can be activated by proteolytic processing. The N-terminal of the prodomain in procaspases contains a highly diverse structure required for caspase activation [150 413]. Meanwhile, caspases themselves are enzymes that can cleave proteins at specific amino acids sequence (Figure 1-7). Caspase can be divided into 3 subfamilies: apoptosis activator, apoptosis executioner and inflammation mediator

ATTENTION: The Singapore Copyright Act applies to the use of this document. Nanyang Technological University Library

caspases. The initiator caspases-2, 8, 9, and 10 are activated by induced dimerization and these initiator caspases will in turn cleave the inactive pro-form of effector caspases-3, 6, and 7. Executioner caspases like caspase-3 will in turn cleave protein substrates within the cell and result in apoptosis (Figure 1-8). Other caspases, including caspase-1, 4, 5, 11 and 12, constitute another group, which is the caspase-1 subfamily. This subfamily is designated inflammatory caspases, because their prime function is to regulate inflammatory processes [151].

Executioner caspases breakdown chromatin and cause apoptosis in 3 ways: activate DNases, inactivate DNA repair enzymes, and breakdown of the structural protein in the nucleus. Inactivation of DNA repair enzymes like poly ADP-ribose polymerase (PARP) prevent the repair of damaged DNA. PARP can repair DNA damage and it can be activated after being cleaved by caspase-3. In addition, degradation of nuclear lamins by caspase-6 results in the breakdown of nuclear membrane [152]. This subsequently causes chromatin condensation and nuclear fragmentation. The activation of DNases, for example caspase-3-activated DNases [153] separates DNA strands into smaller fragments.

Caspase-3 is a key player in apoptosis execution. It is the active form of procaspase-3. Procaspase-3 can be activated by several upstream activators, including caspase-3, caspase-8, caspase-9, caspase-10, CPP32 activating protease, and granzyme B (Gran B). Activated caspase-3 also has many substrates, such as procaspase-3, procaspase-6, procaspase-9, actin, fodrin, lamin, inhibitor of caspase-activated deoxyribonuclease

ATTENTION: The Singapore Copyright Act applies to the use of this document. Nanyang Technological University Library

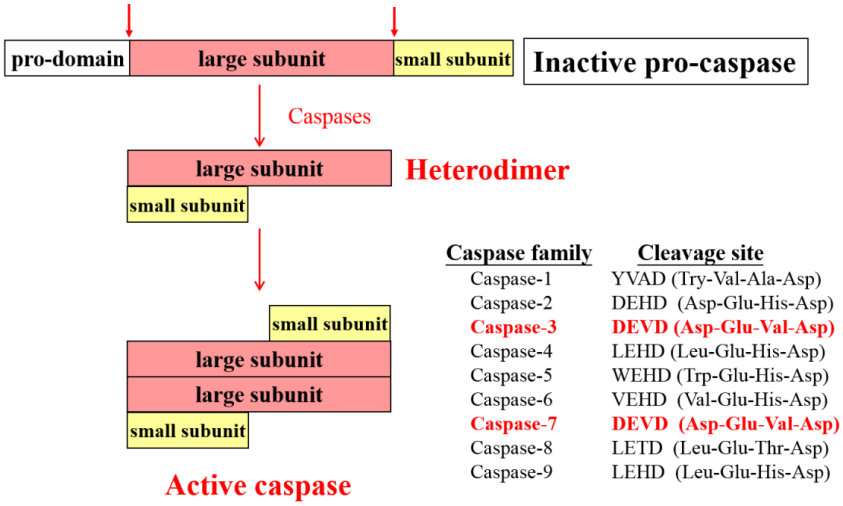

Caspase family	Cleavage site
Caspase-1	YVAD (Try-Val-Ala-Asp)
Caspase-2	DEHD (Asp-Glu-His-Asp)
Caspase-3	**DEVD (Asp-Glu-Val-Asp)**
Caspase-4	LEHD (Leu-Glu-His-Asp)
Caspase-5	WEHD (Trp-Glu-His-Asp)
Caspase-6	VEHD (Val-Glu-His-Asp)
Caspase-7	**DEVD (Asp-Glu-Val-Asp)**
Caspase-8	LETD (Leu-Glu-Thr-Asp)
Caspase-9	LEHD (Leu-Glu-His-Asp)

Figure 1-7. Activation of caspases and their specific cleavage sites. Caspases can be activated from inactive pro-caspase when they are cleaved by other upstream caspases. Each caspase family member has its specific cleavage site, which contains 4-amino acid group. This picture is provided by my supervisor Prof. Kathy Luo.

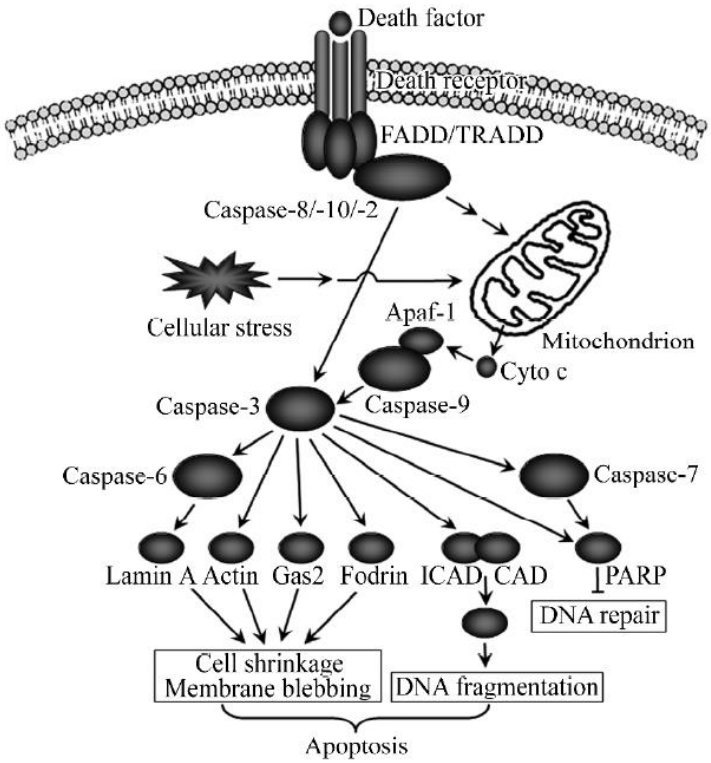

Figure 1-8. Downstream substrates of apoptosis executioner caspases [149]. Reprinted from ref [130] with permission from the Oxford University Press.

ATTENTION: The Singapore Copyright Act applies to the use of this document. Nanyang Technological University Library

(ICAD), steroid response element-binding protein, DNA-PK, PKCγ, PARP, D4-GD1, and so on [149]. Therefore, caspase-3 activation is a central event in apoptosis pathway and can serve as an important early indicator for cell death. Based on this key role of caspase-3, our group has previously developed a caspase-3 biosensor (sensor C3) for detecting apoptosis in living cells [154].

1.6.4 A Caspase-3 Biosensor for Apoptosis Detection

This caspase-3 biosensor was invented by my supervisor, Prof. Kathy Qian Luo, in 2001 [154]. The development of sensor C3 was inspired by the earlier developed new variants of green fluorescent protein (GFP) in Roger Tsien's Lab, the cyan fluorescent protein (CFP) and the yellow fluorescent protein (YFP). These two GFP variants displayed promising fluorescence resonance energy transfer (FRET) effect and could be disrupted by proteolytic cleavage of the linker [155, 156]. In the sensor C3, a CFP protein and a YFP protein was fused with a specialized linker. The linker contains 16 amino acids, including a caspase-3 recognition and cleavage sequence of DEVD (Figure 1-9).

The amino acid sequence of the linker connecting a donor CFP and an acceptor YFP is SGLRSRAQASNS. Four amino acids RAQA in this linker region was replaced with GGDEVDGG. DEVD is a cleavage site of caspase-3 for detecting apoptosis. The whole C3 sensor protein conformation was designed to optimize the FRET effect. Since sensor C3 is a protein made up of a sequence of amino acids, the corresponding gene can be incorporated into the genome system of any living cells through transfection and by allowing the cell to transcribe and translate the C3 sensor continuously without changing the morphology and basic property of the cell. A HeLa-

ATTENTION: The Singapore Copyright Act applies to the use of this document. Nanyang Technological University Library

C3 cell line was established after the invention of the sensor C3 (Figure 1-10). Under normal condition, there is no active caspase-3. Energy can be transferred directly from CFP to YFP under an excitation of 433 nm and the FRET fluorescence is emitted at a

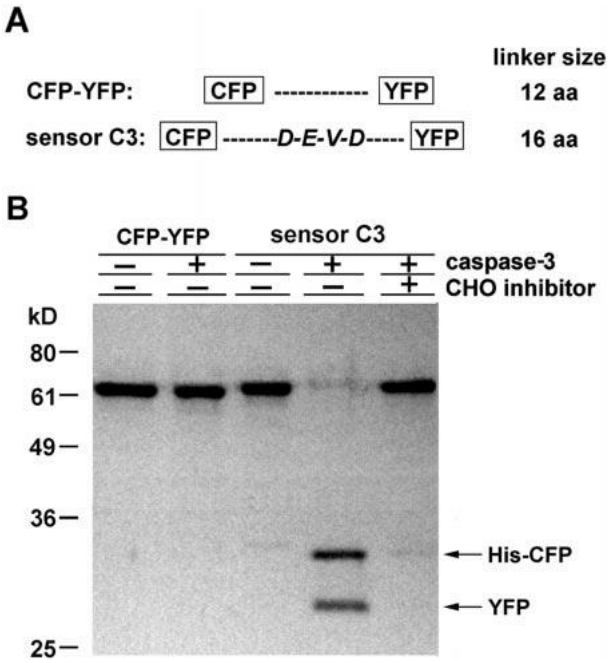

Figure 1-9. **Structure of sensor C3 [154].** Basic design of fusion constructs for CFP-YFP and sensor C3, the latter contains the caspase-3 cleavage sequence DEVD in the linker, the length of which is given in number of amino acid (aa). (B) Western blot results showing the cleavage of the purified sensor C3 protein by caspase-3. The positions of YFP and polyhistidine-tagged CFP are indicated. CHO (Ac-DEVD-CHO) is a caspase-3 specific inhibitor. Reprinted from ref [134] with permission from Elsevier.

wavelength of 535 nm. In the presence of caspase-3, the cysteine–aspartic acid-proteases will cleave the DEVD linker and cause the dissociation of donor and acceptor. Under the same excitation light of 433 nm, only the donor fluorescent protein CFP was excited and the FRET effect was eliminated. Thus, response with the fluorescence emission was at a wavelength of 480 nm.

ATTENTION: The Singapore Copyright Act applies to the use of this document. Nanyang Technological University Library

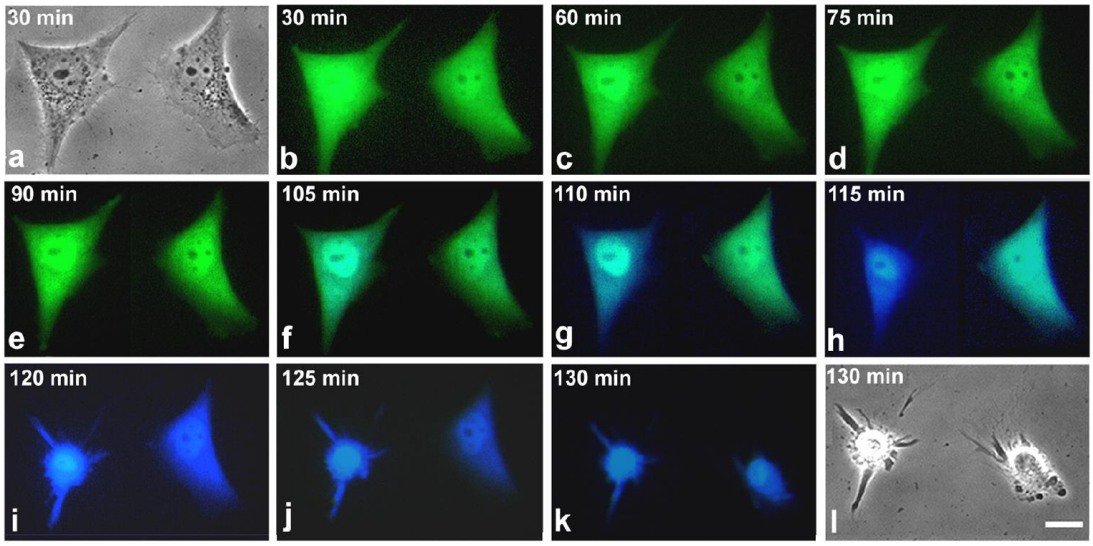

Figure 1-10. FRET imaging of HeLa-C3 cells undergoing apoptosis [154]. HeLa-C3 cells were treated with UV irradiation for 3 min to induce apoptosis. Reprinted from ref [134] with permission from Elsevier.

This sensor C3 has many advantages. First, it is highly sensitive to caspase-3 cleavage. Therefore, it can detect apoptosis which is induced by various stimulus. Second, the FRET efficiency is very high. In the FRET imaging, colour of a single cell can clearly change from green to blue when the cell is undergoing apoptosis. This property can enable the *in vivo* application of the FRET sensor. Third, it can be stably incorporated into the cells without affecting cell morphology and viability [154].

1.6.5 Application of Sensor C3 in Anti-Cancer Drugs Screening

In the past decade, our group has widely applied this sensor C3 in detecting apoptosis during drug screening and evaluation. After the generation of cancer sensor cell line HeLa-C3 [154], we started to apply it into the study of anti-cancer drugs. Consequently, a high throughput screening method was developed [157]. In this method, HeLa-C3 cells were grown in 96-well plates. Upon the treatment with anti-cancer drugs,

ATTENTION: The Singapore Copyright Act applies to the use of this document. Nanyang Technological University Library

apoptosis of HeLa-C3 cells was detected in a fluorescence plate-reader by calculating the emission ratio of YFP over CFP. When the Y/C ratio reduced to 1/3, 80% of cell viability was reduced due to apoptosis. This method specifically detects the apoptotic effects of anti-cancer drugs and differs from the traditional cell viability methods (such as MTT assay) which quantify the overall viability without separating apoptotic and necrotic cell death as well as proliferation inhibition effect. Meanwhile, the same population of cells can be detected at multiple time points during the anti-cancer drug treatment course using this sensor C3. Since this experiment can be set within a single plate, the apoptotic curve can be obtained from multiple drugs with multiple concentrations. This makes it a truly high throughput screening method. Moreover, based on the slope of a Y/C ratio curve, the speed of caspase-3 activation can be determined, which may reveal the possible mechanism of a particular drug. For example, the curve with a steep slope suggests that the drug can directly induce apoptosis, whereas a curve with a gentle decline may indicate that the apoptotic effects are due to cell-cycle inhibition.

Based on this method, our group have conducted drug screening of plentiful herbal compounds [158-166]. Some of the hits were found to effectively induce the apoptosis of cancer cells and inhibit tumor growth [167-169]. One of the promising drug displayed specific anti-cancer effect towards ER positive breast cancer cells in our recent study [169].

In another direction, we also transfected the FRET sensor into endothelial cells to generate a blood vessel sensor cell line HUVEC-C3 [170]. With this cell line, we were able to study tumor induced angiogenesis, and screen for anti-angiogenesis drugs which can potentially inhibit tumor growth and metastasis [170, 171]. When seeding

ATTENTION: The Singapore Copyright Act applies to the use of this document. Nanyang Technological University Library

this sensor endothelial cell line into a microfluidic channel, we were able to mimic the human blood vessels *in vitro* and study the apoptosis of endothelial cells under pulsatile shear stress and diabetes conditions [172-174].

In this thesis, I transfect the sensor C3 plasmid into more cancer cell lines and normal cell lines to establish a sensor cell bank. Multiple breast cancer sensor cell lines were generated to study breast cancer metastasis and screen anti-cancer drugs. I also applied this FRET sensor to detect apoptosis in live animals for the first time. More importantly, apoptosis of CTCs was first investigated in this thesis using the advantageous features of sensor C3. Through this thesis, we have established a large cell bank with more than 30 sensor cell lines, including 10 cell lines from various human cancers, 1 highly metastatic mouse melanoma cell line, >10 lung metastatic breast cancer cell line in different stages, 8 metastatic breast cancer cell line in different organs and 3 normal cell lines. The establishment of this large C3 sensor cell bank will facilitate our future studies in cancer, diabetes, and drug discovery.

1.7 Drug Resistance of Cancer

Resistance of cancer cells to chemotherapy, radiotherapy, and targeted therapy is a major problem of cancer treatment [175]. In breast cancer therapy, systemic agents are effective in 90% of primary breast cancers and 50% of metastases at the beginning of the therapy. However, after a period of time, resistance to therapy is frequently developed and can be expected as the cancer progression occurs. Commonly developed drug resistance is related with the high recurrent rate in breast cancer patients. Although breast cancer patients benefit from the early detection and the defined molecular basis of breast cancer biology, approximately 30% of patients with

ATTENTION: The Singapore Copyright Act applies to the use of this document. Nanyang Technological University Library

early-stage breast cancer have recurrent disease, which is metastatic in most cases [176]. Therefore, a better understanding of the molecular mechanisms of drug resistance is needed to select proper therapeutic strategies which are more suitable to the characteristics of cancer patients.

Drug resistance of cancer cells can be intrinsic or acquired. Intrinsic drug resistance originates from the pre-existence of resistance-mediating factors in cancer cells before receiving treatment. Furthermore, acquired drug resistance usually develops during cancer treatment. Initially, the tumors are sensitive to the therapeutic agents. But after a period of treatment, drug resistance can be produced after genetic mutations, adaptive responses, or the activation of alternative compensatory signalling pathways [177].

Many molecular mechanisms can potentially lead to drug resistance, including drug inactivation, mutation of drug target, drug efflux, DNA damage repair, cell death inhibition, activation of survival signalling pathways, and the epithelial-mesenchymal transition, etc. More recently, it was reported that drug resistance could also be caused by the presence of genetic heterogeneity in cancer cells [178] and cancer stem cells [179]. The principles for the main mechanisms of cancer drug resistance are listed below [175].

1.7.1 Drug Efflux

Several cell membrane transporter proteins are linked to chemo-resistance. The ATP-binding cassette (ABC) transporter family are well-studied drug efflux mediators. The transmembrane proteins regulate the flux across the plasma membrane of multiple chemotherapeutic agents. There are 49 different ABC transporters. The transporter's structure varies in different proteins. But they share two different domains. One is a

ATTENTION: The Singapore Copyright Act applies to the use of this document. Nanyang Technological University Library

highly conserved nucleotide binding domain and the other is a variable transmembrane domain. When anticancer drugs bind to the transmembrane domain, ATP hydrolysis at the nucleotide binding site will drive the conformational change and pump the drugs out of the cell [180]. Multi-drug resistance protein 1 (MDR1), MDR-associated protein 1 (MRP1) and breast cancer resistance protein (BCRP) are involved in many types of cancers with drug resistant. All three transporters can efflux xenobiotics, including taxanes, vinca alkaloids, epidophyllotoxins, anthracyclines, and kinase inhibitors from cells. In addition, MDR1 can cause both intrinsic and acquired drug resistance [181].

1.7.2 Drug Activation and Inactivation

This mechanism is relevant to both chemotherapeutic drugs and targeted therapy agents. It is caused by drug inactivation or a lack of drug activation to certain types of drugs. An example is that platinum drugs can be inactivated by the thiol glutathione [182]. Glutathione transferase [12] superfamily is a group of detoxifying enzymes that can protect cellular macromolecules from electrophilic compounds. Elevation of glutathione S-transferases [12] expression in cancer cells is able to enhance detoxification of the cytotoxic drugs in breast cancer [183].

1.7.3 Alteration in Drug Targets

Alterations in the drug target such as mutations or changes in the expression level may affect the drug response. This mechanism often leads to drug resistance against molecular targeted therapies. One example is the topoisomerase II which is the target for several anticancer drugs including doxorubicin. Topoisomerase II is an enzyme used for preventing super-coiling or under-coiling of DNA. The complex formed by

ATTENTION: The Singapore Copyright Act applies to the use of this document. Nanyang Technological University Library

DNA and topoisomerase II is usually transient. The stabilization of this complex by anticancer drugs will induce DNA damage and inhibit DNA synthesis, which further lead to anti-cancer effects. Cancer cells can generate mutation in the topoisomerase II gene and limit the binding of drugs with topoisomerase II-DNA complex by which it confers resistance to topoisomerase II inhibiting drugs [184].

1.7.4 Apoptosis Inhibition

Resistance to apoptosis of cancer cells can cause their resistance to drug treatment. Cancer cell survival is mediated by a group of anti-apoptotic proteins. The most important anti-apoptotic proteins include Bcl-2 family members, inhibitors of apoptosis proteins [104] and caspase 8 inhibitor FLIP [175]. Gene mutations, amplifications, chromosomal translocations, and overexpression of the genes encoding these proteins will induce resistance to chemotherapy and targeted therapies. Moreover, the upstream regulators of these genes are also pro-survival factors that confer drug resistance. These regulators include nuclear factor -κB (NF-κB), signal transducer and activator of transcription 3 (STAT3) [175] and c-Jun N-terminal kinases (JNK) [185].

1.7.5 DNA Damage Repair

The killing effects of chemotherapy drugs towards cancer cells involves directly (for example, platinum-based drugs) or indirectly (for example, topoisomerase inhibitors) damaging of the DNA. Therefore, repairing DNA damage has a significant role in cancer drug resistance [186]. The molecular basis of DNA damage repair-induced drug resistance is associated with DNA damage response (DDR) mechanism. In normal cells, DNA lesions are quickly recognized by DDR factors, which can activate cell

ATTENTION: The Singapore Copyright Act applies to the use of this document. Nanyang Technological University Library

cycle checkpoints and direct DNA repair. In cancer cells, the accumulation of DDR gene mutation is widely present and can contribute to genomic integrity. Gene mutations of *BRCA1* or *BRCA2* in women are involved in double-strand break (DSB) repair via homologous recombination (HR) and contribute to the development of breast cancers [187, 188]. BRCA1 and BRCA2 proteins have tumor suppression function by promoting DNA repair. BRCA1/2-mutant cancers are initially sensitive to therapies that target DNA, such as cisplatin and PARP inhibitors. However, the restoration of BRCA1/2 functions due to secondary *BRCA1/2* mutations was found to be a mechanism of acquired resistance to DNA damaging drugs in *BRCA1/2*-mutated cancer cells [189].

1.8 Reactive Oxygen Species, Antioxidant and MnSOD

An emerging hallmark of cancer is the reprogramming of energy metabolism [141]. The uncontrolled cell proliferation of tumor cells requires the adjustments of energy metabolism in order to fuel the abnormal cell activity [141]. A group of metabolic by-products, reactive oxygen species (ROS), are produced during energy metabolism from the molecular oxygen [190]. ROS play important roles in various cell activities under physiological and pathological conditions [191]. Thus, increasing interests are focused on the role of ROS in tumor initiation, progression [192] and anti-cancer therapeutic strategies [193]. Understanding the mechanism of ROS and antioxidant system in regulating the cell proliferation, migration, survival, and drug resistance may inspire new insights into the anti-metastasis efforts.

ATTENTION: The Singapore Copyright Act applies to the use of this document. Nanyang Technological University Library

1.8.1 Cell Sources of ROS

ROS are highly reactive molecules, ions or radicals. They have a single unpaired electron in their outermost shell of electrons [194]. There are two types of ROS. The first type are free oxygen radicals, such as superoxide ($O_2^{\bullet-}$), hydroxyl radical ($^{\bullet}OH$), nitric oxide ($NO^{\bullet}$), organic radicals ($R^{\bullet}$), peroxyl radicals ($ROO^{\bullet}$), alkoxyl radicals ($RO^{\bullet}$), thiyl radicals ($RS^{\bullet}$), sulfonyl radicals ($ROS^{\bullet}$), thiyl peroxyl radicals ($RSOO^{\bullet}$), and disulfides (RSSR). The second type are non-radical ROS, including hydrogen peroxide (H_2O_2), ozone/trioxygen (O_3), singlet oxygen ($^1O_2$), hypochloride (HOCl), organic hydroperoxides (ROOH), peroxynitrite (ONO^-), nitrosoperoxycarbonate anion ($O=NOOCO_2^-$), nitrocarbonate anion ($O_2NOCO_2^-$), dinitrogen dioxide (N_2O_2), nitronium (NO_2^+), and highly reactive lipid-or carbohydrate-derived carbonyl compounds [195]. Among all of these ROS, superoxide, hydrogen peroxide and hydroxyl radicals are well-investigated.

In cancer cells, ROS may be generated from multiple mechanisms, including mitochondrial dysfunction, increased metabolic activity, cell receptor signaling oncogene activity, increased activity of oxidases, peroxisomes, cyclooxygenases, lipoxygenases or crosstalk with the immune cells [195]. The major sources of ROS are the mitochondria and the NADPH oxidase (NOX) family (Figure 1-11).

In the mitochondria, ROS are produced as a byproduct of oxidative phosphorylation (Figure 1-11). Superoxide is the initial ROS generated in complexes I and II of the electron transport chain and released to the mitochondrial matrix or the intermembrane space [153]. Mitochondrial membrane is impermeable to the superoxide radical. Thus, the only route for the leakage of superoxide into the cytoplasm is through a mitochondrial permeability transition pore (MPTP) in the outer membrane [196, 197].

ATTENTION: The Singapore Copyright Act applies to the use of this document. Nanyang Technological University Library

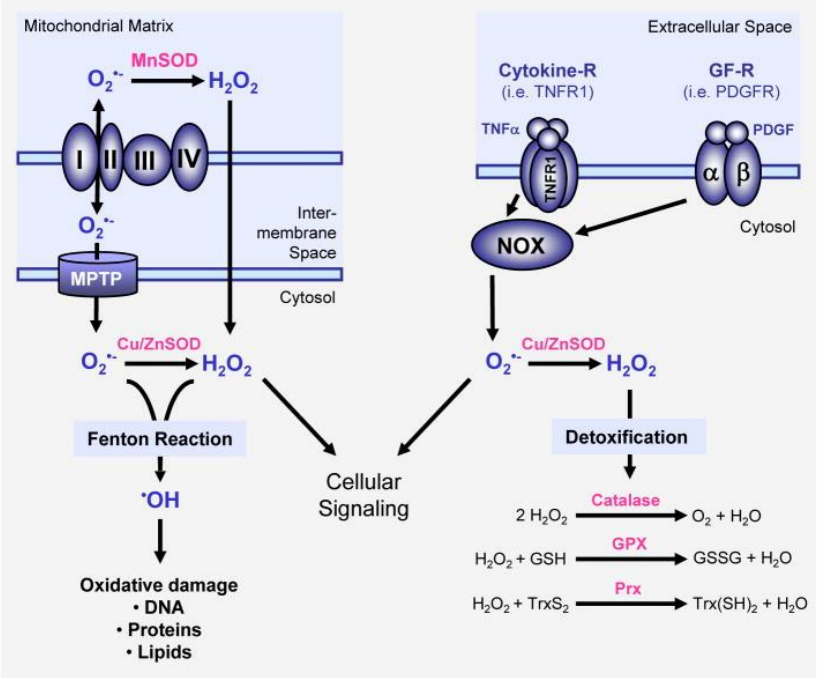

Figure 1-11. **Major mechanisms of ROS generation and detoxification [195].** There are two major ROS source in the cells. One is from the respiratory chain in mitochondria and the other is from the NADPH oxidase (NOX) in the plasma membrane. Reprinted from ref [175] with permission from Elservier.

Superoxide can be further converted to H_2O_2 by manganese superoxide dismutase (MnSOD) in the mitochondrial matrix or by copper/zinc superoxide dismutase (CuZnSOD) in the cytosol [198]. H_2O_2 is an important secondary messenger in the cells and is highly diffusible in cellular membrane systems facilitated by specific aquaporin [199]. Both hydrogen peroxide and superoxide involved in cellular signaling. They can also form hydroxyl radicals (•OH) in the Fenton reaction in the presence of iron ion. Hydroxyl radicals are highly reactive and can damage proteins, DNA, and lipids. In addition, peroxisomes are another major ROS generation sites. Superoxide and H_2O_2 can be generated through xanthine oxidase in the peroxisomal matrix and the peroxisomal membranes [200].

ATTENTION: The Singapore Copyright Act applies to the use of this document. Nanyang Technological University Library

1.8.2 ROS-induced Oxidative Stress

ROS have multiple functions in the cells. Under normal conditions, the effects of ROS are counteracted by antioxidant system in the cells through both enzymatic and non-enzymatic mechanisms. However, an imbalance of ROS and antioxidants will lead to oxidative stress. Excessive ROS in the cells can cause damage by reacting with lipids in the cellular membrane, nucleotides in the DNA, and sulfhydryl groups in proteins. They also cause cross-linking or fragmentation of ribonucleoproteins [191]. The damaging effects of ROS to DNA are carcinogenic [201]. Oxidative DNA damage was reported to be involved in the development of breast cancer [202]. Moreover, because superoxide molecules are produced at the inner mitochondrial membrane and released to the mitochondrial matrix, the mitochondrial DNA (mtDNA) can also be damaged [203].

1.8.3 Cellular Antioxidant System

Under physiological conditions, the intracellular levels of ROS are steadily maintained by an antioxidant system to prevent cells from damage. This system includes non-enzymatic molecules such as glutathione, flavonoids, and vitamin A, C, and E, and antioxidant enzymes which scavenge specific ROS by different members. Superoxide dismutases (SODs) are metalloenzymes that convert superoxide anion into hydrogen peroxide and oxygen. The metal ions utilized by dismutases include copper, zinc, manganese, or iron as cofactors [195]. Three SODs members using different metal ions are localized in different parts of the cell. CuZnSOD is mainly located in the cytosol, while MnSOD is located in mitochondrial matrix. Also, the third member is modified from CuZnSOD, and is localized in the extracellular spaces.

ATTENTION: The Singapore Copyright Act applies to the use of this document. Nanyang Technological University Library

Hydrogen peroxide can be catalyzed into water and oxygen by many different molecules and enzymes. Catalase is an enzyme that is located in the cytosol and peroxisomes and can scavenge hydrogen peroxide [204]. Peroxiredoxin, a thioredoxin peroxidases, is able to catalyze the reduction of hydrogen peroxide, organic hydroperoxides and peroxynitrite. The glutathione system also play important roles in the regulation of hydrogen peroxide level. It includes glutathione (GSH), glutathione reductase, glutathione peroxidases (GPX), and glutathione S-transferases [12]. GSH protects cells from oxidative stress by reducing disulfide bonds to cysteine in cytoplasmic proteins. At the same time, glutathione will be oxidized to glutathione disulfide (GSSG). GSSG can be reduced by glutathione reductase to refill the GSH pools. Under physiological conditions, glutathione is often in its reduced form because of a constitutive activity of glutathione reductase in cells. Another enzyme, glutathione peroxidases (GPX), is able to breakdown hydrogen peroxide and other organic hydroperoxides. In addition, detoxification enzymes glutathione S-transferases can catalyze the conjunction of GSH with many exogenous and endogenous electrophilic compounds. GSTs were found to be overexpressed in many types of tumors. They were able to regulate MAPK pathways and were involved in the development of chemo- resistance [195].

1.8.4 MnSOD in Cancer Progression

MnSOD is the most important antioxidant enzyme with many important functions in cancer growth and progression [205]. It is encoded by *sod2* gene mapping at chromosome 6q25 and translated in ribosome as a precursor form with 223 amino acids. Post-translationally, the MnSOD precursor is transported into the mitochondrial

ATTENTION: The Singapore Copyright Act applies to the use of this document. Nanyang Technological University Library

matrix to become a mature protein with 198 amino acids [206]. MnSOD is essential to protect aerobic life from the toxic effects of oxygen under physiological conditions [207]. The basic function of MnSOD is to convert superoxide radicals, which are produced from the electron transport chain and released to the mitochondrial matrix, into hydrogen peroxide and oxygen. By doing so, the levels of superoxide can be controlled at nanomolar concentration which is the physiological levels of superoxide in mitochondria. Meanwhile, the accumulation of H_2O_2 in cells can also be modulated by MnSOD through affecting the production of superoxide from mitochondrial respiration [208]. Therefore, by controlling the level of superoxide and hydrogen peroxide in the cells, MnSOD is involved in the regulation of cell activities.

MnSOD can prevent mitochondrial dysfunction that is caused by the accumulation of superoxide anion radical and its progeny. MnSOD was found to protect neuron cells from ROS induction, loss of the mitochondrial transmembrane potential and the energy charge which were associated with membrane lipid peroxidation and protein nitration [209]. Another example comes from the treatment of cancer cells with doxorubicin. The major mechanism of doxorubicin in killing cancer cells is through intercalation of DNA and inhibition of topoisomerase II activity [210]. However, doxorubicin also have another important anti-cancer mechanism by generating ROS [211] from redox cycling of the quinone moiety [212], leading to increased iron uptake [213, 214] and the release of iron from internal stores [210], causing further formation of ROS through iron-catalyzed reactions [215].

MnSOD can also regulate multiple signaling pathways through modulating the level of its product H_2O_2, which is an important secondary messenger regulating the normal function of cells [216]. As H_2O_2 can pass through cellular membrane systems,

ATTENTION: The Singapore Copyright Act applies to the use of this document. Nanyang Technological University Library

it is able to influence the activity of hydrogen peroxide-sensitive signaling proteins. These proteins share some features that make them susceptible to oxidation by hydrogen peroxide. One feature is the presence of a deprotonated cysteine residue in its active site. Most cytosolic proteins only have protonated cysteine residues. However, in proteins that can specifically detect hydrogen peroxide, their cysteine residues are deprotonated. Exposure to hydrogen peroxide can lead to reversible oxidation of thiol groups of key cysteine residues in many proteins, including transcription factors, kinases, phosphatases, structural proteins, metabolic enzymes, and ion channels [216]. Therefore, MnSOD can regulate the activity of transcription factors such as HIF-1α [217], AP-1 [218], NF-κB [219] and p53 [220].

The roles of MnSOD in cancer development and progression are controversial, because it was considered both as tumor suppressor and tumor promoter. Early studies reported the low levels of MnSOD in many tumor types [221, 222]. When MnSOD is overexpressed in human melanoma cells, breast cancer cells, and glioma cells, the tumorigenicity could be suppressed [223-225]. However, in several types of human tumors, MnSOD levels were found to be increased [219]. Moreover, MnSOD levels were increased in several types of metastatic tumors than primary tumors [226-228].

The controversial roles of MnSOD may be related with different redox-status of the cells, primarily to the ratio of the endogenous antioxidants that controls $O_2^{\cdot-}/H_2O_2$ ratio (Figure 1-12) [229]. In normal tissues, high levels of MnSOD are expressed to maintain the physiological level of H_2O_2 and its signaling functions. The cells with lower level of MnSOD are under oxidative stress and may consequently transform to cancer cells. In the initial stage of tumor, MnSOD functions as a tumor suppressor. It is because H_2O_2 regulating enzymes are also down-regulated accordingly.

ATTENTION: The Singapore Copyright Act applies to the use of this document. Nanyang Technological University Library

Overexpression of MnSOD in these cells may lead to oxidative stress due to the high level of H_2O_2. In the advanced stage, the levels of MnSOD are upregulated to provide more H_2O_2 to signal the activation of transcription factors which can control the oxidative stress and facilitate the cancer progression and metastasis.

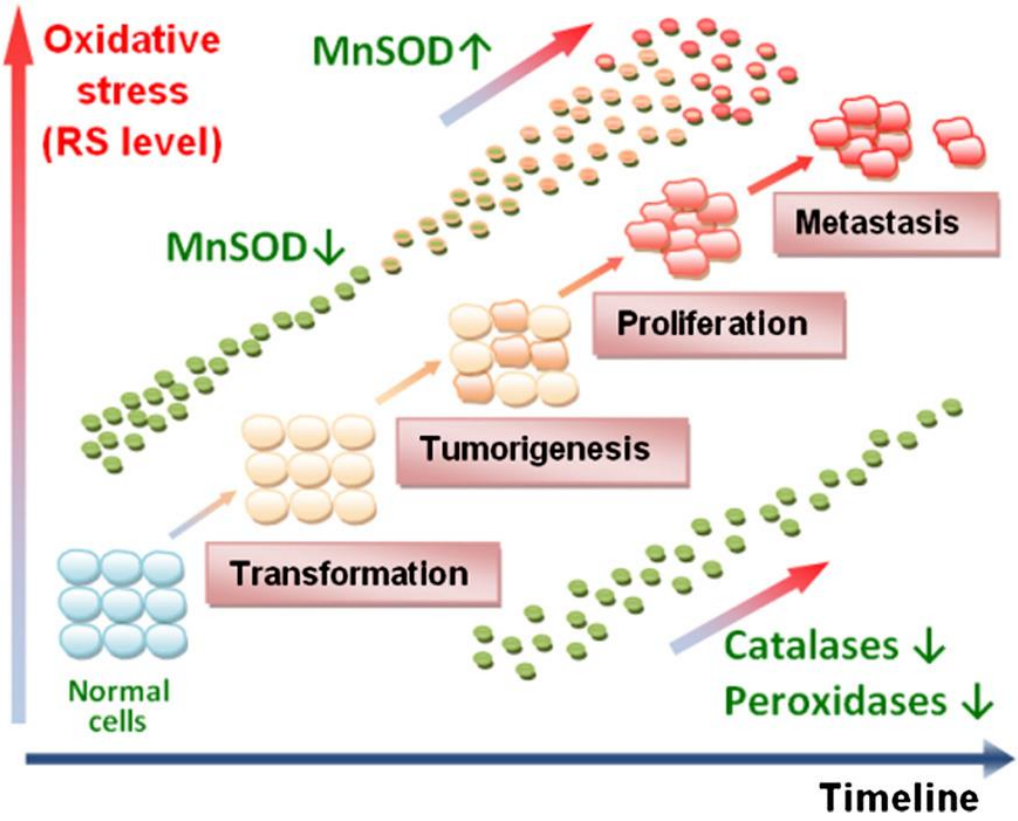

Figure 1-12. The role of MnSOD in cancer progression [229]. MnSOD play dual roles during cancer metastasis. In the early stage, MnSOD is a tumor suppressor and its level is reduced following the tumor progression. In the late stage, MnSOD promote tumor metastasis and its level is increased when the tumor cells become more metastatic. Reprinted from ref [210] with permission from Elsevier.

ATTENTION: The Singapore Copyright Act applies to the use of this document. Nanyang Technological University Library

1.8.5 Strategies to Modulate the Effects of MnSOD

Because of the importance of MnSOD, many strategies have been investigated to modulate the effects of MnSOD [205].

The first strategy is to alter the expression of MnSOD. Human MnSOD was found to be a single-copy gene consisting of five exons interrupted by four introns with typical splice junctions. Seven Sp1 and three AP2 consensus sequences with no TATA box or CAAT box were initially detected in the promoter region of MnSOD. MnSOD gene also contains one NF-κB consensus sequence in the 3'-flanking region [230]. Sp1 is an essential transcriptional activator of MnSOD expression, while AP-2 is a potent repressor of MnSOD expression by interacting with Sp-1 [231]. Interaction of tumor suppressor p53 with Sp1 also represses the MnSOD expression [232]. NF-κB is involved in MnSOD gene expression because a NF-κB response element was identified within an enhancer of MnSOD gene [233]. In addition, nucleophosmin (NPM) was found to be an important cofactor for NF-*κ*B-regulated MnSOD expression [234]. By targeting these transcription factors, MnSOD expression can be modulated in cancer cells [235-237]. Epigenetic mechanisms can also modulate the MnSOD expression [238]. These mechanisms include cytosine hyper methylation within the intron 2 [239] which interferes with NF-*κ*B enhancer, DNA hyper methylation in the promoter region of *sod2* gene [240, 241], and histone modifications of *sod2* gene [242, 243].

The second strategy is the application of SOD mimetics. As many studies have suggested MnSOD as a tumor suppressor, a lot of SOD mimetics were synthesized such as MnTBAP and MnTE-2-PyP^{5+} [229]. MnTBAP is a cell-permeable SOD mimetic that widely used to inhibit cell oxidation [244, 245]. It was applied both *in*

ATTENTION: The Singapore Copyright Act applies to the use of this document. Nanyang Technological University Library

vitro [246] and *in vivo* [247] for protecting cells from oxidative damage. Recent studies revealed that MnTBAP can reduce mitochondrial superoxide-induced oxidative damage in normal cells under treatment with anti-cancer drug doxorubicin [248, 249], and cisplatin [250].

Another modulating strategy is to inhibit the MnSOD activity. However, very few MnSOD specific inhibitors have been identified or synthesized so far. A naturally occurring estrogen metabolite 2-Methoxyestradiol (2-ME) was reported to inhibit the activity of SOD. Both activities of CuZnSOD and MnSOD could be inhibited by 2-ME, leading to the selective killing of cancer cells [251]. 2-ME has shown promising antitumor effects in preclinical studies with both anti-proliferative and antiangiogenic effects [252, 253]. An antiangiogenic study revealed that 2-ME produced antiangiogenic effect by increasing both superoxide production and SOD activity in mitochondria [254]. Clinical trials have also shown 2-ME as a promising anticancer agent in treatment of metastatic breast cancer [255] [256], metastatic prostate cancer [257, 258], and platinum-resistant ovarian cancer [259]. Although 2-ME has been reported with many other mechanisms of action such as microtubule disruption-induced apoptosis [259] and hypoxia-inducible factor (HIF)-1α inhibition [260], increasing evidence suggest its mechanism in inducing oxidative stress in mitochondrial [261-266], which are related to the early reported mechanism of SOD inhibition [251].

ATTENTION: The Singapore Copyright Act applies to the use of this document. Nanyang Technological University Library

1.9 Project Rationale

This thesis mainly focuses on the investigation of the survival mechanism of CTCs under hemodynamic shear stress and understanding the underlying mechanisms of metastasis-derived drug resistance in disseminated breast cancer cells.

Metastasis caused majority of breast tumor related death of cancer patients. Thus extensive interests were raised to elucidate the molecular mechanisms of metastasis including EMT, migration, invasion and microenvironment in the secondary organs. However, strategies targeting the malignant motility and proliferation of primary tumor cells are often inefficient, especially after a breast cancer patient is diagnosed with DTCs in distant organ. Meanwhile, DTCs frequently acquire resistance to systemic chemotherapy which further worsen the prognosis and eventually lead to poor survival of metastatic cancer patient.

One of the key steps of metastasis has not been well-investigated is the survival of CTCs in the blood stream. Although many clinical relevance of CTCs have been emphasized, very few study has investigated the killing mechanism of blood flow and survival mechanism of CTCs in the circulation. Because the blood circulation is a severe microenvironment where over 99.9% CTCs are eliminated, understanding how hemodynamic shear stresses induce the programmed cell death–apoptosis, and what mechanisms underlying the survival of rare metastatic breast cancer cells may enable the design of effective strategies to prevent metastasis. Moreover, because the bloodstream serves as a stringent natural selection field on CTCs, drug resistance of DTCs is very likely acquired during this process by utilizing a shared survival mechanism. Therefore, metastatic tumors are potentially curable if the survival factors in CTCs are identified and effectively inhibited.

ATTENTION: The Singapore Copyright Act applies to the use of this document. Nanyang Technological University Library

To facilitate the mechanism study of cancer metastasis and discovery of anti-metastatic strategies, I also generated a series of apoptosis sensor cell lines and developed multiple novel experimental models. In addition, comparative proteomics analysis was applied to identify more potential driver proteins of metastasis. Our studies will contribute to an improved clinical outcome of MBC treatment.

ATTENTION: The Singapore Copyright Act applies to the use of this document. Nanyang Technological University Library

CHAPTER 2 Material and Methods

2.1 Cell Culture

The human breast cancer cell lines MCF7, T-47D, BT-474, SK-BR-3, MDA-MB-468 and MDA-MB-231, mouse melanoma cell line B16-F10, human hepatocellular carcinoma cell line HepG2, and human lung cancer cell line A549 were purchased from the American Type Culture Collection (ATCC, USA). FRET sensor cell line HeLa-C3 and HUVEC-C3 were previously generated by our laboratory. The MCF7 cell line was cultured in MEM, the BT-474 cell line and A549 cell line were cultured in RPMI 1640 and the other cell lines were cultured in DMEM medium (Invitrogen, USA), all supplemented with 10% fetal bovine serum (FBS) (HyClone, UK) and 1% penicillin-streptomycin (Gibco, USA). All cells were sub-cultured in 100 mm petri dishes (TPP, USA), every 2 to 3 days when it reached between 80 to 90% confluence and maintained in a 5% CO_2 humidity incubator at 37 ℃. The passaging ratio was 1:5 to 1:3 for most of the cell lines. For B16-F10 cell line, ratio 1:10 was adopted in the regular subculture. For experiments setting up, the cells were collected by trypsinization and span down by centrifugation at 1500 rpm for 3 min. Cells suspended in fresh medium were counted for density using a hemocytometer.

2.2 Generation of Stable FRET-based Biosensor Cell Lines

In this thesis, MCF7, BT474, MDA-MB-231, A549, B16-F10, and HepG2 cell lines were transfected with the FRET-based caspase-3/7 sensor plasmid to generate stable sensor cell lines.

Before transfection, a G418 titration test was done in all cell lines to attain the G418 killing curve in order to determine the optimum G418 concentration needed to kill

ATTENTION: The Singapore Copyright Act applies to the use of this document. Nanyang Technological University Library

cells without FRET sensor expression. Briefly, 5000 cells of each cell line were seeded per well in a 96-well plate and varying concentrations (0, 50, 100, 200, 400, 600, 800, and 1000 μg ml^{-1}) of G418 (PAA, Germany) in culture medium were added to 3 wells per concentration. 5000 HeLa-C3 cells were seeded into 3 wells of the 96-well plate and 800 μg ml^{-1} of G418 in MEM medium (Invitrogen) was added to serve as a positive control. The total volume of the medium containing G418 in each well was 100 μl. The duration of the titration test was 10 days, during which the 96-well plate was left in the incubator and the old culture medium containing G418 was replaced with fresh culture medium containing appropriate concentrations of G418 on the fifth day. On the tenth day, MTT assay was performed on the 96-well plate to determine cell viability and hence, to attain the G418 killing curve. After obtaining optimum G418 concentration, sensor C3 plasmid transfection were conducted to all cell lines mentioned above. Lipofectamine 2000 (Invitrogen, USA) were used as transfection reagent in all stable cell line generation in this study. The procedure of transfection are described below:

1. Cells were seeded onto a 6 cm culture dish and grown overnight to approximately 70% confluence.
2. Old medium was removed and FBS-free medium was used to wash the cells twice and then aspirated out.
3. 2 ml of FBS-free medium was added to the dish and then placed in the CO_2 incubator.
4. 120 μl of FBS-free medium was pipetted into a centrifuge tube and 2 μl of caspase-3 biosensor DNA (1 μg μl^{-1}) was added to the DMEM. In another tube,

ATTENTION: The Singapore Copyright Act applies to the use of this document. Nanyang Technological University Library

5 µl of lipofectamine 2000 reagent was diluted with 120 µl FBS-free medium and was incubated at room temperature for 5 min.

5. DNA solution was then added slowly into the liposome solution and mixed well to form a complex.
6. The DNA-liposome complex was incubated at room temperature for 20 min.
7. The complex was then added dropwise into the culture dish with 2 ml FBS-free medium prepared in step 3.
8. After 6 h, transfection medium was replaced with 3 ml of fresh medium containing 10% FBS.
9. 48 h after successful transfection, the culture medium was replaced with complete medium containing optimal concentration of G418 as determined in the G418 titration test to kill untransfected cells.

After selection with G418 for more than 2 weeks, single-cell colonies expressing the C3 sensor were picked up by trypsin using a culture insert (Ibidi, Germany). The harvested sensor cell lines were designated as MCF7-C3, BT474-C3, 231-C3, A549-C3, B16-F10-C3 and HepG2-C3, respectively. All generated stable cell lines were resuspended with freezing medium containing 20% FBS, 10% dimethyl sulfoxide (DMSO) and stored in liquid nitrogen.

2.3 Functional Assays

2.3.1 Determination of Apoptotic Status of Single Cells by FRET imaging

To detect the apoptosis of single cells *in situ*, FRET imaging was conducted through an inverted fluorescence microscope (Observer.Z1, Carl Zeiss, Inc.) using an excitation wavelength of 436 ± 10 nm and a 455-nm dichroic mirror. The emissions of YFP (535 ± 15 nm) and CFP (480 ± 20 nm) were recorded using a computer-controlled camera

ATTENTION: The Singapore Copyright Act applies to the use of this document. Nanyang Technological University Library

(AxioCam MRm, Cal Zeiss, Inc.) with control software of Zen 2012 (Cal Zeiss, Inc.). The digital fluorescence images were then processed using Image-Pro Plus software (Media Cybernetics, Inc.). Composite image with both YFP and CFP channel was used in the measurement of YFP/CFP ratio, which can reflect the FRET efficiency. The outline of a particular cell and neighboring background reference were traced in an Image-Pro Plus software software (Media Cybernetics, USA) for the intensity measurement. For calculation of the YFP/CFP ratio, background value is subtracted from both YFP and CFP channel prior to the subsequent division (Figure 2-1).

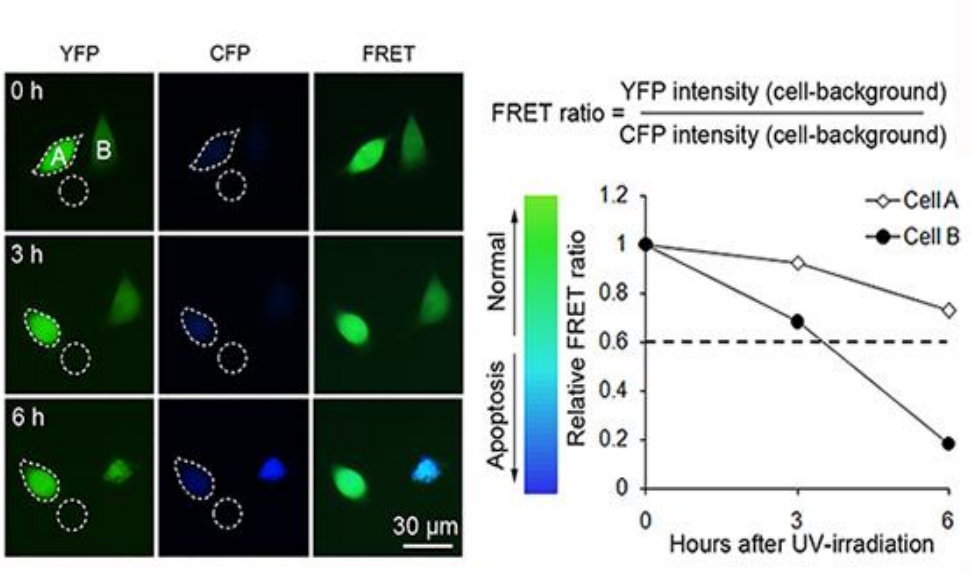

Figure 2-1. Calculation of FRET ratio by measuring the YFP and CFP intensity. Apoptosis was induced in 231-C3 cells by 3 min of UV irradiation. Fluorescent images of 231-C3 cells were separately obtained from YFP (Em = 535 ± 15 nm) and CFP (Em = 480 ± 20 nm) channels excited under the excitation light of CFP (Ex = 436 ± 10 nm), and the images were merged to produce the FRET images. The green FRET images indicate live cells, and blue FRET images indicate apoptotic cells. The FRET ratio was calculated from the fluorescence intensity of YFP and CFP from the circled areas. To compare the apoptotic rates between different cells at various times, the relative emission ratio of YFP/CFP in each cell was calculated by normalizing the initial FRET ratio to 1.0 at t0. Cells were considered apoptotic if their relative FRET ratio was reduced from 1.0 to less than 0.6, which is equivalent to more than a 50% reduction of the FRET effect.

ATTENTION: The Singapore Copyright Act applies to the use of this document. Nanyang Technological University Library

2.3.2 Determination of Cell Apoptosis and Proliferation by Measuring the Fluorescent Intensity of FRET Sensor in Plate Reader

To evaluate the effects of anticancer agents in inducing apoptosis and inhibiting proliferation, fluorescent intensity of the FRET sensor was measured using a VICTOR™ *X*3 plate reader (PerkinElmer, USA). Briefly, 5000 cells in 100 μL culture medium were seeded in each well of 96-well plate for overnight. Anticancer reagents were added into 96-well plate in multiple concentrations, with 5 repeating wells for each concentration. After 0, 24, 48 and 72 hours' treatments, the fluorescent intensity in each well were measured with three sets of filters: Net CFP: Ex = 440 ± 4 nm and Em = 486 ± 5 nm; CFP-YFP FRET: Ex = 440 ± 4 nm and Em = 535 ± 5 nm; Net YFP: Ex= 486 ± 5 nm and Em = 535 ± 5 nm. Background fluorescence was measured from wells containing culture medium and anticancer reagents. To evaluate the apoptotic effects, a Y/C FRET ratio was calculated using the equation: Y/C ratio = of CFP-YFP FRET intensity / Net CFP intensity. The value of net YFP intensity was used to indicate the cell number.

2.3.3 Determination Cell Viability by MTT Assay

3- (4, 5-dimethylthiazol-2-yl)-2, 5-diphenyltetrazolium bromide (MTT) assay was used to determine cell viability in this study by measuring the activity of the enzyme mitochondrial reductase inside the living cells. MTT powder (Sigma-Aldrich) was dissolved in phosphate buffered saline (PBS) at a concentration of 5 mg ml-1 to form the MTT solution. Cells were seeded and grown in 100 μl medium in 96-well plates. 10 μl of the MTT solution was then added into each well and incubated for 2 to 4 h in the CO_2 incubator to allow the reduction of MTT into purple-coloured formazan. 100

ATTENTION: The Singapore Copyright Act applies to the use of this document. Nanyang Technological University Library

μl of 10% sodium dodecyl sulphate (SDS) solution with 0.01 M hydrochloric acid (HCl) was added into each well to dissolve the purple crystals. After overnight incubation in the CO_2 incubator, the optical density (OD) readings of the samples was measured in a plate reader (Perkin-Elmer Victor3), using the wavelength of light absorbance at 595 nm.

2.3.4 Determination of ROS Levels in Living Cells

Cells were pre-loaded with 10 μM CM-H_2DCFDA (Invitrogen, USA), which can be oxidized by ROS into green fluorescence-emitting dichlorofluorescein (DCF), for 30 min and injected into the bloodstream of the zebrafish or the circulatory microfluidic system. At different time points, the injected cells were imaged using an inverted fluorescence microscope with a set of GFP filters. Each observation field was photographed only once, and the exposure time was restricted to 200 milliseconds per photo to minimize photo-stimulation of the dye. The fluorescence intensity of DCF in each single cell was measured using Image-Pro Plus software. The average intensity of cells from five fish and at least five observation areas in the microfluidic system at each time point was calculated. The antioxidant chemical propyl gallate PG (20 μM in DMSO) was used to pre-treat cells for 1 h before subjecting the cells to circulation.

2.3.5 Quantification of Superoxide Generation by Flow Cytometry

To detect fluid shear stress-induced generation of mitochondrial superoxide, cells were preloaded with the mitochondrial superoxide indicator, mitoSOX (10 μM, Invitrogen, USA). After 0, 20, 40, 60, and 120 min in the circulatory microfluidic system, cells were collected from microfluidic system and the mitoSOX fluorescence was measured

ATTENTION: The Singapore Copyright Act applies to the use of this document. Nanyang Technological University Library

immediately using a flow cytometer (LSRII, BD Biosciences, USA). In addition, cells cultured in a non-adhesive coated dish were used as a negative control.

2.3.6 Determination of Morphology and Membrane Potential of Mitochondria in CTCs

Cells were subjected to shear stress treatment in the circulatory microfluidic system for 0, 3 and 6 h. To test the damaging effects of superoxide on mitochondria, MCF7 cells were pretreated with 100 μM MnTBAP, and MDA-MB-231 cells were pretreated with 20 μM 2-ME for 1 h before being subjected to circulation for 6 h. Cells were then collected and immediately resuspended with fresh culture medium containing 100 μM MitoTracker Red-CMXRos (Life technologies, USA). Cell suspensions in 100 μl of Mitotracker solution were added to each well of the poly-lysine-coated 12-well removable chamber (Ibidi, Germany). After 15 min, culture medium containing Mitotracker was removed and cells were washed twice with fresh medium for 10 min. Cells were then fixed in 4% paraformaldehyde for 15 min and washed once. Afterwards, cells were further stained with 2 μg ml^{-1} Hoechst 33342 for 10 min and washed with PBS three times. The slide was mounted with Mowiol® 4-88 overnight before imaging with a confocal microscope (LSM 710, Carl Zeiss, Inc.).

2.3.7 Western Blot Analysis

Cells were lysed in RIPA buffer with protease and phosphatase inhibitors (Sigma-Aldrich). Protein concentrations were determined by a Bradford Assay Kit (Bio-Rad). Fifty micrograms of total protein were used for SDS-PAGE. The protein blots were probed with primary antibodies against MnSOD at 1:3000 (Abcam, UK), CuZnSOD

ATTENTION: The Singapore Copyright Act applies to the use of this document. Nanyang Technological University Library

at 1:1000 (Cell Signaling, USA), and GAPDH at 1:1000 (Cell Signaling, USA) overnight at 4℃, followed by incubation with a secondary goat anti-rabbit IgG at 1:5000 (BioRad, USA) for 1 h at room temperature. The blots were developed using ECL solutions (Thermo Scientific).

2.3.8 Immunofluorescence Staining

For immunofluorescence staining (IF), cells were cultured in a 12-well removable chamber (Ibidi, Germany). After washing with PBS, cells were fixed with 4% paraformaldehyde for 15 min and permeabilized with 0.2% Triton X-100 for 20 min. Cells were then blocked with 3% BSA in PBS containing 0.3 M glycine for 30 min and incubated with rabbit anti-MnSOD antibody (Abcam, UK) at a 1:100 dilutions in PBST containing 3% BSA overnight at 4℃. The cells were further incubated with TRITC-conjugated secondary antibody (Calbiochem, USA) at a 1:100 dilutions in PBST containing 3% BSA for 1 h at room temperature. Slides were mounted with Mowiol® 4-88 (Calbiochem, USA) and then imaged on a fluorescence microscope (Axio Observer Z1, Carl Zeiss, Inc.) equipped with a CCD camera (AxioCam MRm, Cal Zeiss, Inc.).

2.4 Gene Knockdown and Overexpression

2.4.1 MnSOD Inhibition by RNA Interference and SOD inhibitor

The Validated Silencer Select siRNA against MnSOD (5’ UGUCAGGCCUGAUUA UCUAtt-3’) and Silencer Select Negative Control siRNA were purchased from Ambion (Life Technologies, USA). Before transfection, 1×10^6 cells were seeded into 60-mm dishes. After 24 h, the cells were washed and the media was replaced with

ATTENTION: The Singapore Copyright Act applies to the use of this document. Nanyang Technological University Library

OptiMEM (Life Technologies, USA). Cells were then transfected with 100 nM siRNA using Lipofectamine RNAiMAX (Life Technologies) according to the manufacturer's instructions. After overnight incubation, the transfection complex was replaced with regular complete DMEM without antibiotics. After 48 h, cells were transfected the second time using the same procedure. After an additional 48 h (i.e., 96 h after the first transfection), cells were harvested for further experiments.

To inhibit the activity of MnSOD, a superoxide dismutase inhibitor 2-Methoxyestradiol (2-ME, Sigma-Aldrich) was used to pre-treat the cells for 1 h before introducing them into the circulatory microfluidic system.

2.4.2 Overexpression of MnSOD in MCF7 Cells

The pMnSOD plasmid was purchased from Origene [267]. This plasmid was constructed with a pCMV6-Entry vector, and MnSOD was tagged with Myc-DDK at the C-terminal. The MCF7-C3 cells were transiently transfected with pMnSOD plasmid or an empty vector using lipofectamine 3000 (Life Technologies, USA), according to the manufacture's protocol. Briefly, 1×10^6 cells were seeded into 60-mm dishes. After 24 h, the cells were washed and the media was replaced with serum-free media. Cells were then transfected with 2μg MnSOD or vector plasmid DNA plus 5 μl Lipofectamine 3000 transfection reagent (Life Technologies) according to the manufacturer's instructions. 6 h later, the transfection medium was replaced with fresh medium containing 10% FBS and PS. After transfection for 48 h, the cells were collected for further experiments.

ATTENTION: The Singapore Copyright Act applies to the use of this document. Nanyang Technological University Library

2.5 Zebrafish Tumor Models

2.5.1 Zebrafish Feeding and Breeding

All zebrafish experiments were approved by the IACUC of NTU. Wild type and *Tg (fli1:EGFP)* zebrafish were kindly provided by Prof. Christoph Wolfram Winkler from the National University of Singapore. Zebrafish were maintained according to the standard operational guidelines, as described previously [78, 268]. The male and female zebrafish were kept separately in fish tanks with a temperature of 28.5 ℃. The zebrafish were fed twice every day with live brine shrimp. For zebrafish breeding, two males and one female were removed from the main tanks and placed overnight in each side of the breeding tank. The eggs were then collected under standard mating conditions, staged by hours post fertilization (hpf) and raised in the zebrafish embryo medium (E3 medium). Around 200 eggs that were produced in every breeding tank were collected and transferred to a petri dish containing zebrafish medium. The petri dishes were then placed into the 28.5 ℃ incubator for optimal embryonic development. At 22 hpf, 0.5 ml of PTU stock solution was added to 25 ml of zebrafish medium for inhibiting the formation of pigments on the embryos. Eggs seen as white or cloudy were unfertilized or dead eggs. They were removed to prevent contamination.

2.5.2 Microinjection of Sensor Cells into the Zebrafish Circulation

In preparation of microinjection, glass micropipettes were fabricated with a micropipette puller and were subsequently cut with a scalpel to construct an opening of approximately 30 μm, slightly larger than the size of a suspending cancer cell. Next, cancer cells were collected by trypsinization and centrifuged for 3 minutes at 1500 rpm. The cell pellet was washed twice with PBS and resuspended in 50 μl of PBS at a

ATTENTION: The Singapore Copyright Act applies to the use of this document. Nanyang Technological University Library

concentration of 1 × 10^6 cells per 50 µl, and was placed on ice for microinjection. Consequently, the removal of DMEM and the addition of PBS can reduce the aggregation of the cells during microinjection. Using a 10 µl pipette, the highly concentrated cells were loaded into the glass micropipette, and were subsequently fixed onto the pressure injector apparatus. The pressure injector which is controlled by a foot pedal can be calibrated to control the amount of cells injected into the embryo.

Seventy-two hpf zebrafish larvae were anesthetized with 0.01% tricaine and positioned on a wet agarose microinjection pad. A volume of 10 nl of cell suspension was injected into each fish larvae. At different time points post injection, fish larvae were anesthetized with 0.01% tricaine and placed on a thin layer of agarose within an imaging chamber. The chamber was maintained at 35.5 ℃ using a heating stage.

2.5.3 Monitoring Apoptosis of Sensor Cells in Zebrafish Model

A region of interest containing 20-50 cancer cells in each of the five fish was employed for FRET imaging, which was conducted using a motorized fluorescence microscope (Axio Observer Z1, Carl Zeiss, Inc.) and a 455 nm diachronic mirror at an excitation wavelength of 436 ± 10 nm. The emissions of YFP (535 ± 15 nm) and CFP (480 ± 20 nm) were recorded using a computer-controlled camera (AxioCam MRm, Cal Zeiss, Inc.) and Zen 2012 software (Cal Zeiss, Inc.). The digital fluorescence images were then processed using Image-Pro Plus software (Media Cybernetics, Inc.). The tail region of the fish body was selected as the observation area, which has clear separation of different types of blood vessels.

ATTENTION: The Singapore Copyright Act applies to the use of this document. Nanyang Technological University Library

2.5.4 Visualizing the Extravasation Dynamics of Cancer Cells in Zebrafish

To detect and quantify cell extravasation, a GFP filter set (Ex = 480 ± 20 nm, Em = 535 ± 25 nm) was used to observe the distribution of EGFP-labelled vascular endothelial cells in zebrafish. The process of extravasation was visualized using a previously described method [78]. The extravasation rate was calculated using the number of extravasated cells at each time point divided by the total number of cells found within the intersegmental Vessels (ISV) at the initial time point of 4 h.

2.6 Studying Metastasis of Cancer Cells in Nude Mice Models

2.6.1 Experimental Lung Metastasis Model in Nude Mice

All mouse experiments were approved by the Institutional Animal Care and Use Committee (IACUC) of Nanyang Technological University [269]. A suspension of 5 $\times 10^5$ MCF7-C3 and 231-C3 cells in 200 µl of PBS, were independently injected into the tail veins of the eight-week-old female BALB/c nude mice (purchased from BioLasco Company, Taiwan). The mice were killed at different time points, and various tissues were examined for micrometastases using a MVX10 Fluorescence MacroZoom System (Olympus) with FRET filters (Ex = 436 ± 10 nm; Em_1 = 480 ± 20 nm and Em_2 = 535 ± 15 nm). The number of YFP-positive foci per unit area (cm^2) was counted from both sides of all the lung leaves of three mice. Blood samples were collected from the heart after the mouse was killed and transferred to a tube containing the anticoagulant heparin (Sigma-Aldrich). The presence of fluorescent circulating sensor cells was determined by fluorescence microscopy.

ATTENTION: The Singapore Copyright Act applies to the use of this document. Nanyang Technological University Library

2.6.2 Orthotopic Xenograft Model of Breast Cancer in Nude Mice

Human cancer xenograft models were generated by subcutaneous injection of 1×10^6 cancer cells in 100 μl of Matrigel (BD Biosciences, USA) into the mammary fat pad of the nude mice. For mice injected with MCF7 cells, one estrogen pellet (1.7 mg per pellet, Innovative Research of America, USA) was subcutaneously implanted into each mouse 4 days prior to cell injection.

2.6.3 Isolation of Metastatic Cell Lines from Mice Models

Forty-five days after 231-C3 cell injection, a micrometastasis was formed in the lung tissue of the nude mouse. To establish a more metastatic cell line, this micrometastasis was isolated using a Fluorescence MacroZoom System. The isolated lung tissue was cut into small pieces and digested with Type IV Collagenase (200U ml^{-1}, Sigma-Aldrich). After washing twice with fresh medium, cells were cultured in a dish with complete DMEM medium plus 10% FBS. After selection with G418, the obtained pure cell line was designated as 231-M1 and was used for further studies. 231-M1 cells (5×10^5) were then re-injected into another group of nude mice. Ninety days after cell injection, two lung macrometastases were isolated from two different mice using the above-mentioned method and designated as 231-M1A and 231-M1B, respectively.

2.6.4 Histological Analysis of Animal Tissues

After dissection, the animal tissues were placed into cassettes which were placed into a tissue basket. The tissue basket was then loaded into tissue processor machine (Leica). After fixation with 10% neutral buffered formalin (NBF), tissues were dehydrated in a slow and stepwise pace to prevent distortion of the tissue. The following step

ATTENTION: The Singapore Copyright Act applies to the use of this document. Nanyang Technological University Library

involves clearing with histoclear solution. The duration of the process is illustrated in Table 1-1.

Table 2-1. Steps for tissue fixation, dehydration and clearing

Station	Duration (hr)
Formalin	24
DH2O	1
50% Ethanol	1
70% Ethanol	1
90% Ethanol	1
100% Ethanol	1
100% Ethanol	1
100% Ethanol and Histoclear (v:v) 1:1	4
Histoclear	4
Histoclear	2
Wax	1.5
Wax	1.5

Tissues were then embedded in paraffin wax using a tissue embedding machine and made into Formalin Fixed Paraffin Embedded (FFPE) tissue and stored in the form of wax blocks. H&E staining and immunohistochemistry (IHC) were performed on 5-µm paraffin sections using standard protocols (Leica). Before staining, microscopic slides with tissue sections were first deparaffinised with histoclear and then undergo hydration in coplin jars using the following procedures (Table 2-2).

Table 2-2. Steps for deparaffinisation and rehydration of slides

Station	Duration (min)
Histoclear	2
Histoclear	2
100% Ethanol	2
100% Ethanol	2
100% Ethanol	2
90% Ethanol	2
70% Ethanol	2
50% Ethanol	2

ATTENTION: The Singapore Copyright Act applies to the use of this document. Nanyang Technological University Library

For H&E staining, the slides were stained with haematoxylin and Eosin Y using the following protocols followed by mounting with Canada balsam (Table 2-3).

Table 2-3. Steps for H&E staining

Station	Duration (min)
DH2O	1
Haematoxylin	1
Water	2
DH2O	1
Differentiation solution	$\frac{1}{6}$ (or 10s)
Water	5-10
DH2O	1
95% Ethanol	1
Eosin	½
90% Ethanol	¼
100% Ethanol	1
100% Ethanol	2
100% Ethanol	2
Histoclear	2
Histoclear	2

2.6.5 Immunohistochemistry (IHC) Analysis

For the IHC staining on FFPE slides, antigens were retrieved using heated citrate buffer (100 ℃ for 5 min). For the orthotopic xenograft tumors, 5-μm cryosections were directly fixed with 4% paraformaldehyde for 30 min. Slides were then stained using the Rabbit Specific HRP/DAB Detection IHC Kit according to the manufacturer's instructions (Abcam). Before staining, the slides were penetrated with 0.25% of Triton X-100 in PBST solution, blocked with hydrogen peroxide to reduced endogenous peroxidase activity, and blocked with 3% BSA to suppress the unspecific binding with antibodies. The primary rabbit anti-MnSOD and anti-Vimentin antibody (Abcam) used in the IHC experiment was diluted 1:100 in PBST containing 3% BSA and incubated with sections overnight at 4 ℃. After visualisation the target protein with DAB, the slides were counterstained with haematoylin for visualisation of nuclear and

ATTENTION: The Singapore Copyright Act applies to the use of this document. Nanyang Technological University Library

mounted with Canada balsam. The steps are listed below in Table 2-4. The imaging of histological slides was conducted under an Observer.Z1 microscope (Carl Zeiss) and photographed with a CCD color camera (Carl Zeiss).

Table 2-4. Counterstaining with haematoxylin

Station	Duration (min)
Haematoxylin	¼ to 1/3
Running water	1
DI water	1
Differentiating solution	1/60
Running water	4
DI water	1

2.7 Study Apoptosis and Survival of CTCs in a Circulatory Microfluidic System

2.7.1 Establishing a Microfluidic System

To specifically study fluid shear stress-induced apoptosis and ROS generation, a circulatory microfluidic system was assembled (Figure 3-20). In this system, a peristaltic pump (Ismatec, Germany) was used to generate a circulatory pulsatile flow in a microchannel of silicone tubing (Ismatec, Germany) with a diameter of 500 μm and a total length of 1.5 m. The observation chip was constructed by mounting a polydimethylsiloxane (PDMS)-based microfluidic channel to a cover slip. As the tubing length is 1.5 m, which is much longer than the length of PDMS channel (20 mm), the shear stress in the system was calculated based on the parameters of the silicone tubing. Shear stress in the tubing was calculated using Poiseuille's equation [42], $\tau = 4Q\eta/\pi R^3$, where τ is shear stress in dyn cm^{-2}, Q is the flow rate in $cm^3\ s^{-1}$, η is the dynamic viscosity of the fluid (the culture medium can be treated as water at 37°C; $\eta = 0.01$ dyn*s cm^{-2}), and R is the radius of the silicone tubing (250 μm). The flow rate can be increased to achieve higher shear stress. In this experiment, the shear stress was adjusted from 5 to 30 dyn cm^{-2}. To prevent cell attachment to the tubing and

ATTENTION: The Singapore Copyright Act applies to the use of this document. Nanyang Technological University Library

PDMS chip, the whole system was pre-coated with 0.5% Pluronic-f127 (Invitrogen, USA) for 1 h at room temperature before the experiments. Pluronic f127-coated 96-well plates were also used as a negative control for the absence of shear stress.

2.7.2 Detection of Apoptosis of CTCs in the Circulatory Microfluidic System

To detect apoptosis under various fluid shear stresses, MCF7-C3 and 231-C3 cells were collected by 0.05% trypsin containing 0.53 mM EDTA (Gibco, USA), washed twice with PBS and re-suspended in fresh culture media at a cell density of 2×10^5 ml^{-1}. One millilitre of cell suspension was added to the circulatory microfluidic system and was subjected to circulation for varying times at 37℃ in a humidified CO_2 incubator. During observation, the pump was closed to stop the medium flow, and the movement of the sensor cells was retained within the observation chip by closing the two control valves. The rate of apoptosis was determined by FRET imaging using a fluorescence microscope. Cell viabilities before and after circulation were determined using the MTT assay. Briefly, 100 µl of cell suspension was added to each well of a 96-well plate followed by the addition of 10 µl 3-(4,5-dimethylthiazol-2-yl)-2,5-diphenyltetrazolium bromide (MTT, Sigma-Aldrich) solution (5 mg ml^{-1}). Three hours later, the formazan was solubilized overnight by the addition of 100 µl of a 10% SDS solution containing 0.01 M HCl. The optical density was determined by a plate reader at 595 nm.

ATTENTION: The Singapore Copyright Act applies to the use of this document. Nanyang Technological University Library

2.8 Proteomics Analysis

2.8.1 Preparation of Protein Sample for Isobaric Tags for Relative and Absolute Quantification (iTRAQ)-based Proteomics Analysis

Breast cancer cell lines derived from lung metastases in nude mice model as well as their parental cell line were cultured *in vitro* until to a confluence of 80%. Two dishes (10 cm) of MDA-MB-231, 231-C3, 231-M1 and 231-M2 cells were harvested by cell scratcher on ice. Cells were then centrifuged and washed twice with pre-cold PBS. Cell pellets were then lysed with RIPA buffer containing protease and phosphatase inhibitors (Sigma-Aldrich). Protein concentrations were determined by a Bradford Assay Kit (Bio-Rad).

2.8.2 Peptide Digestion

Two hundred micrograms of total protein were loaded to a 12.5% SDS-PAGE gel and subjected to electrophoresis for 15 min at 80 V. Each sample lane was cut into small pieces and washed with 25 mM triethylammonium bicarbonate (TEAB) in 75% ACN. The gel pieces were then dehydrated with 100% ACN and vacuum dried. Reduction was performed using 5 mM Tris 2-carboxyethyl phosphine hydrochloride in 25 mM TEAB buffer at 60 ℃ for 30 min. Reduced samples were then alkylated with 10 mM methyl methanethiosulfonate in 25 mM TEAB buffer at room temperature for 45 min. The gel pieces were then alternately washed in 25 mM TEAB buffer and 25 mM TEAB/75% ACN to remove excess Tris 2-carboxyethyl phosphine hydrochloride and methyl methanethiosulfonate. After another round of dehydration and vacuum drying, the protein samples were conducted an in-gel digestion at 37 ℃ for overnight in 25

ATTENTION: The Singapore Copyright Act applies to the use of this document. Nanyang Technological University Library

mM TEAB buffer containing 10 ng/ml sequencing-grade modified trypsin (Promega Corporation, USA).

2.8.3 Labelling of Peptides with iTRAQ Reagents

Tryptic peptides derived from the 231, 231-C3, 231-M1 and 231-M2 were labeled with iTRAQ isobars 114, 115, 116, and 117 respectively. The iTRAQ labeled peptides were then combined into a fresh tube as a peptide pool. The mixed peptides were then desalted using Sep-Pak Vac C18 cartridges (Waters, Milford, MA), and dried by vacuum centrifugation. The iTRAQ-labeled peptides were then dissolved in 100 µl of sample loading buffer containing 10 mM ammonium acetate in 85% ACN and 1% formic acid. Dissolved peptides were then fractionated using electrostatic repulsion–hydrophilic interaction chromatography. After fractionation, the collected fractions were combined to 28 fractions according to their chromatograms and dried by vacuum centrifugation.

2.8.4 LC-MS/MS Analysis

The peptides were further reconstituted in 0.1% formic acid for LC-MS/MS analysis using a Q-STAR Elite mass spectrometer coupled with an online nano-flow Eksigent HPLC system (Applied Biosystems, MDS-Sciex, Foster City, CA). The LC-MS/MS analysis was performed for three times by injecting the samples in triplicate. The obtained mass spectrometric data was processed with Analyst QS 2.0 software (Applied iosystems/MDS-Sciex) and the protein identification and quantification were conducted with a Protein Pilot 3 Software (Applied Biosystems).

ATTENTION: The Singapore Copyright Act applies to the use of this document. Nanyang Technological University Library

2.8.5 2D-DIGE-based Comparative Proteomics Analysis

Proteomics of three generation of metastatic breast cancer cell lines 231-C3, 231-M1 and 231-M1A were compared to identify the driver proteins that promote malignant proliferation and drug resistance. Two dishes (10 cm) of 231-C3, 231-M1 and 231-M1A cells with 80% confluence were harvested by cell scratcher on ice. Cells were washed twice with pre-cold PBS and centrifuged to remove all liquid. Cell pellets were kept at -80 ℃ for proteomics analysis. Two-dimensional differential in-gel electrophoresis (2D-DIGE) was performed by Applied Biomics (Hayward, CA, USA) to identify the most significantly changed proteins during metastasis. In this study, cell lysate of 231-C3 cells was labelled with Cy2 (Ex492/Em510), 231-M1 cell lysate was labelled with Cy3 (Ex 550/Em570) and 231-M1A cell lysate was labelled with Cy5 (Ex650/Em670). The fluorescence ratio of 124 changed spots were measured. From these 124 spots, I selected 56 spots to do the further LC-MS/MS identification. The spots selection is based on the ratio of Cy5/Cy2 and Cy3/Cy2 are both higher than 1.5 or lower than 1.5 fold.

2.8.6 Bioinformatics Analysis

Gene IDs of the proteins of interest were searched in a batch using PANTHER classification system against NCBI (*Homo sapiens*) dataset. Proteins of interest were classified based on molecular function, biological process and protein classification. The potential interaction networks of proteins of interest was analysed with an Ingenuity pathway analysis [128] system (Qiagen, USA).

ATTENTION: The Singapore Copyright Act applies to the use of this document. Nanyang Technological University Library

2.9 Statistical Analysis

All data are represented as the mean ± SD from three independent experiments. Statistical significance was analysed using a one-tailed Student's *t* test and $*p<0.05$ was considered to be significant.

ATTENTION: The Singapore Copyright Act applies to the use of this document. Nanyang Technological University Library

CHAPTER 3 Generation of Apoptosis Sensor Cell Lines and Development of Novel Experimental Models for Metastasis Study and Anti-Metastatic Drug Discovery

3.1 Introduction

Metastasis is the leading cause of cancer-related death. Most cancers are potentially curable as long as the cancer cells remains localized. Thus the main emphasis of the cancer research and the anti-cancer drug discovery should be focused on metastasis. However, cancer metastasis is a complicated process involving not only dynamic cell behavior of the cancer cells, but also the interactions between the cancer cells and the microenvironment [74]. Diverse molecular, cellular, and environmental events must work together to form secondary tumors [270]. Therefore, appropriate experimental models are critical to the understanding of the metastatic process and the development of new diagnosis and therapeutic strategies.

Various *in vitro* and *in vivo* experiment assays and models were developed for the study of cancer metastasis [271, 272]. Based on these models, a vast amount of knowledge has been acquired. However, in most cases, cell viability could not be simultaneously investigated with the metastatic events. Considering that metastasis is an inefficient process, the evaluation of cancer cell viability in each step is crucial to the understanding of the limiting factors of metastasis.

Here, I employed a FRET-based caspase sensor to monitor the apoptosis of cancer cells during cancer development, metastasis, or under treatment. This FRET sensor was previously invented by our group and has been applied to detect the apoptosis of single cells or a group of cells *in vitro*. In this study, FRET caspase sensor was

ATTENTION: The Singapore Copyright Act applies to the use of this document. Nanyang Technological University Library

introduced into breast cancer cells as well as other cancer cells to generate stable sensor cell lines. Sensor cells were then injected into zebrafish or nude mice to generate xenograft tumors. In another *in vitro* model, I developed a circulatory system to mimic the blood circulation. FRET sensor cells were introduced into the system and the effects of fluid shear force on the viabilities of CTCs were evaluated by measuring the apoptotic and survival rates.

ATTENTION: The Singapore Copyright Act applies to the use of this document. Nanyang Technological University Library

3.2 Results

3.2.1 Generation of Sensor Cell Lines for *in situ* Apoptosis Detection

In this study, series of sensor cell lines were generated by transfecting plasmid of sensor C3 into multiple cancer or normal cell lines. Together with HeLa-C3 and HUVEC-C3 previously generated by our laboratory, we established a sensor cell bank for further mechanism study and drug discovery (Table 3-1). These new stable cell lines were generated from 3 human breast cancer cell lines MDA-MB-231, MCF7 (Figure 3-1), and BT474. Other cell lines include a human lung cancer cell line A549, a human hepatocellular carcinoma cell line HepG2, a mouse melanoma cell line B16-F10, a human melanoma cell line MDA-MB-435, a normal liver cell line L02, and a fibroblast cell line NIH/3T3. We have validated that all these sensor cell lines can be applied to detect apoptosis *in situ* during drug treatment, tumor growth and cancer cell metastasis.

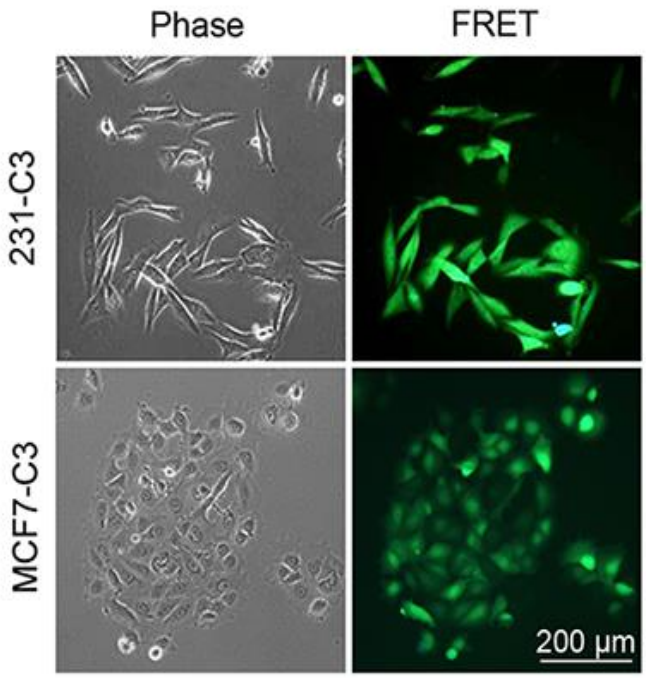

Figure 3-1. Morphologies of two sensor cell lines MCF7-C3 and 231-C3.

ATTENTION: The Singapore Copyright Act applies to the use of this document. Nanyang Technological University Library

Table 3-1. List of C3 sensor cells generated in Prof. Kathy Luo's lab

Category	Cell line	Origin	G418 (μg/ml)	Generated by
Cancer cells (10)	HeLa-C3	Human cervical carcinoma	-	Prof. Kathy Luo [154]
	MDA-MB-231-C3 (231-C3)	Human breast adenocarcinoma	600	This thesis
	MCF-7-C3	Human breast adenocarcinoma	400	This thesis
	BT-474-C3	Human breast ductal carcinoma	400	This thesis
	HepG2-C3	Human hepatocellular carcinoma	500	This thesis
	A549-C3	Human lung carcinoma	300	This thesis
	HCT-15-C3	Human colorectal adenocarcinoma	-	Xichen Zhang
	K562-C3	Human chronic myeloid leukemia	-	Xiaofeng Liu
	B16-F10-C3	Mouse melanoma	700	This thesis
	MDA-MB-435-C3	Human melanoma	500	This thesis
Endotheliu m	HUVEC-C3	Human umbilical vein endothelium	-	Dr. Xiaoming
Normal cells	L02-C3	Human embryo liver cell line	300	This thesis
	3T3-C3	Mouse embryo fibroblast cell line	400	This thesis

3.2.2 Search for Anti-Proliferation Compounds by YFP Intensity

The HeLa-C3 cells were employed for the screening of herbal compounds with pro-apoptotic effects. Besides apoptotic effects, anti-proliferation is also an important aspect of anticancer strategies. Several inhibitors have shown effective anti-proliferation effects by inhibiting kinase activities. For example, the tyrosine kinase inhibitors such as Imatinib (Gleevec), Gefitinib (Iressa), Erlotinib (Tarceva) and Sorafenib (BAY 43-9006) are widely used to inhibit the tumor cell proliferation and

ATTENTION: The Singapore Copyright Act applies to the use of this document. Nanyang Technological University Library

tumor angiogenesis [273, 274]. The traditional functional assays cannot be used to measure the pro-apoptotic effect and anti-proliferative effects simultaneously in the same population of cancer cells. This may cause the omission or misread of the mechanisms of potential anticancer compounds. Therefore, I explored the potential dual application of the sensor C3 in identifying both pro-apoptotic and anti-proliferative mechanisms of anti-cancer compounds.

Here I used endothelial cell line HUVEC-C3 as a model to establish the method (Figure 3-2), which can be further applied in all cancer sensor cell lines generated above. The fluorescence intensity of net YFP (Ex 480 nm/Em535 nm) displayed a linear correlation with the cell viability measured with a standard MTT assay when different number of HUVEC-C3 cells were seeded in 96-well plate (Figure 3-2A). I then define a GI (growth inhibition) index for evaluating the proliferation inhibition rate of a compound at a particular time point T1 (Figure 3-2B). The GI are calculated using an equation: $GI=G_1/G_0 \times 100\%$, where G_1 is the YFP intensity difference between control and treated group, G_0 refer to the YFP intensity of control group. Both G_0 and G_1 are values excluded background fluorescence. In this method, the same population of living cells can be detected for multiple time points. Therefore, T1 can be any time from 0 to many days. During the whole treatment course, cells were measured every 24 h for up to 72 h.

ATTENTION: The Singapore Copyright Act applies to the use of this document. Nanyang Technological University Library

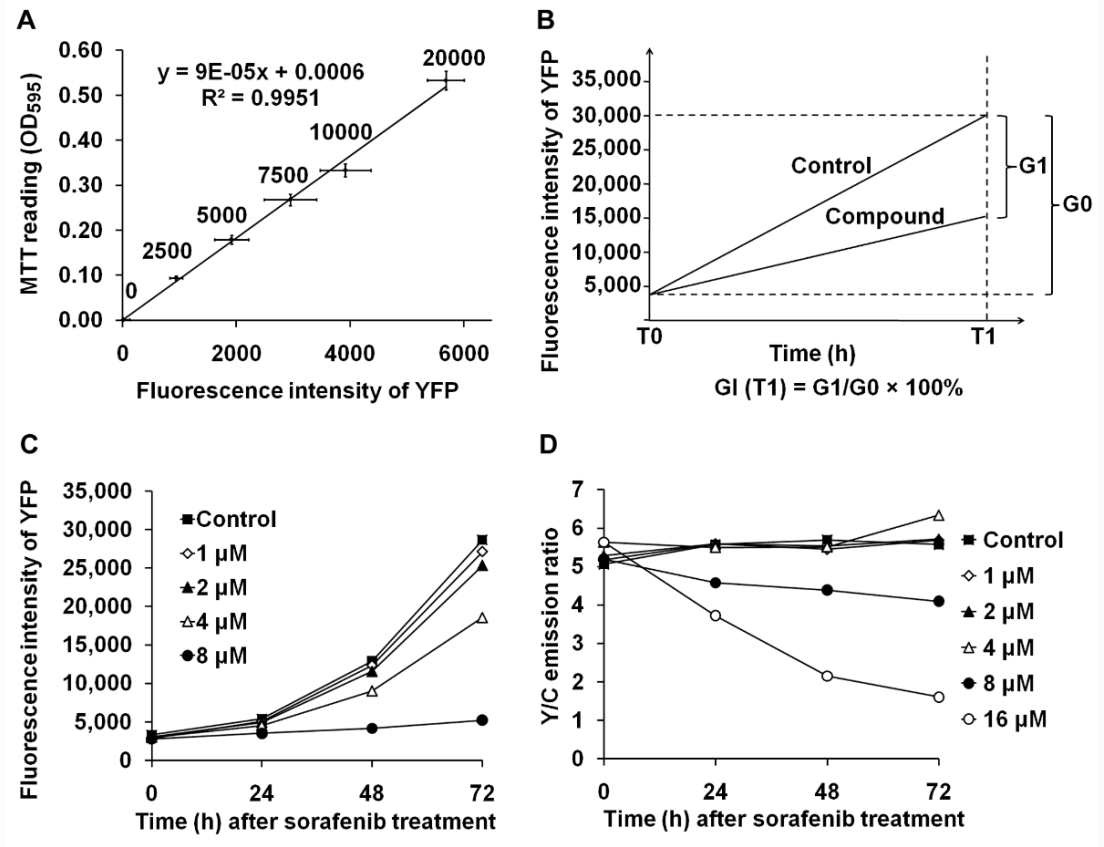

Figure 3-2. Use the increasing net YFP intensity of FRET sensor as an indicator of cell proliferation. (A) Correlation of net YFP intensity with cell viability measured by MTT assay. (B) Calculation of growth inhibition index (GI) of a compound from the net YFP intensity. (C) Measurement of the anti-proliferation effects of sorafenib on HUVEC-C3 cells d by net YFP intensity. (D) Measure the apoptotic effects of sorafenib on HUVEC-C3 cells d by FRET ratio.

I then validated this proliferation measurement method using an antiangiogenic drug sorafenib, which can reduce proliferation of endothelial cells by inhibiting Raf and VEGFR2 in endothelial cells. Sorafenib at concentration above 4 μM inhibited the proliferation of HUVEC-C3 cells (Figure 3-2C). At 72 h, the GI for 4 μM sorafenib was calculated to be 40% and the GI for 8 μM was calculated to be 97%. This decrease of cell viability was not caused by apoptotic effects, because sorafenib at concentrations below 8 μM displayed little apoptosis-inducing effect as illustrated by

ATTENTION: The Singapore Copyright Act applies to the use of this document. Nanyang Technological University Library

the Y/C ratio curves. Only when the concentration of sorafenib was at 16 μM, obvious apoptotic effects was detected in HUVEC-C3 cells (Figure 3-2D).

By combining the measurements of Y/C ratio and net YFP intensity, I established an integrative anti-cancer drug screening platform. The mechanism of a particular compound can be clarified as different categories within a single 96-well plate, including toxicity compounds, proliferation inhibition compounds, vascular disrupting agents (VDA) and angiogenesis inhibiting agents (AIA) or compounds with multiple effects. Meanwhile, potential side effects can be indicated in an early screening stage by measuring Y/C ratio and net YFP intensity in L02-C3 and 3T3-C3 cells (Table 3-2).

Table 3-2. A drug screening platform to determine various drug mechanisms

FRET sensor stable cell line	Cell properties	FRET effect (Y/C ratio change) Apoptosis	Net YFP (Intensity change) Proliferation
Cancer cell line with C3 sensor	Cancer cells	Induce apoptosis of cancer cells	Inhibit proliferation of cancer cells
HUVEC-C3	Blood vessel endothelial cells	Vascular disrupting agents (VDA)	Angiogenesis inhibiting agents (AIA)
L02-C3 /3T3-C3	Normal liver cells	Toxicity to normal tissue	Inhibit normal cells proliferation

3.2.3 Development of a CTCs models in Zebrafish

Discovery of the agents that can prevent the progression of metastatic tumors or inhibit the proliferation of secondary tumors is a big challenge. The current *in vitro* methods for studying metastasis normally focus on cell migration and invasion. However, cell motility is only a small part of the superpower of metastatic cancer cells. Strategies inhibiting migration and invasion may not be effective enough in the real *in vivo*

ATTENTION: The Singapore Copyright Act applies to the use of this document. Nanyang Technological University Library

condition. The current *in vivo* metastasis models in mouse are always time consuming and inefficient in the search for anti-metastatic drugs. Therefore, in this study, I developed a new tumor model by injecting sensor cancer cells into a transparent vertebrate animal, larval zebrafish (Figure 3-3).

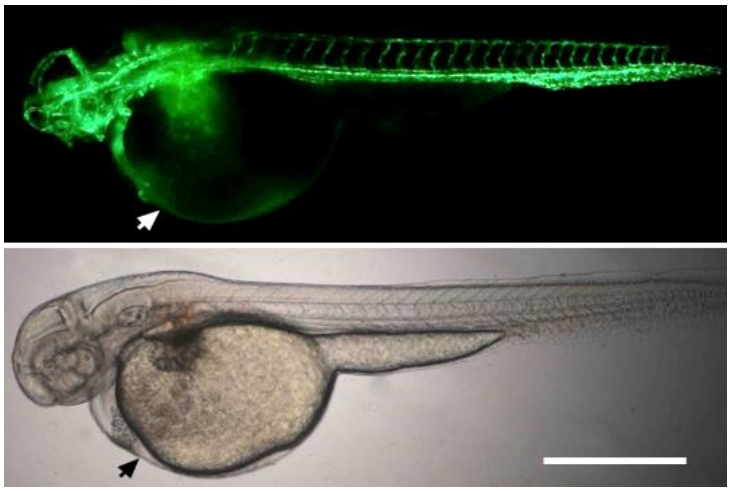

Figure 3-3. Side view of transparent body of a *fli1:EGFP* transgenic zebrafish. Scale bar, 1 mm. Arrows indicate the site for microinjection to achieve CTCs.

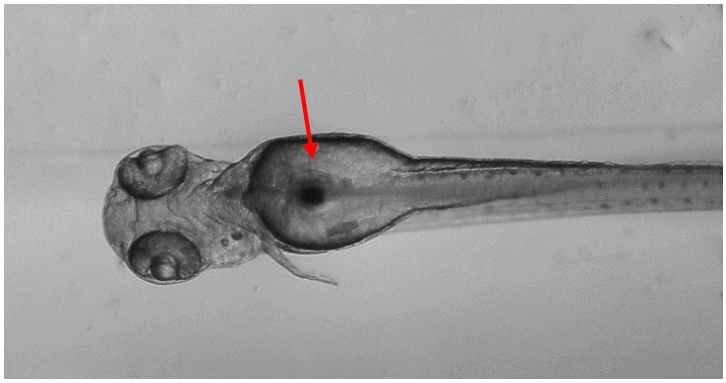

Figure 3-4. Tumor inoculation site in zebrafish body (bottom view). Red arrow indicates microinjection site to generate xenograft tumors.

ATTENTION: The Singapore Copyright Act applies to the use of this document. Nanyang Technological University Library

Two metastasis models were established in this study by using different inoculation methods. One inoculation method is to inject sensor cells directly into the blood circulation at the site behind the heart of zebrafish (indicated by arrows in Figure 3-3). Using this method, sensor cells were injected into the bloodstream and became CTCs in zebrafish circulation (shown by green fluorescence in Figure 3-3). The other method is to inject sensor cells subcutaneously into the abdomen (yolk sac at early stage) to form a solid tumor (Figure 3-4). Two types of zebrafish were used. One is wide type zebrafish without any fluorescence in the whole body (Figure 3-4). The other type is a transgenic line *fli1:EGFP* which express EGFP in their blood vessels (Figure 3-3).

I first evaluated the potential utilization of the C3 sensor in zebrafish model. HeLa-C3 and HepG2-RFP cells were mixed and injected together into the blood circulation of a wild type zebrafish. From 2 to 72 hours post injection (hpi), HeLa-C3 cells were observed to undergo apoptosis by FRET imaging (blue cells in Figure 3-5). By contrast, although the cell number can be quantified with the traditional single color GFP method (shown by RFP channel), it is hard to correlate the decreased cell number with cell viability and apoptosis. Therefore, the sensor C3 is very effective in detecting apoptosis *in vivo* and can be applied to the future studies of cancer metastasis and cancer therapy.

In the first zebrafish model, sensor cells were directly introduced into the blood circulation. These cells were circulated in the bloodstream and distributed in the whole body. Apoptosis of sensor cells were monitored by FRET imaging (Figure 3-6). Therefore, the survival ability of different sensor cells could be compared. At the same time, a transgenic zebrafish *fli1:EGFP* was used to display the structure of blood

ATTENTION: The Singapore Copyright Act applies to the use of this document. Nanyang Technological University Library

vessels and visualize the extravasation dynamics of cancer cells (Figure 3-7). The invasiveness of each single cell thus can be determined in a zebrafish body.

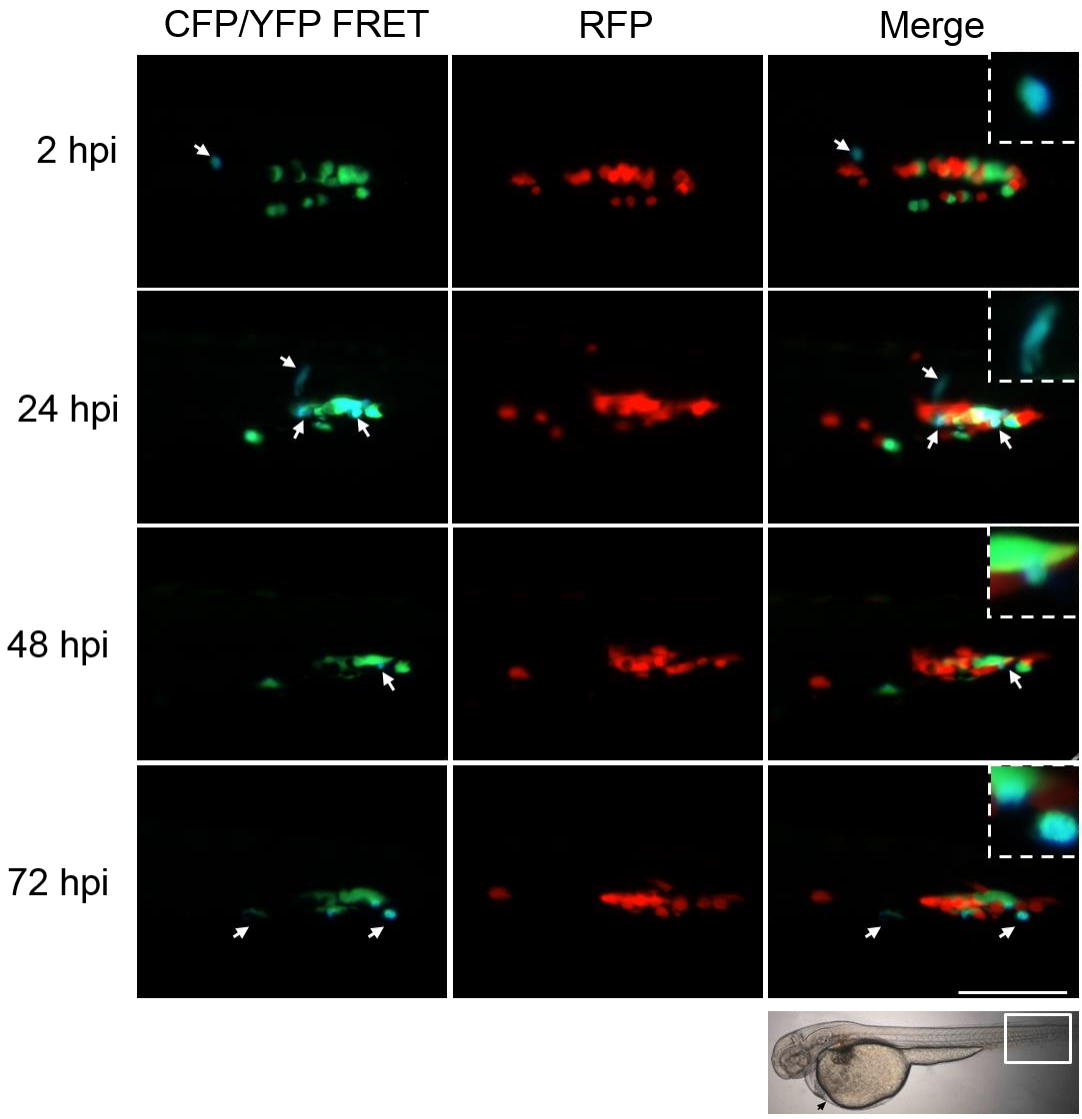

Figure 3-5. Co-injection of HeLa-C3 cells and HepG2-RFP cells into the blood stream of wild type zebrafish. The same zebrafish was observed at different time points (2, 24,48,72 h) after cell injection. Apoptosis of HeLa-C3 cells were revealed by CFP/YFP FRET imaging. Enlarged blue cells in the merged picture indicate the apoptotic HeLa-C3 cells. Observation window of zebrafish is indicated below by a white box. Scale bar, 100 μm.

ATTENTION: The Singapore Copyright Act applies to the use of this document. Nanyang Technological University Library

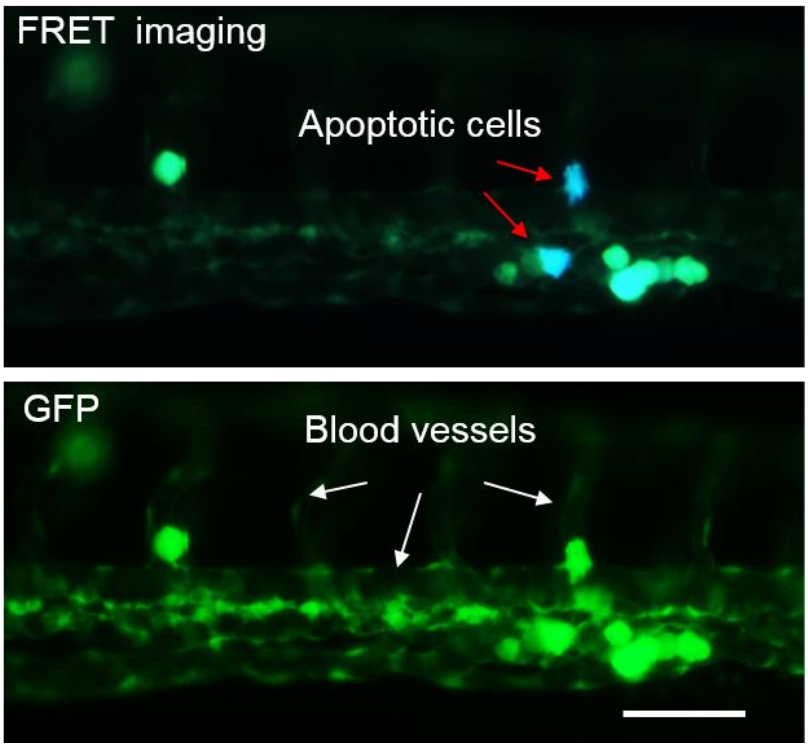

Figure 3-6. Detecting apoptosis of cancer cells in zebrafish circulation by FRET imaging. MCF7-C3 cells were microinjected into zebrafish circulation. Apoptosis of sensor cells were observed after 24 h. Scale bar, 100 μm.

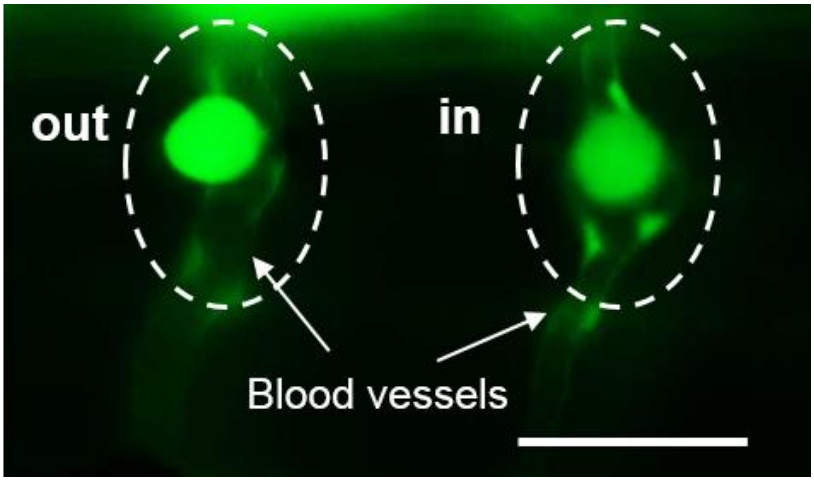

Figure 3-7. Extravasation of cancer cells from blood vessels of zebrafish. Two 231-C3 cells were observed in the ISV area of fli1:EGFP zebrafish. One cell (left) exited the ISV by penetrating the endothelial thin layer. The other cell (right) was still within the ISV. Bright area of zebrafish blood vessel is the nucleus of endothelial cells. Scale bar, 50 μm.

ATTENTION: The Singapore Copyright Act applies to the use of this document. Nanyang Technological University Library

The CTCs model in zebrafish was further applied to search for potential anti-metastatic drugs. Three kinase inhibitors displayed promising effects in reducing the survival and inhibiting extravasation of cancer cells in zebrafish model. They are inhibitors against phosphatidylinositide 3-kinase (PI3K) (LY294002), focal adhesion kinase (FAK) (Y15) and Rho-associated protein kinase [179] (Y27632). 231-C3 cells were pre-treated with 20 μM PI3K inhibitor (LY294002), 10 μM FAK inhibitor (Y15), and 10 μM ROCK inhibitor (Y27632) for 1 h, respectively, before being injected into zebrafish. Pre-treatment with all three inhibitors did not produce any apoptotic effect on 231-C3 cells at both 4 and 24 h *in vitro* (Figure 3-8). However, in zebrafish circulation, PI3K inhibitor significantly increased the apoptotic rate from 6.1 ± 1.0% to 15.3 ± 2.0% at 24 h (Figure 3-9A). Interestingly, pre-treating cells with inhibitors of FAK and ROCK also significantly enhanced apoptosis of CTCs in zebrafish. The ROCK inhibitor produced the highest level of apoptosis (20.7 ± 2.4%) among the three inhibitors at 24 h (Figure 3-9A).

The pre-treatment of 231-C3 cells with the PI3K, FAK, and ROCK inhibitors also significantly reduced their rates of extravasation from 33.4 ± 6.3% to 15.9 ± 4.3%, 12.9 ± 10.4% and 16.0 ± 4.1%, respectively, after injection into zebrafish for 24 h (Figure 3-9B). The underlying mechanisms may be because these three signaling pathways regulated cell survival, cell adhesion and cytoskeleton reorganization respectively.

ATTENTION: The Singapore Copyright Act applies to the use of this document. Nanyang Technological University Library

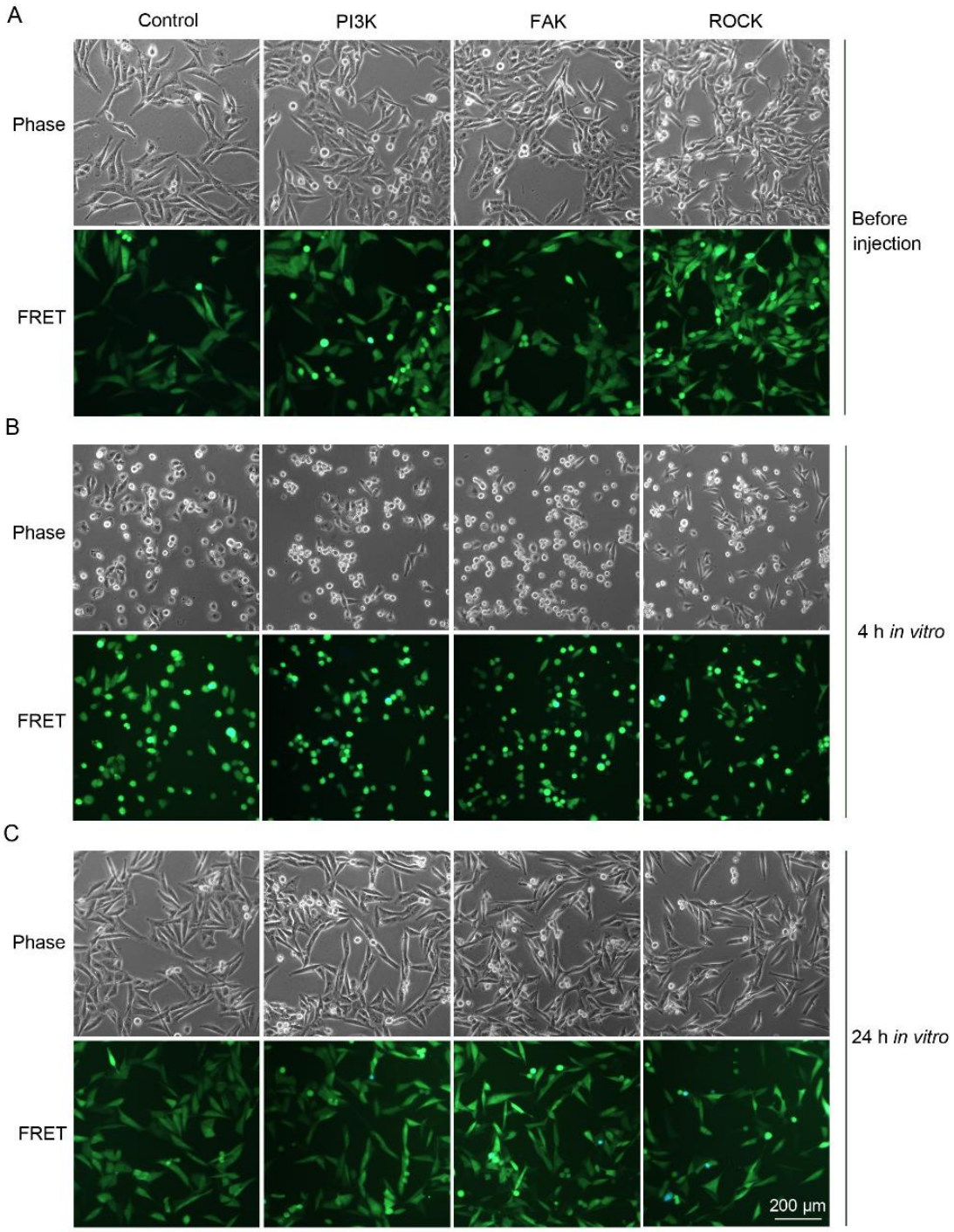

Figure 3-8. Three inhibitors did not induce apoptosis of 231-C3 cells *in vitro*. (A) 231-C3 cells were pre-treated the PI3K inhibitor (LY294002, 20 μM), FAK inhibitor (Y15, 10 μM), or ROCK inhibitor (Y27632, 10 μM) for 1 h. (B) Trypsinized 231-C3 cells were seeded in a 6-well plate for 4 h. (C) 24 h after 231-C3 cells were seeded in a 6-well plate.

ATTENTION: The Singapore Copyright Act applies to the use of this document. Nanyang Technological University Library

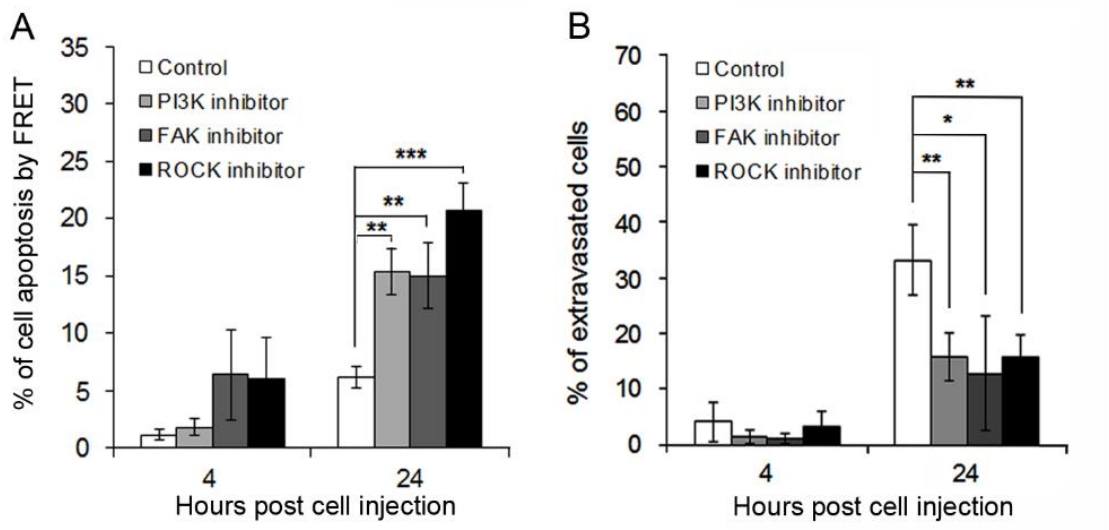

Figure 3-9. Malignant phenotype of 231-C3 cells can be reversed by blocking three important signaling pathways in zebrafish. 231-C3 cells were pre-treated with the PI3K inhibitor (LY294002, 20 μM), FAK inhibitor (Y15, 10 μM), or ROCK inhibitor (Y27632, 10 μM) for 1 h before injection into the circulatory system of zebrafish. The rates of apoptosis (A) and extravasation (B) in zebrafish were determined at 4 and 24 hpi. At least five fish containing 10-20 sensor cells were examined for each experimental condition. The results represent the mean ± SD from three independent experiments. *p< 0.05, **p< 0.01, ***p< 0.001 by Student t test.

3.2.4 Development of a Xenograft Tumor Model in Zebrafish

To generate a xenograft tumor in zebrafish, many cancer cell lines with sensor C3 were injected subcutaneously into the abdomen of zebrafish larvae, including breast cancer cell line 231-C3 and MCF7-C3, cervical cancer cell line HeLa-C3, lung cancer cell line A549-C3 and metastatic melanoma cell line B16-F10-C3. All of these cells can form solid tumor after 24 h. But only solid tumors formed by B16-F10-C3 cells were able to proliferate in the zebrafish body whereas tumors formed by other sensor cells shrunk after 3-5 days. This is not surprising because B16-F10 is a highly metastatic cell line which has been selected in mouse circulation for multiple times [275]. An essential capacity of metastatic cancer cells is that they can adapt to the new

ATTENTION: The Singapore Copyright Act applies to the use of this document. Nanyang Technological University Library

microenvironment and initiate proliferation in it. Therefore, a B16-F10-C3 tumor grown in an alien zebrafish body can function as an ideal drug screening model to identify potential drugs that can inhibit the growth of secondary tumor. To generate the tumor, a suspension of 20 to 40 B16-F10-C3 cells was injected into 48 hpf zebrafish embryos. The injected cells formed a growing mass 24 hpi and subsequently increased in size over the next several days (Figure 3-10). Most of the B16-F10-C3 tumor bearing fish died after 6-8 days because of exhausting of nutrition.

The malignant proliferation of B16-F10-C3 tumors was associated with their ability to stimulate angiogenesis in a fish body. When I injected wild-type B16-F10 cells into *fli1:EGFP* zebrafish whose blood vessels displayed green fluorescence, the solid tumor recruited endothelial cells carrying green fluorescence and stimulated the sprouting and network-formation of these endothelial cells after 3 days (Figure 3-11). With the blood supply from zebrafish, the tumor mass could gain enough nutrition for their growth. Moreover, the CTCs that fell off from the primary tumor mass were able to extravasate and proliferate in zebrafish tissue (Figure 3-12) and even developed secondary tumors in the tail of zebrafish (Figure 3-13). These results further proved that the B16-F10-C3 xenograft tumors in zebrafish have a real tumor mass instead of an aggregate of cell pellets.

ATTENTION: The Singapore Copyright Act applies to the use of this document. Nanyang Technological University Library

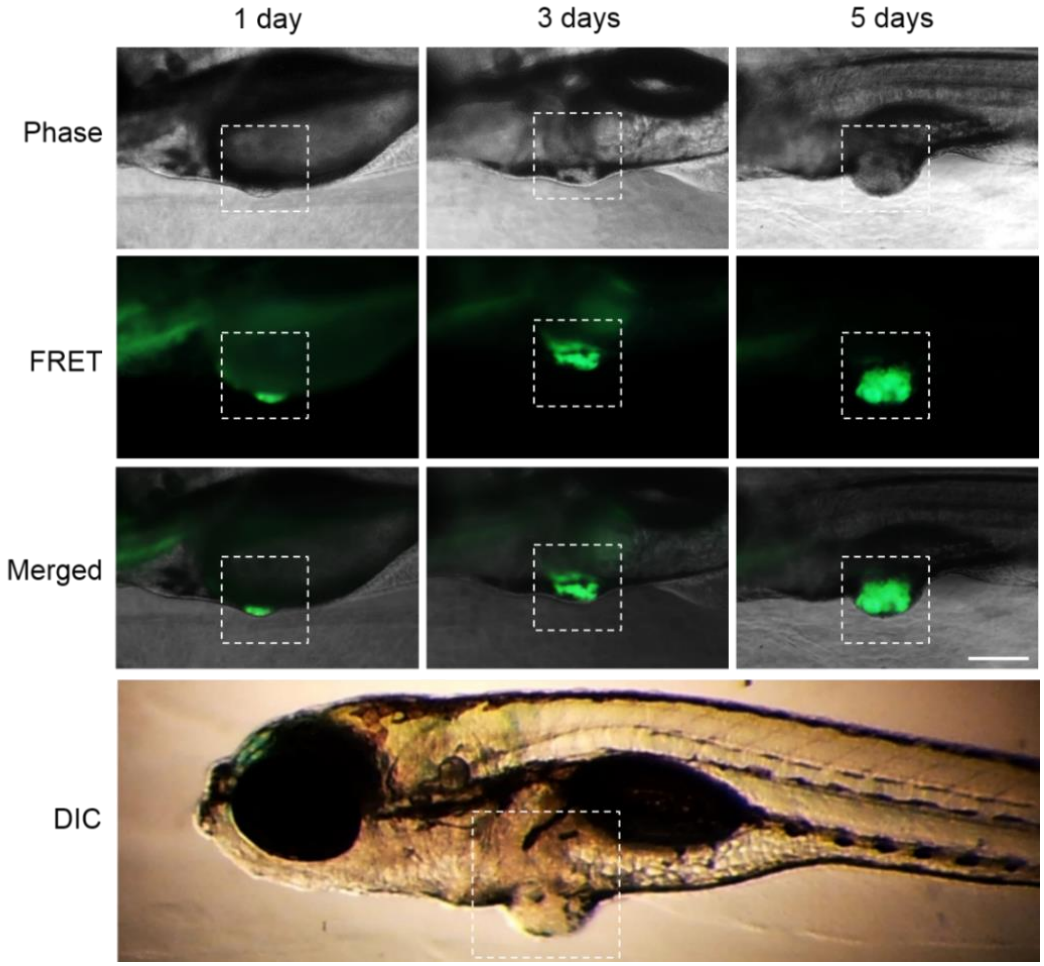

Figure 3-10. Growth of a B16-F10-C3 tumor in a zebrafish body. B16-F10-C3 cells were injected into 48 hpf zebrafish embryos. The growth of a B16-F10-C3 xenograft tumor was checked by FRET imaging at 1, 3, and 5 days post injection (dpi). The position and size of the tumor were imaged under differential interference contrast (DIC) microscopy 5 days after injection. Scale bar, 200 μm.

ATTENTION: The Singapore Copyright Act applies to the use of this document. Nanyang Technological University Library

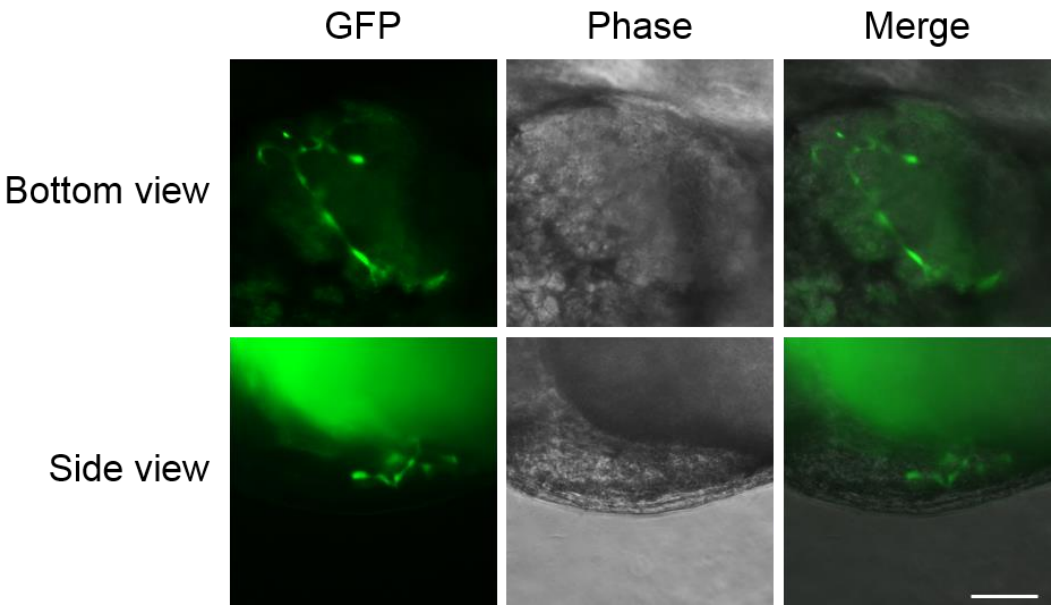

Figure 3-11. Angiogenesis in a B16-F10 xenograft tumor. After 3 days, wild type B16-F10 cells formed a solid tumor. Sprouting of blood vessel endothelial cells into the xenograft tumor was imaged in a GFP channel. *Fli1:EGFP* transgenic zebrafish was used in this experiments to display endothelial cells (with green fluorescence). Scale bar, 100 μm.

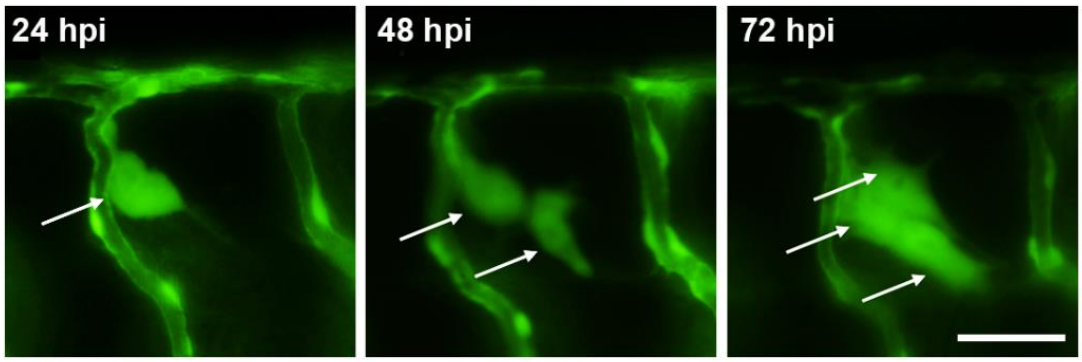

Figure 3-12 Extravasation and proliferation of B16-F10-C3 cells in a zebrafish body. A B16-F10-C3 cell (indicated by white arrows) was found underwent proliferation after extravasation in zebrafish tissue. Scale bar, 50 μm.

ATTENTION: The Singapore Copyright Act applies to the use of this document. Nanyang Technological University Library

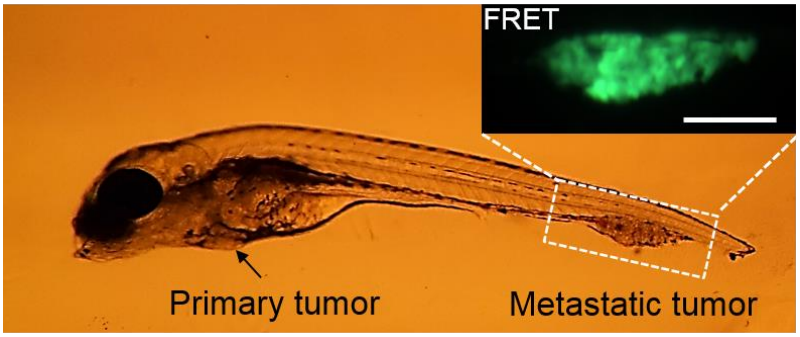

Figure 3-13. Circulating B16-F10-C3 cells developed a metastatic tumor after 5 days. Some circulating B16-F10-C3 cells fell off from the injection site and traveled to the tail of zebrafish. Subsequently, they proliferated and formed a metastatic tumor (indicated by a dashed box). The apoptotic status of metastatic tumor was checked by FRET imaging. Scale bar, 200 μm.

3.2.5 Evaluation of Anti-Metastatic Drugs in Zebrafish Xenograft Tumor Model

Before applying the zebrafish xenograft tumor model for anti-cancer drug testing, the apoptosis-detection ability of sensor C3 was evaluated by UV-irradiation. A tumor-bearing zebrafish was exposed to UV-light for 3 min. FRET imaging was conducted to detect apoptosis of B16-F10-C3 cells before and 6 h after UV-irradiation. As shown in Figure 3-14, it can be seen that there is a distinct changed in the color of the tumor from green to blue 6 h after UV exposure. This result demonstrates the feasibility of this model and also suggests that the tumor formed inside the embryo is not only susceptible to drug treatment but also to other external apoptotic stimulus. Hence, in additional to drug screening, this model may have other applications such as testing water quality and determining radiotoxicity.

ATTENTION: The Singapore Copyright Act applies to the use of this document. Nanyang Technological University Library

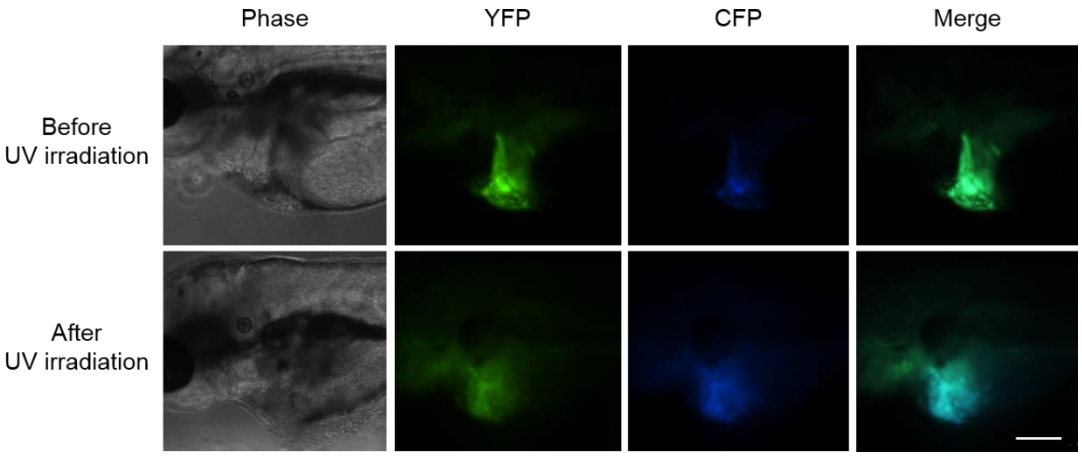

Figure 3-14. Apoptosis detection in a B16-F10-C3 xenograft tumor after UV-irradiation. A zebrafish bearing a B16-F10-C3 xenograft tumor was exposed to UV-light for 3 min. Apoptosis within the tumor was detected by FRET imaging. The merged image of B16-F10-C3 tumor appeared green (normal) before UV-irradiation and changed to blue (underwent apoptosis) after UV-irradiation. Scale bar, 200 μm.

An advantage of zebrafish tumor model is that the anti-cancer efficiency, side effects, as well as pharmacokinetic properties of a drug can be evaluated simultaneously [276, 277]. In this study, I first determined the maximum drug concentration applicable for the subsequent testing of anti-cancer efficiency. Zebrafish larvae were treated with different concentrations based on reported ranges used *in vitro*. Five fish were tested in every concentration of each drug. Five compounds were evaluated, including chemotherapy drugs of paclitaxel, vincristine, and doxorubicin and Raf inhibitor sorafenib, as well as PI3K inhibitor LY294002. The numbers of viable fish after drug treatment for 1-5 days are listed in Table 3-3, Table 3-4, Table 3-5, Table 3-6, and Table 3-7, respectively. Interestingly, three chemotherapy drugs displayed low toxicity to zebrafish in applied concentrations, while two inhibitors killed zebrafish at higher concentrations.

ATTENTION: The Singapore Copyright Act applies to the use of this document. Nanyang Technological University Library

Table 3-3. Embryos viability after LY294002 treatment

Concentration (μM)	Number of embryos alive			
	24 h	48 h	72 h	96 h
20	0/5	0/5	0/5	0/5
10	3/5	3/5	3/5	3/5
5	5/5	5/5	5/5	5/5

Table 3-4. Embryos viability after sorafenib treatment

Concentration (μM)	Number of embryos alive				
	24 h	48 h	72 h	96 h	120 h
8	0/5	0/5	0/5	0/5	0/5
4	5/5	3/5	0/5	0/5	0/5
2	5/5	5/5	4/5	0/5	0/5
1	5/5	5/5	5/5	5/5	1/5
0.5	5/5	5/5	5/5	5/5	3/5

Table 3-5. Embryos viability after vincristine treatment

Concentration [278]	Number of embryos alive				
	24 h	48 h	72 h	96 h	120 h
250	5/5	5/5	5/5	5/5	4/5
125	5/5	5/5	5/5	5/5	4/5
62.5	5/5	5/5	5/5	5/5	5/5
31.25	5/5	5/5	5/5	5/5	5/5
15.625	5/5	5/5	5/5	5/5	4/5

Table 3-6. Embryos viability after paclitaxel treatment

Concentration [278]	Number of embryos alive				
	24 h	48 h	72 h	96 h	120 h
200	5/5	5/5	4/5	3/5	2/5
100	5/5	5/5	5/5	4/5	4/5
50	5/5	5/5	5/5	5/5	5/5
25	5/5	5/5	5/5	5/5	5/5
12.5	5/5	5/5	5/5	5/5	5/5

Table 3-7. Embryos viability after doxorubicin treatment

Concentration (μM)	Number of embryos alive				
	24 h	48 h	72 h	96 h	120 h
10	5/5	5/5	5/5	5/5	4/5
5	5/5	5/5	5/5	5/5	4/5
2.5	5/5	5/5	5/5	5/5	4/5
1.25	5/5	5/5	5/5	5/5	5/5
0.625	5/5	5/5	5/5	5/5	5/5

ATTENTION: The Singapore Copyright Act applies to the use of this document. Nanyang Technological University Library

From the results obtained, it was concluded that the maximum concentrations applicable in the subsequent experiments for LY294002, sorafenib, vincristine, paclitaxel and doxorubicin are 5 μM, 1 μM, 250 nM, 100 nM, and 10 μM, respectively.

I then verified the effects of the drugs on B16-F10-C3 cells based on the concentrations obtained from the previous embryos drug viability analysis. The cells were treated with the drugs respectively and observed for 24 and 48 h. As shown in Figure 3-15, doxorubicin was the only one that significantly induced apoptosis of B16-F10-C3 cells at 24 and 48 h. Paclitaxel caused cytoplasmic contraction [279] without inducing any apoptosis. This may be related with the resistance of B16-F10 cells to paclitaxel [269]. Vincristine also modulated the cell morphologies but did not trigger apoptosis within 48 h. Two inhibitors of LY 294002 and sorafenib did not show any apoptotic effects *in vitro*.

Interestingly, when I conducted drug evaluation in zebrafish model, the effects of five drugs were different from the *in vitro* results. PI3K inhibitor LY294002 was the only compound that successfully inhibited the growth of B16-F10-C3 xenograft tumor in zebrafish (Figure 3-16). Apoptosis of B16-F10-C3 were not detected in the early stage of LY294002 treatment. Only when the fish were treated with LY294002 for more than 5 days, apoptosis were detected in the shrunk tumor (Figure 3-17).

ATTENTION: The Singapore Copyright Act applies to the use of this document. Nanyang Technological University Library

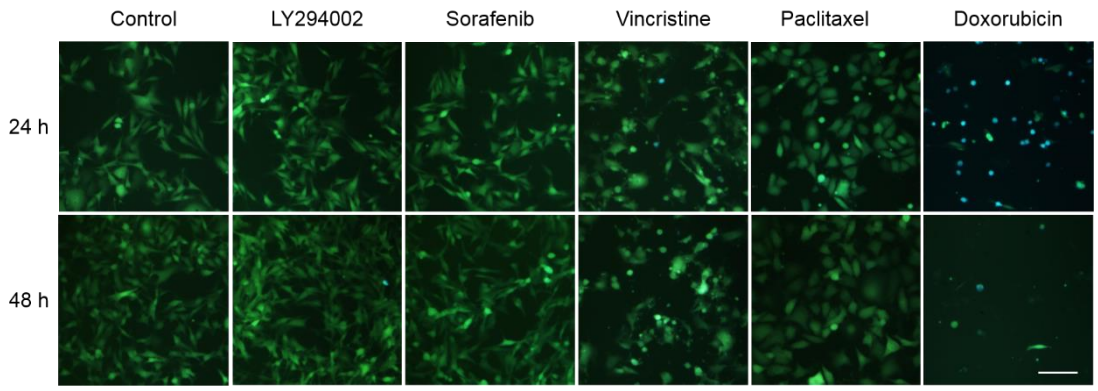

Figure 3-15. Apoptotic effects of five drugs in treating B16-F10-C3 cells *in vitro*. B16-F10-C3 cells were treated with 5 μM LY294002, 1 μM 1 μM, 250 nM 250 nM, 100 nM paclitaxel, and 10 μM doxorubicin for 24 and 48 h. Apoptosis were detected by FRET imaging, where normal cells appeared in green and apoptotic cells appear in blue color. Scale bar, 100 μm.

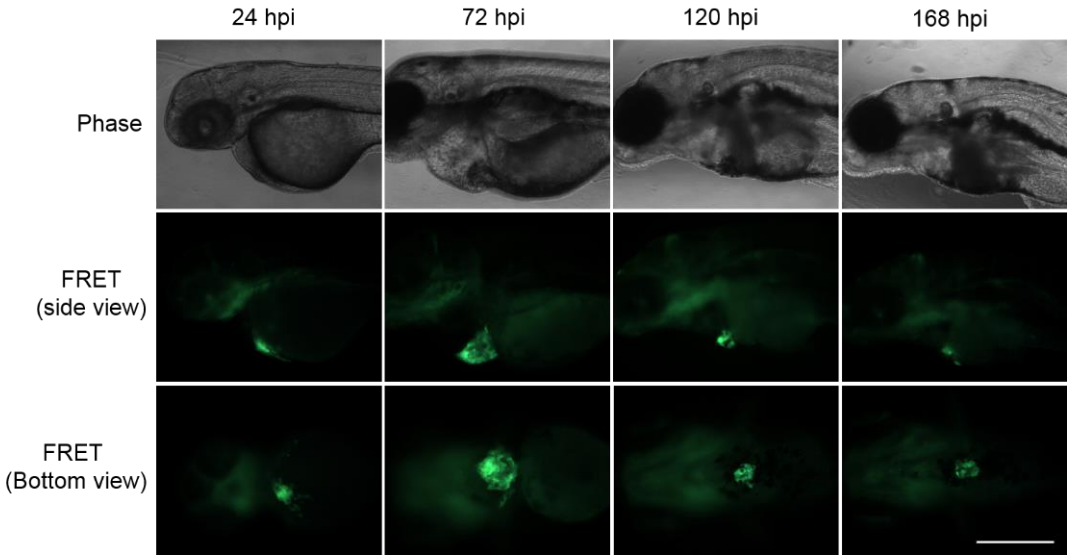

Figure 3-16. LY294002 inhibited growth of B16-F10-C3 xenograte tumor in zebrafish. The tumor sizes were revealed by FRET imaging from a side view or a bottom view. Scale bar, 400 μm.

ATTENTION: The Singapore Copyright Act applies to the use of this document. Nanyang Technological University Library

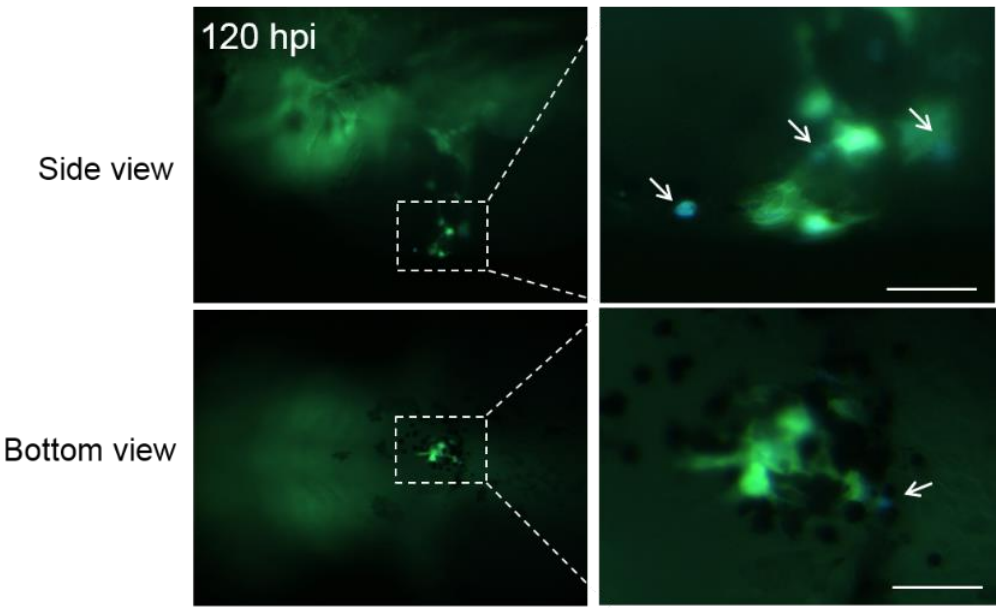

Figure 3-17. Apoptosis of B16-F10-C3 cells in xenograft tumor after LY treatment. Apoptotic B16-F10-C3 cells are indicated by white arrows. 5 μM LY294002 were used to treat the zebrafish with a xenograft tumor for 5 days. Scale bars, 100 μm.

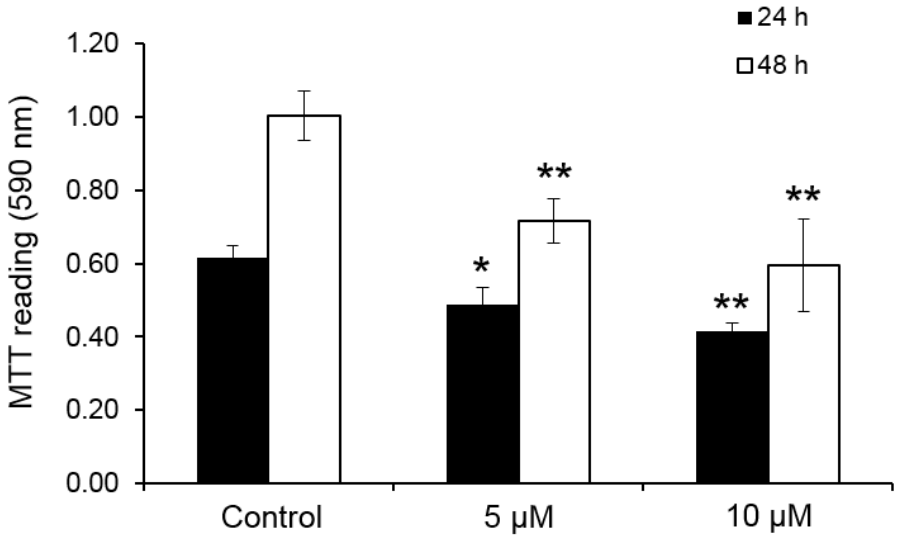

Figure 3-18. LY294002 inhibits the proliferation of B16-F10-C3 cells *in vitro*. Cell viability of B16-F10-C3 cells treated with 0, 5 and 10 μM of PI3K inhibitor LY294002 for 24 and 48 h were measured by MTT assay. Results are shown as optical density of MTT reading at 590 nm.

ATTENTION: The Singapore Copyright Act applies to the use of this document. Nanyang Technological University Library

These results indicate that the anti-cancer effect of LY294002 on B16-F10-C3 tumor is due to growth inhibition rather than apoptosis-inducing mechanism. The apoptosis of B16-F10-C3 cells in the late stage of LY294002 treatment is probably related to inhibited cell proliferation. In the *in vitro* experiments, LY294002 was found to inhibit the proliferation of B16-F10-C3 cells under concentrations of 5 and 10 μM (Figure 3-18) without inducing any apoptosis (Figure 3-15). In zebrafish tumor xenograft model, the effect of LY294002 was more significant than that in the *in vitro* analysis. This may be because the microenvironment of a zebrafish body is much harsher to B16-F10-C3 cells than that of the culture medium a petri-dish.

However, the results from chemotherapy drugs of vincristine, doxorubicin and paclitaxel show otherwise. Even though drugs were administered for up to 168 hpi, there were still obvious signs of tumor growth. One reason could be the drug resistance of B16-F10-C3 cells, which can be indicated by vincristine and paclitaxel treatment *in vitro* (Figure 3-15). Another reason may be related to the drug ABME (absorption, distribution, metabolism and elimination). During the period of drug administration, in the embryos that were treated with doxorubicin, orange or red stain can be seen at the location of the gut (Figure 3-19). This is a clear indication that the drug that was added into the zebrafish medium was indeed absorbed into the embryo and subsequently distributed, metabolized and eliminated by the fish body.

ATTENTION: The Singapore Copyright Act applies to the use of this document. Nanyang Technological University Library

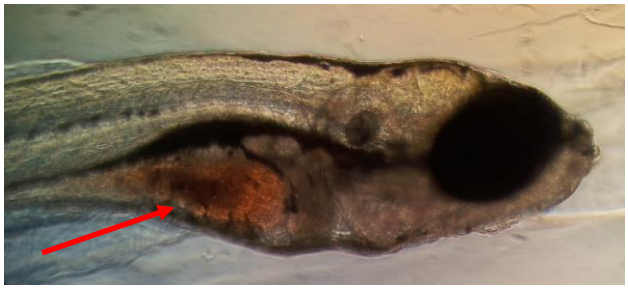

Figure 3-19. Accumulation of doxorubicin in the gut of a zebrafish embryo after 24 h. Zebrafish embryo (48 hpf) were placed in fish medium containing 10 μM anticancer drug doxorubicin for 24 h. Red arrow indicate the accumulation of red compound in the gut of zebrafish embryo.

3.2.6 Development of a Circulatory Microfluidic System for CTC Study

To facilitate the study of the viability of CTCs during circulation, I invented a circulatory microfluidic system to mimic the blood circulation (Figure 3-20A). This system uses a peristaltic pump (Ismatec, Germany) to drive the circulation of culture medium through a microfluidic channel (Figure 3-20B).

The engaging and disengaging of the roller with the silicon tubing in the peristaltic pump can mimic the heart beat and generate a pulsatile outflow (Figure 3-21). The beat rate can be controlled by adjusting the pump speed. For example, a beat rate of 75 bpm can be achieved when the pump speed was set up at 9 rpm. The main part of the microchannel is a silicon tubing (Figure 3-20C). For the outflow area, a silicon tubing with a length of 1 m and a diameter of 0.52 mm was used to mimic the arteries in the human body. For the roller engaging area, a special 2-stop PharMed tubing (Ismatec, Germany) was used. The size of 2-stop tubing has a range from 0.51 to 1.52 to achieve different flow rates in the outflow tubing. By adjusting the flow rate of the culture medium, designed shear stresses can be produced. For instance, a flow rate of 15.4 μl sec^{-1} can generate a shear stress of 15 dyne cm^{-2}, which is equivalent to the

ATTENTION: The Singapore Copyright Act applies to the use of this document. Nanyang Technological University Library

average pulsatile shear stress encountered in human arteries. A PDMS-based observation chip was connected to the silicon tubing to enable the real-time observation (Figure 3-20C). Through this chip, cell status such as cell morphologies, deformation, apoptosis, ROS generation can be monitored in a circulatory environment.

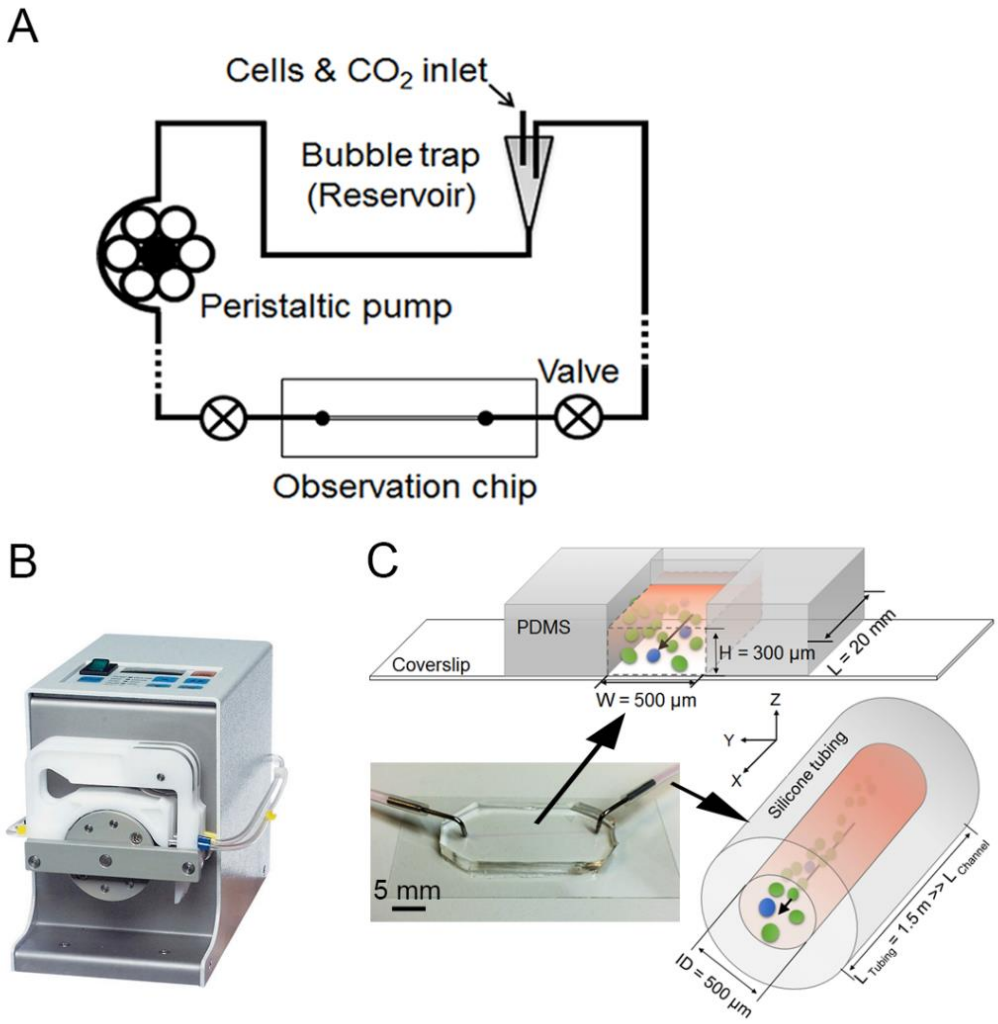

Figure 3-20. A circulatory microfluidic system for CTCs study *in vitro*. (A) Diagram of the circulatory microfluidic system. (B) A peristaltic pump was used to drive the circulation. (C) A PDMS-based observation chip was used for real-time monitoring of cell status.

ATTENTION: The Singapore Copyright Act applies to the use of this document. Nanyang Technological University Library

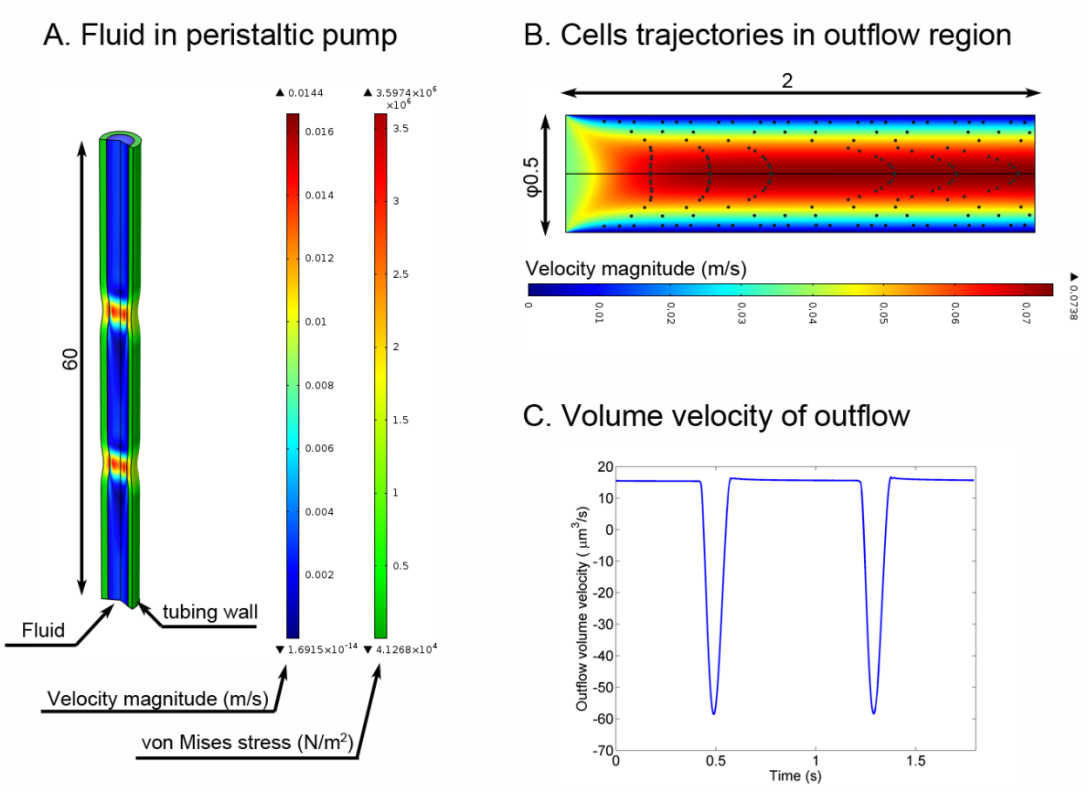

Figure 3-21. Simulation of the fluid shear stress that cancer cells encountered in the circulatory microfluidic system. (A) The engaging and disengaging of the rollers caused flow fluctuations. The engaging speed of the roller was 75 beats per minute. The fluid viscosity was 0.01 dyne cm^{-2}. (B) The flow fluctuations oscillated the cell trajectories. The cell concentration was 5×10^5 ml^{-1}. (C) The oscillation of the volume velocity with time was simulated with the same input in (A) and (B). Units are mm if not indicated.

3.3 Discussion and conclusion

In this study, I have generated multiple apoptosis sensor cell lines from various cancer cell lines and two normal cell lines (Table 3-1). Together with HeLa-C3 cells [154] and HUVEC-C3 cells [170] previously generated by our group, we established an apoptosis sensor cell bank. This cell bank contains cell lines representing multiple types of cancer and blood vessel endothelial cells as well as normal cells. All these cell lines can be applied for high-throughput screening of anti-cancer drugs that can induce

ATTENTION: The Singapore Copyright Act applies to the use of this document. Nanyang Technological University Library

apoptosis of cancer cells using the methods established by our group previously [157]. Moreover, detecting apoptosis as a single mechanism during drug screening may lead to the missing of many promising compounds that can inhibit tumor growth and progression via other mechanisms, such as suppressing proliferation, inhibiting angiogenesis and reducing metastasis. In two of our recent studies, we employed sensor endothelial cells to study angiogenesis and search for anti-angiogenic agents [170, 171]. This mechanism also potentially contributes to the cancer study and screening of anti-cancer drugs. In this thesis, I further extended the application of FRET sensor C3 in cancer research and drug discovery.

First, I explored the application of the net YFP value as an indicator of cell proliferation. Because the amount of YFP protein in each single cell should be quite stable, the total YFP intensity could be employed to measure the change of cell numbers. Therefore, when combining the measurements of Y/C ratio and net YFP intensity, the apoptotic effect and proliferation inhibitory effect of a tested compound could be evaluated simultaneously. Currently, identifying the agents that can inhibit cell proliferation is more important than the compounds only with toxic effects. The reason is that toxic compounds often affect DNA, mitochondria or cell cycle, which work in the same mechanisms as traditional chemotherapy drugs. The effects of these compounds are prominent, but their limitations are also well known, such as extensive side effects and drug resistance. Increasing drug discovery interests are shifting to the identification of specific kinase inhibitors such as inhibitors of EGFR, Raf, PI3K and mTOR [124]. These inhibitors usually do not directly induce apoptosis. Instead, most of these protein targets are associated with the proliferation of cancer cells. Therefore, searching for compounds with anti-proliferative effects may be more productive in drug

ATTENTION: The Singapore Copyright Act applies to the use of this document. Nanyang Technological University Library

discovery. In addition, I also developed an integrative drug screening platform for identifying multiple drug mechanisms in a single experiment (Table 3-2). The drug mechanisms can include toxic effects and anti-proliferative effects either in tumor cells, endothelial cells, or in normal cells.

Second, in this study, the FRET-based caspase sensor was applied to detect apoptosis *in vivo* for the first time. Apoptosis sensor cells were injected into zebrafish to generate either CTCs or solid tumors. Both models can be used to study cancer development and search for anti-metastatic drugs. Interestingly, a PI3K inhibitor LY294002 was found to inhibit both survival of CTCs in zebrafish circulation and proliferation of xenograft tumor in zebrafish. Although the apoptotic effect was not detected *in vitro* when cancer cells were treated with LY294002, the survival, extravasation and proliferation of cancer cells in zebrafish were significantly inhibited. Without LY treatment, cancer cells displayed high malignancy in zebrafish, even it is an allogeneic microenvironment. Inhibiting PI3K by LY294002 significantly reduced the malignancy of B16-F10-C3 cells in zebrafish. These results not only suggest that studying the drug effects is more reliable *in vivo* than that in *in vitro*, but also indicate that the zebrafish xenograft models developed in this study can be applied for the drug discovery in the future.

Third, I developed a new circulatory microfluidic system to mimic the blood circulation *in vitro*. Compared with the traditional microfluidic system which grows cells in the chip, this system allows the cells to be circulated in a microfluidic channel with culture medium. This system is specifically designed for studying of CTCs. The circulation of culture medium containing cancer cells was driven by a peristaltic pump, which mimics the function of a human heart. Moreover, multiple parameters of

ATTENTION: The Singapore Copyright Act applies to the use of this document. Nanyang Technological University Library

circulation in a human body can be simulated in this system, including heart beat rates, pulsatile flow, hemodynamic shear stress, diameter and length of human arteries as well as the environmental factors such as temperature and pH values. With this system, the viability, proliferation and invasiveness of CTCs can be well investigated. This system is thus extensive employed in the experiments in the following chapters of this thesis.

In summary, major achievements of this chapter include:

1. A caspase sensor cell bank was established for further mechanism study and drug discovery.
2. An integrative anti-cancer drug screening platform was developed by combining the apoptosis measurements using Y/C ratio and proliferation monitoring using net YFP intensity.
3. A CTCs model in zebrafish was developed and applied for searching of potential anti-metastatic drugs.
4. A zebrafish xenograft tumor model was developed based on the caspase FRET sensor and was applied for anti-cancer drug testing. A pan-PI3K inhibitor LY294002 was evaluated to suppress the proliferation of malignant melanoma cells in zebrafish.
5. A circulatory microfluidic system was invented to mimic the blood circulation and study the survival of CTCs.

ATTENTION: The Singapore Copyright Act applies to the use of this document. Nanyang Technological University Library

CHAPTER 4 Studying the Effects and Mechanisms of Hemodynamic Shear Stress-Induced Apoptosis of CTCs

4.1 Introduction

Circulation is the only route by which cancer cells move from the primary tumor site to a distant location. Once tumor cells enter the bloodstream, they can be killed by several mechanisms: 1) anoikis due to the detachment of cancer cells from the extracellular matrix and disruption of the actin cytoskeleton, which leads to cell rounding; 2) hemodynamic shear stress generated from blood flow and collisions between CTCs and blood cells and endothelial cells lining the vessel wall; and 3) immune destruction mediated by natural killer cells [141, 280-284]. Among these three mechanisms, the effect of hemodynamic shear on CTCs viability is least understood [281]. Thus, understanding how cancer cells survive hemodynamic shear stress may provide new insights into how CTCs became the true seeds of secondary tumors during metastasis [55].

Previously, several *in vivo* and *in vitro* model systems have been used to investigate the survival of cancer cells in response to different shear force conditions. For example, more than 99% of B16 melanoma cells were destroyed after 24 h of intravenous injection into the tail vein of mice [136, 278, 285, 286], while little or no cell death (0-20%) was observed after cells were introduced into the vein of the chorioallantoic membrane (CAM) in chick embryo or mouse liver models [73, 287, 288]. Under various fluid shear forces generated using a corn-plate viscometer or a tubing circuit, more than 80% of B16 cells died under higher shear stress (29 dyne cm^{-2}) after 4 h, while only 20% of the cells died under lower shear stress (5.9 dyne cm^{-2}) [289].

ATTENTION: The Singapore Copyright Act applies to the use of this document. Nanyang Technological University Library

Moreover, metastatic PC-3 cancer cells are more resistant to high fluid shear stress generated using a syringe needle compared to normal epithelial cells [290].

In this study, I assessed the effects of shear flow on CTCs apoptosis, a topic that remains largely unstudied [281]. Our group have designed a biosensor that can detect apoptosis via detecting caspase-3 activation, which is the most important event of apoptotic process [291]. This sensor was constructed by fusing the genes encoding two variants of GFP, CFP and YFP, with a specialized linker containing a caspase-3 cleavage sequence, DEVD (Figure 1-9). When plasmid DNA containing the caspase sensor was introduced into cancer cells, the transfected cells constitutively produced the sensor protein, which could be cleaved by activated execution caspases, including caspase-3, caspase-6 and caspase-7. Once the sensor protein was cleaved, it no longer produced fluorescence resonance energy transfer (FRET) [156, 292], and as a result, the color of the sensor cells changed from green to blue [154]. We have shown that these FRET-based sensor cells can detect apoptosis induced by various death inducers, including UV-irradiation and anti-cancer drugs such as paclitaxel, vincristine, etoposide, in single cells or a population of cells in real time [154, 170, 293].

Based on this apoptosis sensor, I developed novel *in vivo* and *in vitro* systems. I first introduced the FRET-sensor construct (sensor C3) into two breast cancer cell lines with different metastatic potential: metastatic MDA-MB-231-C3 (231-C3) and non-metastatic MCF7-C3. These sensor cells were introduced into two model systems to compare the resistance of metastatic and non-metastatic cells to shear flow-induced apoptosis. The first system is an *in vivo* system that uses zebrafish as a model due to its transparent body, which allows for the direct study of cancer cell metastasis, including visualizing extravasation dynamics [78] and hypoxia-induced dissemination

ATTENTION: The Singapore Copyright Act applies to the use of this document. Nanyang Technological University Library

of cancer cells [294]. The second system is a hemodynamic microfluidic system, which enables mechanistic studies under fluid shear stress, mimicking the physiological conditions of the bloodstream.

ATTENTION: The Singapore Copyright Act applies to the use of this document. Nanyang Technological University Library

4.2 Results

4.2.1 Metastatic Breast Cancer Cells Survive Better after Intravenous Injection in Mouse

To compare the survival of the two breast cancer cell lines with different metastatic capacities during hematogenous dissemination, an equal number (5×10^5) of 231-C3 and MCF7-C3 cells were separately injected into nude mice through the tail vein. At different times after the injection, the mice were sacrificed, and the distribution of the sensor cells on the surface of lung was visualized by YFP fluorescence using a Fluorescence MacroZoom System (Figure 4-1). The numbers of YFP-positive foci were counted from both sides of all lung leaves of three mice and converted to the number per unit area (cm^2). After 4 h, both cell lines appeared on the surface of the lung, indicating their successful arrest in this first capillary bed encountered (Figure 4-1).

From 4 h to 1 day, cell numbers counted from fluorescence positive foci were dramatically decreased with 96.6% loss of MCF7-C3 cells and 95.5% loss of 231-C3 cells (Figure 4-1 and Figure 4-2). This result suggests that shear force-induced cell deformation (necrosis) have played the main role in cell losing, which may not be selective to cancer cells with different metastatic ability. Nonetheless, 2.19 fold more of 231-C3 cells survived in the first 24 h compared to MCF7-C3 cells. The most interesting phase was from 1 day to 2 days. As shown in Figure 4-1 and 4-2, only 8.5% of MCF7-C3 cells survived in these 24 h. In contrast, the survival rate for 231-C3 cells was 38.9%, which was 4.6 fold higher than that of MCF7-C3 cells. As a result, 395 ± 8 of 231-C3 foci survived in each cm^2 area of lung tissue within the first 2 days

ATTENTION: The Singapore Copyright Act applies to the use of this document. Nanyang Technological University Library

and this number was maintained at a value of 307 ± 115 foci/cm^2 until 4 days post cell injection.

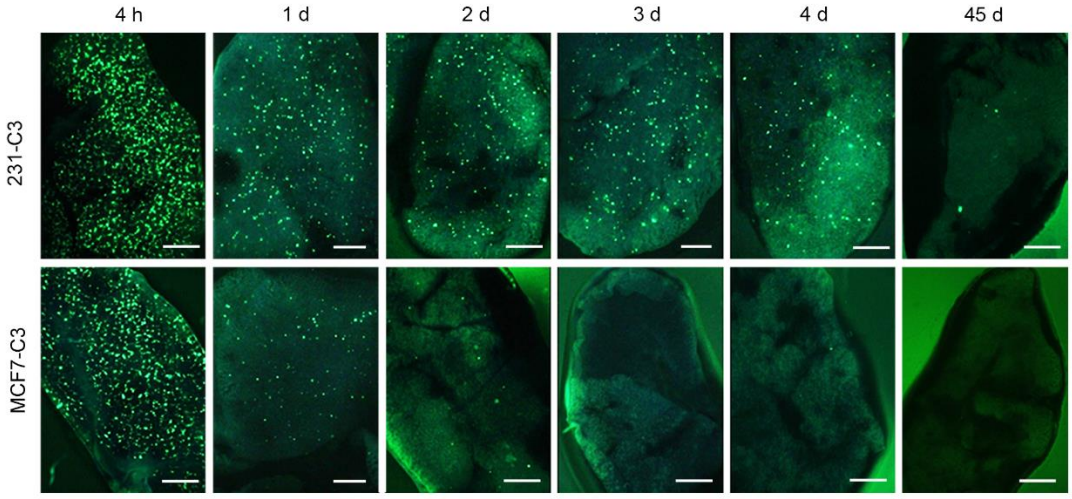

Figure 4-1. Distributions of 231-C3 and MCF7-C3 sensor cells in the lung of nude mice. Approximately 5×105 231-C3 and MCF7-C3 cells were injected into the tail vain of nude mice. The distribution of these sensor cells on the surface of the lung was imaged using a Fluorescence MacroZoom System at the indicated times. h=hours, d=days.

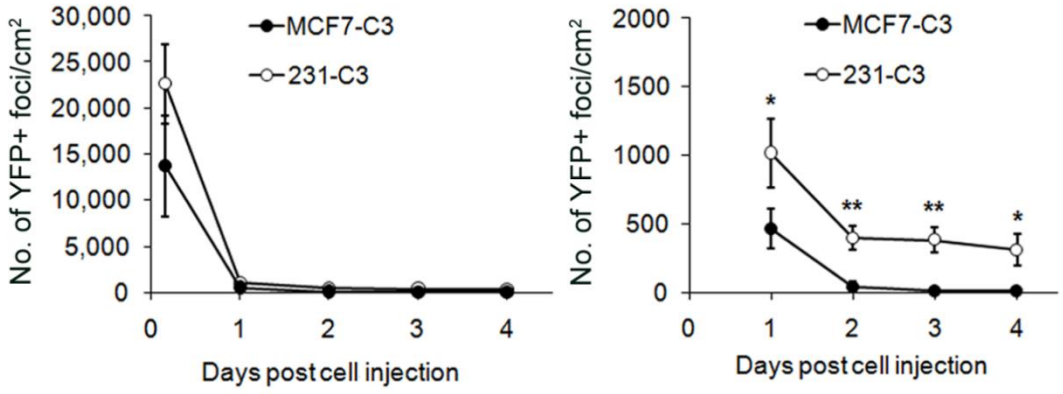

Figure 4-2. Quantification of viable sensor cells in lung after intravenous injection. The numbers of YFP-positive foci of MCF7-C3 and 231-C3 cells in the lung tissue were quantified from 0-4 days (left panel) and 1-4 days (right panel). N=3 in each time point.

ATTENTION: The Singapore Copyright Act applies to the use of this document. Nanyang Technological University Library

Eventually, several micrometastases were formed in the lung tissue after 45 days (Figure 4-1), with a maximal diameter of 200 μm (Figure 4-1). In another mouse reserved for a long term observation, visible macrometastases were detected by H&E staining after 90 days (Figure 4-3B). No visible MCF7-C3 colony was observed by FRET imaging (Figure 4-1) or detected by H&E staining after 45 days, demonstrating that 231-C3 cells are more metastatic than MCF7-C3 cells. I also assessed the presence of the sensor cells in other parts of the mouse. No sensor cell was detected after 1 day from blood samples and other organs such as liver, spleen, kidney, heart and bone.

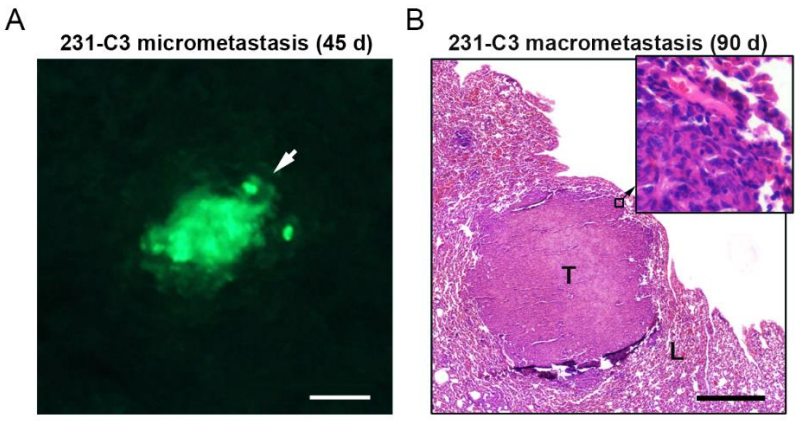

Figure 4-3. Lung metastases formed by 231-C3 cells. A micrometastasis (indicated by white arrow) formed in lung 45 days after injection. Scale bar, 100 μm. (B) H&E staining of a 231-C3 macrometastasis tumor (T) in the lung tissue (L) 90 days after injection. Scale bar, 500 μm.

4.2.2 Metastatic Cells Resist to Apoptosis in the Mouse Circulation

High resolution FRET imaging analysis revealed the rate of apoptosis to be 5-fold higher among non-metastatic MCF7-C3 cells compared to metastatic 231-C3 cells (30.2 ± 11.0% vs. 5.8 ± 2.6%) in day 1 (Figure 4-4A and B). The rate of apoptosis remained below 10% among 231-C3 cells (Figure 4-4B), and this was in keeping with the higher numbers of live YFP+ foci detected (Figure 4-2). These results suggest that

ATTENTION: The Singapore Copyright Act applies to the use of this document. Nanyang Technological University Library

the apoptosis played very important roles in the elimination of CTCs. As metastatic 231-C3 cells were more resistant to apoptosis induced by the host environmental factors compared to MCF7-C3 cells, they had higher potential to survive and form visible distant metastasis.

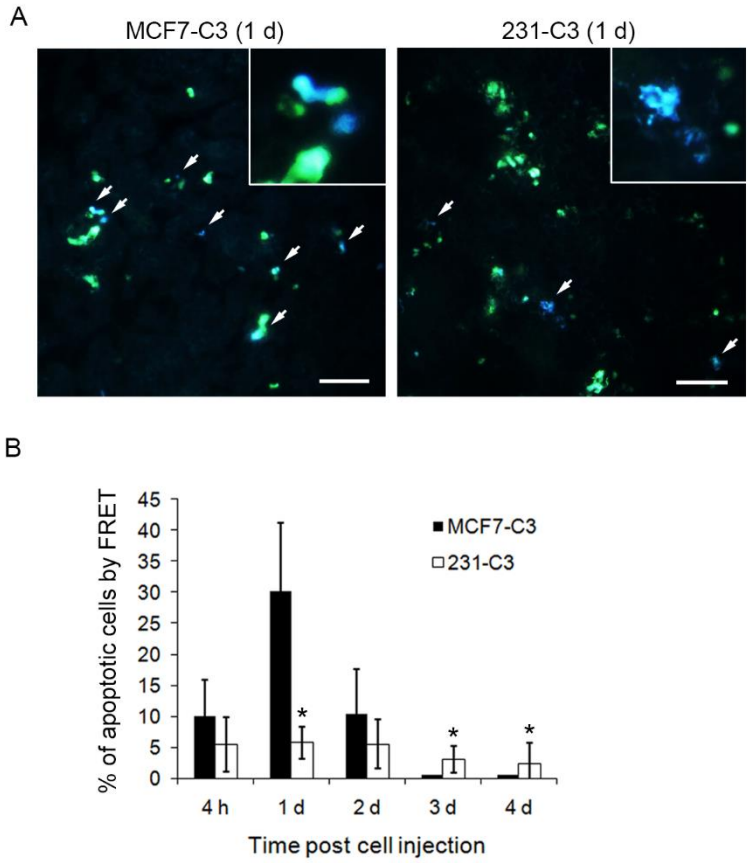

Figure 4-4. Quantification of apoptosis of sensor cells in lung after intravenous injection. The percentage of apoptotic cells in the lung tissue was quantified from FRET images at different time points after cell injection. The results represent the mean ± SD from all lungs of three mice at each time point (n = 3). *p < 0.05, **p < 0.01 by Student t test: 231-C3 cells vs. MCF7-C3 cells.

ATTENTION: The Singapore Copyright Act applies to the use of this document. Nanyang Technological University Library

4.2.3 Metastatic Breast Cancer Cells Resist Apoptosis in the Circulatory System of Zebrafish

To determine whether apoptosis of cancer cells occurred in circulation or after extravasation in an animal model, I employed zebrafish as a study model for CTCs because their transparent body allows us to visualize cancer cell dissemination and extravasation dynamics *in vivo*. A transgenic zebrafish *Tg(fli1:EGFP)* expressing enhanced GFP in endothelial cells was used to display the vascular system (Figure 4-5).

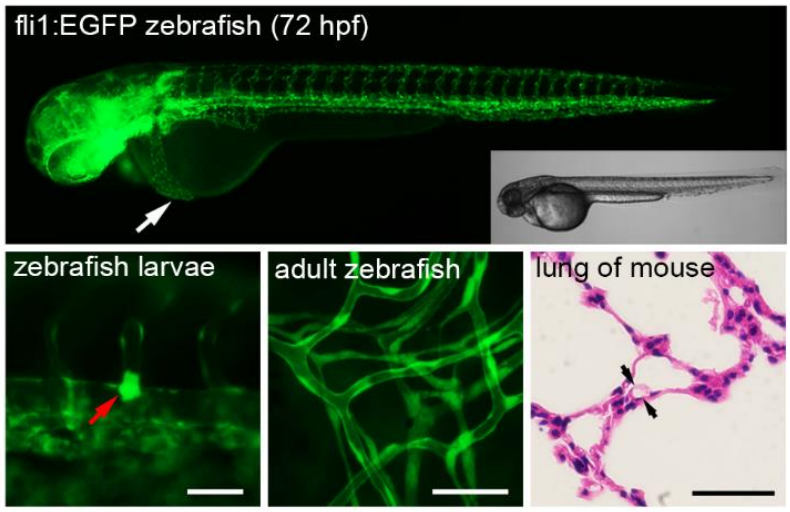

Figure 4-5. Blood circulation of zebrafish. Transgenic *Tg(fli1:EGFP)* zebrafish larvae expressing EGFP in the vascular system were imaged under fluorescence and DIC microscopy at 72 hpf. White arrow indicates the injection site of cancer cells. The diameter of blood vessels in zebrafish larvae were compared with the capillaries in adult zebrafish and the mouse pulmonary alveolus. A cancer cell having a larger size than the small blood vessel is indicated by a red arrow.

ATTENTION: The Singapore Copyright Act applies to the use of this document. Nanyang Technological University Library

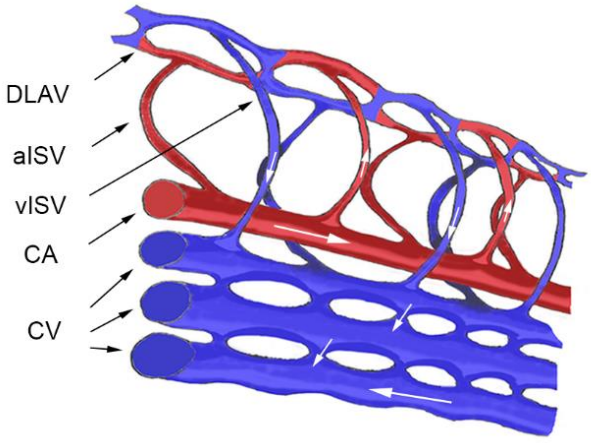

Figure 4-6. The schematic diagram illustrates the structures of the blood vessels in the observation window. DLAV: dorsal longitudinal anastomotic vessel, aISV: arterial intersegmental vessel, vISV: venous intersegmental vessel, CA: caudal artery, CV: caudal vein.

Approximately 50-100 sensor cells were injected into the pericardium of 72 hpf fish larvae (indicated by arrows in Figure 4-5), and approximately 20-50 cells entered into circulation. The tail region of the fish body was selected as the observation area, which has clear separation of the artery, vein and intersegmental vessels (ISV) (Figure 4-6). With this system, I tracked how CTCs traveled in the vascular system. After microinjection, the sensor cells were absorbed and pumped out to the whole body immediately by the heart. Afterwards, cells were circulating in large vessels like CA and CV. The blood flow in large arteries such as caudal artery (CA) was very fast, which may cause severe mechanical stress to CTCs. A portion of cells were trapped by small vessels like ISV (Figure 4-7) and CV plexus because of size restriction. These arrests may help cancer cells to avoid high shear stress. However, in this zebrafish model I observed that even the CTCs arrested by the aISV were still under continuous pulsatile beating by the blood flow. Moreover, these cells might return to circulation again via moving through small vessels after many minutes (Figure 4-8). The only way

ATTENTION: The Singapore Copyright Act applies to the use of this document. Nanyang Technological University Library

for cancer cells to completely avoid mechanical force is to extravasate from blood vessels and invade into the zebrafish tissue (Figure 4-9).

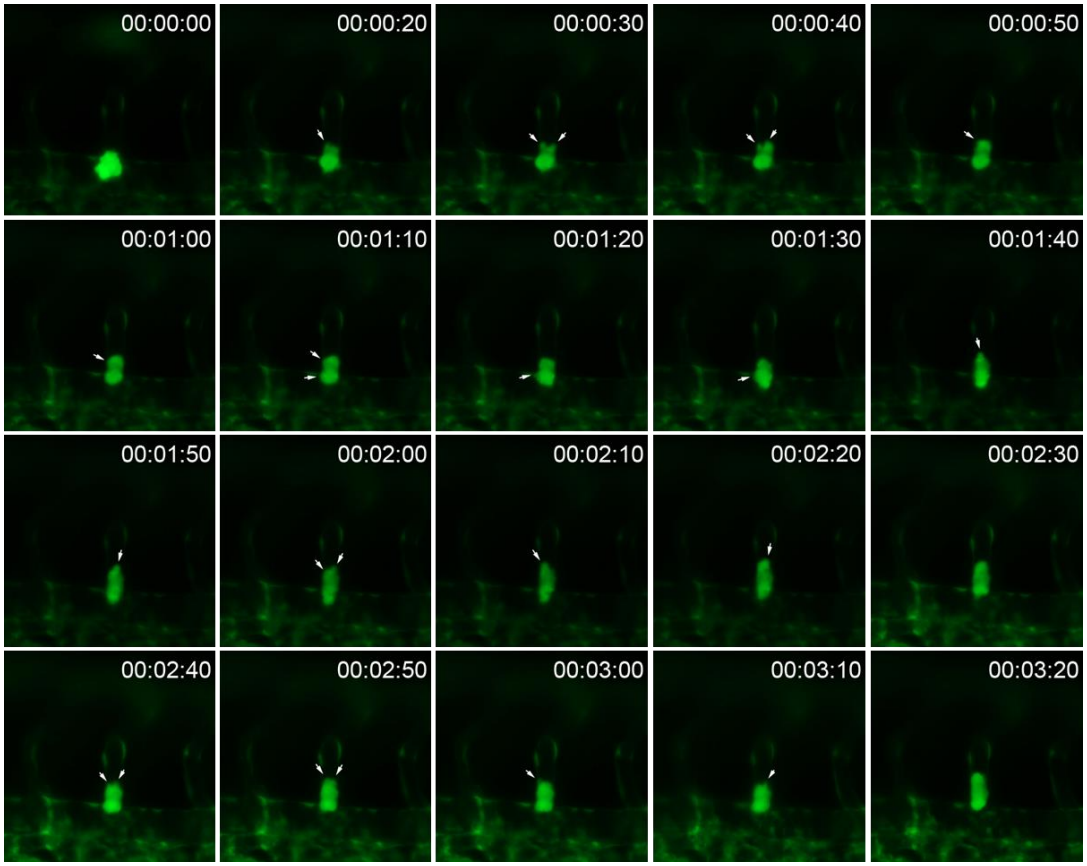

Figure 4-7. Process of a 231-C3 cell entering the aISV. A 231-C3 cell was arrested by ISV in the beginning. The cell had a size larger than the ISV and entered the ISV by active morphological deformation. White arrows indicate protrusion formation. Time shows hours, minutes and seconds.

The apoptotic status of sensor cells in blood circulation of zebrafish was determined by FRET imaging (Figure 4-10). In the short-interval observation, the apoptotic rate of non-metastatic MCF7-C3 cells began to increase at 6 hpi and reached a maximum level of 45.7% at 15 hpi, whereas the apoptotic rate of metastatic 231-C3 cells did not significantly increase in the first 24 hpi and only reached its highest level of 20.6 ± 9.2% at 72 hpi in the long-term observation (Figure 4-11).

ATTENTION: The Singapore Copyright Act applies to the use of this document. Nanyang Technological University Library

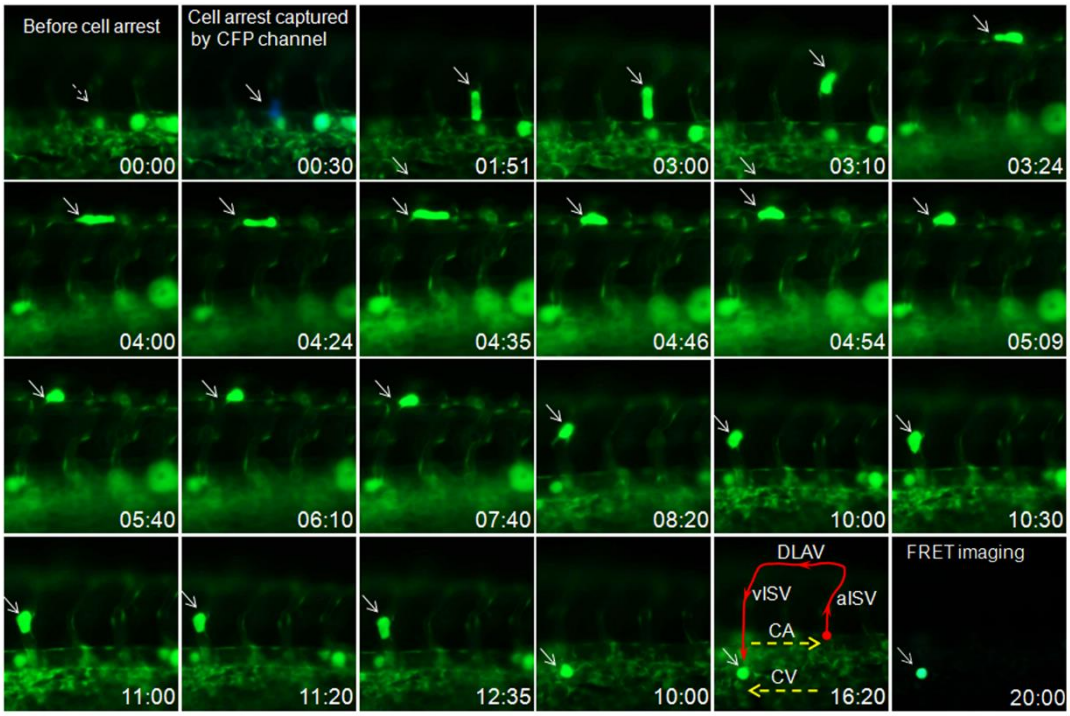

Figure 4-8. Travel route of cancer cell in small vessels of zebrafish. A MCF7-C3 cell was arrested by ISV. The cell migrated from the aISV to the DLAV and vISV following the blood flow (direction indicated by yellow arrows), and it finally returned to the circulation in CV after 20 min (traveling route indicated by red arrows). Time shows minutes and seconds.

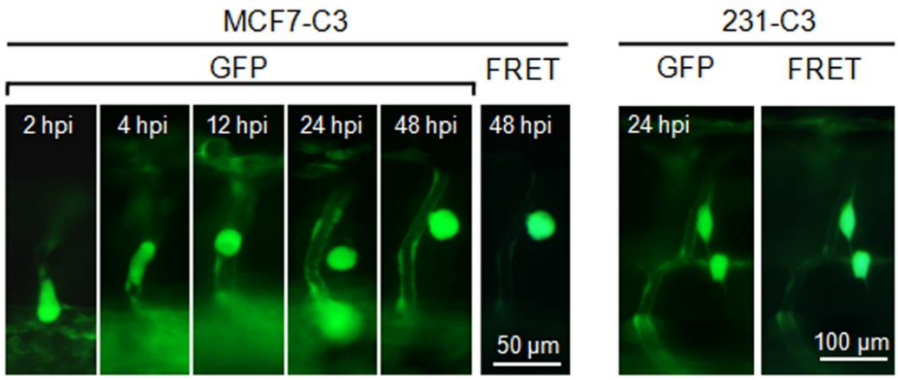

Figure 4-9. Extravasation of a MCF7-C3 cell and a 231-C3 cell from the ISV. Imaging from GFP channel in left panel shows the process of a MCF7-C3 cell being arrested by an ISV, migrating and changing shape within ISV, extravasating from ISV and migrating out of ISV. A FRET image indicates the cell is viable after extravasation at 48 hpi. Right panel shows that two 231-C3 cells have extravasated from ISV remain viable after 24 h.

ATTENTION: The Singapore Copyright Act applies to the use of this document. Nanyang Technological University Library

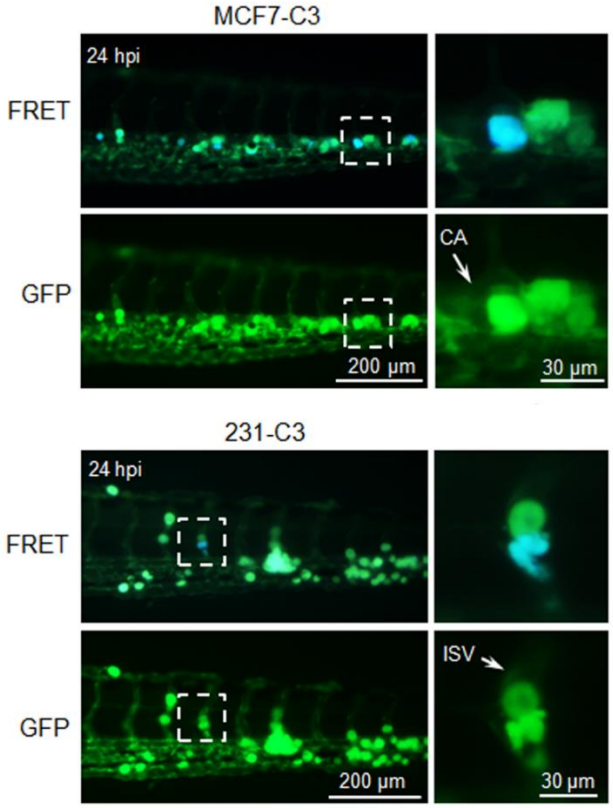

Figure 4-10. Representative image of sensor cell apoptosis in the zebrafish circulation. Apoptotic cells appeared in blue color by FRET imaging at 24 hpi. Representative apoptotic MCF7-C3 and 231-C3 cells were indicated by dashed boxes and enlarged in right panels.

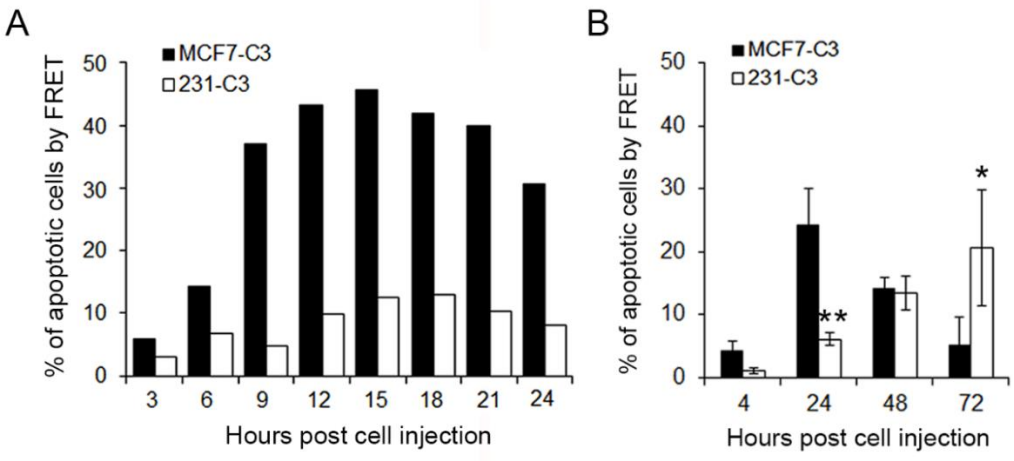

Figure 4-11. Quantification of apoptosis of CTCs in the zebrafish circulation. FRET images of MCF7-C3 and 231-C3 cells were quantified in short-intervals with 24 h (A) and in a long observation time of 3 days (B) from 200-300 cells at each time point.

ATTENTION: The Singapore Copyright Act applies to the use of this document. Nanyang Technological University Library

These results show that metastatic 231-C3 cells are more resistant to apoptosis in circulation than the non-metastatic MCF7-C3 cells, which is consistent with our previous findings in the mouse model.

4.2.4 Hemodynamic Shear Force in Zebrafish Circulation Triggers Apoptosis of CTCs

CTCs can be destroyed by the immune system, anoikis and hemodynamic shear force. However, the immuno-elimination of CTCs may not occur in the 3- to 6-day-old zebrafish whose immune system is not fully developed at this stage. Anoikis is also unlikely to cause CTCs to die in this zebrafish model, as I observed that the injected sensor cells were able to adhere to fish endothelial cells during circulation. I next explored whether hemodynamic shear stresses can trigger apoptosis in CTCs.

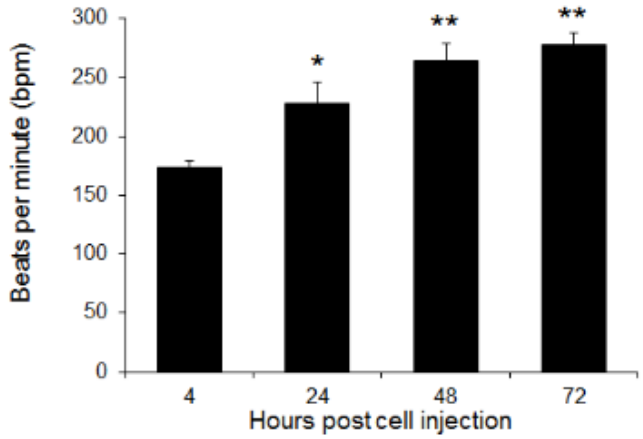

Figure 4-12. Heartbeat rates of developing zebrafish larvae. Heart beats per minute of control zebrafish were counted at the time of 4, 24, 48 and 72 h post microinjection of sensor cells.

First, as described above, all CTCs were under pulsatile mechanical force from blood stream, even when they were arrested in the small vessels. Second, I measured

ATTENTION: The Singapore Copyright Act applies to the use of this document. Nanyang Technological University Library

the heartbeats of zebrafish during their development from 3 to 6 days post fertilization (dpf), and found that the rates increased from 173.6 ± 5.4 beats per min (bpm) at 4 hpi to 277.7 ± 10.0 bpm at 72 hpi (Figure 4-12). This increasing of heart rate sould elevate hemodynamic shear stresses on the injected sensor cells which might account for the increased apoptosis in 231-C3 cells observed only in zebrafish larvae (from 6.1 ± 1.0% at 24 hpi to 20.6 ± 9.2% at 72 hpi) (Figure 4-11B), but not in mouse model (Figure 4-4).

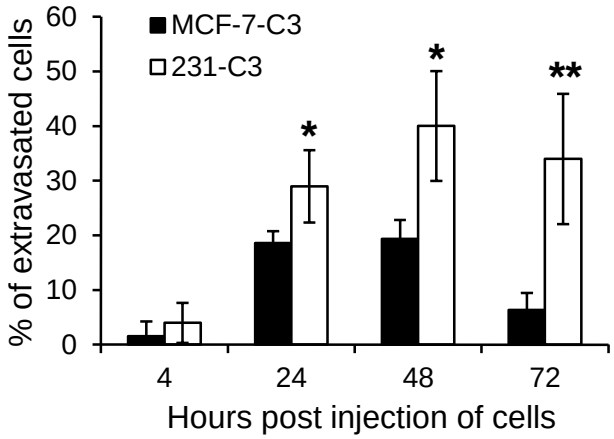

Figure 4-13. Extravasation rates of sensor cells in the ISV of the tail region. At least five fish were analyzed in each experiment. Each fish containing at least 20-50 sensor cells located in the tail region was imaged with a fluorescence microscope. Three independent experiments were conducted for both MCF7-C3 and 231-C3 cells. The results represent the mean ± SD *p < 0.05, **p < 0.01 by Student t test: 231-C3 cells vs. MCF7-C3 cells.

Third, I explored the association of extravasation (Figure 4-9), a crucial event in metastasis, with cell viability in circulation. Extravasation was found to be an efficient event in zebrafish, because over 20% of cells were able to extravasate in both cell lines in the first 24 h (Figure 4-13). However, as metastatic 231-C3 cells had higher viability over non-metastatic MCF7-C3 cells, they also displayed a greater tendency to extravasate from the ISV (Figure 4-13) and malignancy to invade into the adjacent

ATTENTION: The Singapore Copyright Act applies to the use of this document. Nanyang Technological University Library

tissues (Figure 4-9) before the peak of apoptosis. Correspondingly, up to 40% of 231-C3 cells were found embedded in the tissues adjacent to the ISV 48 hpi, whereas fewer MCF7-C3 cells (19.4 ±3.5%) had extravasated (Figure 4-13). In addition, more 231-C3 cells (19.8 ± 4.6%) survived in the tail region of zebrafish than MCF7-C3 cells (5.9 ±1.6%) at 72 hpi (Figure 4-14). Most of these viable 231-C3 cells at 72 hpi were observed in the ISV region (Figure 4-15A) and already extravasated from the ISV as shown in the enlarged image in Figure 4-15B. No cell could survive in the large vessel (CA and CV) after 72 h unless they form an aggregate to resist large shear stress there (Figure 4-15C). I further correlated the viability of sensor cells with their localizations in or out of the ISV. For cells within the ISV, the percentage of viable sensor cells was rapidly decreased from > 95% at 4 hpi to <10% at 72 hpi for both 231-C3 and MCF7-C3 cells (Figure 4-14B, bars with darker colours). In contrast, the cells extravasated the ISV had significantly higher survival rates (Figure 4-14B, bars with lighter colours). In particular, the percentage of viable 231-C3 cells that were outside the ISV was 3-fold higher than the cells inside the ISV at 72 hpi. Taken together, these observations support our hypothesis that hemodynamic shear force can induce apoptosis of CTCs. Metastatic 231-C3 cells can survive longer in blood circulation, thus having more time to extravasate and avoid the hemodynamic shear stress environment.

ATTENTION: The Singapore Copyright Act applies to the use of this document. Nanyang Technological University Library

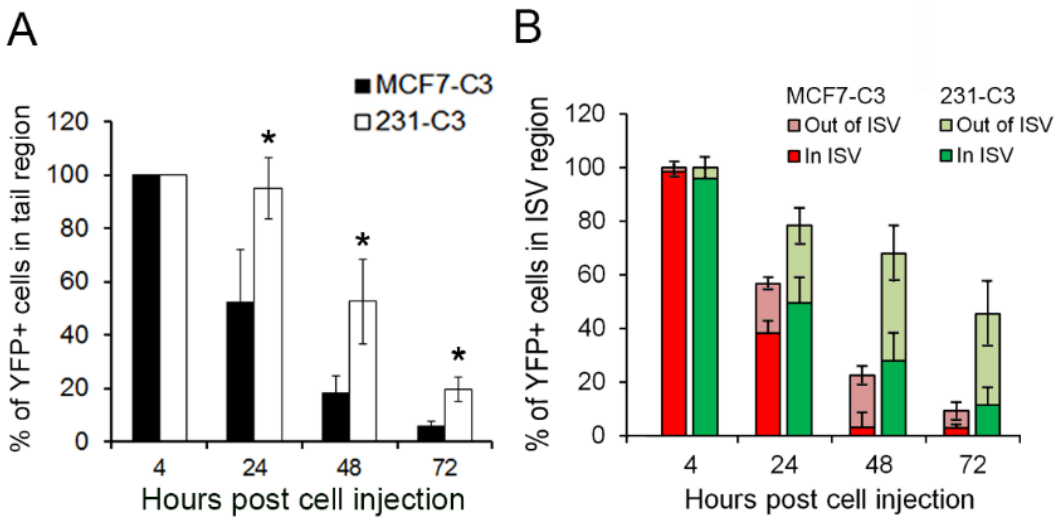

Figure 4-14. Viability of sensor cells in the tail region of zebrafish. (A) Percentage of YFP+ 231-C3 and MCF7-C3 cells located in the whole tail region. (B) Percentage of YFP+ 231-C3 and MCF7-C3 cells located in and out of the ISV. At least five fish were analysed in each experiment, with at least 20-50 sensor cells located in the tail region of each fish. Three independent experiments were conducted for both MCF7-C3 and 231-C3 cells. Data represent the mean ± SD. *p<0.05, **p<0.01 by Student's t test comparing 231-C3 *vs.* MCF7-C3 cells.

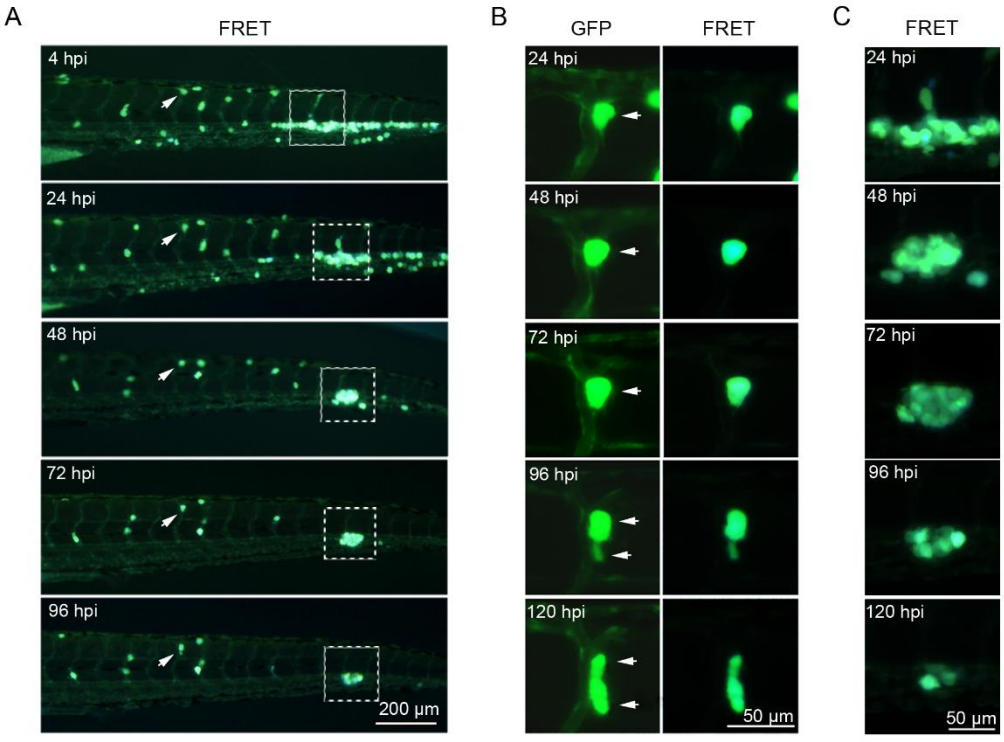

ATTENTION: The Singapore Copyright Act applies to the use of this document. Nanyang Technological University Library

Figure 4-15. Survival of 231-C3 cells in zebrafish. (A) The distribution of 231-C3 cells in zebrafish circulation was continuously observed in the same fish by FRET imaging for 96 hpi. (B) A 231-C3 cell divided into two cells in zebrafish body after extravasation between 96-120 hpi. (C) 231-C3 cells resisted shear stress and survived longer within large vessels by forming an aggregate.

4.2.5 Fluid Shear Stresses Trigger Apoptosis of Sensor Cells in a Circulatory Microfluidic System

To further determine the effects of hemodynamic shear stresses on cell viability, I developed a novel circulatory microfluidic system to mimic physiological fluid shear stresses encountered in circulation (Figure 3-20A). In this system, apoptosis of the sensor cells was determined by FRET imaging through a PDMS-based observation chip (Figure 4-16). Non-metastatic MCF7-C3 cells exhibited a much higher apoptotic rate, with a maximum rate of 18.9% at 16 h, while the metastatic 231-C3 cells displayed a much lower apoptotic rate of <4.6% in the first 20 h (Figure 4-17).

More importantly, I observed that increasing shear stresses from 5 to 30 dyne cm^{-2} significantly enhanced the rate of apoptosis in both types of cells (Figure 4-18). Lower shear stress of 5 dyne cm^{-2}, which is closer to the average shear stress in the bloodstream of human veins [295] [296], induced lower levels of apoptosis in both MCF7-C3 ($7.2 \pm 1.9\%$) and 231-C3 ($3.9 \pm 1.7\%$) cells and these were similar to the

ATTENTION: The Singapore Copyright Act applies to the use of this document. Nanyang Technological University Library

apoptotic rates obtained from the non-adhesive condition

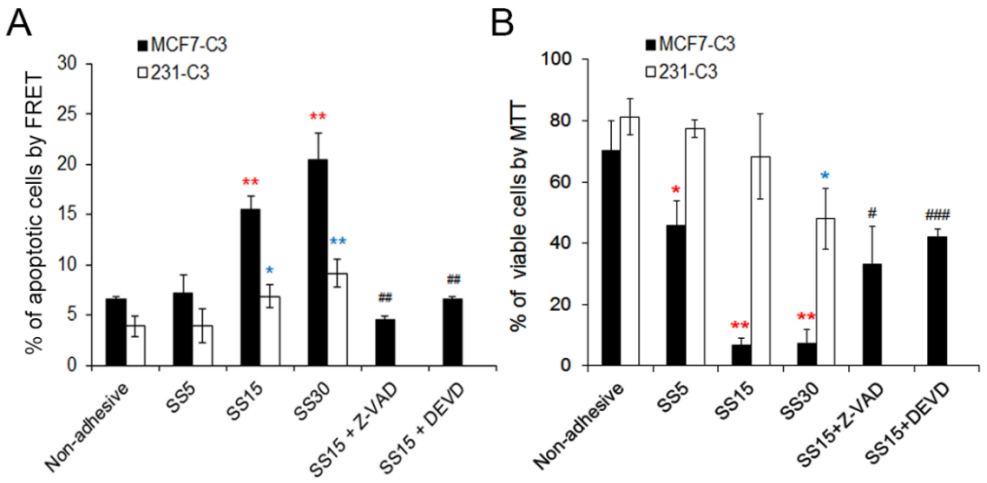

(

Figure 4-19).

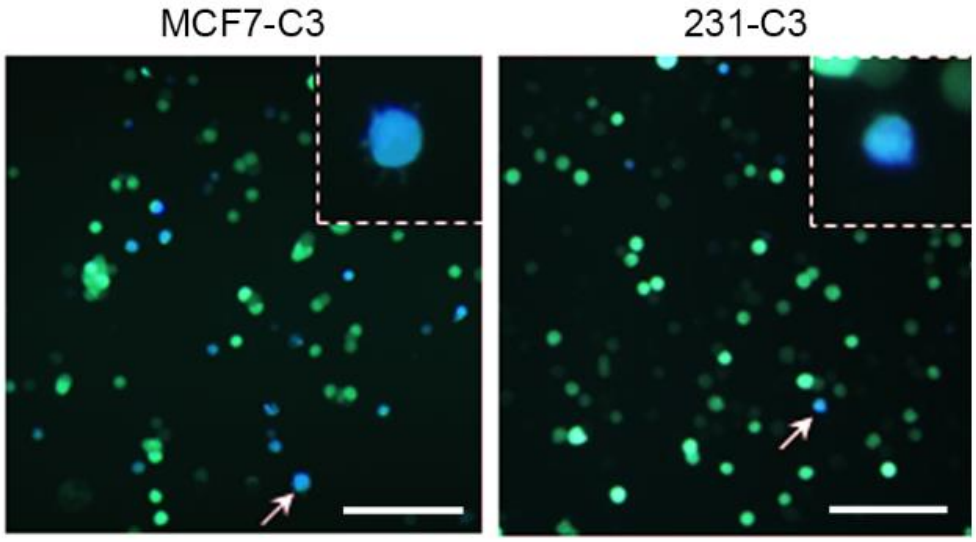

Figure 4-16. Apoptosis of sensor cells in the circulatory microfluidic system. Apoptosis was detected in both MCF7-C3 and 231-C3 cells by FRET imaging through an observation chip after 18 h circulation under a shear stress of 15 dyne cm^{-2}. Apoptotic cells appear in blue color, as indicated by white arrows and enlarged in the dashed boxes. Scale bars, 100 μm.

ATTENTION: The Singapore Copyright Act applies to the use of this document. Nanyang Technological University Library

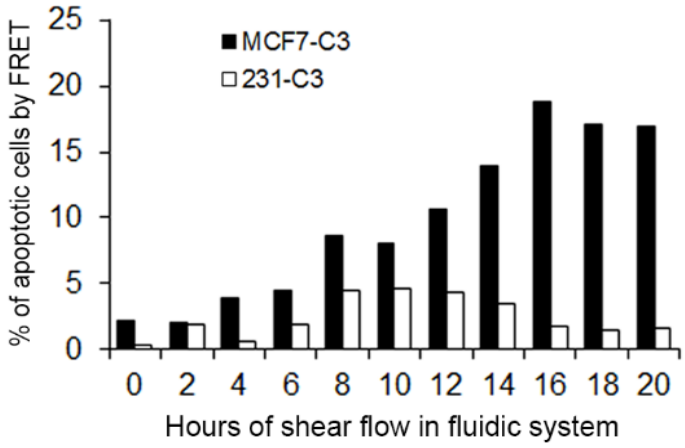

Figure 4-17. Quantification of apoptosis of CTCs in microfluidic system. The apoptosis of MCF7-C3 and 231-C3 cells in circulation under a shear stress of 15 dyne cm^{-2} was determined by FRET imaging from 0 to 20 h. The apoptotic rates were calculated from more than 200 cells in each time point.

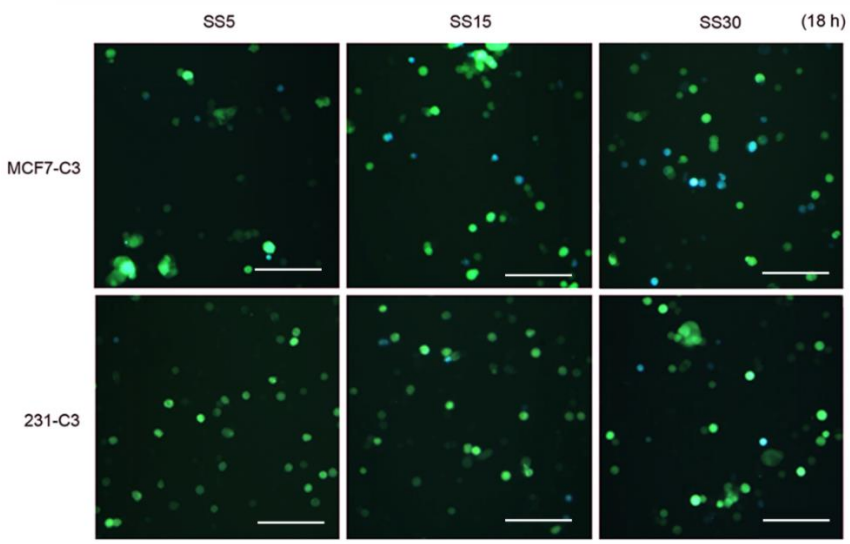

Figure 4-18. FRET images of MCF7-C3 and 231-C3 cells after circulation under different shear stresses. Shear stresses of 5 dyne cm^{-2} (SS5), 15 dyne cm^{-2} (SS15) and 30 dyne cm^{-2} (SS30) were generated by controlling the flow rates. Cells were circulated for 18 h in the microfluidic system before subjecting to FRET imaging.

ATTENTION: The Singapore Copyright Act applies to the use of this document. Nanyang Technological University Library

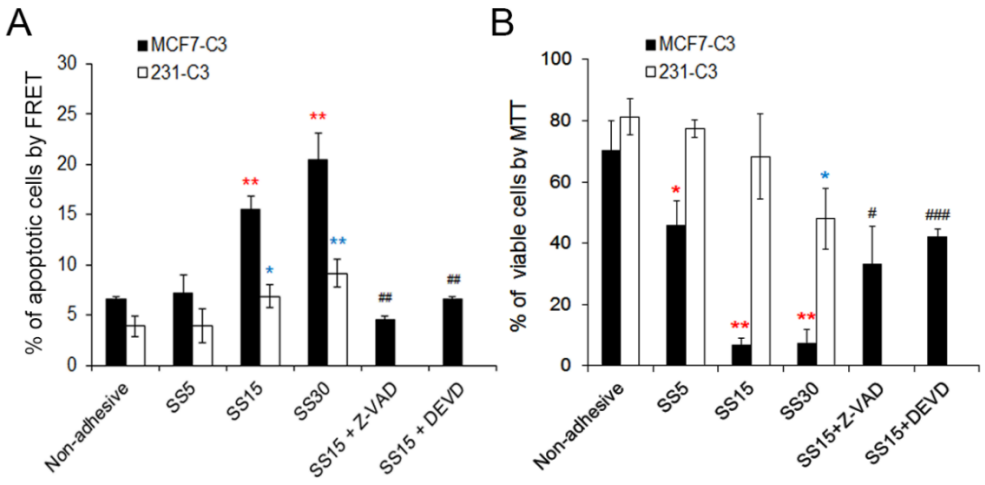

Figure 4-19. Quantification of apoptosis under different shear stresses and treatments. MCF7-C3 and 231-C3 cells were subjected to various shear stresses (5, 15 and 30 dyne cm^{-2}). Cells grown in non-adhesive-coated wells were used as a negative control. MCF7-C3 cells pretreated with pan-caspase inhibitor Z-VAD-FMK (Z-VAD, 20 μM) and caspase-3/7 inhibitor Ac-DEVD-CHO (DEVD, 10 μM) for 1 h were also subjected to fluid shear stress of 15 dyne cm^{-2}. Apoptotic rates were determined by FRET imaging.

Higher shear stresses of 15 and 30 dyne cm^{-2} resulted in much higher levels of apoptosis, which was more prominent in non-metastatic MCF7-C3 cells with an apoptotic rate of 20.4% ± 2.7% compared to the metastatic 231-C3 cells with an apoptotic rate of (9.2% ± 1.4%) (Figure 4-18 and Figure 4-19A). Elevated apoptosis in MCF7-C3 cells also resulted in significant reduction of cell viability (Figure 4-19B). Finally, I pre-treated the MCF7-C3 cells with a pan-caspase inhibitor or a caspase-3/7 inhibitor and circulated them at 15 dyne cm^{-2} for 18 h. The FRET imaging analysis revealed that both inhibitors significantly reduced the level of apoptosis (Figure 4-19A). Furthermore, the results of the MTT assay showed that the inhibitor treatments also increased cell viability from 6.8 ± 2.3% to 33.1 ± 12.4 % (Ac-DEVD-CHO) and 42.1 ± 2.6 % (Z-VAD-FMK) (Figure 4-19B). These results suggest that hemodynamic shear stress can destroy cancer cells by activating apoptosis and

ATTENTION: The Singapore Copyright Act applies to the use of this document. Nanyang Technological University Library

metastatic cancer cells are more resistant to this type of cell death than non-metastatic cells.

4.2.6 Fluid Shear Stress Increases ROS Generation in CTCs

To investigate how fluid shear stresses induced apoptosis of cancer cells in circulation, I measured the level of ROS by pre-incubating cells with a ROS-detecting dye CM-H_2DCFDA (10 μM) for 30 min before injecting them into the zebrafish circulation or microfluidic system. CM- H_2DCFDA is an indicator for ROS in cells. It can passively diffuse into cells, where its acetate groups are cleaved by intracellular esterases and its thiol-reactive chloromethyl group reacts with intracellular glutathione and other thiols. Subsequent oxidation of DCFDA by hydrogen peroxide and hydroxyl radicals can produce a green fluorescent adduct that is trapped inside the cell. As shown in Figure 4-20A, the fluorescence intensity of oxidized CM-H_2DCFDA, DCF, was low in both MCF7 and MDA-MB-231 cells in zebrafish circulation 5 min after injection and clearly increased after 60 and 120 min of circulation in both MCF7 and MDA-MB-231 cells, indicating that ROS was generated in circulating cells regardless of their metastatic potential (Figure 4-20B). Elevation of intracellular ROS levels was similarly detected in cells circulated in the microfluidic system under a shear stress of 15 dyne cm^{-2} (Figure 4-20 and Figure 4-21). Pre-treatment with an anti-oxidant agent PG (20 μM) for 1 h significantly reduced ROS levels in both cell lines (Figure 4-22).

ATTENTION: The Singapore Copyright Act applies to the use of this document. Nanyang Technological University Library

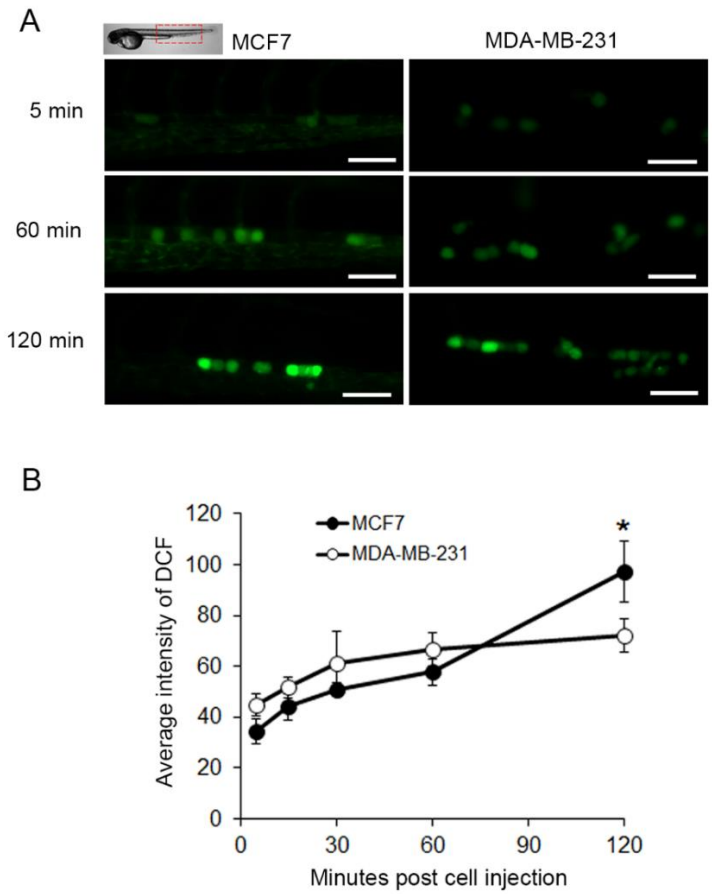

Figure 4-20. MCF7 and MDA-MB-231 cells pre-loaded with 10 μM CM-H2DCFDA were injected into the bloodstream of 3 dpf zebrafish. (A) Fluorescence images of cells in zebrafish circulation. Scale bars, 50 μm. (B) Fluorescence intensities of DCF in 100-200 cells from more than 10 fish were measured to quantify the levels of ROS.

ATTENTION: The Singapore Copyright Act applies to the use of this document. Nanyang Technological University Library

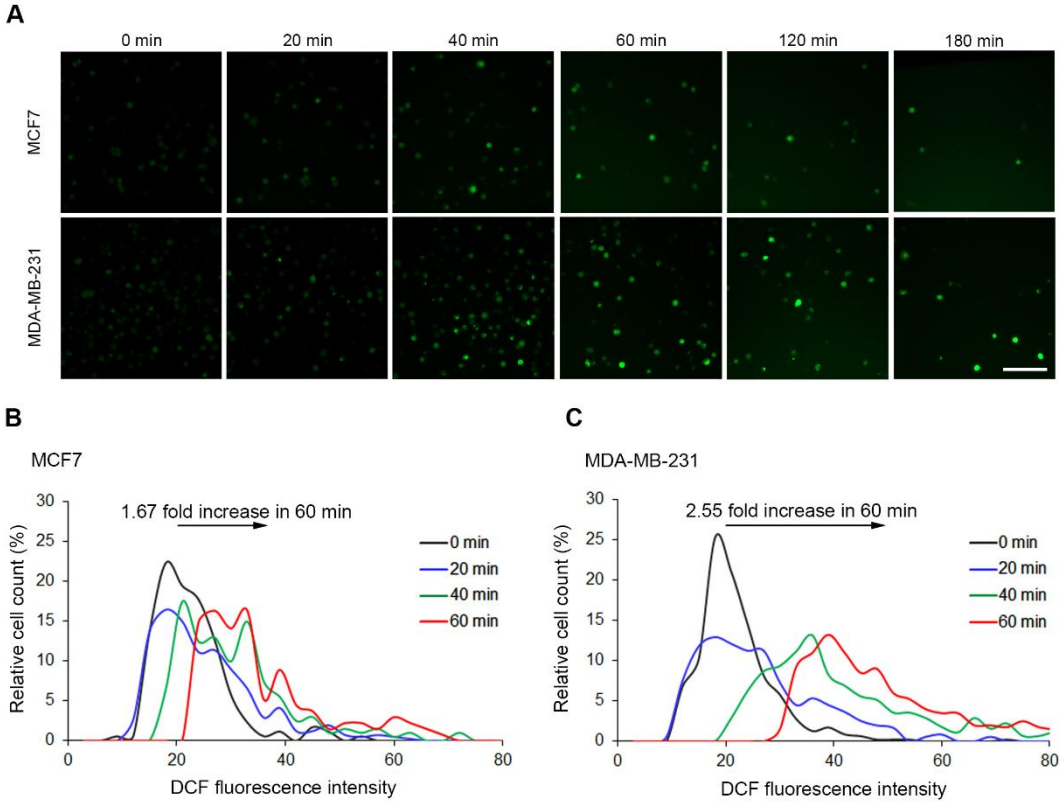

Figure 4-21. Fluid shear stresses promote ROS generation in circulating cancer cells. (A) Production of H_2O_2 in MCF7 and MDA-MB-231 cells was monitored by pre-staining cells with 10 μM CM-H2DCFDA. Cells with positive staining of DCF were captured after 0, 20, 40, 60, 120 and 180 min circulation in shear stress of 15 dyn cm^{-2}. Scale bar, 100 μm. The levels of ROS in MCF7 (B) and MDA-MB-231 (C) were determined by measuring the fluorescence intensity of DCF in each cell. The fluorescence intensities of more than 200 cells were converted into distribution curves.

ATTENTION: The Singapore Copyright Act applies to the use of this document. Nanyang Technological University Library

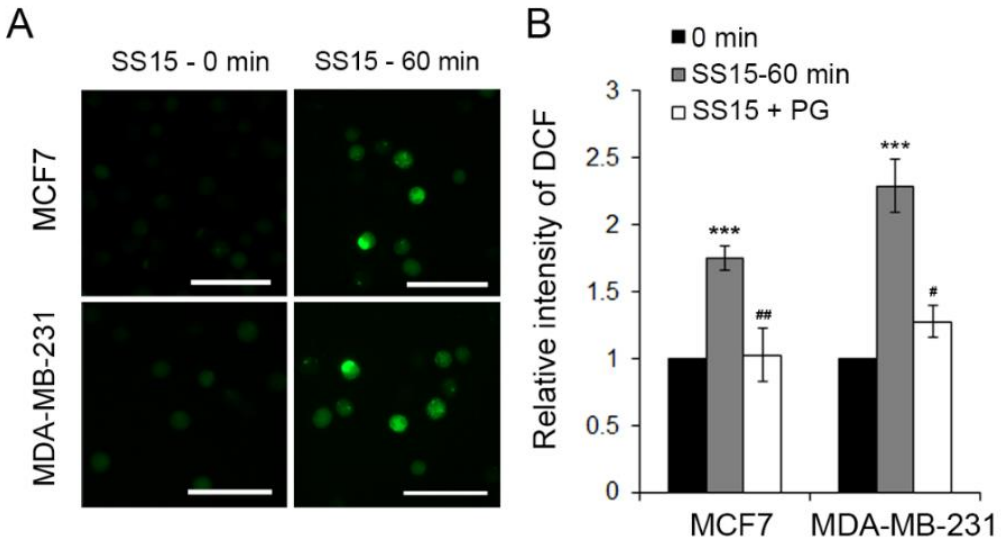

Figure 4-22. ROS generation in microchannel can be inhibited by PG treatment. ROS was detected by CM-H2DCFDA staining in MCF7 and MDA-MB-231 cells after circulating in the microfluidic system with a shear stress of 15 dyne cm-2 for 60 min. The ROS levels were determined by measuring the fluorescence intensity of DCF in each cell of more than 200 cells. PG (20 μM) was used to inhibit ROS generation. The results represent the mean ± SD from three independent experiments. *p<0.05, **p<0.01 and ***p<0.001 by Student's t test vs. time point of 0 min.

4.2.7 Fluid Shear Stress Elevated the Levels of Superoxide in Mitochondria

Since PG is known to scavenge superoxide and hydroxyl radicals [297, 298], I postulated that the type of ROS produced by fluid shear stress in circulating cells was superoxide. To test this hypothesis, MCF7 and MDA-MB-231 cells were pre-loaded with a mitochondrial superoxide specific dye MitoSOX Red and circulated in the microfluidic system under the shear stress of 15 dyne cm^{-2}. MitoSOX Red is a mitochondrial superoxide indicator derived from dihydroethidium. This dye is used for highly selective detection of superoxide in the mitochondria of live cells. Oxidation of MitoSOX Red indicator by superoxide results in hydroxylation and yield red fluorescence with the emission at 590 nm. The levels of fluorescence intensity of

ATTENTION: The Singapore Copyright Act applies to the use of this document. Nanyang Technological University Library

MitoSOX increased for about 2-fold at 60 min in both types of cells which are significantly higher than the levels generated under static condition (Figure 4-23B). These results suggest that fluid shear stress can elevate the levels of superoxide in both metastatic and non-metastatic CTCs.

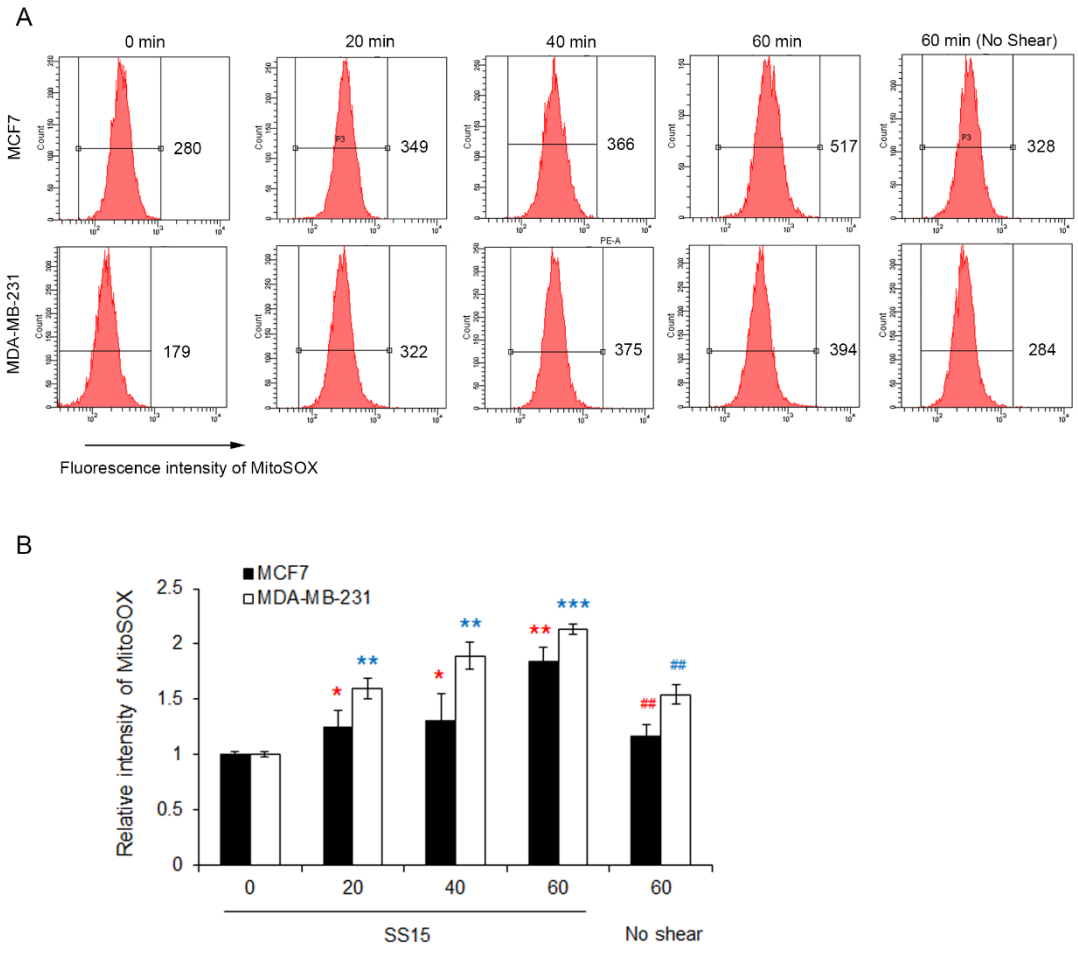

Figure 4-23. Mitochondrial superoxide production was detected by MitoSOX. Cells stained with 10 μM MitoSOX were analysed by flow cytometry. Non-adhesive conditions with no shear were used as a negative control. (B) The average intensity from 10000 cells was calculated in each sample and the results represent the mean ± SD from three independent experiments. *p<0.05, **p<0.01 and ***p<0.001 by Student's t test vs. time point of 0 min. ##p<0.01 vs. condition of 15 dyne cm^{-2} for 60 min.

ATTENTION: The Singapore Copyright Act applies to the use of this document. Nanyang Technological University Library

4.2.8 Excessive Superoxide Generation by Fluid Shear Stress Damages Mitochondria and Causes Caspase-dependent Apoptosis

Superoxide molecules have the potential to induce apoptosis by increasing mitochondrial membrane permeability. In this study, I found that shear stress significantly induced the fragmentation of mitochondria in MCF7 cells after 3h (Figure 4-24A). Time lapse imaging (Figure 4-25) showed that the mitochondria shrank to ring-shape after detachment from dish. When exposed to fluid shear stress, the mitochondria in MCF7 cells started to fragment after 1 h of circulation and reached severe levels after 2-3 h (Figure 4-25). The elevation of mitochondrial superoxide by shear stress (< 1 h in Figure 4-24A and Figure 4-25A) was in accordance to this time point. This mitochondrial fragmentation is shear stress-dependent as little fragmentation was detected in MCF7 cells under non-adhesive condition with no shear stress (Figure 4-25A). Moreover, inhibiting the accumulation of superoxide by pretreating cells with antioxidant PG also reduced mitochondrial fragmentation in MCF7 cells (Figure 4-25B). I then evaluated mitochondrial integrity by MitoTracker Red CMXRos, which is mitochondrial membrane potential (MMP)-sensitive. Loss of MitoTracker staining was not observed before 3 h but was clearly detected in 36.5 ± 13.8 % of MCF7 cells after 6 h circulation. Interestingly, when excessive superoxide was eliminated by a superoxide scavenger, MnTBAP, which mimics SOD enzyme [299], mitochondrial fragmentation was delayed and the MMP in MCF7 cells could be retained after 6 h circulation (Figure 4-24 and Figure 4-25B).

ATTENTION: The Singapore Copyright Act applies to the use of this document. Nanyang Technological University Library

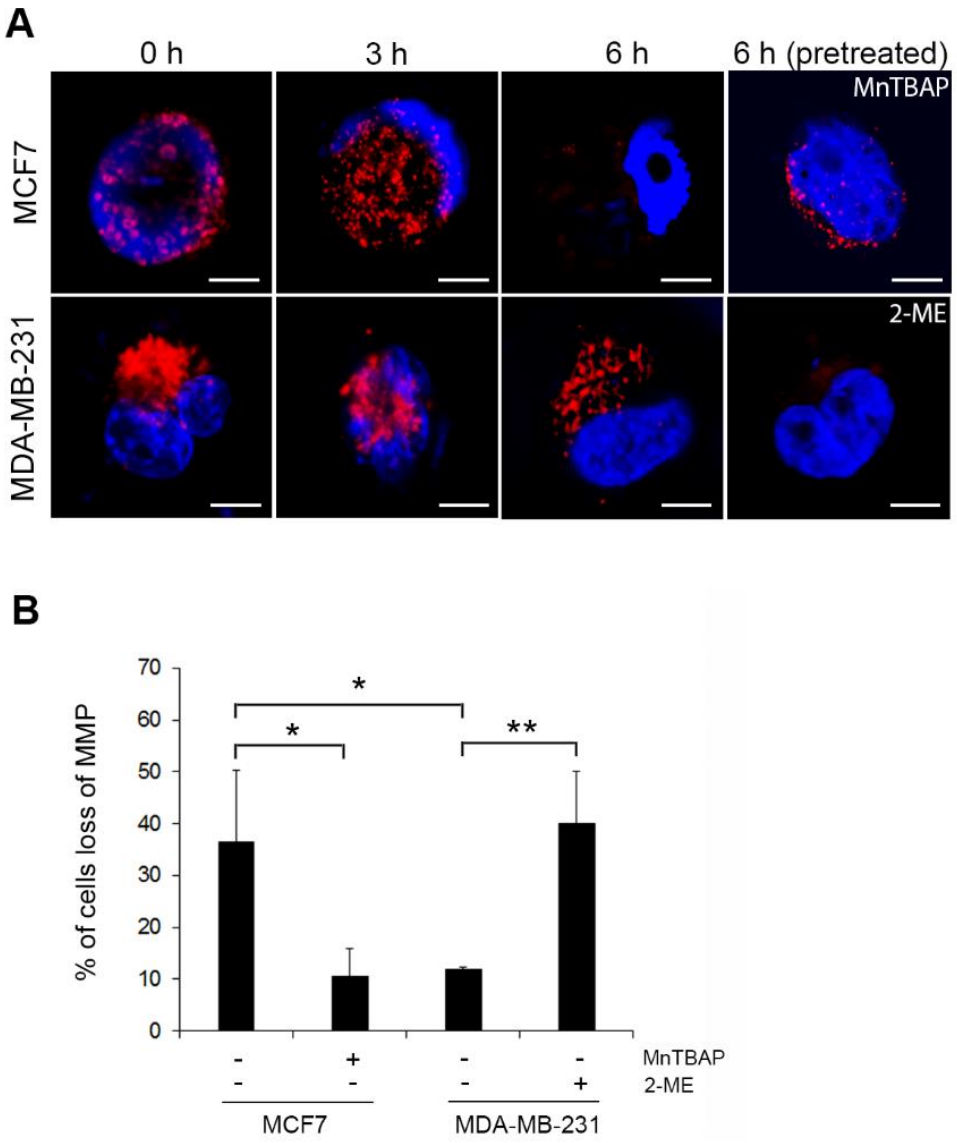

Figure 4-24. Fluid shear stress damages mitochondria by inducing oxidative stress. (A) Mitochondrial membrane potential (MMP) was examined by staining with MitoTracker Red-CMXRos in MCF7 and MDA-MB-231 cells after 0, 3 and 6 h of circulation. MnTBAP (100 μM) was used to pre-treat MCF7 cells and 2-ME (20 μM) was used to pre-treat MDA-MB-231 cells before circulating. Scale bars, 5 μm. (B) The percentage of cells with loss of MMP was quantified from more than 200 cells. The results represent the mean ± SD from three independent experiments. *p<0.05 and **p<0.01 by Student's t test vs. control.

ATTENTION: The Singapore Copyright Act applies to the use of this document. Nanyang Technological University Library

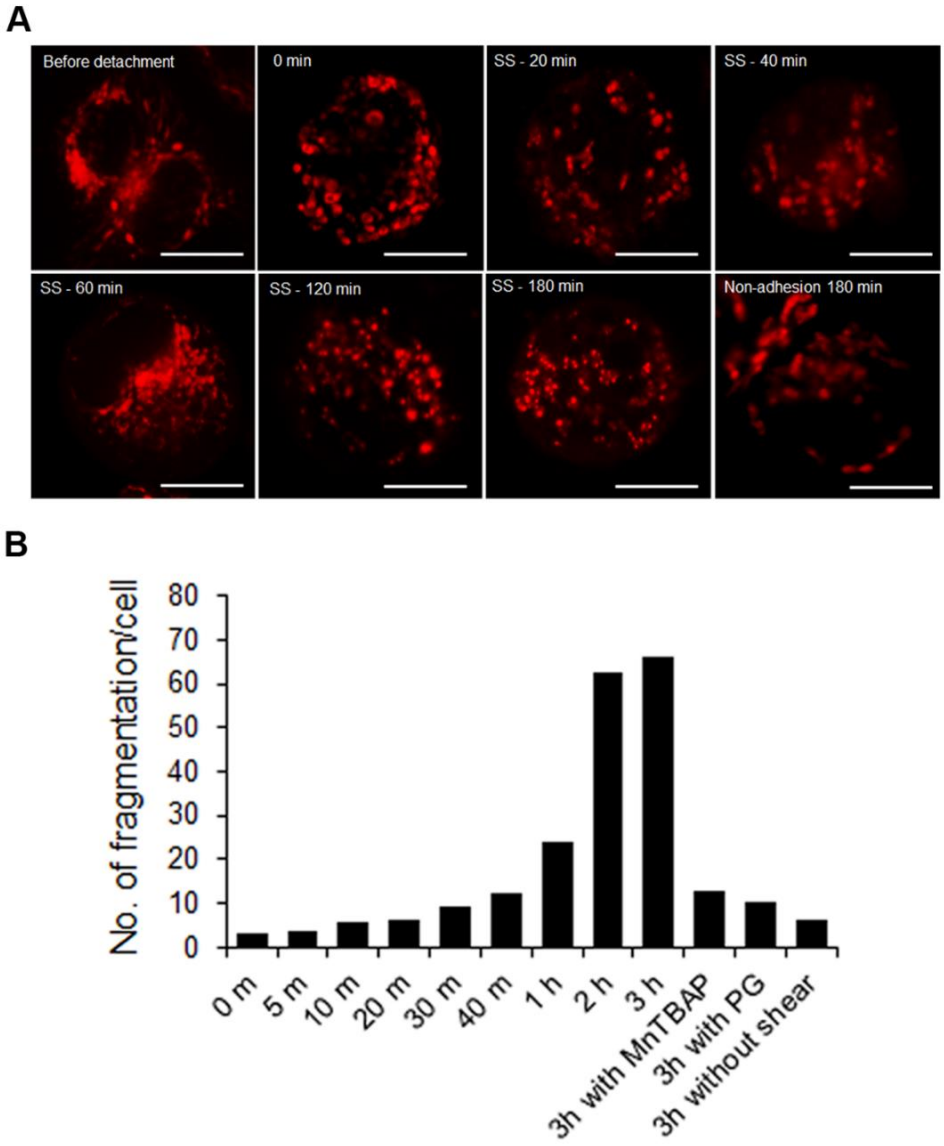

Figure 4-25 Fluid shear stress caused fragmentation of mitochondria in circulating MCF7 cells. (A) Mitochondrial morphologies of MCF7 cells after 0, 20, 40, 60, 120 and 180 min circulation were monitored by MitoTracker Red. Cells grown in non-adhesive dish were used as negative control. Scale bars, 10 μm. (B) The fragmentation of mitochondria in circulated MCF7 cells was quantified from 10-15 cells in each condition. A fragmentation was counted if its diameter is less than the average diameter of mitochondria in attached cells. The average number of fragmentations were calculated and presented in the following bar graph.

ATTENTION: The Singapore Copyright Act applies to the use of this document. Nanyang Technological University Library

Mitochondrial integrity appeared to be unaffected in MDA-MB-231 cells when circulated in the microfluidic system for 3 and 6 h. At the time point of 3 h, no obvious fragmentation of the mitochondria was observed. After 6 h circulation, most of MDA-MB-231 cells retained their mitochondrial integrity (Figure 4-24A) and only 10% cells displayed lost MMP (Figure 4-24B). However, inhibiting SOD activity by pretreatment with 2-ME [251] produced a marked loss of MitoTracker staining in 231-C3 cells (Figure 4-24A and B).

4.2.9 Antioxidant Chemicals Protect CTCs from Fluid Shear Stress-Induced Apoptosis

To validate that fluid shear stress can trigger apoptosis of CTCs through ROS overproduction, I measured the apoptosis and survival of circulating MCF7-C3 cells under the protection with antioxidant chemicals. Results indicated that antioxidant agent PG and SOD mimetic MnTBAP significantly reduced apoptotic rate (Figure 4-26A) and increased cell viability (Figure 4-26B) after 18 h circulation. Because the level of shear-induced cell death was much lower in metastatic 231-C3 cells, no protective effect was observed in after PG pretreatment. These results further confirm that hemodynamic shear stress can elevate the level of ROS in cancer cells while they are circulating in the bloodstream, which could consequently kill the cells. Metastatic cells are more resistant to hemodynamic shear stress-induced apoptosis due to their higher antioxidant ability.

ATTENTION: The Singapore Copyright Act applies to the use of this document. Nanyang Technological University Library

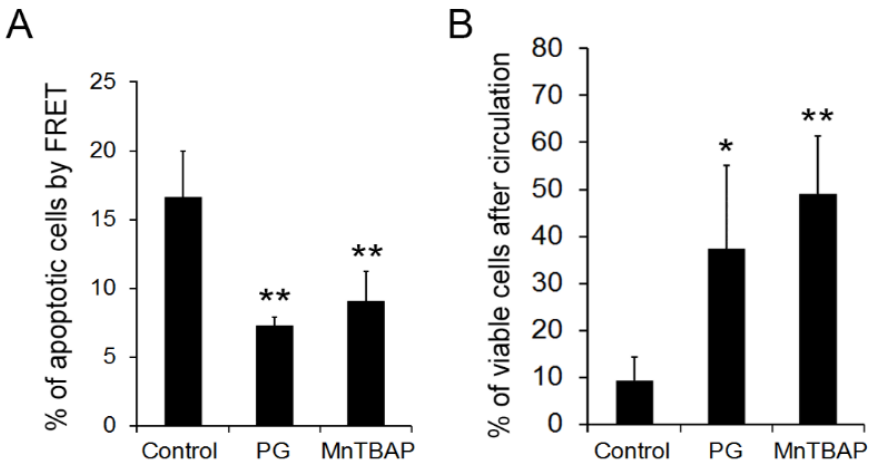

Figure 4-26. Antioxidant compounds protect circulating MCF7-C3 cells. MCF7-C3 cells were pre-treated with or without the antioxidant PG (20 μM) or MnTBAP (100 μM) and circulated for 18 h. (A) Apoptotic rates were measured in sensor cells by FRET imaging. (B) The viability of MCF7-C3 cells from A was quantified using the MTT assay. The results represent the mean ± SD from three independent experiments. *p<0.05 and **p<0.01 by Student's t test vs. control.

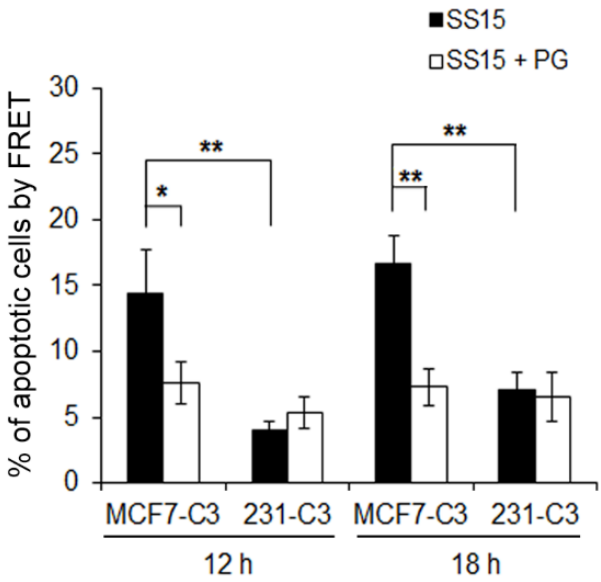

Figure 4-27. Antioxidant PG displayed less protection effect in 231-C3 cells. Both cell lines were circulated for 12 and 18 h with or without antioxidant PG (20 μM). Apoptotic rates of both cells were quantified by FRET imaging. The results represent the mean ± SD from three independent experiments. *p<0.05 and **p<0.01 by Student's t test.

ATTENTION: The Singapore Copyright Act applies to the use of this document. Nanyang Technological University Library

4.3 Discussion

Majority of CTCs are eliminated by the bloodstream [55], but a small portion of breast cancer cells are able to survive and develop distant metastases in approximately 10-15% of breast cancer patients within 3 years [41]. Despite the importance of these metastatic CTCs, little is known about the effects of shear flow on the viability of CTCs [133] as well as the molecular mechanism in which metastatic CTCs survive in circulation. This study addresses the above questions by facilitating the use of integrative model systems.

In contrast to previous CTCs studies in which necrotic cell death was measured based on cell membrane integrity [42, 278, 286, 289, 300], I investigated the apoptotic effects exerted by the bloodstream on metastatic cancer cells as they frequently resist programmed cell death or apoptosis [301]. In this study, a FRET-based caspase senor [154] was employed for real-time detection of apoptosis in the circulatory conditions. This type of real-time detection of apoptosis at the single cell level in fresh animal tissues cannot be achieved by conventional apoptotic assays, including immunostaining using anti-caspase-3 antibody, TUNEL assays and labeling with fluorescent dyes, such as Hoechst 33342. Although fluorescent proteins such as GFP and RFP (red fluorescence protein) are widely used to locate cancer cells during metastasis in nude mice, they are less frequently used to detect apoptotic cells *in vivo*, as it is not easy to observe nuclear fragmentation of cells in animal tissues [302-306]. With the FRET sensor cells, apoptosis can be readily visualized by observing the change of color from green to blue in response to caspase activation in FRET images.

Three *in vitro* and *in vivo* models were utilized to study the survivability of CTCs *in situ*, including an experimental metastatic mouse model [302, 305, 307], a zebrafish

ATTENTION: The Singapore Copyright Act applies to the use of this document. Nanyang Technological University Library

tumor model [78, 308] and a novel *in vitro* microfluidic system. In contrast to previous *in vitro* models which only focus on achieving the vascular shear stress in corn-plate viscometers [289, 309, 310] or syringe needles [42], our circulatory microfluidic system can mimic multiple parameters of the blood circulatory system, such as a pulsatile shear stress, an average heartbeat rate, the typical length and diameter of a blood vessel, and a normal body temperature. More importantly, after circulation in the microfluidic system, survived cells can be collected for further molecular analyses, which is not achievable in traditional animal models or other shear stress-mimicking systems. Extensive investigation of fluid shear stress on cancer cells survival during and after circulation could be performed through this circulatory microfluidic system.

MCF7-C3 cells representing cancer cells with a lower metastatic potential, were eliminated rapidly in the blood circulation of nude mouse and zebrafish, which was contributed by over 30% of apoptosis in 24 h. In the microfluidic system, fluid shear stress as a single factor induced apoptosis and eliminated MCF7-C3 cells within 18 h. These results provide direct evidence to the notion that apoptosis significantly contributes to the destruction of CTCs in breast cancer patients [311] and associates with the dormancy state of CTCs [312]. Mitochondria function as a mechanosensor of fluid shear stress to trigger CTCs for apoptosis. Because mitochondria are localized along the microtubules, they can be affected by the dynamic changes of the cytoskeleton structures [313]. When shear forces act on CTCs, the most toxic ROS, superoxide molecules, are immediately accumulated in the mitochondria (<1 h), and subsequently caused mitochondrial fragmentation (1-3 h), loss of MMP (3-6 h) and caspase-dependent apoptotic events (12-18 h) (Figure 4-27). Mitochondrial ROS-

ATTENTION: The Singapore Copyright Act applies to the use of this document. Nanyang Technological University Library

activated intrinsic apoptotic cascade is associated with the interactions of the proteins in the mitochondrial permeability transition complex [314].

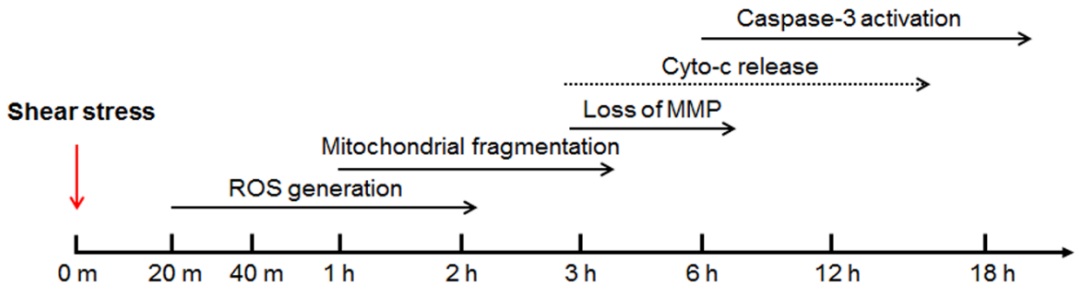

Figure 4-28. Time lines of fluid shear stress-induced cell damage.

In summary, major finding in this chapter include:

1. Apoptosis played a major role in the elimination of CTCs in nude mice and zebrafish. Metastatic breast cancer cells are more resistant to apoptosis induced by the blood stream and therefore have higher potential to survive and form distant metastasis.
2. Physiological shear stress in the bloodstream triggered apoptosis of CTCs by elevating the levels of ROS in both metastatic and non-metastatic cancer cells in circulation.
3. Excessive superoxide generation induced by fluid shear stress damages mitochondria and causes caspase-dependent apoptosis of CTCs.
4. This elevated level of ROS may be more harmful to non-metastatic cells, as they have lower levels of antioxidant scavengers. Antioxidant chemicals can protect CTCs from fluid shear stress-induced apoptosis.

ATTENTION: The Singapore Copyright Act applies to the use of this document. Nanyang Technological University Library

CHAPTER 5 Downregulating MnSOD to Sensitize CTCs to Hemodynamic Shear Stress-induced Apoptosis and Adjuvant Therapy with Doxorubicin

5.1 Introduction

Preventing metastasis is the biggest challenge in cancer treatment. However, metastatic tumor cells do not respond well to conventional treatments and often develop resistance [315]. The disease is thus progressive and prognoses are often poor. Breast cancer–specific mortality is caused almost exclusively by metastatic disease. However, breast cancer is potentially curable as long as the cancer remains localized to the breast and regional nodes. Eliminating CTCs within the bloodstream is thus the key challenge in breast cancer treatment, since treatment becomes merely palliative once the disease disseminates further than the breast and regional nodes. The relative 5-year survival rates of women with metastatic breast cancer is 22%, compared to 72% in those with Stage III disease. Therefore, novel therapeutics to eliminate CTCs will translate into a very significant survival gain.

Cancer cells gain access into circulation by either actively invading into nearby lymphatic vessels [34] as well as capillaries or passively falling into the bloodstream via leaky blood vessels formed during angiogenesis [316] or during surgery [317]. Once cancer cells enter the bloodstream, they are susceptible to several death mechanisms such as anoikis [282] and immune-mediated destruction [318]. Another important death mechanism is hemodynamic shear stresses [133] which are generated from the blood flow and from collisions between cells in the blood and endothelial cells lining the vessel wall [319]. Hemodynamic shear stresses range from 0.5 to 4.0

ATTENTION: The Singapore Copyright Act applies to the use of this document. Nanyang Technological University Library

dyne cm^{-2} in venous circulation and 4.0 to 30.0 dyne cm^{-2} in arterial circulation [295]. Most CTCs are destroyed when they are exposed to blood circulation, however, the underlying mechanisms of hemodynamic shear flow in killing CTCs remain unclear [133]. Elucidating the effect of shear flow on CTCs will provide new insights on how CTCs survive this stress and travel to distant sites where they establish metastatic colonies [55].

Moreover, the experienced shear stress may confer some resistance to chemotherapy upon the survival CTCs. Current guidelines to breast cancer treatment recommend adjuvant systemic therapy following surgical resection of the primary tumor to target micrometastasis and CTCs. Anthracycline-based chemotherapy regimens are among the first recommended regimens and among them, doxorubicin (DOX) [320] is one of the commonly used agents. In spite of such treatments, distant disease recurrence often occurs. This has been postulated to be a consequence of tumor resistance to conventional treatments – a hypothesis further supported by observations that metastatic disease often responds less effectively to treatment and is associated with poor prognoses. There has been extensive research into the mechanisms contributing to DOX resistance, including the over-expression of P-glycoprotein, multidrug resistance-associate proteins [321] and anti-apoptotic proteins Bcl-2, Bcl-xL [142, 322, 323]. However, they fail to explain why treatment efficacy to DOX in metastatic cancers is only half of those observed in the primary tumors [320, 324]. I therefore hypothesized that there may be an association between the metastatic potential and treatment resistance within breast cancers.

Reactive oxygen species (ROS) is a potential trigger of apoptosis that can link hemodynamic shear stress together with DOX treatment. Our previous studies

ATTENTION: The Singapore Copyright Act applies to the use of this document. Nanyang Technological University Library

demonstrated that shear stress induced apoptosis of endothelial cells under pulsatile shear stress by damaging the mitochondria and generating ROS [172-174]. Besides inhibiting DNA topoisomerase II, DOX also damage cells by triggering the production of ROS, including superoxide [248, 325] and hydroxyl radicals [326].

MnSOD is the most important antioxidant enzyme in cells, which scavenges the excessive ROS in the mitochondria [327]. High levels of MnSOD expression were detected in clinical samples of several metastatic cancers, including breast [228], gastric [226, 227] and colorectal cancers [227], rendering MnSOD a potential metastatic marker. Overexpression of MnSOD also promoted the survival of cancer cells in the presence of tumor necrosis factor (TNF) [328], interleukin-1 (IL-1), anticancer drugs, ionizing radiation [329] or under anoikis condition [330]. However, the mechanisms by which MnSOD is elevated in metastatic tumors and whether high levels of MnSOD can promote breast cancer metastasis and their drug resistance during adjuvant systemic therapy remain a mystery.

ATTENTION: The Singapore Copyright Act applies to the use of this document. Nanyang Technological University Library

5.2 Results

5.2.1 Metastatic Breast Cancer Cell Line Express Higher Level of MnSOD

In chapter 4, I revealed that metastatic 231-C3 cells are more resistant to fluid shear stress-induced mitochondrial damage and apoptosis than non-metastatic MCF7-C3 cells. The results also showed that anti-oxidant agents PG and SOD mimetic MnTBAP could protect MCF7-C3 cells from fluid shear stress-induced oxidative stresses and apoptosis, while a SOD inhibitor 2-ME significantly sensitized MDA-MB-231 cells to fluid shear stress-induced mitochondrial damage. In considering that superoxide was the initiate ROS generated in mitochondrial stimulated by fluid shear stress, I hypothesized that antioxidant enzyme superoxide dismutase may be associated with the resistance of metastatic 231-C3 cells against fluid shear stress. I next evaluated cellular levels of two known superoxide dismutases, mitochondrial MnSOD and cytosolic CuZnSOD. MnSOD levels were 2.6-fold higher in metastatic 231-C3 cells compared to non-metastatic MCF7-C3 cells, while CuZnSOD levels were similar. Neither MnSOD nor CuZnSOD levels were enhanced after 12 h circulation (Figure 5-1).

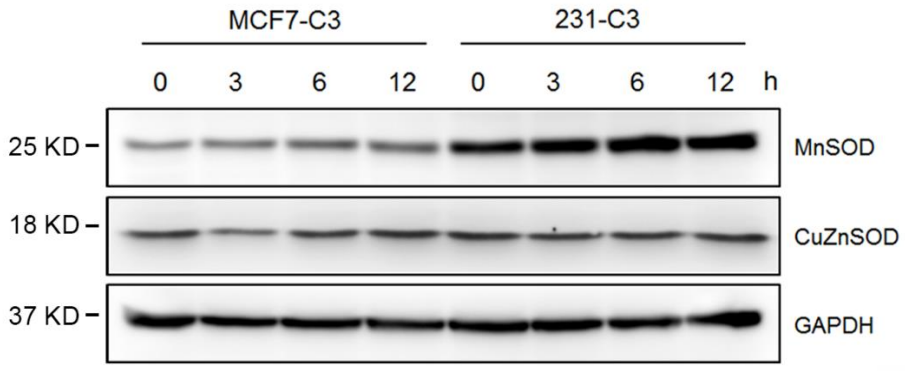

Figure 5-1. Western blot analysis of two superoxide dismutases. MCF7-C3 and 231-C3 cells were circulated for 0, 3, 6, 12 h in the circulatory microfluidic system. Levels of CuZnSOD and MnSOD before and after circulation were measured by Western blotting. GAPDH was used as an input control.

ATTENTION: The Singapore Copyright Act applies to the use of this document. Nanyang Technological University Library

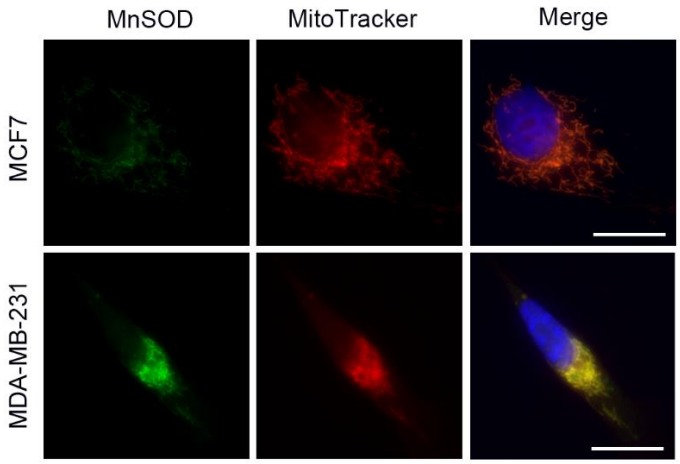

Figure 5-2. Co-localization of MnSOD and MitoTracker in MCF7 and MDA-MB-231 cells. MnSOD was revealed by immunostaining with FITC-conjugated secondary antibody. Mitochondrion was stained with MitoTracker (Red) and nuclear was labelled with Hoechst 33342 (Blue).

5.2.2 Higher Level of MnSOD Protect Metastatic Cells against Shear Force

As MnSOD is localized in the mitochondria (Figure 5-2), higher expression levels of this enzyme can protect 231-C3 cells from oxidative stress during circulation. To confirm the key role of MnSOD in protecting CTCs from shear stress-mediated apoptosis, the expression of MnSOD was knocked down in 231-C3 cells by transfection with MnSOD-specific siRNA (siMnSOD) (Figure 5-3). Silencing MnSOD in 231-C3 cells resulted in a significant increase in apoptosis (16.1 ± 2.6% compared to 6.5 ± 0.7% in cells transfected with negative siRNA (siNeg)) and a corresponding drop in cell viability (32.0 ± 15.0 % compared to 66.9 ± 6.9% in the siNeg control group) following treatment with a fluid shear stress of 15 dyne cm^{-2} for 18 h. A similar effect was achieved by treating 231-C3 cells with the SOD inhibitor 2-ME (Figure 5-4A and B).

ATTENTION: The Singapore Copyright Act applies to the use of this document. Nanyang Technological University Library

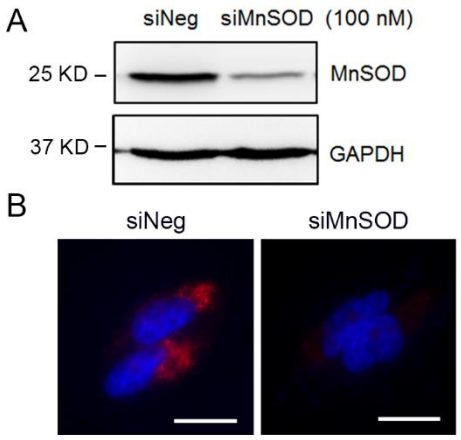

Figure 5-3. Silencing the expression of MnSOD by siRNA in 231-C3 cells. The expression levels of MnSOD in 231-C3 cells transfected with MnSOD specific siRNA (siMnSOD, 20 nM) or negative control siRNA (siNeg) were analyzed by Western blotting (A) and immunofluorescence staining (B). Scale bars, 10 μm.

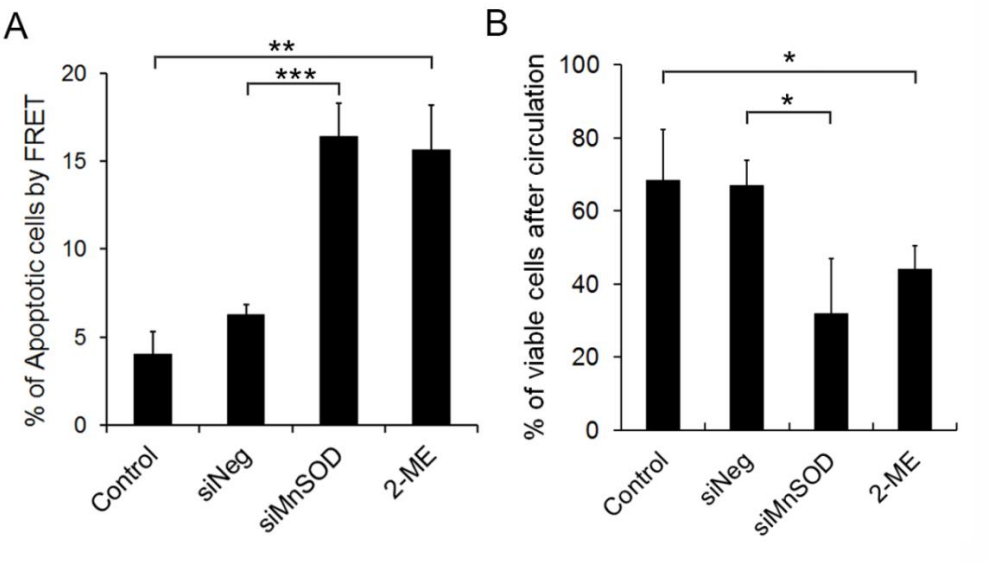

Figure 5-4. Downregulation of MnSOD sensitized 231-C3 cells to fluid shear stress-induced apoptosis. After silencing MnSOD or inhibiting MnSOD activity by pre-treating 231-C3 cells with 20 μM 2-ME, cells were circulated for 18 h. Their apoptotic rates were quantified by FRET imaging (A) and viability was quantified using the MTT assay (B).

ATTENTION: The Singapore Copyright Act applies to the use of this document. Nanyang Technological University Library

5.2.3 Overexpression of MnSOD in Non-Metastatic Cells Reduce Apoptosis and Enhance Their Survival in Circulation

I also overexpressed MnSOD in MCF7-C3 cells by transiently transfecting cells with a MnSOD plasmid (Figure 5-5). Consequently, overexpression of MnSOD in MCF7-C3 cells resulted in a significant reduction in apoptosis (6.7 ±1.8% compared to 18.1 ± 6.0% in cells transfected with a vector plasmid) and increased viability in circulation (21.7 ±4.0% compared to 8.1 ±1.0% in the vector control group, Figure 5-6A and B).

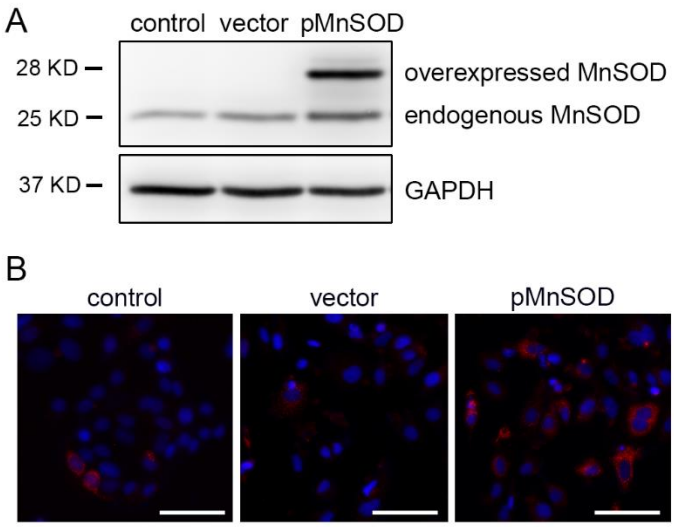

Figure 5-5. Overexpress MnSOD in MCF7-C3 cells by transient transfection. The expression levels of MnSOD in MCF7-C3 cells transfected with MnSOD plasmid or vector alone were analyzed by Western blotting (A) and IF (B). Scale bars, 100 μm.

ATTENTION: The Singapore Copyright Act applies to the use of this document. Nanyang Technological University Library

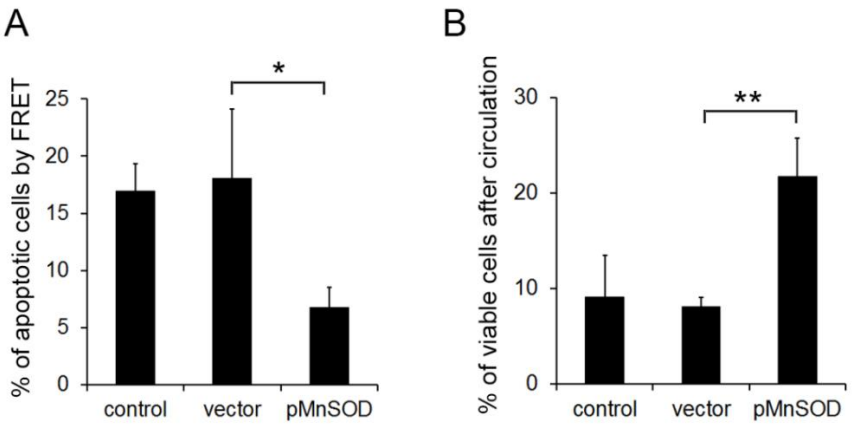

Figure 5-6. MnSOD overexpression protected MCF7-C3 cells from fluid shear stress-induced apoptosis. 24 h after transfection, cells were circulated for 18 h and their apoptotic rates were quantified by FRET imaging. (B) The viability of MCF7-C3 cells was quantified using the MTT assay.

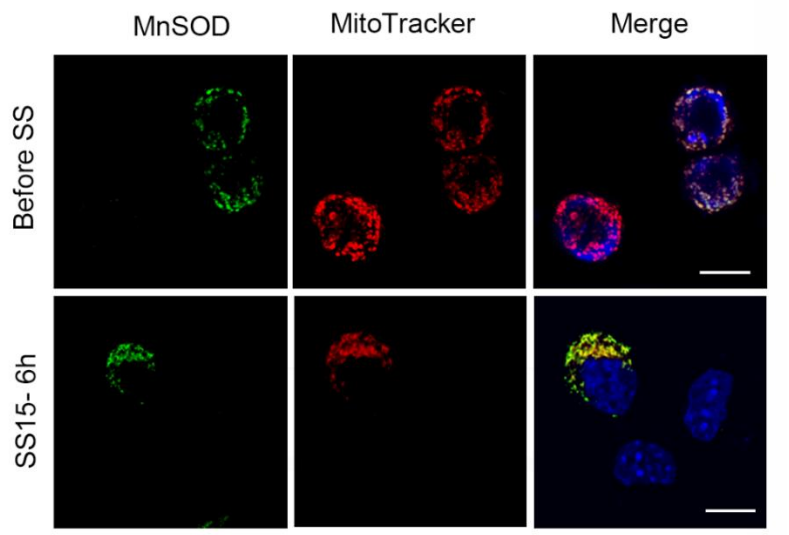

Figure 5-7. High expression level of MnSOD in rare MCF7 cells protected them from mitochondrial damage. MnSOD was stained with FITC-conjugated secondary antibody (green). Mitochondrial integrity was indicated by MitoTracker staining (red). Nuclear was labelled with Hoechst 33342 (blue). After 6 h circulation, some cells lost their mitochondrial integrity. Scale bars, 10 μm.

ATTENTION: The Singapore Copyright Act applies to the use of this document. Nanyang Technological University Library

5.2.4 Successfully Survived MCF7-C3 Cells Displayed High Level and Stable Expression of MnSOD

More interestingly, MnSOD expression was greatly heterogeneous among individual MCF7 cells. IF staining showed that most MCF7-C3 cells were MnSOD negative while only a small portion of the cells had high levels of MnSOD (Figure 5-5B). These MnSOD positive cells were able to maintain normal morphologies and retained their MMPs after 6 h circulation (Figure 5-7), and survive after 18 h circulation. I collected these survived MCF7-C3 cells as a new cell line MCF7-S1. After approximately one-month culture, the MCF7-S1 cells still displayed high levels and stable expression of MnSOD (Figure 5-8). Additionally, MCF7-S1 cells were more resistant to shear stress-induced apoptosis (Figure 5-9A) and survived better in circulation (Figure 5-9B). All these results suggest that MnSOD can protect CTCs from shear stress-induced mitochondrial damage and apoptosis.

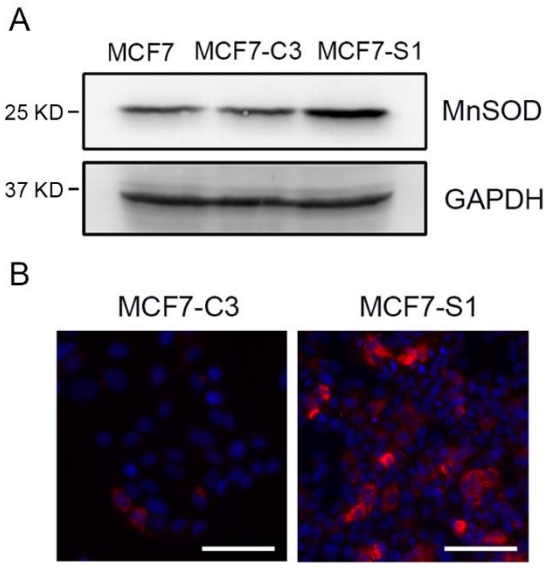

Figure 5-8. Subculture of survived MCF7-C3 cells as a new cell line MCF7-S1 from microfluidic system after 18 h circulation. The expression levels of MnSOD in MCF7, MCF7-C3 and MC7-S1 cells were analyzed by Western blotting (A) and immunostaining (B).

ATTENTION: The Singapore Copyright Act applies to the use of this document. Nanyang Technological University Library

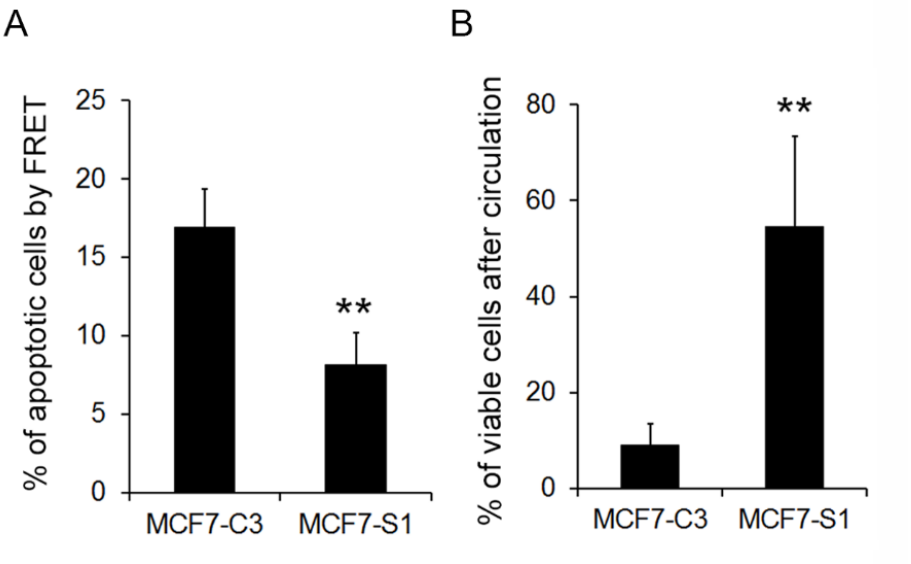

Figure 5-9. MCF7-S1 displayed stronger survivability than parental MCF7 cells in circulation by resisting apoptosis. MCF7-C3 and MCF7-S1 cells were circulated for 18 h. Their apoptotic rates were quantified by FRET imaging (A) and their viability was quantified using the MTT assay.

5.2.5 Expression of MnSOD are Heterogeneous in Xenograft Breast Tumors

Heterogeneity of MnSOD expression in breast cancer cells was further evaluated in both *in vitro* and *in vivo* samples. IHC staining revealed that MnSOD expression is heterogeneous in individual cells in xenograft tumors from mice. In MCF7 xenografts, weak to moderate staining was observed in only a few of cells. In MDA-MB-231 xenografts, MnSOD staining was more intense and in a greater proportion of cells (Figure 5-10).

ATTENTION: The Singapore Copyright Act applies to the use of this document. Nanyang Technological University Library

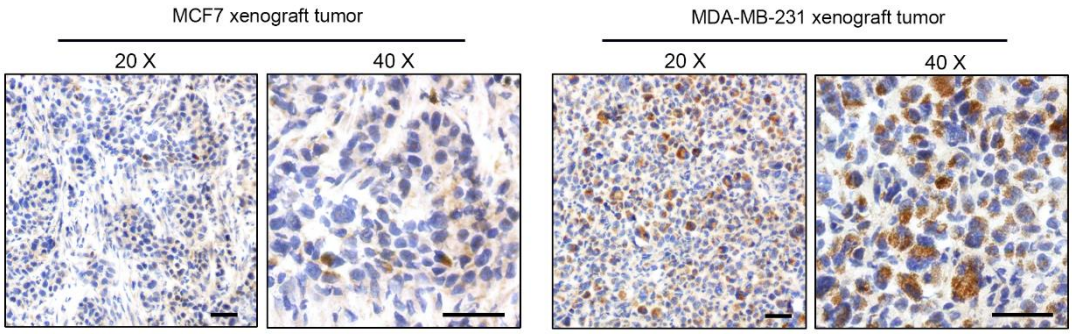

Figure 5-10. Heterogeneity of MnSOD expression in xenograft tumors. IHC staining of MnSOD was conducted on cryo-sections of the xenograft tumors of MCF7 and MDA-MB-231 from nude mice. Scale bars, 50 μm.

5.2.6 Expression of MnSOD in Breast Cancer Cell Lines are Heterogeneous

Protein levels of MnSOD were also evaluated in six breast cancer cell lines, representing different subtypes: MCF7 and T-47D (ER+/HER2-), BT474 (ER+/HER2+), SK-BR-3 (ER-/HER2+), MDA-MB-468 and MDA-MB-231 (triple negative) [331]. The immunofluorescence (IF) results showed that there is a clear heterogeneity of MnSOD expression in all six breast cancer cell lines examined (Figure 5-11). Two triple negative breast cancer cell lines (MDA-MB-468 and MDA-MB-231), which are most malignant, have the highest MnSOD expression (Figure 5-11 and 5-12). CuZnSOD was relatively similar across the cell lines (Figure 5-12).

ATTENTION: The Singapore Copyright Act applies to the use of this document. Nanyang Technological University Library

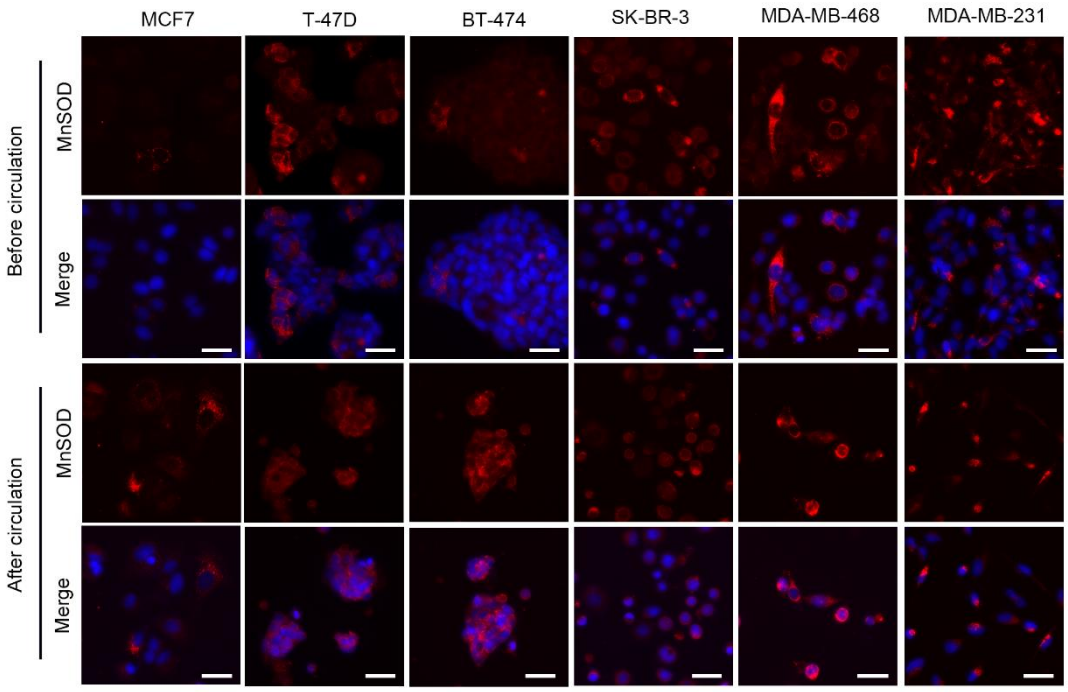

Figure 5-11. Heterogeneity of MnSOD in breast cancer cell lines before and after circulation. Immunofluorescence staining experiments of MnSOD were conducted in six breast cancer cell lines before and after 18 h of circulation. MnSOD proteins were stained in red and the nucleus was stained in blue by Hoechst 33342. Scale bars, 20 μm.

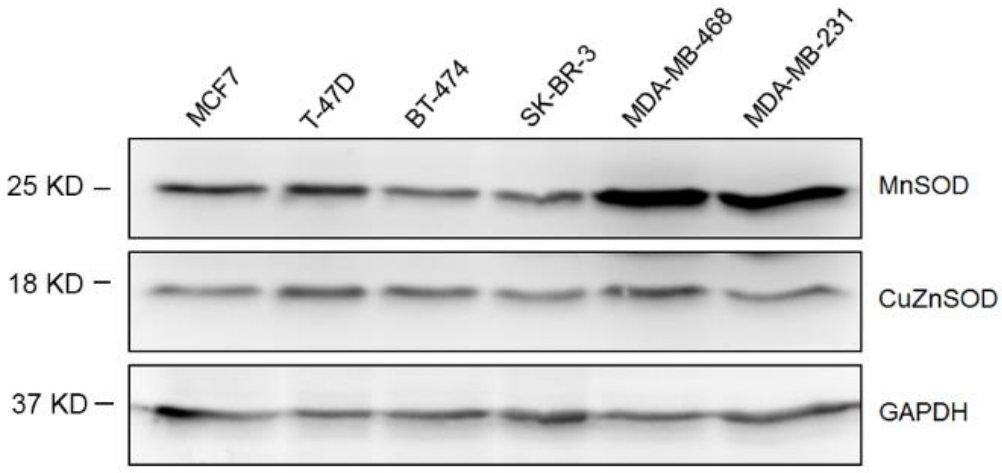

Figure 5-12. Western blot analysis of MnSOD and CuZnSOD in six breast cancer cell lines.

ATTENTION: The Singapore Copyright Act applies to the use of this document. Nanyang Technological University Library

5.2.7 MnSOD Level Determines the Survivability of Single Breast Cancer Cells in Circulation

To further establish the relationship between MnSOD levels and survival rates under shear stresses, all six breast cancer cell lines were circulated in the microfluidic system for 18 h. IF analysis showed that all survived cells were stained positive with MnSOD in contrast to the heterogeneous expression of MnSOD before circulation (Figure 5-11). Quantitative analysis showed that there is a highly positive linear correlation between the number of MnSOD positive cells before circulation and the number of viable cells after circulatory treatment (R^2 = 0.9614) (Figure 5-13). This result suggests that only the CTCs with high expression levels of MnSOD can survive the fluid shear stress-induced apoptosis in circulation.

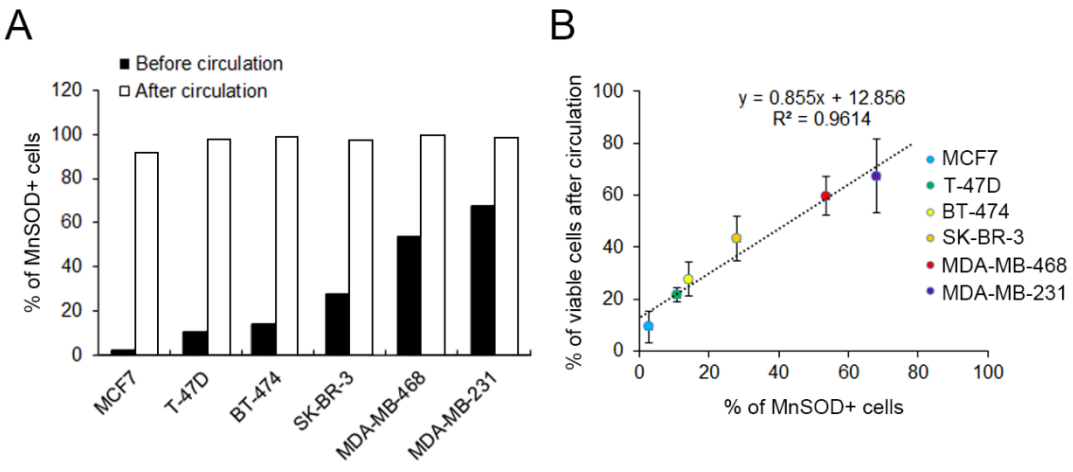

Figure 5-13 Correlation of MnSOD level with cell survivability in circulation. (A) Quantification of MnSOD positive cells before and after circulation from six breast cancer cell lines. (B) The survival rates of six breast cancer cell lines were determined using the MTT assay after circulation for 18 h in a microfluidic system. The correlation between the percentage of MnSOD-positive cells before circulation and the percentage of viable cells after circulation was illustrated using a linear curve with an R2 value of 0.9614. The results represent the mean ± SD from three independent experiments. All cells subjected to the circulatory microfluidic system in this figure were under a shear stress of 15 dyne cm^{-2}.

ATTENTION: The Singapore Copyright Act applies to the use of this document. Nanyang Technological University Library

5.2.8 Reducing MnSOD Level Suppresses the Survival of Metastatic Breast Cancer Cells in Mouse Circulation

Next, I validated the association between MnSOD level and metastasis in an experimental lung metastasis mouse model. A series of metastatic 231-C3 cells were isolated from lung metastases in nude mice after 231-C3 cells were injected into the tail vein for 45 and 90 days, respectively (Figure 5-14). The cell line derived from 231-C3 (1st generation) metastasis was named as 231-M1 (2nd generation) and the cell lines generated from 231-M1 metastatic tumors were named as 231-M1A and 231-M1B (3rd generation). After 90 days, more mice developed lung metastasis injected with 231-M1 than 231-C3 cells (Figure 5-15A and B). More importantly, the average number of lung metastatic nodules increased 14-fold from an average of 3.7 $\pm$ 0.8 nodules per mice injected with 231-C3 cells to 53.2 $\pm$ 34.6 nodules per mice injected with 231-M1 cells (Figure 5-15B and C). Consistent with our postulation that MnSOD-expressing cells are the ones that can better survive in circulation, MnSOD expression was much more intense and homogenous in lung metastasis derived from 231-M1 cells than that of 231-C3 cells in tumor tissues (Figure 5-16).

I then compared the expression levels of MnSOD between the parental 231-C3 cells and metastasis-derived cells. Western blot results showed that MnSOD level progressively increased with each generation, with the third-generation cell lines 231-M1A and 231-M1B expressing the highest levels of MnSOD (Figure 5-17A). Consistent with our results in microfluidic system, elevated level of MnSOD in metastatic cell lines were due to elimination of cells with low MnSOD level. Immunostaining analysis showed that MnSOD expression became more homogenous

ATTENTION: The Singapore Copyright Act applies to the use of this document. Nanyang Technological University Library

and almost all 231-M1A cells demonstrated strong MnSOD staining compared to the parental 231-C3 cells (Figure 5-17B).

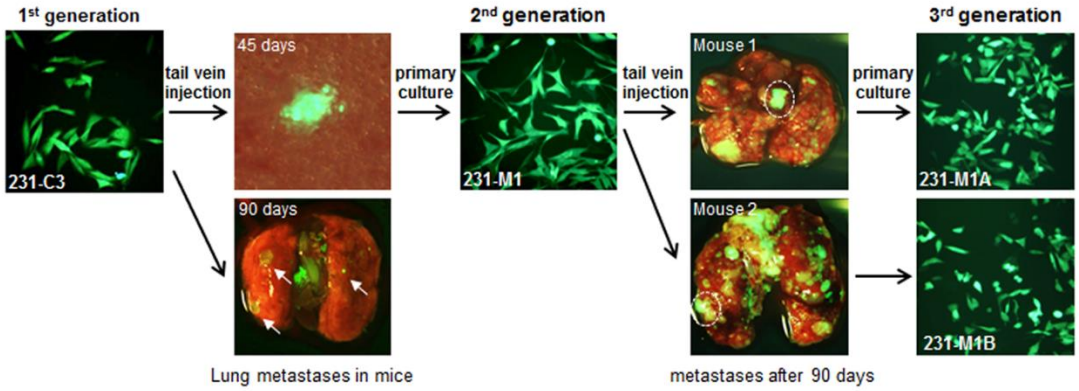

Figure 5-14. Generation of high metastatic cell lines from 231-C3 cells in a mouse model. Three generations of metastatic breast cancer cells originating from the 231-C3 sensor cells were isolated from experimental lung metastases in nude mice.

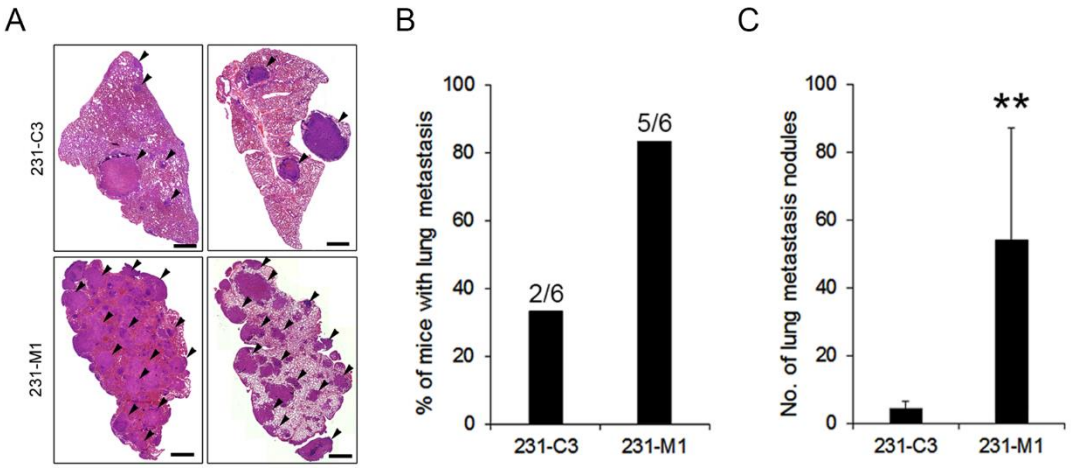

Figure 5-15. 231-M1 cells were more metastatic than 231-C3 cells in mice model. (A) Representative images of H&E staining for lung metastases (indicated by black arrows) 90 days after injection of 231-C3 or 231-M1 cells. Scale bars, 1 mm. Quantification of lung metastases from H&E staining. The percentage of mice with lung metastases was calculated by analyzing all lung leaves (left panel). The number of lung metastatic nodules was calculated from the left lobe of the lungs in all mice (n=6) (right panel). $^{**}p<0.01$ by Student's t test.

ATTENTION: The Singapore Copyright Act applies to the use of this document. Nanyang Technological University Library

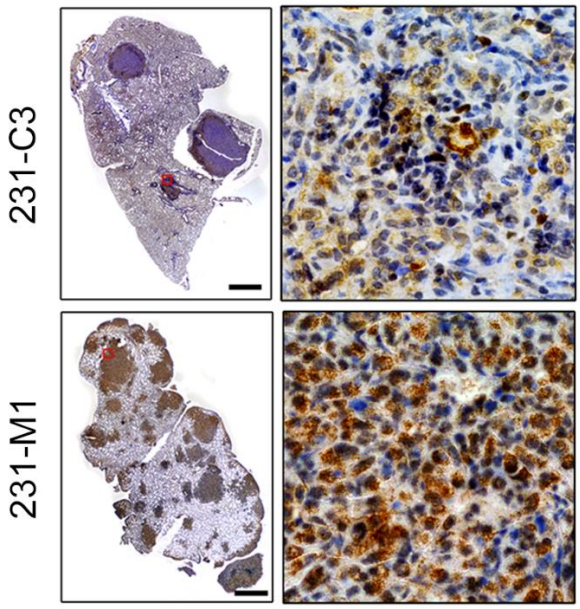

Figure 5-16. 231-M1 metastatic tumors displayed higher level and more homogenous MnSOD expression. IHC staining of MnSOD was conducted in the sections of lung tissue 90 days after intravenous injection of 231-C3 or 231-M1 cells. The left panels show the overall expression in the whole left lobe (scale bars, 1 mm) and the right panels show the enlarged details of MnSOD expression in the metastatic tumors.

Cells with high levels and homogenous expressions of MnSOD exhibited a striking correlation with strong abilities of survival and metastasis in the nude mouse tumor model. To further validate the role of MnSOD in promoting the survival and metastasis of CTCs, I reduced the expression of MnSOD in both 231-C3 and 231-M1 cells using siRNA and injected the cells into the tail veins of nude mice. When no siRNA was introduced, greater cell viability was observed in 231-M1 than 231-C3 cells from day 1 to day 4 in the lung tissues of nude mice. In particular at day 4, 5.3-fold more of 231-M1 cells were detected in each cm^2 area of lung tissue than the parental 231-C3 cells. When MnSOD expressions were knocked down (Figure 5-18A), the survival abilities of both 231-C3 and 231-M1 cells in mouse circulation were dramatically reduced 4 days after injection (Figure 5-18B and C). These results

ATTENTION: The Singapore Copyright Act applies to the use of this document. Nanyang Technological University Library

indicated that reducing MnSOD expression may potentially decrease the survival ability of metastatic breast cancer cells in circulation and suppress breast cancer metastasis.

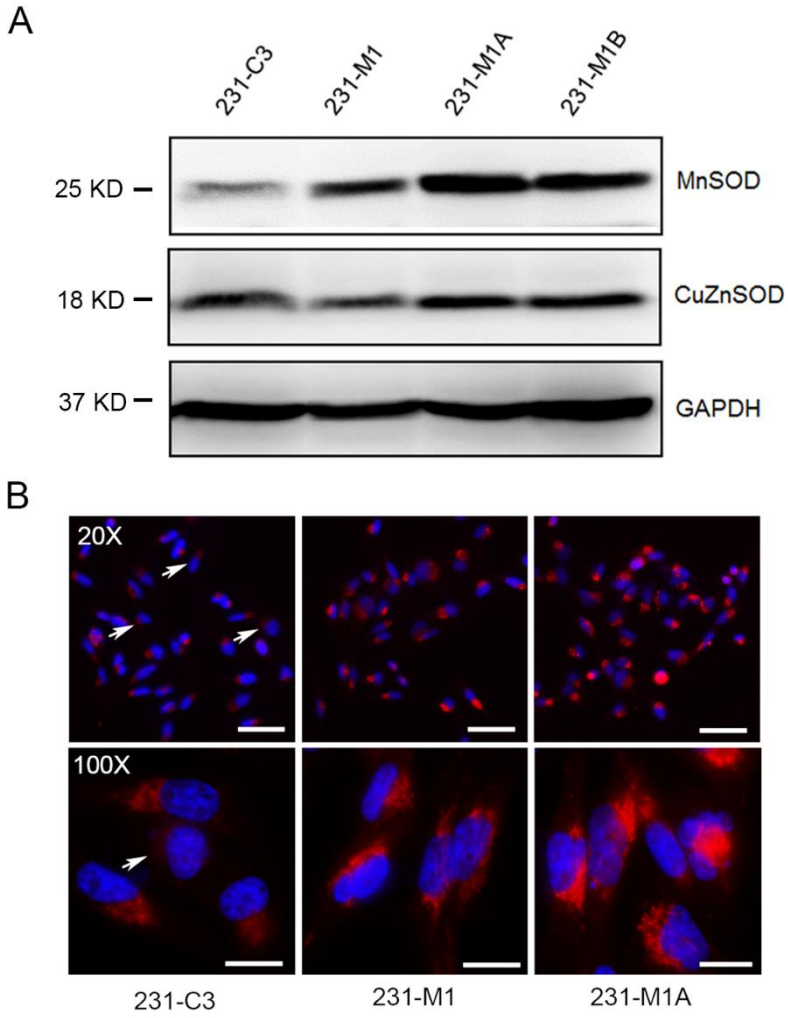

Figure 5-17. Expression levels of MnSOD in three generations of metastatic cell lines. (A) The expressions of MnSOD and CuZnSOD in three generations of 231-C3 family of metastatic cell lines were compared by Western blot analysis. GAPDH was used as an input control. (B) IF staining of MnSOD in three generations of 231 family of metastatic cell lines. The upper panels show overall expression level in the cells observed with a 20 ×objective (scale bars, 50 μm). The lower panels show the details of MnSOD in cells observed with a 100 × objective (scale bars, 10 μm). Cells with low levels of MnSOD are indicated by white arrows.

ATTENTION: The Singapore Copyright Act applies to the use of this document. Nanyang Technological University Library

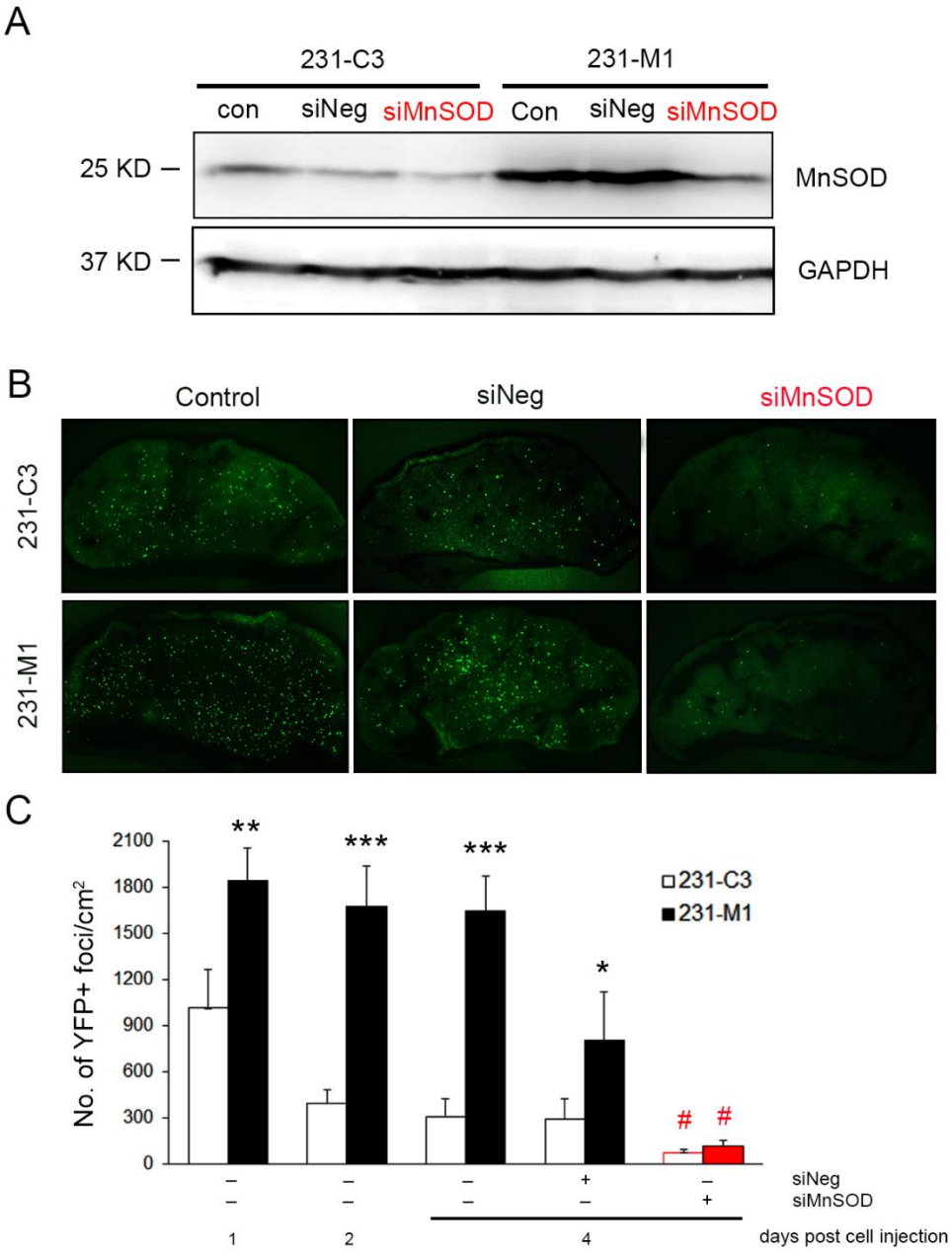

Figure 5-18. Knocking-down MnSOD reduced the survival of metastatic cancer cells in mouse circulation. (A) Western blot assay of MnSOD expression after transfection with negative siRNA (siNeg) or MnSOD siRNA (siMnSOD). (B) Representative images of 231-C3 and 231-M1 cells on the lung surface 4 days after injection with or without siRNA transfection. (C) Quantification of YFP-positive foci on the lung surface from 1-4 days with or without siRNA transfection (n = 5).

ATTENTION: The Singapore Copyright Act applies to the use of this document. Nanyang Technological University Library

5.2.9 Reducing MnSOD Levels Sensitize Metastatic Breast Cancer Cells to Doxorubicin Treatment

The parental 231-C3 cells were selected within the blood circulation to obtain metastatic cells with high levels of MnSOD. I postulated that these tumor cells have stronger ability to handle oxidative stress, and thus develop resistance to ROS generating agents such as doxorubicin and radiation therapy.

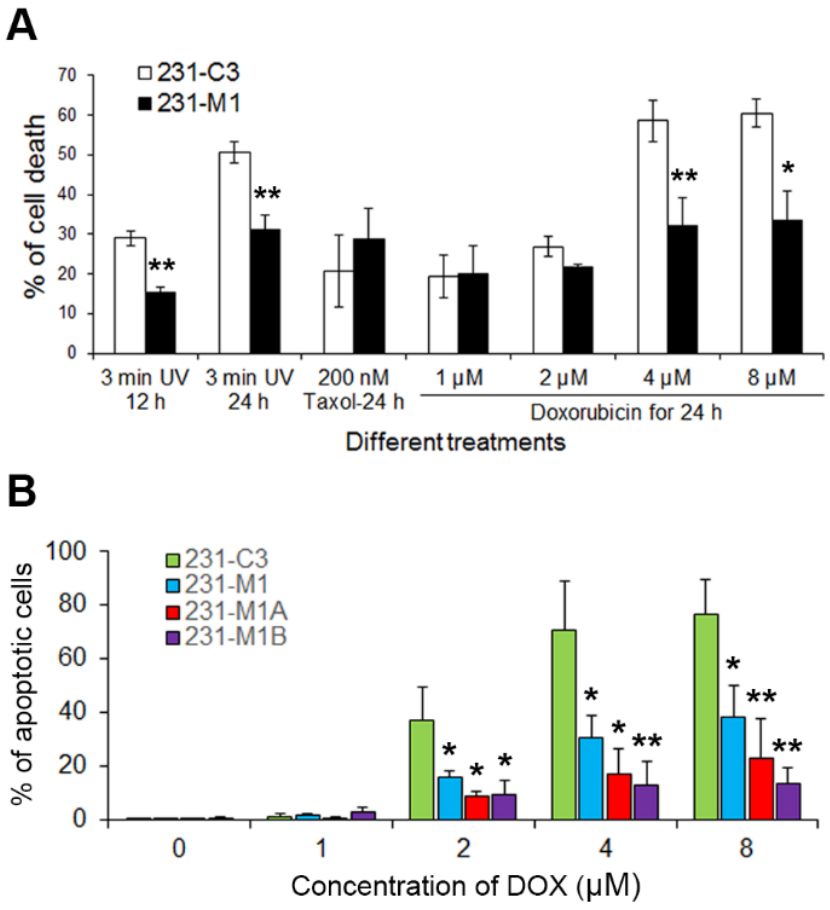

Figure 5-19. Metastatic cancer cells are more resistant to treatment with redox agents. (A) 231-C3 and 231-M1 cells were treated with 3 min UV irradiation, 200 nM of Taxol and doxorubicin in concentrations of 1, 2, 4 and 8 μM. After 12 or 24 h, the percentages of cell death were measured using MTT assay. (B) Apoptotic rates of 231-C3, 231-M1, 231-M1A and 231-M1B cell lines were quantified from FRET imaging following treatment with 0, 1, 2, 4, 8 μM of doxorubicin for 24 h.

ATTENTION: The Singapore Copyright Act applies to the use of this document. Nanyang Technological University Library

To test this hypothesis, I treated 231-C3 and 231-M1 cells with UV-irradiation, doxorubicin and Taxol. As shown in Figure 5-19A, 231-M1 cells displayed stronger resistance to UV and doxorubicin treatment than 231-C3 cells, while Taxol, which did not generate ROS directly, displayed no significant difference in the percentage of cell death in both cell lines. I further compared doxorubicin resistance between the three generations of 231-C3 cells. Apoptotic rates was decreased in 231-M1, 231-M1A and M1B cells compared with the parental cell line 231-C3 (Figure 5-19B). In particular, 76.7 ± 12.9 % of apoptotic 231-C3 cells were detected after 24 h's treatment with 8 μM doxorubicin. While only 38.3 ± 12.0% of 231-M1 cells, 22.8 ± 14.9 % of 231-M1A and 13.3 ± 6.3% of 231-M1B cells were undergoing apoptosis.

Doxorubicin was able to generate superoxide within 1 h (Figure 5-20A) and damage mitochondria in 3-6 h (Figure 5-20B). Cells with mitochondrial damage lost their MMP and underwent caspase-3 dependent apoptosis after 12 h (Figure 5-20B).

To understand the role of MnSOD in mediating doxorubicin resistance, MnSOD was knocked down by specific siRNA. All four cell lines were sensitized to doxorubicin treatment after siRNA transfection (Figure 5-21). In all four cell lines, 60-80% cells underwent apoptosis when treated with 4 μM doxorubicin for 24 h (Figure 5-21A and B). Even at 2 μM, which is near the plasma concentration of doxorubicin in cancer patients after 6 h of administration, doxorubicin successfully induced over 50% of apoptosis (Figure 5-21B) and reduced cell viability to less than 20% in all four cell lines (Figure 5-22). These results prove that high levels of MnSOD neutralize the therapeutic effects of doxorubicin and downregulating the expression of MnSOD can sensitize metastatic breast cancer cells to doxorubicin treatment.

ATTENTION: The Singapore Copyright Act applies to the use of this document. Nanyang Technological University Library

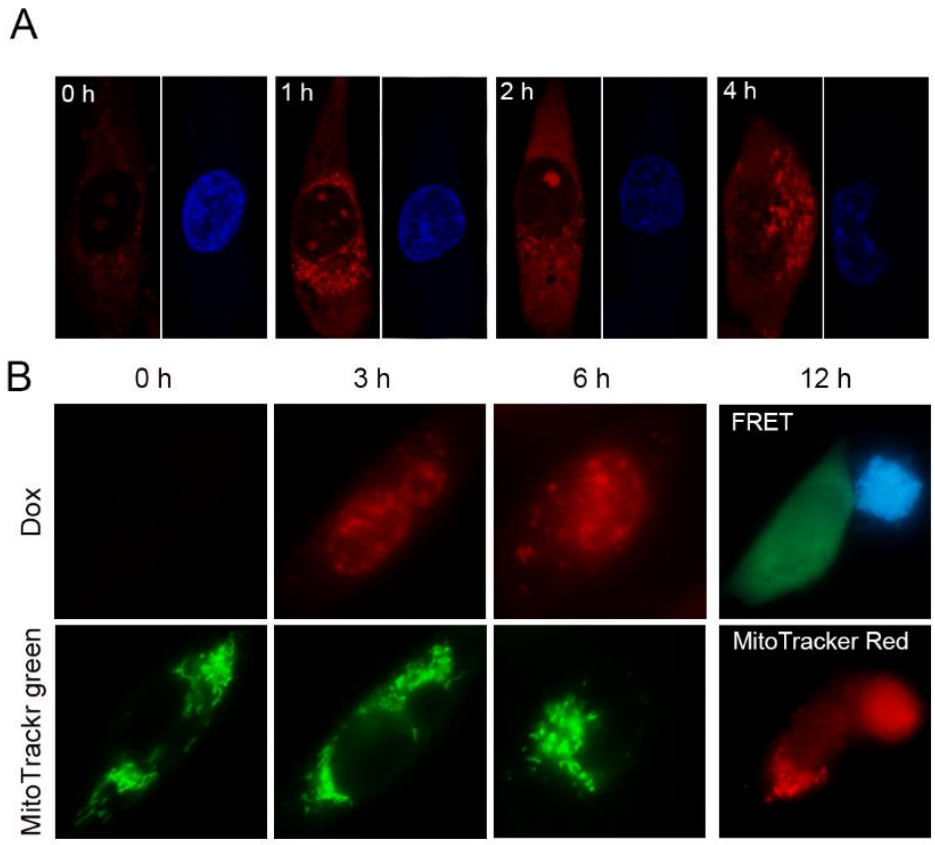

Figure 5-20. Doxorubicin generates superoxide in mitochondrial and induces mitochondrial damage. (A) After treatment with 4 μM doxorubicin for 0, 1, 2, 4 h, generation of mitochondrial superoxide in MDA-MB-231 cells was detected by 5 μM mitoSOX. The nucleus was stained with 1 μg ml^{-1} Hoechst 33342 (blue). (B) Mitochondrial morphologies of MDA-MB-231 cells were imaged with 100 nM MitoTracker Green (green) following treatment with 4 μM doxorubicin for 0, 3 and 6 h. Mitochondrial morphologies of 231-C3 cells were imaged with MitoTracker Red (100 nM) following treatment with 4 μM doxorubicin for 12 h. Live cell (green) and apoptotic cell (blue) were assessed by FERT imaging.

ATTENTION: The Singapore Copyright Act applies to the use of this document. Nanyang Technological University Library

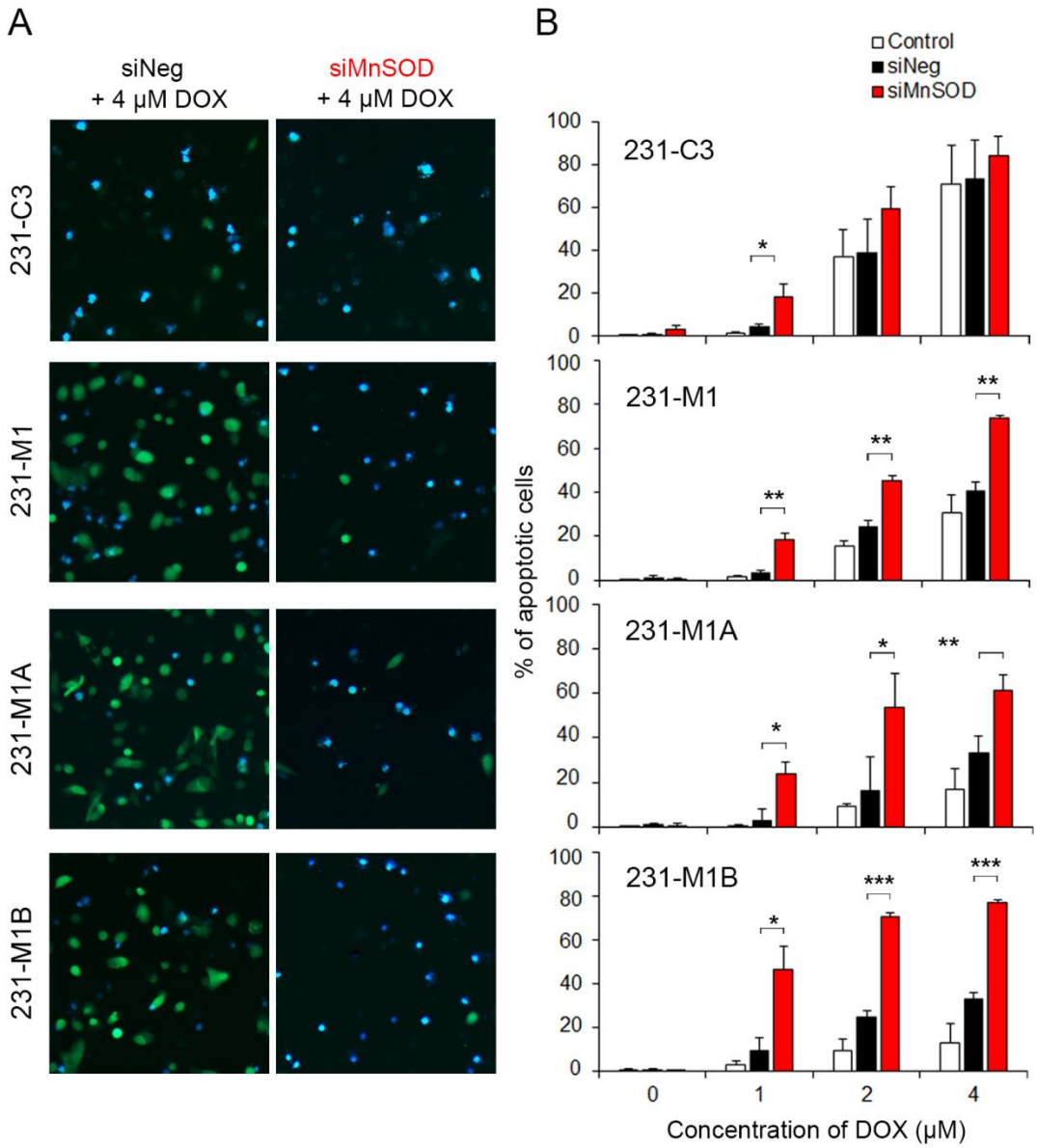

Figure 5-21. Silencing MnSOD sensitizes metastatic cells to doxorubicin-induced apoptosis. (A) 231-C3, 231-M1, 231-M1A and 231-M1B cells were transfected with negative siRNA (siNeg) or MnSOD siRNA (siMnSOD) followed by treatment with 4 μM doxorubicin for 24 h. Apoptotic cells (blue cells) was detected by FRET imaging. (B) 231-C3, 231-M1, 231-M1A and 231-M1B cells with or without siRNA transfection were treated with 0, 1, 2, and 4 μM doxorubicin for 24 h and apoptotic rates were quantified by FRET imaging. The results represent the mean ± SD from three independent experiments. *p<0.05, **p<0.01, ***p<0.001 using Student's t test compared with the control group or as otherwise indicated in the graphs.

ATTENTION: The Singapore Copyright Act applies to the use of this document. Nanyang Technological University Library

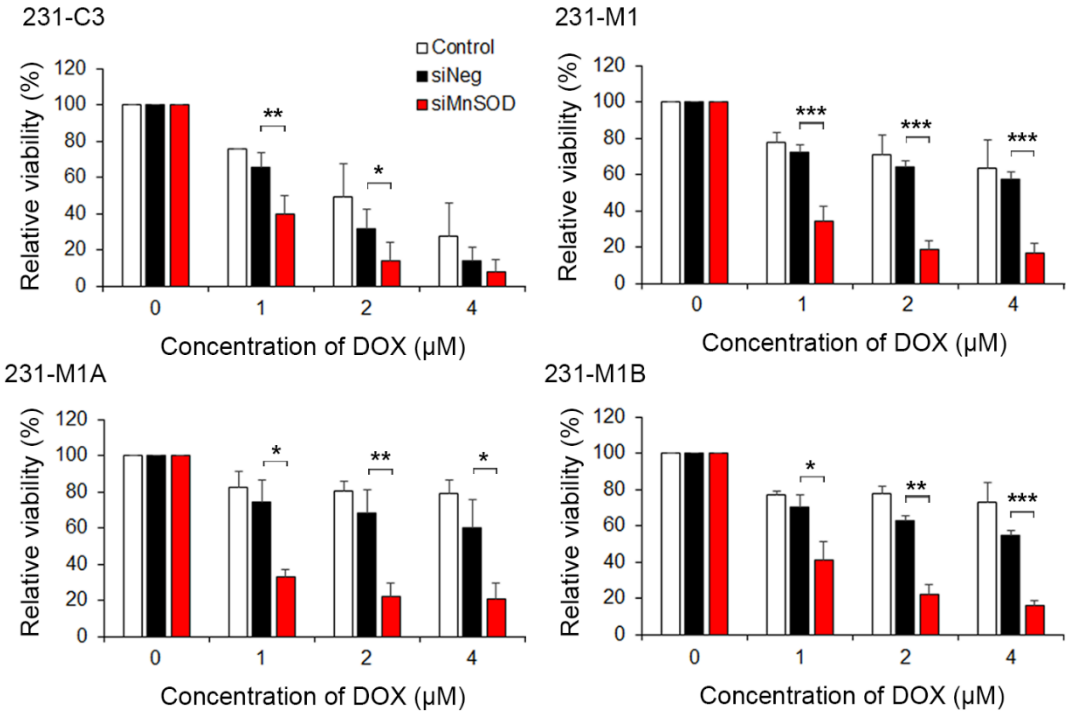

Figure 5-22. Silencing MnSOD reduces doxorubicin resistance in metastatic breast cancer cells. Relative viabilities of 231-C3, 231-M1, 231-M1A and 231-M1B cells after treatments with 0, 1, 2, 4 μM doxorubicin were analyzed using MTT assay. The results represent the mean ± SD from three independent experiments. *p<0.05, **p<0.01, ***p<0.001 using Student's t test compared with the control group or as otherwise indicated in the graphs.

5.2.10 Metastasized Human Breast Tumors Expressed More Homogenous MnSOD than Their Heterogeneous Primary Tumors after Recurrence

To investigate the clinical relevance of this study, Dr. Tan Ern Yu from Tan Tock Seng Hospital helped me to identify three cases of invasive breast cancers and provided with three pairs of formalin-fixed, paraffin-embedded (FFPE) tissue samples from both the primary tumor and the distant metastasis (Figure 5-23). All three patients were diagnosed with recurrent disease after surgical excision of the primary tumors. IHC analysis of the clinical samples revealed that some cells within the primary tumor exhibited strong MnSOD staining (red arrows) while others had

ATTENTION: The Singapore Copyright Act applies to the use of this document. Nanyang Technological University Library

weak staining of MnSOD. In contrast, high and homogenous expressions of MnSOD were observed in all three clinical samples of the metastasized tumor cells to the cervical lymph node, pleura and femur bone respectively (Figure 5-23). The patients' information is summarized in Table 5-1.

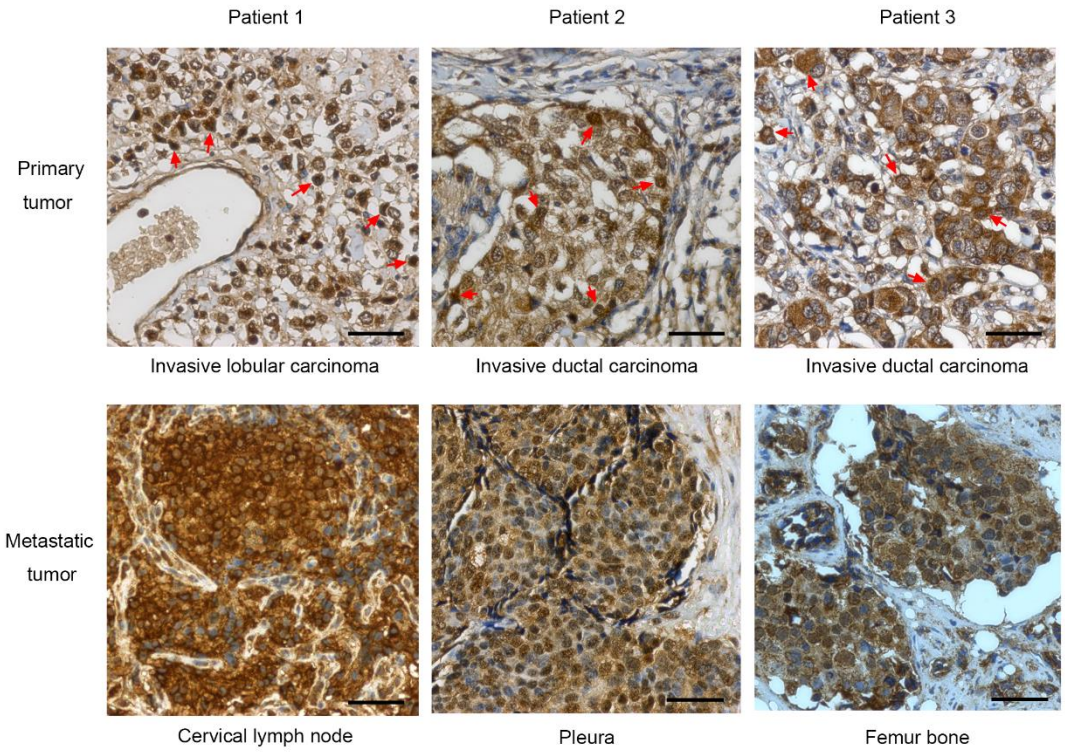

Figure 5-23. Recurrent human breast tumors display more homogenous expression pattern in metastatic sites than primary tumors. FFPE samples of primary tumors and distant recurrent metastases from three cases of invasive breast carcinoma patients were analysed for MnSOD expression by IHC staining. Cells with high levels of MnSOD expression in the primary tumors were indicated with red arrows. Scale bars, 100 μm.

ATTENTION: The Singapore Copyright Act applies to the use of this document. Nanyang Technological University Library

Table 5-1. Information of three cases of breast cancer patients with primary and metastatic tumors

Case number	Primary/ recurrent	Year of occurrence	Tumor histology	ER[1]	HER2[2]	Metastasis site
1	Primary	2009	Invasive lobular carcinoma	Positive	Negative	
	Recurrent	2012		Positive	Positive	Cervical lymph node
2	Primary	2006	Invasive ductal carcinoma with minor mucinous component	Positive	Negative	
	Recurrent	2007		Negative	Unknown	Pleura
3	Primary	2007	Invasive ductal carcinoma	Positive	Negative	
	Recurrent	2008		Unknown	Unknown	Femur bone

[1]ER: Estrogen receptor; [2]HER2: Human epidermal growth factor receptor 2.

5.3 Discussion

Here, I report a novel approach to prevent metastasis of breast cancer cells. By reducing the level of antioxidant enzyme MnSOD in metastatic CTCs, they can be sensitized to hemodynamic shear stress-induced apoptosis and adjuvant systemic therapy with doxorubicin. This new mechanism is derived from step-by-step discoveries (Figure 5-24). First, I verified that apoptosis contributed mainly to the elimination of CTCs in blood circulation, which can be resisted by metastatic breast cancer cells. Apoptosis was found to be triggered by fluid shear stress through overproduction of mitochondrial ROS, which damaged the mitochondria and initiate caspase-dependent apoptosis in CTCs. Metastatic breast cancer cells could resist apoptosis by possessing high levels of MnSOD which protected them from oxidative

ATTENTION: The Singapore Copyright Act applies to the use of this document. Nanyang Technological University Library

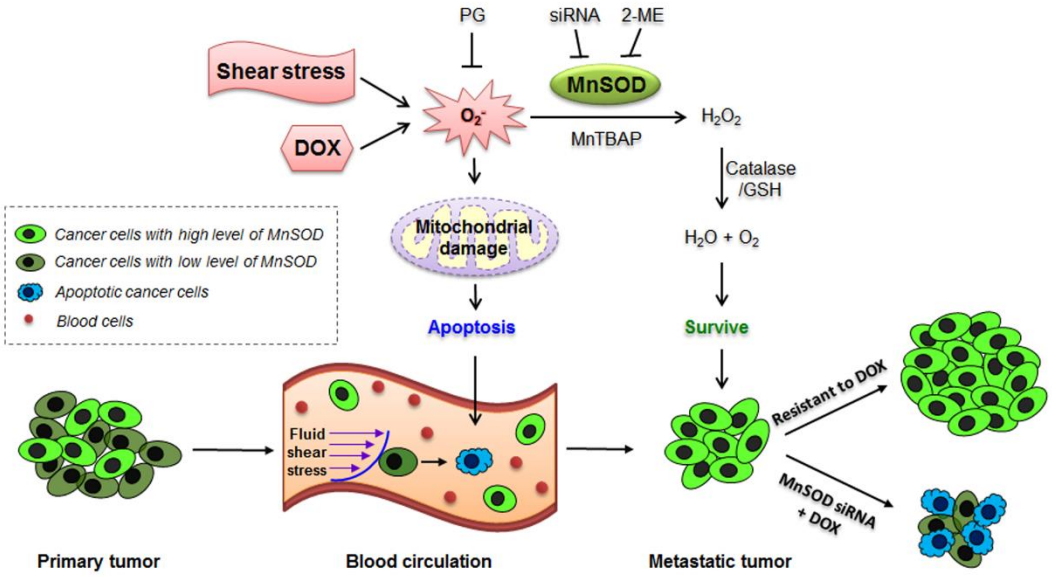

Figure 5-24. Proposed mechanism of MnSOD in promoting survival of metastatic breast cancer cells in blood circulation and drug resistance after metastasis.

stress and apoptosis induced by shear force. Second, breast cancer cells display heterogeneous levels of MnSOD. Only cells with high levels of MnSOD have the ability to survive in circulation and form secondary tumors. In addition, these high levels of MnSOD in metastatic CTCs contribute to the drug resistance of redox agent doxorubicin, a common chemotherapy drug applied in the adjuvant systemic therapy of breast cancer. By reducing the levels of MnSOD in metastatic breast cancer cells, it can not only suppress their survival in blood circulation, but also sensitize these cells to doxorubicin treatment.

ROS, including superoxide anions, hydrogen peroxide, and hydroxyl radicals, are the by-products of oxygen metabolism. They modulate cell fate and growth during metastatic progression of cancer cells under various stress conditions, such as a hypoxic environment [332, 333], cell detachment [334], shear stress [335, 336], and microenvironment interactions [332, 337]. Cells use natural detoxification systems

ATTENTION: The Singapore Copyright Act applies to the use of this document. Nanyang Technological University Library

including superoxide dismutase (SOD), catalase, and glutathione peroxidase to convert ROS into non-toxic molecules such as water and oxygen. Manganese superoxide dismutase (MnSOD) is one of the most important antioxidant enzymes, as it is localized in the mitochondria where superoxide, the most toxic type of ROS, is produced. MnSOD discomposes the mitochondrial superoxide to hydrogen peroxide, which can be further converted into water and oxygen by catalase and other antioxidant enzymes or antioxidant agents such as glutathione [205]. Overexpression of MnSOD was found to promote the survival of cancer cells under different stress conditions, such as in the presence of interleukin-1 (IL-1), tumor necrosis factor (TNF), anticancer drugs (such as doxorubicin and mitomycin C), ionizing radiation [328, 329], hyperthermia [338] and anoikis [330]. More importantly, high levels of MnSOD expression have been detected in clinical samples of several metastatic cancers, including gastric [227, 339], colorectal [227] and breast cancers [228] as well as metastatic MDA-MB-231 breast cancer cells [340, 341].

MnSOD protects metastatic CTCs from fluid shear force-induced oxidative stress and apoptosis depending on its level in the mitochondria. In the primary tumor, cancer cells are widely heterogeneous [342]. I detected remarkable heterogeneity in the MnSOD levels of individual breast cancer cells before they entered circulation. Cells with high levels of MnSOD effectively scavenged toxic superoxide, thereby preventing mitochondrial damage and subsequent apoptosis initiation. Conversely, cells with low levels of MnSOD were eliminated by circulation via apoptosis. Considering that the expression of MnSOD was not significantly upregulated by fluid shear stress at 12 h, I provide an explanation to the phenomenon that overall MnSOD

ATTENTION: The Singapore Copyright Act applies to the use of this document. Nanyang Technological University Library

level was elevated in the metastatic tumor which was also indicated by previously clinical studies [226, 228, 329].

MnSOD was considered as a tumor suppressor by earlier studies [343-345], however, several pieces of recent evidence have suggested that MnSOD can enhance the malignancy of tumor cells by promoting resistance to anoikis [330] or by sustaining the Warburg effect [346]. This study reveals a new mechanism of MnSOD in promoting cancer metastasis. Downregulation of MnSOD expression by specific siRNA or inhibiting the activity of MnSOD by SOD inhibitor, 2-ME, significantly increased apoptosis and reduced cell viability of 231-C3 cells in circulation. Conversely, overexpression of MnSOD increased the survivability of MCF7-C3 cells by reducing apoptosis. A positive correlation between the percentage of MnSOD-positive cells and their survivability against fluid shear stresses was established from six breast cancer cell lines. Furthermore, in animal experiments, the therapeutic potential of MnSOD siRNA was demonstrated by attenuating the survivability of metastatic breast cancer cells and their metastatic potential. Herein, I provide the first evidence suggesting the link between MnSOD and cancer cell survivability under hemodynamic shear stress, ultimately identifying MnSOD as a novel marker and therapeutic target for metastatic breast cancer.

Intriguingly, high expression levels of MnSOD also confer the doxorubicin resistance of metastatic breast cancer cells. When CTCs with low levels of MnSOD were eliminated, the high MnSOD levels in the survived cells also protected them against doxorubicin-induced apoptosis by removing excessive superoxide. This was strongly demonstrated when the downregulation of MnSOD levels by siRNA was able to reverse doxorubicin resistance within these highly metastatic breast cancer cells (Fig.

ATTENTION: The Singapore Copyright Act applies to the use of this document. Nanyang Technological University Library

7G). In view of the therapeutic potential of our findings, doxorubicin administration should be avoided in the adjuvant systemic therapy if the primary tumor and CTCs were diagnosed with high levels of MnSOD. A feasible strategy to eliminate these cells would be a combinatorial approach to reduce MnSOD levels before adjuvant therapy with doxorubicin, henceforth effectively killing cells by apoptosis.

As a conclusion, MnSOD can be employed as a novel prognostic marker to predict the metastatic potentials of invasive breast tumors and CTCs, and second, be used as a guideline to provide appropriate treatment recommendations. Third, MnSOD can also serve as a new molecular target in preventing breast cancer metastasis. Therapies targeting MnSOD expression or inhibiting its activity can potentially prevent the development of metastatic disease and reduce breast cancer specific mortality.

In summary, major finding in this chapter include:

1. Metastatic breast cancer cell line express higher level of antioxidant enzyme MnSOD, which scavenger excessive superoxide generation under shear stress and can protect CTCs from shear stress-mediated apoptosis.
2. Expression of MnSOD is heterogeneous in a series of breast cancer cells lines, xenograft breast tumors and human breast carcinoma samples. The MnSOD level determines the survivability of in individual breast cancer cells in circulation.
3. Reducing MnSOD level in metastatic breast cancer cells not only decrease their survivability against to shear stress-induced apoptosis in circulation, but also sensitize them to the treatment by redox-agent doxorubicin. Therefore,

ATTENTION: The Singapore Copyright Act applies to the use of this document. Nanyang Technological University Library

downregulating MnSOD have the potential to inhibit metastasis of breast cancer cells.

ATTENTION: The Singapore Copyright Act applies to the use of this document. Nanyang Technological University Library

CHAPTER 6 Identification of Molecular Markers Associated with the Survival, Proliferation and Therapy Resistance of Metastatic Breast Cancer Cells by Comparative Proteomics Analysis

6.1 Introduction

Targeting the survival of CTCs in bloodstream may reduce the malignancy and prevent the metastasis of breast cancers. Moreover, identification of the driver proteins that promote the survival of CTC will extend our understanding of metastasis-derived therapy resistance. In Chapter 5, I identified MnSOD as an important mediator of the resistance of CTCs to hemodynamic shear stress-induced apoptosis which also confer doxorubicin resistance in DTCs. MnSOD can prevent oxidative stress in the early stage. However, CTCs may also benefit from some other molecular mechanisms such as evading apoptosis by activating anti-apoptotic pathways or modifying cytoskeleton structure which can protect mitochondria from mechanical stresses.

To further elucidate the survival mechanisms of CTCs, I conducted comparative proteomics analysis in metastatic cells that were isolated from lung metastases in mouse model with the assistant from Prof. Newman Sze's laboratory in School of Biological Sciences of Nanyang Technological University. I have isolated two groups of metastatic cell lines. The first group includes three cell lines which all produce the caspase-3 sensor: (1) a breast cancer cell line derived from a micrometastasis in the lung of a mouse (231-M1), (2) a breast cancer cell line derived from a dormant tumor in the lung of a mouse (231-M2), and (3) the parental cell line of M1 and M2 derived from triple negative breast cancer MDA-MB-231 (231-C3). The second group includes three cell lines including 231-C3, 231-M1 and a more metastatic cell line of

ATTENTION: The Singapore Copyright Act applies to the use of this document. Nanyang Technological University Library

231-M1A derived from a lung macrometastases of M1 cells (add the Figure showing the 3 generations of these cell lines). As the cells from these two groups were all originated from the same TNBC MDA-MB-231 cell line and exhibited very different metastatic capacities in mouse, they can serve as valuable sources for identifying metastatic markers and improving our knowledge on how cancer cells gain metastatic abilities.

Two different proteomics analysis methods were used to compare the protein expression profiles in these metastatic breast cancer cell lines. One is the iTRAQ (isobaric tags for relative and absolute quantification) analysis, a liquid chromatography (LC)-based separation method. The other is 2D-DIGE (2 dimensional differential in-gel electrophoresis), an acrylamide gel-based method. Previous studies have compared these two proteomics methods and concluded that these two methods are complementary in nature. And their differences could result from variations in experimental procedures and sample preparation [347, 348].

ATTENTION: The Singapore Copyright Act applies to the use of this document. Nanyang Technological University Library

6.2 Results

6.2.1 Collection of Protein Samples from Micrometastasis and Dormant Metastasis-derived Cell Lines

I have isolated two metastatic breast cancer cell lines from experimental lung metastases in nude mouse model (Figure 6-1). The cell line 231-M1 was derived from a 45-day micrometastasis in lung. The other cell line 231-M2 was derived from a 120-day dormant metastasis in another mouse. 231-M1 micrometastasis was a well-developed tumor in the lung of nude mouse. However, 231-M2 metastasis was constituted with scattered sensor cells. Only some of those scattered cells were able to survive and proliferate to produce this stable cell line of 231-M2. These two cell lines displayed different growth phenotypes thus they can be used to discover new driver proteins for metastasis. The reason is that both cell lines have successfully survived from hemodynamic shear stress. Therefore, they may share the same survival factors during circulation and extravasation. On the other hand, they displayed different capacities to adapt to the new microenvironment and proliferate to become a metastatic tumor, which could due to their differences in proteins that regulate proliferation after extravasation. I therefore collect whole cell lysate from these two cell lines for comparative proteomics analysis using an iTRAQ method.

ATTENTION: The Singapore Copyright Act applies to the use of this document. Nanyang Technological University Library

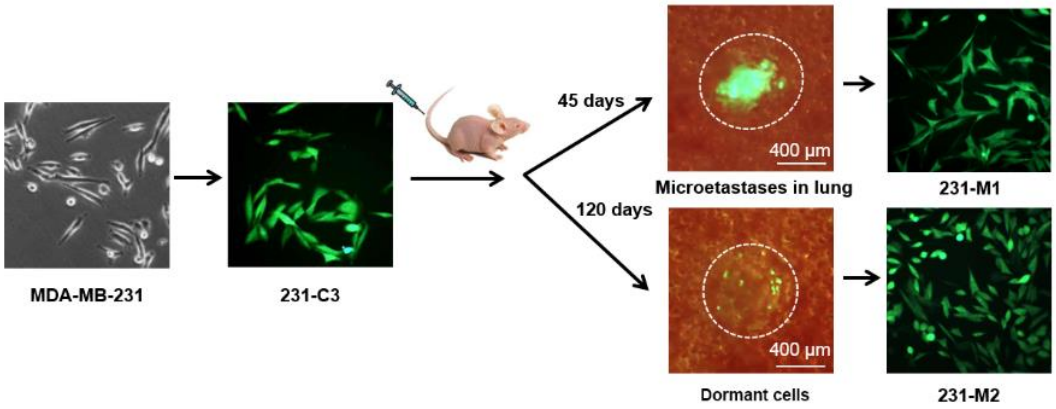

Figure 6-1. Isolation of metastatic cell lines of 231-M1 and 231-M2 from 231-C3 derived lung metastases. 231-C3 cells generated from stable transfection of C3 sensor in triple negative breast cancer cell line MDA-MB-231 were injected into the blood circulation of nude mice via tail vein. A micrometastasis formed in the lung tissue of a mouse 45 days after cell injection was isolated and cultured as 231-M1 cell. A dormant tumor formed in the lung tissue of another mouse 120 days after cell injection was isolated and cultured in vitro as 231-M2 cells.

6.2.2 Comparative Proteomics Analysis by iTRAQ Method

Comparative proteomics analysis using an iTRAQ method was conducted to compare the protein expression levels in 4 cell lines including MDA-MB-231, 231-C3, 231-M1 and 231-M2 (Figure 6-2). A total of 1362 target proteins were identified and quantified with estimated false discovery rate (FDR) of <1%. Prof. Newman Sze's laboratory employed the two stringent inclusion criteria to filter the data set: (1) at least two unique peptides with >95% confidence, and (2) unused ProtScore ≥2 corresponding to ≥99% confidence. A total of 521 proteins were quantified with high confidence. I set up a cut-off of 1.3-fold change (>1.3 or <0.77) to define up- or down-regulation of protein levels. Compared to parental 231-C3 cells, 88 proteins were found upregulated and 72 proteins were downregulated in 231-M1 cells. 231-M2 cells have 66 upregulated proteins and 49 downregulated proteins compared to 231-C3 cells (Figure

ATTENTION: The Singapore Copyright Act applies to the use of this document. Nanyang Technological University Library

6-3).

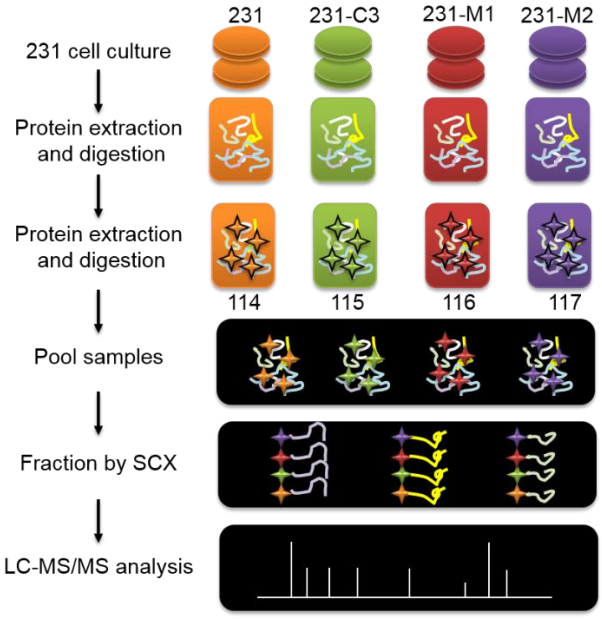

Figure 6-2. Schematic diagram of iTRAQ-based proteomics analysis workflow. The proteomics of 4 cell lines MDA-MB-231 (231), 231-C3, 231-M1 and 231-M2 was compared using iTRAQ-analysis. Digested protein sample of MDA-MB-231 was labelled with the isobaric tags 114; 231-C3 was labelled with 115; 231-M1 was labelled with 116; and 231-M2 cells was labelled with 117, respectively.

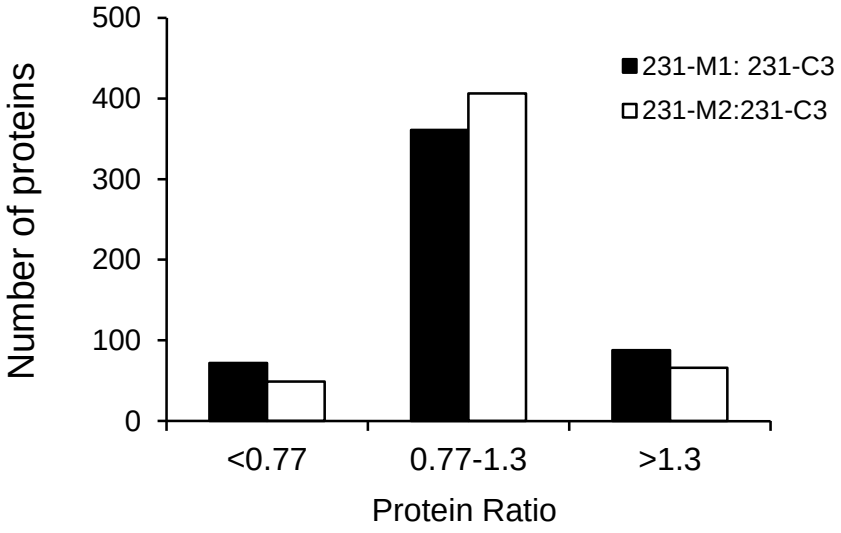

Figure 6-3. Distribution of the relative expression levels of proteins.

ATTENTION: The Singapore Copyright Act applies to the use of this document. Nanyang Technological University Library

6.2.3 Differentially Expressed Proteins with Same Trends in 231-M1 and 231-M2 Cells are Associated with Cytoskeleton and Structural Function

42 proteins were upregulated and 21 proteins were downregulated in both 231-M1 and 231-M2 cells compared to 231-C3 cell line (red bars in Figure 6-4). Survival in bloodstream is required for all cells infiltrated the lung tissue, including those successfully formed a micrometastasis or remained as a dormant tumor. Thus, these 63 proteins are hypothesized to be related with the survival of CTCs in circulation.

The biological functions of these 63 proteins were further classified by PANTHER classification system against NCBI (*H. sapiens*). 13 of 63 proteins (21%) were classified as cytoskeletal proteins, and another 6 proteins were classified as structural proteins (Figure 6-5). 12 proteins were detected with high confidence and they were listed in Table 6-1. The parameters to define the high confidence of a protein include: the numbers of unique peptide are equal to or more than 5, p-value is less than 0.05, and error factor is lower than 2.0.

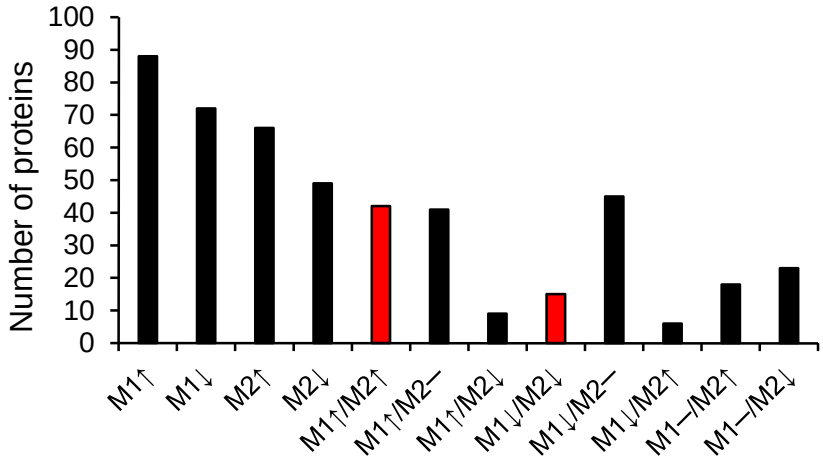

Figure 6-4. Differentially expressed proteins in 231-M1 and M2 cells compared with 231-C3 cells. ↑: >1.3; —: >0.77, <1.3; ↓: <0.77.

ATTENTION: The Singapore Copyright Act applies to the use of this document. Nanyang Technological University Library

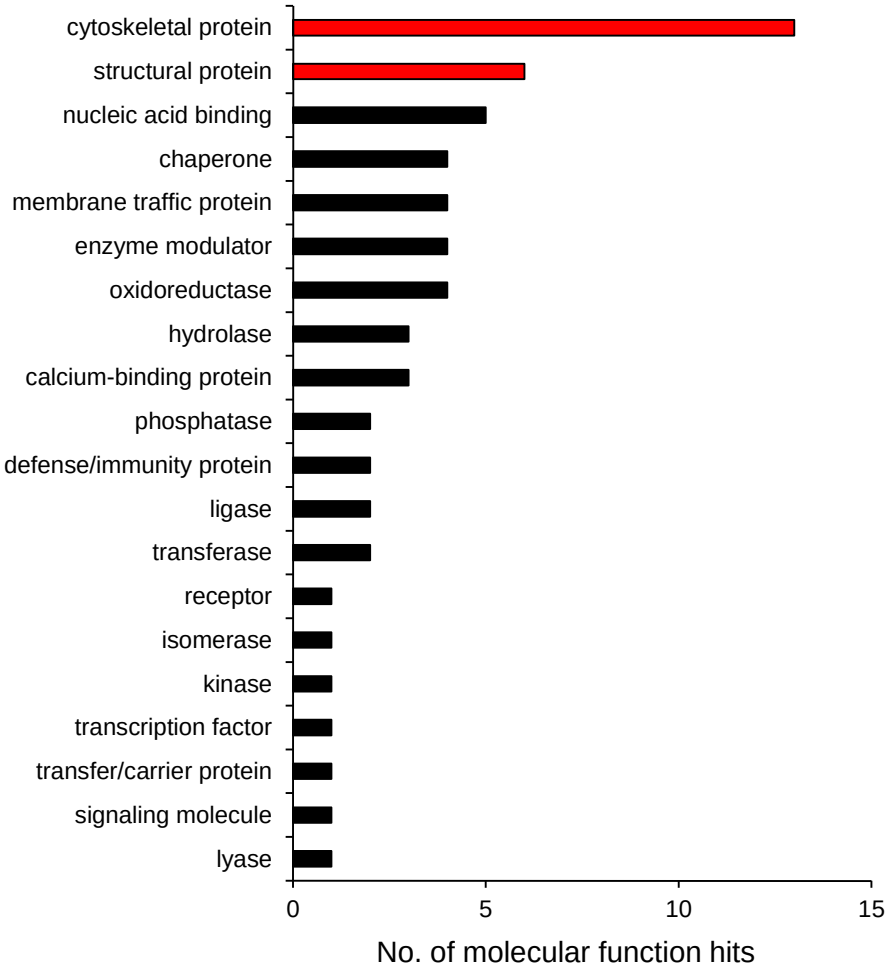

Figure 6-5. Classification of molecular functions of differentially expressed proteins with same trends in 231-M1 and 231-M2 cells.

In this list, 7 proteins were upregulated and 5 proteins were downregulated in both 231-M1 and M2 cells when compared to the parental 231-C3 cells. The expression levels of three important hits, including vimentin, hsp-70 and plectin, were further validated by Western blot analysis (Figure 6-6).

ATTENTION: The Singapore Copyright Act applies to the use of this document. Nanyang Technological University Library

Table 6-1. Differentially expressed proteins with the same trends in 231-M1 and M2 cells

No	Accessions	Gene description	Gene symbol	No. of unique peptide	231 - M1	231-M2	Molecular function
1	H0YG33	Heat shock 70 kDa protein 1A/1B	HSPA1B*	14	2.94	1.84	Chaperone
2	P04075	Fructose-bisphosphate aldolase A	ALDOA	8	2.88	1.89	Structure protein
3	P21980	Protein-glutamine gamma-glutamyl transferase 2	TGM2	6	2.29	1.72	Acyltransferase
4	P08670	Vimentin	VIM*	48	2.27	1.94	Structure protein
5	P02545	Prelamin-A/C	LMNA	17	1.89	1.32	Structure protein
6	Q15149	Plectin	PLEC*	60	1.85	1.47	Actin binding protein
7	P08133	Annexin A6	ANXA6	13	1.47	1.50	Structure protein
8	Q09666	Neuroblast differentiation-associated protein AHNAK	AHNAK	29	0.68	0.65	Cell migration
9	P08729	Keratin, type II cytoskeletal 7	KRT7	7	0.58	0.39	Structure protein
10	Q14315	Filamin-C	FLNC	13	0.52	0.28	Actin binding protein
11	B2ZZ89	Spectrin beta non-erythrocytic 1	SPTBN1	12	0.50	0.75	Actin binding protein
12	P50454	Serpin H1	SERPIN H1	5	0.29	0.64	Serine protease inhibitor

*: indicates proteins validated by Western blotting.

Very interestingly, most of these 12 high confidence proteins are associated with EMT program, such as vimentin [349], plectin [350], Hsp70 [351], ALDOA [349], TGM2 [352] and cytokeratin 7 [353]. However, the experimental metastasis model used this study did not involve the early steps of metastasis such as primary tumor growth and EMT. Instead, the cancer cells were injected directly into the blood

ATTENTION: The Singapore Copyright Act applies to the use of this document. Nanyang Technological University Library

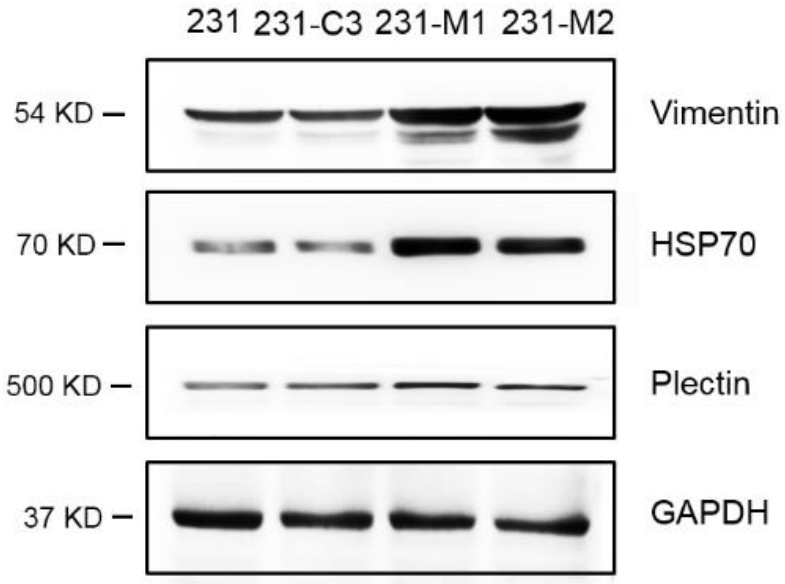

Figure 6-6. Western blot validation of three proteins identified by iTRAQ.

circulation through tail vein. The EMT process in this experiment in reality was completed by the effect of trypsin. Nevertheless, after selection by circulation and lung tissue microenvironments, successfully survived cancer cells displayed higher level of EMT markers than before. Taking vimentin as an example, this protein is a well-known EMT maker which is a type of mesenchymal intermediate filament protein and has low expression level in epithelial cells. After proteomics analysis, I found that the expression level of vimentin was up-regulated for more than 2 times in 231-M1 cells and 1.94 times in 231-M2 cells. Western blot analysis also confirmed the upregulation of vimentin in both 231-M1 and M2 cells (Figure 6-6). To explore the interactions of all these differentially expressed proteins with similar trends in 231-M1 and M2 cells, a protein interactive network was created by Ingenuity pathway analysis systems (Figure 6-7). In consistent with our hypothesis, this pathway network suggested that the upregulated proteins (red) and downregulated proteins (green) identified by

ATTENTION: The Singapore Copyright Act applies to the use of this document. Nanyang Technological University Library

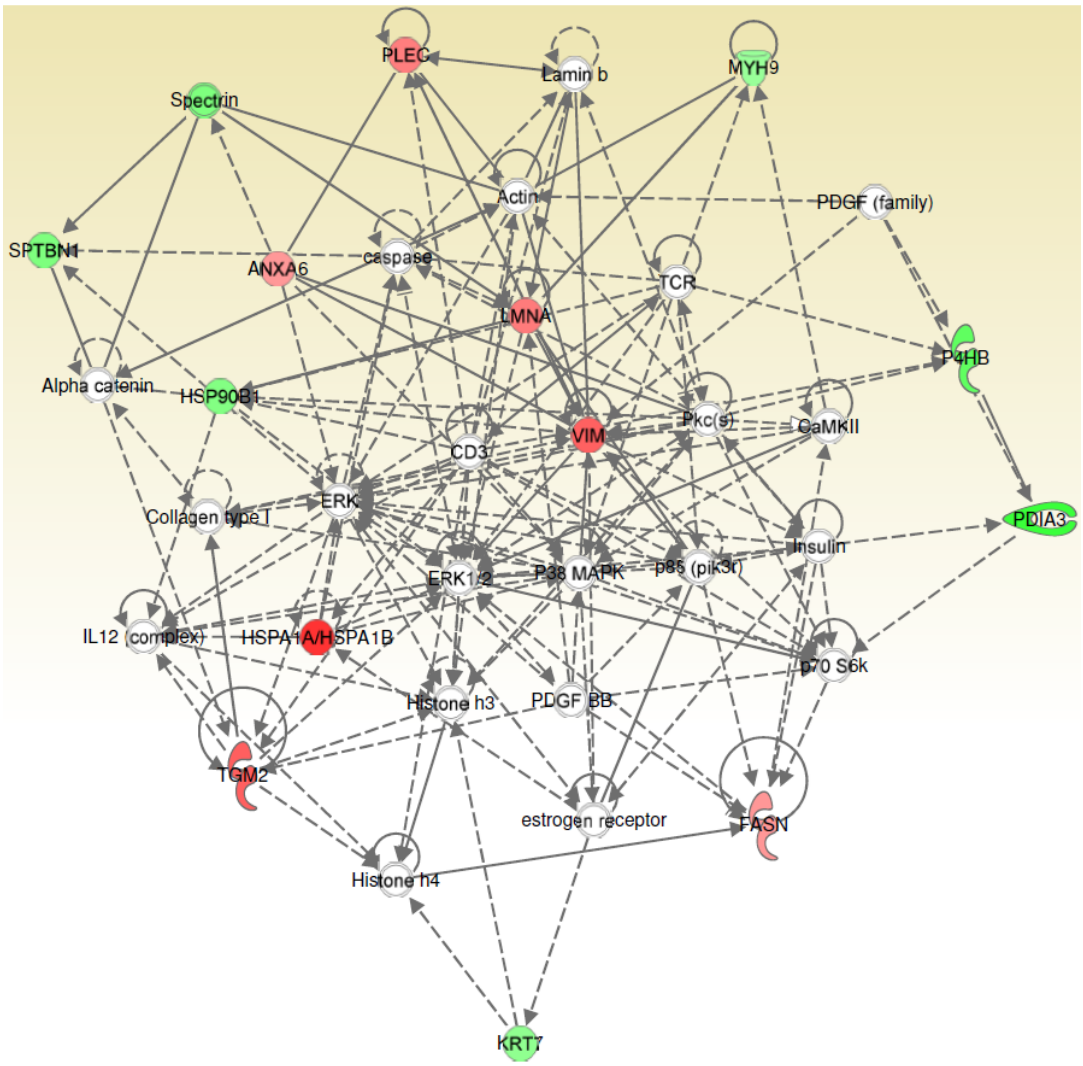

Figure 6-7. Differentially regulated molecular networks from 231-C3 to 231-M1 cells. Red color indicates the upregulated proteins and green color indicates downregulated proteins in 231-M1 and M2 cells compared with 231-C3 cell line.

proteomics analysis are associated with cytoskeleton reorganization, cell stress response, cell proliferation as well as apoptosis resistance, all of which can contribute to the enhanced survival ability of metastatic CTCs. Specifically, the most common junctions of the network include: vimentin (VIM), laminin A (LMNA), and actin which are cytoskeleton proteins playing important functions in EMT. In addition to cytoskeleton proteins, other pro-oncogenic proteins were also identified including

ATTENTION: The Singapore Copyright Act applies to the use of this document. Nanyang Technological University Library

ERK and p70S6k, which are key regulating kinases in cell proliferation; P38 MAPK which is associated with cellular response to environmental stresses; p85 (pik3r) which is a subunit of PI3K that can regulate survival, proliferation and invasiveness of cancer cells.

6.2.4 Differentially Expressed Proteins with Different Trends between 231-M1 and 231-M2 Cells are Associated with Cell Proliferation and Metabolism

142 proteins were differentially expressed in 231-M1 and 231-M2 cells with different regulation trends (Figure 6-4). They include 41 proteins upregulated in 231-M1 but did not change in 231-M2, 9 proteins upregulated in 231-M1 but downregulated in 231-M2, 45 proteins down regulated in 231-M1 but did not change in 231-M2, 6 proteins downregulated in 231-M1 but upregulated in 231-M2, 18 proteins did not change in 231-M1 but upregulated in 231-M2 and 23 proteins did not change but downregulated in 231-M2.

The molecular functions of these 142 proteins were also classified by PANTHER classification system against NCBI (H. sapiens). Interestingly, only 7 proteins were cytoskeleton and structural proteins (indicated by red bars in Figure 6-8). Majority of these proteins were related to nucleic acid binding and oxidoreductase as well as other cellular activities which are related to cell proliferation and metabolism. Another 12 proteins were identified with high confidence as listed in Table 6-2 using the same parameters in Table 6-1. As these proteins were differentially expressed with different trends in 231-M1 and 231-M2 cells, they may be more related to the progression of disseminated tumor cells after extravasation. The cells that can grow into a secondary tumor must have overcome the limitations of new microenvironment. The functions

ATTENTION: The Singapore Copyright Act applies to the use of this document. Nanyang Technological University Library

of these identified 12 proteins can meet these requirements. For example, fatty acid synthase (FASN) which is upregulated in 231-M1 cells (231-M1/231-C3 = 1.49) but downregulated in 231-M2 cells (231-M2/231-C3 = 0.64) plays important roles in stimulating tumor cell proliferation and survival of cancer cells, and is associated with metastasis of breast cancer cells [354]. Another protein Calreticulin which is downregulated in 231-M1 cells but did not change in 231-M2 cells could suppress the

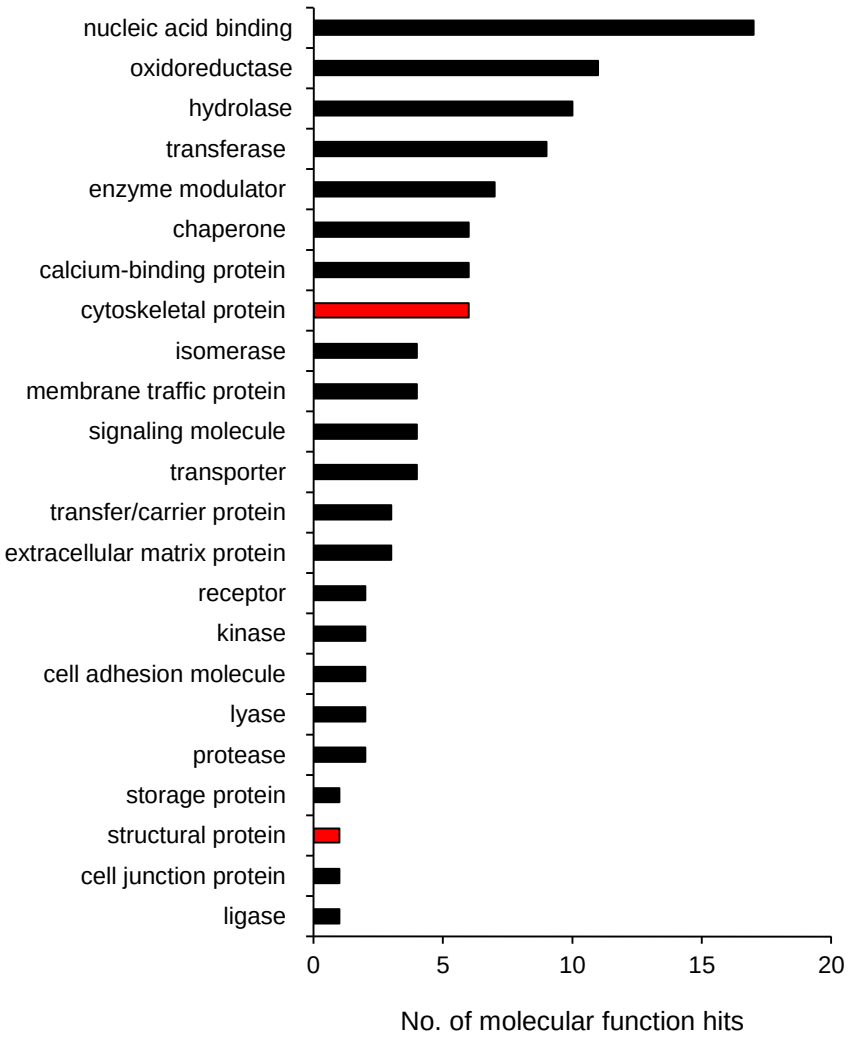

Figure 6-8. Classification of molecular functions of differentially expressed proteins with different trends in 231-M1 and M2 compared to 231-C3 cells.

ATTENTION: The Singapore Copyright Act applies to the use of this document. Nanyang Technological University Library

colony formation of PC-3 cells and inhibit the growth and metastasis of prostate cancer cells [355]. If this group of proteins can be further validated by functional assays, they can be used as new biomarkers for diagnosing metastatic breast cancer.

Table 6-2. Differentially expressed proteins with different trends in 231-M1 and M2 cells compared with 231-C3 cell line.

No	Accessions	Gene description	Gene symbol	No. of unique peptide	231-M1	231-M2	Molecular function
1	F5GZ16	26S proteasome non-ATPase regulatory subunit 2	PSMD2	6	1.79	1.07	Enzyme modulator
2	P49327	Fatty acid synthase	FASN	11	1.49	0.64	Metabolic pathways
3	P14618	Pyruvate kinase isozymes M1/M2	PKM2	41	1.42	0.84	Metabolic pathways
4	P42704	Leucine-rich PPR motif-containing protein	LRPPRC	11	0.64	1.20	Protein kinase
5	P35579	Myosin-9	MYH9	46	0.63	0.90	Actin binding protein
6	P14625	Endoplasmin	HSP90B1	6	0.52	0.79	Chaperone
7	P27797	Calreticulin	CALR	3	0.48	1.11	Calcium-binding protein
8	Q14697	Neutral alpha-glucosidase AB	GANAB	11	0.42	0.82	Glucosidase
9	P07237	Protein disulfide-isomerase	P4HB	12	0.41	1.02	Metabolic pathways
10	P30101	Protein disulfide-isomerase A3	PDIA3	5	0.33	0.79	Metabolic pathways
11	P07339	Cathepsin D	CTSD	9	1.27	2.21	Aspartic protease
12	P06576	ATP synthase subunit beta	ATP5B	19	1.08	1.75	DNA binding protein

ATTENTION: The Singapore Copyright Act applies to the use of this document. Nanyang Technological University Library

6.2.5 Collection of Protein Samples from Macrometastasis-derived Cell Lines

After 231-M1 cell line was generated, these cells were injected back into nude mice to produce more metastatic tumors (Figure 5-14). After 90 days, 231-M1 cells formed obvious lung metastases in 5 out of 6 nude mice (Figure 5-15). The number of 231-M1 foci was also significantly high than that of 231-C3 lung metastases. I then isolated sensor cells from the biggest metastatic tumor and generated a stable cell line of 231-M1A. Unlike 231-M1 and 231-M2 cells, 231-M1A cells were derived from a macrometastasis with an approximate tumor size of 2 mm. Therefore, 231-M1A cells can truly represent the cancer cells that had completed all the metastatic process with high malignancy. Moreover, 231-M1A cells also exhibited high resistance to doxorubicin treatment. For example, even under a treatment with 8 μM doxorubicin, very little apoptosis was detected after 24 h. To identify driver proteins conferring proliferation and drug resistance in 231-M1 and 231-M1A cells, I separately prepared total cell lysates from 231-C3, 231-M1, and 231-M1A cells.

6.2.6 Conduct 2D-DIGE Proteomic Analysis to Identify New Driver Proteins from Highly Metastatic Breast Cancer Cells

I further compared protein expression profiles between 231-C3, 231-M1, and 231-M1A cells using another comparative proteomics analysis-2D DIGE method with the help of Dr. Hongjin Huang from Applied Biomics Inc. in USA (Figure 6-9). This method allows me to visually compare the levels of protein(s) at the same spot between three cell lines. As shown in Figure 6-9, the proteins that have high expression levels in 231-C3 cells appear in green color and the proteins with high expression levels in

ATTENTION: The Singapore Copyright Act applies to the use of this document. Nanyang Technological University Library

231-M1 or 231-M1A cells appear in red color. If the levels of the same protein are similar between two compared cell lines, the merged dots will appear in an orange color. The differences between 231-M1 and 231-M1A cells were also compared. Using this method, the fluorescence intensity ratios between 231-M1 and 231-C3, 231-M1A and 231-C3, 231-M1A and 231-M1 were calculated from 125 spots. I selected 56 spots whose fluorescence intensity ratios in 231-M1A/231-C3 and 231-M1/C3 were increased or reduced for 1.5 fold and determined their identification by LCMS/MS (Figure 6-9). 52 protein was identified by LCMS/MS analysis. These 52 proteins were further classified into different subtypes by molecular function, biological process and protein classification using Panther analysis (Figure 6-10).

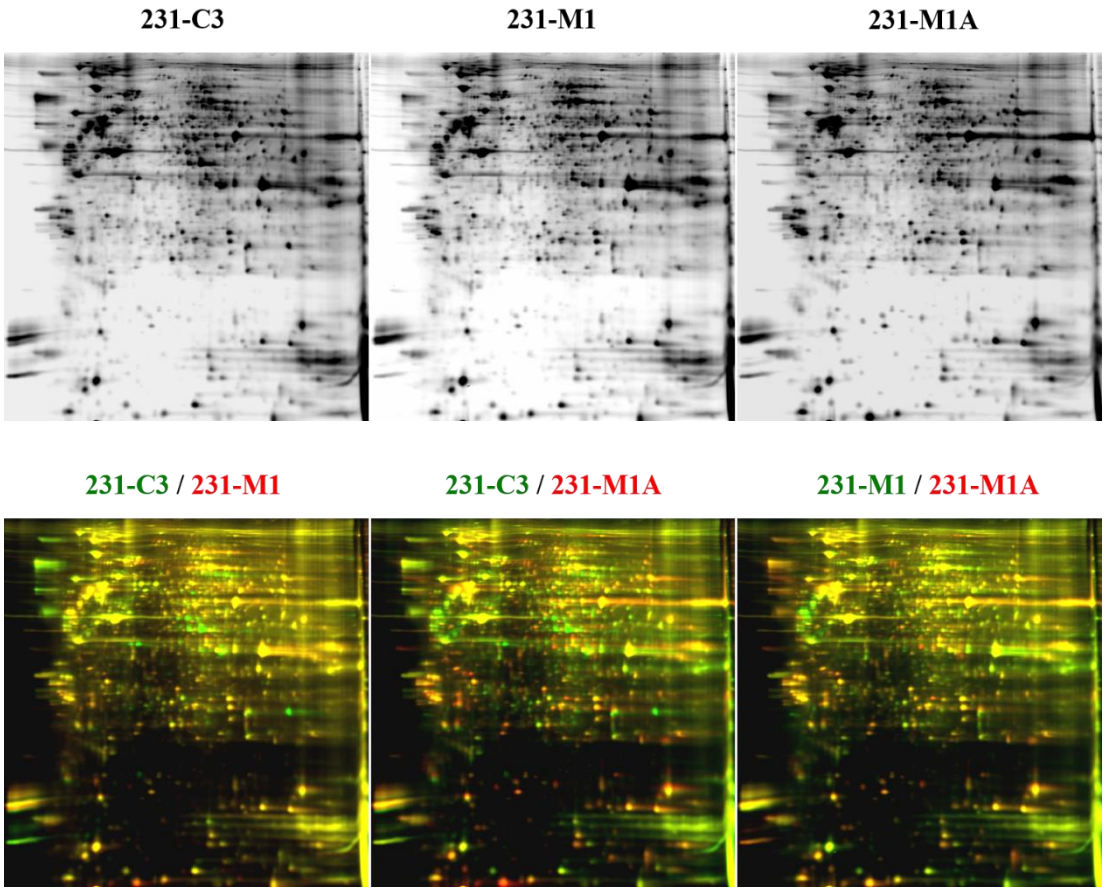

Figure 6-9. Representative images of two-dimensional differential in-gel electrophoresis (2D-DIGE).

ATTENTION: The Singapore Copyright Act applies to the use of this document. Nanyang Technological University Library

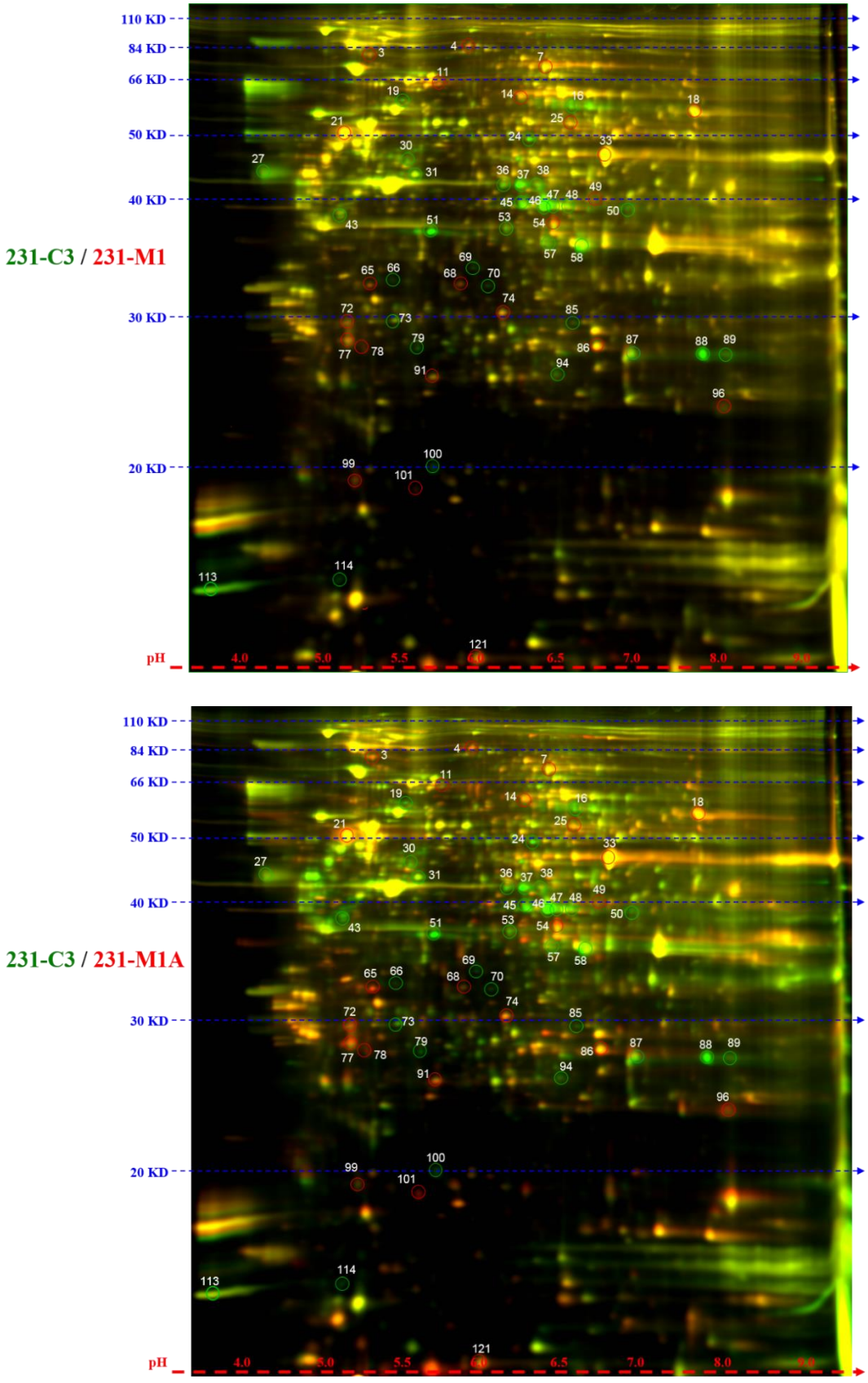

Figure 6-10. Selection of 56 spots from 2D-DIGE for LC-MS/MS identification.

ATTENTION: The Singapore Copyright Act applies to the use of this document. Nanyang Technological University Library

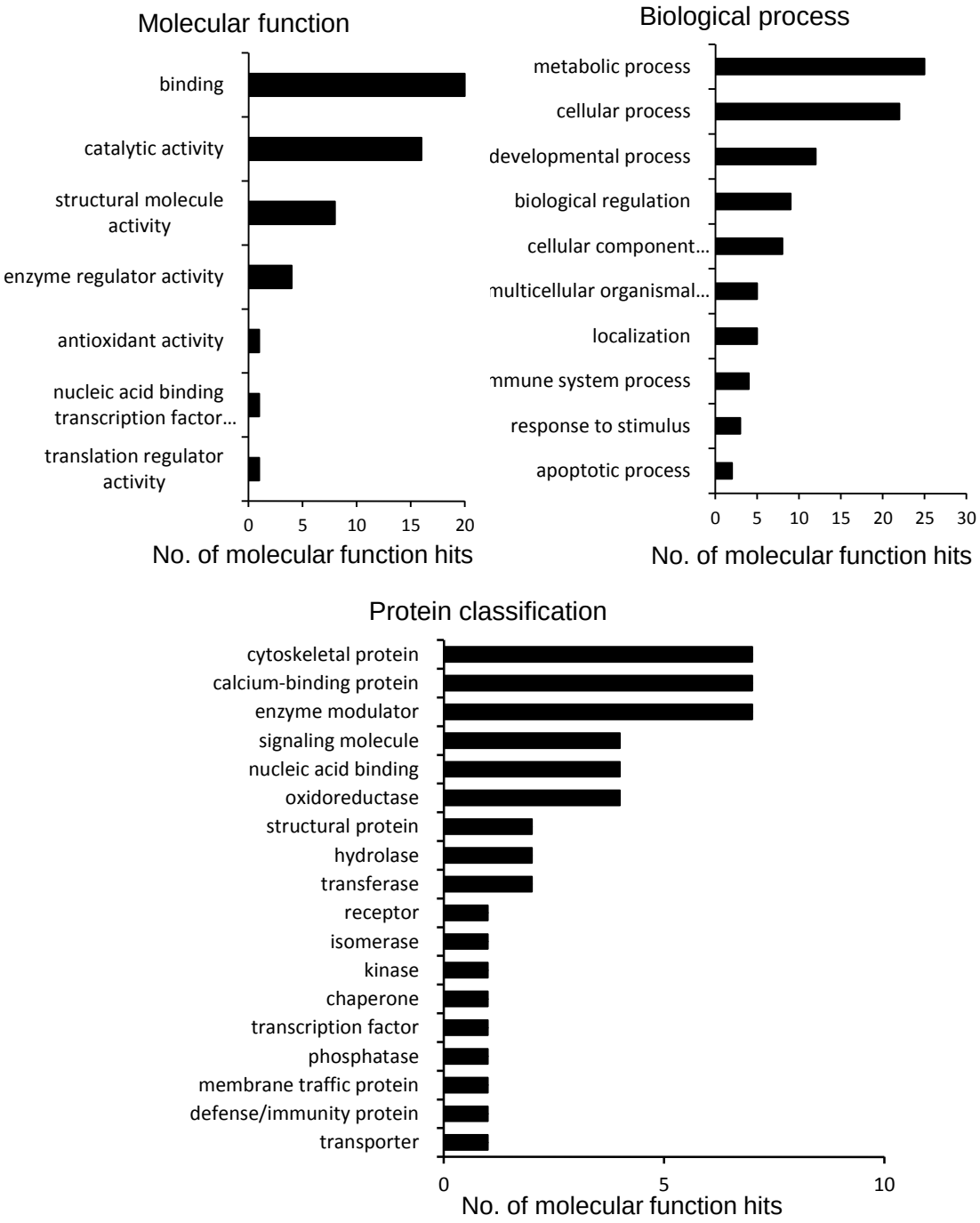

Figure 6-11. Classification of differentially expressed proteins by molecular function, biological process, and protein classification from 2D DIGE proteomics.

Based on the protein classification, I have identified 8 structural proteins (Table 6-3) and 23 metabolic proteins (Table 6-4). Structural proteins may be related with the survival of CTCs in circulation and the migration ability in lung tissue. The metabolic

ATTENTION: The Singapore Copyright Act applies to the use of this document. Nanyang Technological University Library

proteins may regulate the anti-oxidant ability as well as proliferation of metastatic cells in lung.

Table 6-3. List of structural proteins that differentially expressed in 231-M1 and 231-M1A cells compared to 231-C3 cells.

No	Accession	Gene description	Gene symbol	M1 :C3	M2 :C3	Molecular function
1	Q15691	Microtubule-associated protein RP/EB family member 1	MAPRE1	2.1	6.6	non-motor microtubule binding protein
2	P06396	Gelsolin	GSN	2.1	4.2	non-motor actin binding protein;calcium-binding protein
3	P07437	Tubulin beta chain	TUBB	1.4	2.4	Tubulin
4	P26038	Moesin	MSN	1.8	1.9	actin family cytoskeletal protein
5	P13645	Keratin, type I cytoskeletal 10	KRT10	-3.5	-1.5	structural protein;intermediate filament
6	P63261	Actin, cytoplasmic 2	ACTG1	-2.1	-1.9	actin and actin related protein
7	P04264	Keratin, type II cytoskeletal 1	KRT1	-1.6	-3.1	structural protein;intermediate filament
8	P31943	Heterogeneous nuclear ribonucleoprotein H	HNRNPH 1	-3.8	-4.2	ribosomal protein

Table 6-4. List of metabolic proteins that differentially expressed in 231-M1 and 231-M1A cells compared to 231-C3 cells.

No	Accession	Gene description	Gene symbol	231-M1 : 231-C3	231-M2 : 231-C3	Molecular function
1	P52566	Rho GDP-dissociation inhibitor 2	ARHGDIB	1.8	3	G-protein modulator
2	P52565	Rho GDP-dissociation inhibitor 1	ARHGDIA	1.6	3	G-protein modulator

ATTENTION: The Singapore Copyright Act applies to the use of this document. Nanyang Technological University Library

3	P60174	Triosephosphate isomerase	TPI1	1.5	2.8	isomerase
4	P04083	Annexin A1	ANXA1	1.5	2.8	-
5	P11413	Glucose-6-phosphate 1-dehydrogenase	G6PD	1.6	2.7	dehydrogenase
6	P21980	Protein-glutamine gamma-glutamyltransferase 2	TGM2	1.6	2.7	acyltransferase
7	Q16555	Dihydropyrimidinase-related protein 2	DPYSL2	1.7	2.1	hydrolase
8	P31949	Protein S100-A11	S100A11	1.6	2	calmodulin
9	P09525	Annexin A4	ANXA4	2.1	1.8	-
10	P08133	Annexin A6	ANXA6	2.3	1.5	-
11	Q01081	Splicing factor U2AF 35 kDa subunit	U2AF1	-2.9	-1.6	ribonucleoprotein
12	P62826	GTP-binding nuclear protein Ran	RAN	-2.3	-1.8	small GTPase
13	P40925	Malate dehydrogenase, cytoplasmic	MDH1	-2.3	-2	dehydrogenase
14	Q5VZL5	Zinc finger MYM-type protein 4	ZMYM4	-2.1	-2.1	transcription factor, kinase inhibitor
15	P31943	Heterogeneous nuclear ribonucleoprotein H	HNRNPH1	-3.3	-2.2	ribosomal protein
16	P62136	Serine/threonine-protein phosphatase PP1-alpha catalytic subunit	PPP1CA	-1.9	-2.4	protein phosphatase, calcium-binding protein
17	O14618	Copper chaperone for superoxide dismutase	CCS	-4.1	-2.7	cation transporter, oxidoreductase
18	P48556	26S proteasome non-ATPase regulatory subunit 8	PSMD8	-3.9	-2.9	enzyme modulator
19	Q9UNE7	E3 ubiquitin-protein ligase CHIP	STUB1	-4.7	-3	chaperone
20	P60842	Eukaryotic initiation factor 4A-I	EIF4A1	-2.5	-3.6	RNA helicase
21	P61978	Heterogeneous nuclear ribonucleoprotein K	HNRNPK	-3	-4.3	mRNA splicing factor, enzyme modulator
22	Q9BV57	1,2-dihydroxy-3-keto-5-methylthiopentene dioxygenase	ADI1	-4	-4.8	oxidoreductase
23	Q9H4M9	EH domain-containing protein 1	EHD1	-4.6	-5.3	membrane traffic protein, G-protein modulator, calcium-binding protein

ATTENTION: The Singapore Copyright Act applies to the use of this document. Nanyang Technological University Library

6.3 Discussion

Metastasis of cancer cell is a complicated process, not only requiring cell motility, but also involving various cellular activities, such as cell survival, cell metabolism and cellular responses to various types of stresses [270]. To provide a more comprehensive understanding of molecular basis of metastasis and identify functional metastatic biomarkers for breast cancer, I conducted proteomics analysis to compare the protein profiles between members of a family of breast cancer cell lines with different metastatic capacities. These cell lines were isolated from lung metastases in an experimental metastasis model in nude mice.

In an iTRAQ-based proteomics analysis, cells derived from a micrometastasis, or a dormant metastasis in the lung of mouse, were compared with their parental cell line. The identified protein hits were classified into two subgroups: one subgroup contains proteins differentially expressed in the same trends in micrometastasis and dormant metastasis-derived cell lines; the other subgroup has proteins differentially produced in different trends in these two cell lines. Interesting differences were found between these two subgroups. Proteins identified from subgroup 1 are mostly cytoskeleton and structural proteins while majority proteins in subgroup 2 are nucleic acid binding proteins as well as proteins with important functions in cell metabolism. In the second 2D-DIGE-based comparative proteomics analysis, I identified some differentially expressed proteins from cells derived from a highly metastatic tumor in comparison with the micrometastasis derived cell lines as well as their parental cell line. In good alignment with the iTRAQ results, the 2D-DIGE results also revealed that most of the differentially regulated proteins identified from 231-M1A and 231-M1 cells are

ATTENTION: The Singapore Copyright Act applies to the use of this document. Nanyang Technological University Library

predominantly associated with cell metabolism, followed by cellular process and structural function.

Based on these results, two distinct phases of cancer cell dissemination can be defined. The first phase is the traveling of CTCs in bloodstream and the landing of DTCs at the secondary organ. The second phase is the adaption and proliferation of DTCs in the new microenvironment. The regulatory proteins in these two phases are different. In the first phase, cytoskeleton and structural proteins play more important roles in the survival and morphological changes of the cells. In the second phase, metabolism and cellular process proteins are more important regulators for form solid metastatic tumors.

Very interestingly, most of the identified regulators in the first phase are EMT-related cytoskeleton proteins or chaperones. EMT is believed to play important roles in the breakthrough of cancer cells from primary tumor in the early stage of metastasis [61]. However, the role of EMT program in the survival of CTCs against hemodynamic shear stress is not clear. In this study, I found that several intermediate filament proteins are changed in metastasis-derived cell lines, including vimentin, keratin, and laminin. These proteins have been well studied and considered as EMT markers [70]. The upregulation of vimentin and downregulation of cytokeratin in 231-M1 and 231-M2 cells suggested that these proteins are essential for the survival of CTCs. One possible mechanism is that these EMT markers can modify the cell stiffness [356]. Meanwhile, they are also associated with the morphology, organization [357] and membrane potential of mitochondria [358]. Therefore, under hemodynamic shear stress, softer intermediate filaments with vimentin may protect CTCs from physical shear stress-related damage, while stiffer intermediate filament with

ATTENTION: The Singapore Copyright Act applies to the use of this document. Nanyang Technological University Library

cytokeratin could cause mitochondrial dysfunction and losing mitochondrial membrane potential which could further induce apoptosis of CTCs.

The proteins of interests in the second phase are more related to cell proliferation and cell metabolism. Strategies targeting these proteins may potentially inhibit the proliferation of metastatic breast cancer cells in the secondary organ. A good example is protein FASN. This protein was upregulated in 231-M1 cells, however, downregulated in 231-M2 cells. This protein was reported recently to be a metabolic marker of cell proliferation rather than malignancy in ovarian cancer and its precursor cells [354, 359]. The other two proteins that are upregulated in 231-M1 but downregulated in 231-M2 cells are PSMD2 and PKM2. Both of them were found to regulate cell proliferation and promote apoptotic progression [360-362].

In addition, most of the proteins of interests identified from the highly metastatic cells by 2D-DIGE analysis are associated with cell metabolism and cellular process. Interestingly, majority of these proteins are related with drug resistance of tumor cells. For example, TGM2 was reported to control sensitivity of breast cancer cells to the chemotherapeutic drug doxorubicin [363]; G6PD activity was also found to modulate doxorubicin resistance [364]; ARHGDIB was able to mediate the chemoresistance to cisplatin [365]; S100A11 could govern the chemoresistance of non-small cell lung carcinoma cells [366]. All these proteins are upregulated in 231-M1 cells when compared to the parental 231-C3 cells, and expressed in 231-M1A cells at the highest level.

In summary, major finding in this chapter include:

1. Using iTRAQ- and 2D-DIGE-based comparative proteomics analysis, I have identified many potential anti-metastatic markers for breast cancer.

ATTENTION: The Singapore Copyright Act applies to the use of this document. Nanyang Technological University Library

2. All identified proteins were split into key regulators of two distinct phases of cancer cell dissemination. One group of regulators are EMT-related cytoskeleton proteins or chaperones which regulate the metastatic process before dissemination. The other group of regulators regulate the proliferation and cell metabolism of disseminated tumor cells to develop metastatic tumor.
3. All these important metastatic regulators identified from this study can be further validated by functional assays and applied as functional biomarkers for metastatic breast cancer cells.

ATTENTION: The Singapore Copyright Act applies to the use of this document. Nanyang Technological University Library

ATTENTION: The Singapore Copyright Act applies to the use of this document. Nanyang Technological University Library

CHAPTER 7 Conclusions and Future Directions

The main objective of this thesis is to find effective strategies to inhibit the survival and proliferation of metastatic breast cancer cells. Breast cancer in the advanced stage causes 90% death of breast cancer patients [37]. While in the earlier stage before the dissemination of cancer cells to distant organs via the blood circulation, the survival rates of breast cancer patients are much higher. For example, in the stage III, when breast cancer cells invade into multiple lymph nodes and surrounding tissues, the relative 5-year survival rate in cancer patients is still very high (>72%). Therefore, potential effective strategies should include 1) eliminating the CTC in blood circulation, and 2) suppressing the proliferation of DTCs in the secondary site. Moreover, metastatic breast cancer cells frequently develop chemo resistance against the most commonly used anti-cancer drugs, such as doxorubicin. Understanding the molecular mechanism of the acquired doxorubicin resistance during metastasis may also improve the survival as well as the quality of life of breast cancer patients. One of the least understood steps during metastasis is the survival of metastatic CTCs in the blood circulation. This is because two important questions have not been answered. One is how hemodynamic shear stress induces apoptosis of CTCs and the other is what mechanisms are used by the metastatic breast cancer cells to resist shear stress-induced damage in circulation, and become the seeds of secondary tumors.

To address these questions, I first overcame the technical obstacles of CTCs' study by generating multiple apoptosis sensor cell lines and integrated them into several novel experimental models. These sensor cell lines express a FRET-based caspase-3 sensor and were applied to monitor apoptosis of CTCs during circulation. The integrative experimental models include an experimental lung metastasis model in

ATTENTION: The Singapore Copyright Act applies to the use of this document. Nanyang Technological University Library

nude mouse, a zebrafish CTCs model, a zebrafish xenograft tumor model, and a circulatory microfluidic system to mimic the blood circulation. These technologies have dramatically facilitated the mechanism study of CTCs in this thesis. Moreover, all these methods can be applied as an anti-metastatic drug discovery platform in the future. A sensor cell bank including cells from multiple types of cancers and several metastatic breast cancer cell lines generated in this thesis can be directly used in the high throughput screening of anticancer agents with different mechanisms, such as apoptosis-inducing, proliferation inhibition and metastasis prevention. The zebrafish CTCs model and the circulatory microfluidic system can be applied to identify the strategies that can reduce the survivability of CTCs in blood circulation or inhibit the extravasation. Furthermore, a zebrafish xenograft tumor model utilizing highly malignant B16-F10-C3 cells can be applied for identification of anti-proliferation agents targeting the metastatic tumor in the future.

A major contribution of this thesis is that I elucidated the mechanism of hemodynamic shear stress-induced apoptosis of CTCs and identified an important survival factor MnSOD in metastatic CTCs. Hemodynamic shear force could affect CTCs in several aspects. Mitochondria localized on the cytoskeleton could be disturbed immediately when the cells were exposed to shear stress. Subsequently, mitochondrial dysfunction, ROS generation, mitochondrial damage as well as caspase-dependent apoptotic cascade were sequentially triggered. The mitochondrial antioxidant enzyme can block this chain reaction by scavenging excessive superoxide in mitochondria and protect CTCs from oxidative stress. I observed that levels of MnSOD in individual breast cancer cells were heterogeneous. Therefore, cells with high levels of MnSOD should have higher metastatic potential as they can better

ATTENTION: The Singapore Copyright Act applies to the use of this document. Nanyang Technological University Library

survive from the blood flow and have higher chance to develop into secondary tumors. These results can explain the phenomenon observed by many clinical studies that MnSOD levels were increased in metastatic tumors. I confirmed the therapeutic potential of inhibiting MnSOD by injecting metastatic cells with MnSOD being knocked down into microfluidic system or blood circulation of nude mice. Metastatic cells were obviously eliminated by fluid shear stress when their MnSOD levels were reduced. In the future, strategies that can downregulate the expression or inhibit the activity of MnSOD in metastatic breast cancer cells should be developed. These strategies have been approved by this thesis to be able to prevent the survival of CTCs in circulation and thus can eliminate CTCs in an early stage.

Moreover, MnSOD also confer resistance of metastatic breast cancer cells to the chemotherapy drug doxorubicin, which is most commonly used in adjuvant therapy of breast cancer. An important part of anticancer mechanism of doxorubicin is to kill cancer cells by generating ROS. The cells with high level of MnSOD not only survive in blood circulation successfully, but also resist to doxorubicin treatment using the same anti-oxidant mechanism. Therefore, the cancer recurrent rate is usually very high and the prognosis is poor in MBC patients. A new strategy to overcome the doxorubicin resistance in MBC cells has therefore been developed in this study by reducing the MnSOD level in MBC cells before doxorubicin treatment. Meanwhile, our study provides an important piece of information to the MBC treatment regime. In MBC patients diagnosed with high level of MnSOD, doxorubicin usage should be avoided, unless the combination strategies of MnSOD inhibition are developed.

In addition, I identified a lot of potential biomarkers for MBC. They are classified into three subgroups: cytoskeleton proteins which modulate the survival of CTCs,

ATTENTION: The Singapore Copyright Act applies to the use of this document. Nanyang Technological University Library

cellular process proteins which govern the cell proliferation in the secondary tumor site and metabolism proteins which are associated with proliferation, survival, and acquired drug resistance of MBC cells. All these biomarkers have potentials to be developed as novel markers for MBC diagnosis, prognosis or as therapeutic targets. Another important direction is to find the key driver proteins that regulate the increasing or decreasing of biomarkers identified in this study. The potential driver proteins can be oncogenes, epigenetic modifications or EMT transcription factors.

In conclusion, all studies in this thesis potentially provide new technologies, new knowledge as well as new strategies to the improvement of metastatic breast cancer research and treatment. Relying on the outcome from several cultured breast cancer cell lines together with some *in vitro* and *in vivo* experimental models, all these achievements are still preliminary before clinical application. Further efforts should be put on the validation with more breast cancer cell lines (e.g. multiple cell lines from a similar subtype), as well as more precision animal models (e.g. using of orthotropic breast tumor metastasis model). More importantly, sufficient clinical samples should be analysed to achieve the druggability of the potential anti-metastatic targets or agents.

ATTENTION: The Singapore Copyright Act applies to the use of this document. Nanyang Technological University Library

References

1. Terese Winslow. **Breast Anatomy Female.** National Cancer Institute, http://www.cancer.gov/types/breast/patient/breast-treatment-pdq, 2011.
2. Terese Winslow. **Modified Radical Mastectomy.** Breast Cancer Treatment, National Cancer Institute, http://www.cancer.gov, 2012.
3. Stewart BW, Wild C, International Agency for Research on Cancer, World Health Organization: **World cancer report 2014**. Lyon, France Geneva, Switzerland: International Agency for Research on Cancer WHO Press; 2014.
4. Eheman CR, Shaw KM, Ryerson AB, Miller JW, Ajani UA, White MC: **The changing incidence of in situ and invasive ductal and lobular breast carcinomas: United States, 1999-2004**. *Cancer epidemiology, biomarkers & prevention : a publication of the American Association for Cancer Research, cosponsored by the American Society of Preventive Oncology* 2009, **18**(6):1763-1769.
5. Teo MC, Soo KC: **Cancer trends and incidences in Singapore**. *Japanese journal of clinical oncology* 2013, **43**(3):219-224.
6. Hulka BS, Stark AT: **Breast cancer: cause and prevention**. *Lancet* 1995, **346**(8979):883-887.
7. Kerlikowske K, Grady D, Barclay J, Sickles EA, Ernster V: **Effect of age, breast density, and family history on the sensitivity of first screening mammography**. *Jama* 1996, **276**(1):33-38.
8. Colditz GA, Rosner BA, Speizer FE: **Risk factors for breast cancer according to family history of breast cancer. For the Nurses' Health Study Research Group**. *Journal of the National Cancer Institute* 1996, **88**(6):365-371.
9. King MC, Marks JH, Mandell JB, New York Breast Cancer Study G: **Breast and ovarian cancer risks due to inherited mutations in BRCA1 and BRCA2**. *Science* 2003, **302**(5645):643-646.
10. Endogenous H, Breast Cancer Collaborative G, Key TJ, Appleby PN, Reeves GK, Roddam AW, Helzlsouer KJ, Alberg AJ, Rollison DE, Dorgan JF *et al*: **Circulating sex hormones and breast cancer risk factors in postmenopausal women: reanalysis of 13 studies**. *British journal of cancer* 2011, **105**(5):709-722.
11. Lee MM, Lin SS: **Dietary fat and breast cancer**. *Annual review of nutrition* 2000, **20**:221-248.
12. Hamajima N, Hirose K, Tajima K, Rohan T, Calle EE, Heath CW, Jr., Coates RJ, Liff JM, Talamini R, Chantarakul N *et al*: **Alcohol, tobacco and breast cancer--collaborative reanalysis of individual data from 53 epidemiological studies, including 58,515 women with breast cancer and 95,067 women without the disease**. *British journal of cancer* 2002, **87**(11):1234-1245.
13. Danaei G, Vander Hoorn S, Lopez AD, Murray CJ, Ezzati M, Comparative Risk Assessment collaborating g: **Causes of cancer in the world: comparative risk assessment of nine behavioural and environmental risk factors**. *Lancet* 2005, **366**(9499):1784-1793.
14. Andrieu N, Easton DF, Chang-Claude J, Rookus MA, Brohet R, Cardis E, Antoniou AC, Wagner T, Simard J, Evans G *et al*: **Effect of chest X-rays on**

ATTENTION: The Singapore Copyright Act applies to the use of this document. Nanyang Technological University Library

the risk of breast cancer among BRCA1/2 mutation carriers in the international BRCA1/2 carrier cohort study: a report from the EMBRACE, GENEPSO, GEO-HEBON, and IBCCS Collaborators' Group. *Journal of clinical oncology : official journal of the American Society of Clinical Oncology* 2006, **24**(21):3361-3366.

15. Liu Q, Wuu J, Lambe M, Hsieh SF, Ekbom A, Hsieh CC: **Transient increase in breast cancer risk after giving birth: postpartum period with the highest risk (Sweden)**. *Cancer causes & control : CCC* 2002, **13**(4):299-305.
16. Collaborative Group on Hormonal Factors in Breast C: **Breast cancer and breastfeeding: collaborative reanalysis of individual data from 47 epidemiological studies in 30 countries, including 50302 women with breast cancer and 96973 women without the disease**. *Lancet* 2002, **360**(9328):187-195.
17. Anderson GL, Limacher M, Assaf AR, Bassford T, Beresford SA, Black H, Bonds D, Brunner R, Brzyski R, Caan B *et al*: **Effects of conjugated equine estrogen in postmenopausal women with hysterectomy: the Women's Health Initiative randomized controlled trial**. *Jama* 2004, **291**(14):1701-1712.
18. Cuzick J, Sestak I, Bonanni B, Costantino JP, Cummings S, DeCensi A, Dowsett M, Forbes JF, Ford L, LaCroix AZ *et al*: **Selective oestrogen receptor modulators in prevention of breast cancer: an updated meta-analysis of individual participant data**. *Lancet* 2013, **381**(9880):1827-1834.
19. Clark K: **Efficacy of bilateral prophylactic mastectomy in women with a family history of breast cancer**. *Journal of insurance medicine* 1999, **31**(1):41-43.
20. Goss PE, Ingle JN, Ales-Martinez JE, Cheung AM, Chlebowski RT, Wactawski-Wende J, McTiernan A, Robbins J, Johnson KC, Martin LW *et al*: **Exemestane for breast-cancer prevention in postmenopausal women**. *The New England journal of medicine* 2011, **364**(25):2381-2391.
21. Thune I, Brenn T, Lund E, Gaard M: **Physical activity and the risk of breast cancer**. *The New England journal of medicine* 1997, **336**(18):1269-1275.
22. Bernstein L, Henderson BE, Hanisch R, Sullivan-Halley J, Ross RK: **Physical exercise and reduced risk of breast cancer in young women**. *Journal of the National Cancer Institute* 1994, **86**(18):1403-1408.
23. Messina MJ, Persky V, Setchell KD, Barnes S: **Soy intake and cancer risk: a review of the in vitro and in vivo data**. *Nutrition and cancer* 1994, **21**(2):113-131.
24. Reis-Filho JS, Pusztai L: **Gene expression profiling in breast cancer: classification, prognostication, and prediction**. *Lancet* 2011, **378**(9805):1812-1823.
25. Rakha EA, El-Sayed ME, Reis-Filho J, Ellis IO: **Patho-biological aspects of basal-like breast cancer**. *Breast cancer research and treatment* 2009, **113**(3):411-422.
26. Parker JS, Mullins M, Cheang MC, Leung S, Voduc D, Vickery T, Davies S, Fauron C, He X, Hu Z *et al*: **Supervised risk predictor of breast cancer based on intrinsic subtypes**. *Journal of clinical oncology : official journal of the American Society of Clinical Oncology* 2009, **27**(8):1160-1167.

ATTENTION: The Singapore Copyright Act applies to the use of this document. Nanyang Technological University Library

27. Nielsen TO, Hsu FD, Jensen K, Cheang M, Karaca G, Hu Z, Hernandez-Boussard T, Livasy C, Cowan D, Dressler L *et al*: **Immunohistochemical and clinical characterization of the basal-like subtype of invasive breast carcinoma**. *Clinical cancer research : an official journal of the American Association for Cancer Research* 2004, **10**(16):5367-5374.
28. Reis-Filho JS, Lakhani SR: **Breast cancer special types: why bother?** *The Journal of pathology* 2008, **216**(4):394-398.
29. Bauer KR, Brown M, Cress RD, Parise CA, Caggiano V: **Descriptive analysis of estrogen receptor (ER)-negative, progesterone receptor (PR)-negative, and HER2-negative invasive breast cancer, the so-called triple-negative phenotype: a population-based study from the California cancer Registry**. *Cancer* 2007, **109**(9):1721-1728.
30. Badve S, Dabbs DJ, Schnitt SJ, Baehner FL, Decker T, Eusebi V, Fox SB, Ichihara S, Jacquemier J, Lakhani SR *et al*: **Basal-like and triple-negative breast cancers: a critical review with an emphasis on the implications for pathologists and oncologists**. *Modern pathology : an official journal of the United States and Canadian Academy of Pathology, Inc* 2011, **24**(2):157-167.
31. Tan AR, Swain SM: **Therapeutic strategies for triple-negative breast cancer**. *Cancer journal* 2008, **14**(6):343-351.
32. Podo F, Buydens LM, Degani H, Hilhorst R, Klipp E, Gribbestad IS, Van Huffel S, van Laarhoven HW, Luts J, Monleon D *et al*: **Triple-negative breast cancer: present challenges and new perspectives**. *Molecular oncology* 2010, **4**(3):209-229.
33. McSherry EA, Donatello S, Hopkins AM, McDonnell S: **Molecular basis of invasion in breast cancer**. *Cellular and molecular life sciences : CMLS* 2007, **64**(24):3201-3218.
34. Ran S, Volk L, Hall K, Flister MJ: **Lymphangiogenesis and lymphatic metastasis in breast cancer**. *Pathophysiology : the official journal of the International Society for Pathophysiology / ISP* 2010, **17**(4):229-251.
35. Baccelli I, Schneeweiss A, Riethdorf S, Stenzinger A, Schillert A, Vogel V, Klein C, Saini M, Bauerle T, Wallwiener M *et al*: **Identification of a population of blood circulating tumor cells from breast cancer patients that initiates metastasis in a xenograft assay**. *Nature biotechnology* 2013, **31**(6):539-544.
36. Stage IA, Stage, I. B., Stage, I. I. A., Stage, I. I. B., Stage, I. I. I. A., Stage, I. I. I. B., & Stage, I. V.: **Breast Cancer Staging**. *American joint committee on cancer* 2009.
37. Bendre M, Gaddy D, Nicholas RW, Suva LJ: **Breast cancer metastasis to bone: it is not all about PTHrP**. *Clinical orthopaedics and related research* 2003(415 Suppl):S39-45.
38. Chua B, Ung O, Taylor R, Boyages J: **Frequency and predictors of axillary lymph node metastases in invasive breast cancer**. *ANZ journal of surgery* 2001, **71**(12):723-728.
39. Lauria R, Perrone F, Carlomagno C, De Laurentiis M, Morabito A, Gallo C, Varriale E, Pettinato G, Panico L, Petrella G *et al*: **The prognostic value of lymphatic and blood vessel invasion in operable breast cancer**. *Cancer* 1995, **76**(10):1772-1778.

ATTENTION: The Singapore Copyright Act applies to the use of this document. Nanyang Technological University Library

40. Laurent TC, Fraser JR: **Hyaluronan**. *FASEB journal : official publication of the Federation of American Societies for Experimental Biology* 1992, **6**(7):2397-2404.
41. Weigelt B, Peterse JL, van 't Veer LJ: **Breast cancer metastasis: markers and models**. *Nature reviews Cancer* 2005, **5**(8):591-602.
42. Barnes JM, Nauseef JT, Henry MD: **Resistance to fluid shear stress is a conserved biophysical property of malignant cells**. *PLoS One* **7**(12):e50973.
43. Gupta GP, Massague J: **Cancer metastasis: building a framework**. *Cell* 2006, **127**(4):679-695.
44. Vanharanta S, Massague J: **Origins of metastatic traits**. *Cancer Cell*, **24**(4):410-421.
45. Scully OJ, Bay BH, Yip G, Yu Y: **Breast cancer metastasis**. *Cancer Genomics Proteomics* 2012, **9**(5):311-320.
46. Hunter KW, Crawford NP, Alsarraj J: **Mechanisms of metastasis**. *Breast cancer research : BCR* 2008, **10 Suppl 1**:S2.
47. Talmadge JE, Fidler IJ: **AACR centennial series: the biology of cancer metastasis: historical perspective**. *Cancer research* 2010, **70**(14):5649-5669.
48. Bonnomet A, Brysse A, Tachsidis A, Waltham M, Thompson EW, Polette M, Gilles C: **Epithelial-to-mesenchymal transitions and circulating tumor cells**. *Journal of mammary gland biology and neoplasia* 2010, **15**(2):261-273.
49. Fidler IJ, Kim SJ, Langley RR: **The role of the organ microenvironment in the biology and therapy of cancer metastasis**. *J Cell Biochem* 2007, **101**(4):927-936.
50. Nowell PC: **The clonal evolution of tumor cell populations**. *Science* 1976, **194**(4260):23-28.
51. Fidler IJ, Kripke ML: **Metastasis results from preexisting variant cells within a malignant tumor**. *Science* 1977, **197**(4306):893-895.
52. Kripke ML, Gruys E, Fidler IJ: **Metastatic heterogeneity of cells from an ultraviolet light-induced murine fibrosarcoma of recent origin**. *Cancer research* 1978, **38**(9):2962-2967.
53. Bernards R, Weinberg RA: **A progression puzzle**. *Nature* 2002, **418**(6900):823.
54. Greaves M, Maley CC: **Clonal evolution in cancer**. *Nature* 2012, **481**(7381):306-313.
55. Fidler IJ: **The pathogenesis of cancer metastasis: the 'seed and soil' hypothesis revisited**. *Nature reviews Cancer* 2003, **3**(6):453-458.
56. Reya T, Morrison SJ, Clarke MF, Weissman IL: **Stem cells, cancer, and cancer stem cells**. *Nature* 2001, **414**(6859):105-111.
57. Bonnet D, Dick JE: **Human acute myeloid leukemia is organized as a hierarchy that originates from a primitive hematopoietic cell**. *Nature medicine* 1997, **3**(7):730-737.
58. Barabe F, Kennedy JA, Hope KJ, Dick JE: **Modeling the initiation and progression of human acute leukemia in mice**. *Science* 2007, **316**(5824):600-604.
59. Hermann PC, Huber SL, Herrler T, Aicher A, Ellwart JW, Guba M, Bruns CJ, Heeschen C: **Distinct populations of cancer stem cells determine tumor growth and metastatic activity in human pancreatic cancer**. *Cell stem cell* 2007, **1**(3):313-323.

ATTENTION: The Singapore Copyright Act applies to the use of this document. Nanyang Technological University Library

60. Mani SA, Yang J, Brooks M, Schwaninger G, Zhou A, Miura N, Kutok JL, Hartwell K, Richardson AL, Weinberg RA: **Mesenchyme Forkhead 1 (FOXC2) plays a key role in metastasis and is associated with aggressive basal-like breast cancers**. *Proceedings of the National Academy of Sciences of the United States of America* 2007, **104**(24):10069-10074.
61. Thiery JP: **Epithelial-mesenchymal transitions in tumour progression**. *Nature reviews Cancer* 2002, **2**(6):442-454.
62. Thompson EW, Newgreen DF, Tarin D: **Carcinoma invasion and metastasis: a role for epithelial-mesenchymal transition?** *Cancer research* 2005, **65**(14):5991-5995; discussion 5995.
63. Hay ED: **An overview of epithelio-mesenchymal transformation**. *Acta anatomica* 1995, **154**(1):8-20.
64. Behrens J, Mareel MM, Van Roy FM, Birchmeier W: **Dissecting tumor cell invasion: epithelial cells acquire invasive properties after the loss of uvomorulin-mediated cell-cell adhesion**. *The Journal of cell biology* 1989, **108**(6):2435-2447.
65. Batlle E, Sancho E, Franci C, Dominguez D, Monfar M, Baulida J, Garcia De Herreros A: **The transcription factor snail is a repressor of E-cadherin gene expression in epithelial tumour cells**. *Nature cell biology* 2000, **2**(2):84-89.
66. Tsai JH, Yang J: **Epithelial-mesenchymal plasticity in carcinoma metastasis**. *Genes Dev* 2013, **27**(20):2192-2206.
67. Bracken CP, Gregory PA, Kolesnikoff N, Bert AG, Wang J, Shannon MF, Goodall GJ: **A double-negative feedback loop between ZEB1-SIP1 and the microRNA-200 family regulates epithelial-mesenchymal transition**. *Cancer research* 2008, **68**(19):7846-7854.
68. Ohkubo T, Ozawa M: **The transcription factor Snail downregulates the tight junction components independently of E-cadherin downregulation**. *J Cell Sci* 2004, **117**(Pt 9):1675-1685.
69. Yang J, Weinberg RA: **Epithelial-mesenchymal transition: at the crossroads of development and tumor metastasis**. *Developmental cell* 2008, **14**(6):818-829.
70. Kalluri R, Weinberg RA: **The basics of epithelial-mesenchymal transition**. *The Journal of clinical investigation* 2009, **119**(6):1420-1428.
71. Fidler IJ: **Metastasis: guantitative analysis of distribution and fate of tumor embolilabeled with 125 I-5-iodo-2'-deoxyuridine**. *Journal of the National Cancer Institute* 1970, **45**(4):773-782.
72. Kienast Y, von Baumgarten L, Fuhrmann M, Klinkert WE, Goldbrunner R, Herms J, Winkler F: **Real-time imaging reveals the single steps of brain metastasis formation**. *Nature medicine* 2010, **16**(1):116-122.
73. Chambers AF, Groom AC, MacDonald IC: **Dissemination and growth of cancer cells in metastatic sites**. *Nature reviews Cancer* 2002, **2**(8):563-572.
74. Nguyen DX, Bos PD, Massague J: **Metastasis: from dissemination to organ-specific colonization**. *Nature reviews Cancer* 2009, **9**(4):274-284.
75. Labelle M, Hynes RO: **The initial hours of metastasis: the importance of cooperative host-tumor cell interactions during hematogenous dissemination**. *Cancer discovery* 2012, **2**(12):1091-1099.

ATTENTION: The Singapore Copyright Act applies to the use of this document. Nanyang Technological University Library

76. Orr FW, Wang HH: **Tumor cell interactions with the microvasculature: a rate-limiting step in metastasis**. *Surgical oncology clinics of North America* 2001, **10**(2):357-381, ix-x.
77. Gupta GP, Nguyen DX, Chiang AC, Bos PD, Kim JY, Nadal C, Gomis RR, Manova-Todorova K, Massague J: **Mediators of vascular remodelling co-opted for sequential steps in lung metastasis**. *Nature* 2007, **446**(7137):765-770.
78. Stoletov K, Kato H, Zardouzian E, Kelber J, Yang J, Shattil S, Klemke R: **Visualizing extravasation dynamics of metastatic tumor cells**. *J Cell Sci* 2010, **123**(Pt 13):2332-2341.
79. Ell B, Kang Y: **SnapShot: Bone Metastasis**. *Cell* 2012, **151**(3):690-690 e691.
80. Howard JH, Bland KI: **Current management and treatment strategies for breast cancer**. *Current opinion in obstetrics & gynecology* 2012, **24**(1):44-48.
81. Berry DA, Ueno NT, Johnson MM, Lei X, Caputo J, Smith DA, Yancey LJ, Crump M, Stadtmauer EA, Biron P *et al*: **High-dose chemotherapy with autologous hematopoietic stem-cell transplantation in metastatic breast cancer: overview of six randomized trials**. *Journal of clinical oncology : official journal of the American Society of Clinical Oncology* 2011, **29**(24):3224-3231.
82. Association of Breast Surgery at B: **Surgical guidelines for the management of breast cancer**. *European journal of surgical oncology : the journal of the European Society of Surgical Oncology and the British Association of Surgical Oncology* 2009, **35 Suppl 1**:1-22.
83. Sekine H: **[Survey of the history and the future for breast cancer radiotherapy]**. *Nihon rinsho Japanese journal of clinical medicine* 2012, **70 Suppl 7**:18-22.
84. Zagar TM, Marks LB: **Breast cancer radiotherapy and coronary artery stenosis: location, location, location**. *Journal of clinical oncology : official journal of the American Society of Clinical Oncology* 2012, **30**(4):350-352.
85. Doval DC, Dutta K, Batra U, Talwar V: **Neoadjuvant chemotherapy in breast cancer: review of literature**. *Journal of the Indian Medical Association* 2013, **111**(9):629-631.
86. Schwartz J: **Current combination chemotherapy regimens for metastatic breast cancer**. *American journal of health-system pharmacy : AJHP : official journal of the American Society of Health-System Pharmacists* 2009, **66**(23 Suppl 6):S3-8.
87. Huober J, Thurlimann B: **The Role of Combination Chemotherapy in the Treatment of Patients with Metastatic Breast Cancer**. *Breast care* 2009, **4**(6):367-372.
88. Fornander T, Rutqvist LE, Cedermark B, Glas U, Mattsson A, Silfversward C, Skoog L, Somell A, Theve T, Wilking N *et al*: **Adjuvant tamoxifen in early breast cancer: occurrence of new primary cancers**. *Lancet* 1989, **1**(8630):117-120.
89. **Tamoxifen for early breast cancer: an overview of the randomised trials. Early Breast Cancer Trialists' Collaborative Group**. *Lancet* 1998, **351**(9114):1451-1467.
90. Fisher B, Costantino JP, Wickerham DL, Redmond CK, Kavanah M, Cronin WM, Vogel V, Robidoux A, Dimitrov N, Atkins J *et al*: **Tamoxifen for**

ATTENTION: The Singapore Copyright Act applies to the use of this document. Nanyang Technological University Library

prevention of breast cancer: report of the National Surgical Adjuvant Breast and Bowel Project P-1 Study. *Journal of the National Cancer Institute* 1998, **90**(18):1371-1388.

91. Valavaara R, Pyrhonen S, Heikkinen M, Rissanen P, Blanco G, Tholix E, Nordman E, Taskinen P, Holsti L, Hajba A: **Toremifene, a new antiestrogenic compound, for treatment of advanced breast cancer. Phase II study**. *European journal of cancer & clinical oncology* 1988, **24**(4):785-790.
92. Howell A, Robertson JF, Quaresma Albano J, Aschermannova A, Mauriac L, Kleeberg UR, Vergote I, Erikstein B, Webster A, Morris C: **Fulvestrant, formerly ICI 182,780, is as effective as anastrozole in postmenopausal women with advanced breast cancer progressing after prior endocrine treatment**. *Journal of clinical oncology : official journal of the American Society of Clinical Oncology* 2002, **20**(16):3396-3403.
93. Baselga J, Norton L, Albanell J, Kim YM, Mendelsohn J: **Recombinant humanized anti-HER2 antibody (Herceptin) enhances the antitumor activity of paclitaxel and doxorubicin against HER2/neu overexpressing human breast cancer xenografts**. *Cancer research* 1998, **58**(13):2825-2831.
94. de Bono JS, Bellmunt J, Attard G, Droz JP, Miller K, Flechon A, Sternberg C, Parker C, Zugmaier G, Hersberger-Gimenez V *et al*: **Open-label phase II study evaluating the efficacy and safety of two doses of pertuzumab in castrate chemotherapy-naive patients with hormone-refractory prostate cancer**. *Journal of clinical oncology : official journal of the American Society of Clinical Oncology* 2007, **25**(3):257-262.
95. Amiri-Kordestani L, Blumenthal GM, Xu QC, Zhang L, Tang SW, Ha L, Weinberg WC, Chi B, Candau-Chacon R, Hughes P *et al*: **FDA approval: ado-trastuzumab emtansine for the treatment of patients with HER2-positive metastatic breast cancer**. *Clinical cancer research : an official journal of the American Association for Cancer Research* 2014, **20**(17):4436-4441.
96. Lin NU, Carey LA, Liu MC, Younger J, Come SE, Ewend M, Harris GJ, Bullitt E, Van den Abbeele AD, Henson JW *et al*: **Phase II trial of lapatinib for brain metastases in patients with human epidermal growth factor receptor 2-positive breast cancer**. *Journal of clinical oncology : official journal of the American Society of Clinical Oncology* 2008, **26**(12):1993-1999.
97. Finn RS, Crown JP, Lang I, Boer K, Bondarenko IM, Kulyk SO, Ettl J, Patel R, Pinter T, Schmidt M *et al*: **The cyclin-dependent kinase 4/6 inhibitor palbociclib in combination with letrozole versus letrozole alone as first-line treatment of oestrogen receptor-positive, HER2-negative, advanced breast cancer (PALOMA-1/TRIO-18): a randomised phase 2 study**. *The Lancet Oncology* 2015, **16**(1):25-35.
98. Stockler M, Wilcken NR, Ghersi D, Simes RJ: **Systematic reviews of chemotherapy and endocrine therapy in metastatic breast cancer**. *Cancer treatment reviews* 2000, **26**(3):151-168.
99. Guth U, Huang DJ, Dirnhofer S, Rochlitz C, Wight E: **Distant metastatic breast cancer as an incurable disease: a tenet with a need for revision**. *Cancer journal* 2009, **15**(1):81-86.
100. Swain SM, Baselga J, Kim SB, Ro J, Semiglazov V, Campone M, Ciruelos E, Ferrero JM, Schneeweiss A, Heeson S *et al*: **Pertuzumab, trastuzumab, and**

ATTENTION: The Singapore Copyright Act applies to the use of this document. Nanyang Technological University Library

docetaxel in HER2-positive metastatic breast cancer. *The New England journal of medicine* 2015, **372**(8):724-734.

101. Cleator S, Heller W, Coombes RC: **Triple-negative breast cancer: therapeutic options**. *The Lancet Oncology* 2007, **8**(3):235-244.
102. Gucalp A, Traina TA: **Triple-negative breast cancer: adjuvant therapeutic options**. *Chemotherapy research and practice* 2011, **2011**:696208.
103. Coley HM: **Mechanisms and strategies to overcome chemotherapy resistance in metastatic breast cancer**. *Cancer treatment reviews* 2008, **34**(4):378-390.
104. Gradilone A, Naso G, Raimondi C, Cortesi E, Gandini O, Vincenzi B, Saltarelli R, Chiapparino E, Spremberg F, Cristofanilli M *et al*: **Circulating tumor cells (CTCs) in metastatic breast cancer (MBC): prognosis, drug resistance and phenotypic characterization**. *Annals of oncology : official journal of the European Society for Medical Oncology / ESMO* 2011, **22**(1):86-92.
105. Cristofanilli M, Budd GT, Ellis MJ, Stopeck A, Matera J, Miller MC, Reuben JM, Doyle GV, Allard WJ, Terstappen LW *et al*: **Circulating tumor cells, disease progression, and survival in metastatic breast cancer**. *The New England journal of medicine* 2004, **351**(8):781-791.
106. Hayes DF, Cristofanilli M, Budd GT, Ellis MJ, Stopeck A, Miller MC, Matera J, Allard WJ, Doyle GV, Terstappen LW: **Circulating tumor cells at each follow-up time point during therapy of metastatic breast cancer patients predict progression-free and overall survival**. *Clinical cancer research : an official journal of the American Association for Cancer Research* 2006, **12**(14 Pt 1):4218-4224.
107. Budd GT, Cristofanilli M, Ellis MJ, Stopeck A, Borden E, Miller MC, Matera J, Repollet M, Doyle GV, Terstappen LW *et al*: **Circulating tumor cells versus imaging--predicting overall survival in metastatic breast cancer**. *Clinical cancer research : an official journal of the American Association for Cancer Research* 2006, **12**(21):6403-6409.
108. Cristofanilli M, Broglio KR, Guarneri V, Jackson S, Fritsche HA, Islam R, Dawood S, Reuben JM, Kau SW, Lara JM *et al*: **Circulating tumor cells in metastatic breast cancer: biologic staging beyond tumor burden**. *Clinical breast cancer* 2007, **7**(6):471-479.
109. Dawood S, Broglio K, Valero V, Reuben J, Handy B, Islam R, Jackson S, Hortobagyi GN, Fritsche H, Cristofanilli M: **Circulating tumor cells in metastatic breast cancer: from prognostic stratification to modification of the staging system?** *Cancer* 2008, **113**(9):2422-2430.
110. Gazzaniga P, Naso G, Gradilone A, Cortesi E, Gandini O, Gianni W, Fabbri MA, Vincenzi B, di Silverio F, Frati L *et al*: **Chemosensitivity profile assay of circulating cancer cells: prognostic and predictive value in epithelial tumors**. *International journal of cancer Journal international du cancer* 2010, **126**(10):2437-2447.
111. Engell HC: **Cancer cells in the circulating blood; a clinical study on the occurrence of cancer cells in the peripheral blood and in venous blood draining the tumour area at operation**. *Acta chirurgica Scandinavica Supplementum* 1955, **201**:1-70.

ATTENTION: The Singapore Copyright Act applies to the use of this document. Nanyang Technological University Library

112. Myerowitz RL, Edwards PA, Sartiano GP: **Carcinocythemia (carcinoma cell leukemia) due to metastatic carcinoma of the breast: report of a case**. *Cancer* 1977, **40**(6):3107-3111.
113. Gallivan MV, Lokich JJ: **Carcinocythemia (carcinoma cell leukemia). Report of two cases with English literature review**. *Cancer* 1984, **53**(5):1100-1102.
114. Sile CC, Perry DJ, Nam L: **Small cell carcinocythemia**. *Archives of pathology & laboratory medicine* 1999, **123**(5):426-428.
115. Seronie-Vivien S, Mery E, Delord JP, Fillola G, Tkaczuk J, Voigt JJ, Bugat R: **Carcinocythemia as the single extension of breast cancer: report of a case and review of the literature**. *Annals of oncology : official journal of the European Society for Medical Oncology / ESMO* 2001, **12**(7):1019-1022.
116. Racila E, Euhus D, Weiss AJ, Rao C, McConnell J, Terstappen LW, Uhr JW: **Detection and characterization of carcinoma cells in the blood**. *Proceedings of the National Academy of Sciences of the United States of America* 1998, **95**(8):4589-4594.
117. Terstappen LW, Rao C, Gross S, Weiss AJ: **Peripheral blood tumor cell load reflects the clinical activity of the disease in patients with carcinoma of the breast**. *International journal of oncology* 2000, **17**(3):573-578.
118. Guller U, Zajac P, Schnider A, Bosch B, Vorburger S, Zuber M, Spagnoli GC, Oertli D, Maurer R, Metzger U *et al*: **Disseminated single tumor cells as detected by real-time quantitative polymerase chain reaction represent a prognostic factor in patients undergoing surgery for colorectal cancer**. *Annals of surgery* 2002, **236**(6):768-775; discussion 775-766.
119. Gaforio JJ, Serrano MJ, Sanchez-Rovira P, Sirvent A, Delgado-Rodriguez M, Campos M, de la Torre N, Algarra I, Duenas R, Lozano A: **Detection of breast cancer cells in the peripheral blood is positively correlated with estrogen-receptor status and predicts for poor prognosis**. *International journal of cancer Journal international du cancer* 2003, **107**(6):984-990.
120. Alix-Panabieres C, Pantel K: **Challenges in circulating tumour cell research**. *Nature reviews Cancer* 2014, **14**(9):623-631.
121. Alix-Panabieres C, Pantel K: **Circulating tumor cells: liquid biopsy of cancer**. *Clinical chemistry* 2013, **59**(1):110-118.
122. Parkinson DR, Dracopoli N, Petty BG, Compton C, Cristofanilli M, Deisseroth A, Hayes DF, Kapke G, Kumar P, Lee J *et al*: **Considerations in the development of circulating tumor cell technology for clinical use**. *Journal of translational medicine* 2012, **10**:138.
123. Pantel K, Brakenhoff RH, Brandt B: **Detection, clinical relevance and specific biological properties of disseminating tumour cells**. *Nature reviews Cancer* 2008, **8**(5):329-340.
124. Ramirez JM, Fehm T, Orsini M, Cayrefourcq L, Maudelonde T, Pantel K, Alix-Panabieres C: **Prognostic relevance of viable circulating tumor cells detected by EPISPOT in metastatic breast cancer patients**. *Clinical chemistry* 2014, **60**(1):214-221.
125. Friedlander TW, Ngo VT, Dong H, Premasekharan G, Weinberg V, Doty S, Zhao Q, Gilbert EG, Ryan CJ, Chen WT *et al*: **Detection and characterization of invasive circulating tumor cells derived from men with metastatic**

ATTENTION: The Singapore Copyright Act applies to the use of this document. Nanyang Technological University Library

castration-resistant prostate cancer. *International journal of cancer Journal international du cancer* 2014, **134**(10):2284-2293.

126. Bednarz-Knoll N, Alix-Panabieres C, Pantel K: **Plasticity of disseminating cancer cells in patients with epithelial malignancies**. *Cancer metastasis reviews* 2012, **31**(3-4):673-687.
127. Pantel K, Deneve E, Nocca D, Coffy A, Vendrell JP, Maudelonde T, Riethdorf S, Alix-Panabieres C: **Circulating epithelial cells in patients with benign colon diseases**. *Clinical chemistry* 2012, **58**(5):936-940.
128. Meng S, Tripathy D, Frenkel EP, Shete S, Naftalis EZ, Huth JF, Beitsch PD, Leitch M, Hoover S, Euhus D *et al*: **Circulating tumor cells in patients with breast cancer dormancy**. *Clinical cancer research : an official journal of the American Association for Cancer Research* 2004, **10**(24):8152-8162.
129. Braun S, Naume B: **Circulating and disseminated tumor cells**. *Journal of clinical oncology : official journal of the American Society of Clinical Oncology* 2005, **23**(8):1623-1626.
130. Yu M, Bardia A, Wittner BS, Stott SL, Smas ME, Ting DT, Isakoff SJ, Ciciliano JC, Wells MN, Shah AM *et al*: **Circulating breast tumor cells exhibit dynamic changes in epithelial and mesenchymal composition**. *Science* 2013, **339**(6119):580-584.
131. Muller A, Homey B, Soto H, Ge N, Catron D, Buchanan ME, McClanahan T, Murphy E, Yuan W, Wagner SN *et al*: **Involvement of chemokine receptors in breast cancer metastasis**. *Nature* 2001, **410**(6824):50-56.
132. Deneve E, Riethdorf S, Ramos J, Nocca D, Coffy A, Daures JP, Maudelonde T, Fabre JM, Pantel K, Alix-Panabieres C: **Capture of viable circulating tumor cells in the liver of colorectal cancer patients**. *Clinical chemistry* 2013, **59**(9):1384-1392.
133. Wirtz D, Konstantopoulos K, Searson PC: **The physics of cancer: the role of physical interactions and mechanical forces in metastasis**. *Nature reviews Cancer*, **11**(7):512-522.
134. Goldmann E: **The Growth of Malignant Disease in Man and the Lower Animals, with special reference to the Vascular System**. *Proceedings of the Royal Society of Medicine* 1908, **1**(Surg Sect):1-13.
135. Iwasaki T: **Histological and experimental observations on the destruction of tumour cells in the blood vessels**. *The Journal of Pathology and Bacteriology* 1915, **20**(1):85-105.
136. Zeidman I, Mc CM, Coman DR: **Factors affecting the number of tumor metastases; experiments with a transplantable mouse tumor**. *Cancer research* 1950, **10**(6):357-359.
137. Zeidman I, Buss JM: **Transpulmonary passage of tumor cell emboli**. *Cancer research* 1952, **12**(10):731-733.
138. Weiss L, Mayhew E, Rapp DG, Holmes JC: **Metastatic inefficiency in mice bearing B16 melanomas**. *British journal of cancer* 1982, **45**(1):44-53.
139. Stackpole CW: **Distinct lung-colonizing and lung-metastasizing cell populations in B16 mouse melanoma**. *Nature* 1981, **289**(5800):798-800.
140. Barbera-Guillem E, Smith I, Weiss L: **Cancer-cell traffic in the liver. I. Growth kinetics of cancer cells after portal-vein delivery**. *International journal of cancer Journal international du cancer* 1992, **52**(6):974-977.

ATTENTION: The Singapore Copyright Act applies to the use of this document. Nanyang Technological University Library

141. Hanahan D, Weinberg RA: **Hallmarks of cancer: the next generation**. *Cell* 2011, **144**(5):646-674.
142. Adams JM, Cory S: **The Bcl-2 apoptotic switch in cancer development and therapy**. *Oncogene* 2007, **26**(9):1324-1337.
143. Evan G, Littlewood T: **A matter of life and cell death**. *Science* 1998, **281**(5381):1317-1322.
144. Lowe SW, Cepero E, Evan G: **Intrinsic tumour suppression**. *Nature* 2004, **432**(7015):307-315.
145. Kerr JF, Wyllie AH, Currie AR: **Apoptosis: a basic biological phenomenon with wide-ranging implications in tissue kinetics**. *British journal of cancer* 1972, **26**(4):239-257.
146. Hacker G: **The morphology of apoptosis**. *Cell and tissue research* 2000, **301**(1):5-17.
147. Elmore S: **Apoptosis: a review of programmed cell death**. *Toxicologic pathology* 2007, **35**(4):495-516.
148. Krysko DV, Vanden Berghe T, D'Herde K, Vandenabeele P: **Apoptosis and necrosis: detection, discrimination and phagocytosis**. *Methods* 2008, **44**(3):205-221.
149. Fan TJ, Han LH, Cong RS, Liang J: **Caspase family proteases and apoptosis**. *Acta biochimica et biophysica Sinica* 2005, **37**(11):719-727.
150. Slee EA, Adrain C, Martin SJ: **Executioner caspase-3, -6, and -7 perform distinct, non-redundant roles during the demolition phase of apoptosis**. *The Journal of biological chemistry* 2001, **276**(10):7320-7326.
151. Martinon F, Tschopp J: **Inflammatory caspases: linking an intracellular innate immune system to autoinflammatory diseases**. *Cell* 2004, **117**(5):561-574.
152. Ruchaud S, Korfali N, Villa P, Kottke TJ, Dingwall C, Kaufmann SH, Earnshaw WC: **Caspase-6 gene disruption reveals a requirement for lamin A cleavage in apoptotic chromatin condensation**. *The EMBO journal* 2002, **21**(8):1967-1977.
153. Han D, Williams E, Cadenas E: **Mitochondrial respiratory chain-dependent generation of superoxide anion and its release into the intermembrane space**. *Biochem J* 2001, **353**(Pt 2):411-416.
154. Luo KQ, Yu VC, Pu Y, Chang DC: **Application of the fluorescence resonance energy transfer method for studying the dynamics of caspase-3 activation during UV-induced apoptosis in living HeLa cells**. *Biochemical and biophysical research communications* 2001, **283**(5):1054-1060.
155. Heim R, Tsien RY: **Engineering green fluorescent protein for improved brightness, longer wavelengths and fluorescence resonance energy transfer**. *Current biology : CB* 1996, **6**(2):178-182.
156. Tsien RY: **The green fluorescent protein**. *Annual review of biochemistry* 1998, **67**:509-544.
157. Tian H, Ip L, Luo H, Chang DC, Luo KQ: **A high throughput drug screen based on fluorescence resonance energy transfer (FRET) for anticancer activity of compounds from herbal medicine**. *British journal of pharmacology* 2007, **150**(3):321-334.
158. Han QB, Tian HL, Yang NY, Qiao CF, Song JZ, Chang DC, Luo KQ, Xu HX: **Polyprenylated xanthones from Garcinia lancilimba showing apoptotic**

ATTENTION: The Singapore Copyright Act applies to the use of this document. Nanyang Technological University Library

effects against HeLa-C3 cells. *Chemistry & biodiversity* 2008, **5**(12):2710-2717.

159. Han QB, Yang NY, Tian HL, Qiao CF, Song JZ, Chang DC, Chen SL, Luo KQ, Xu HX: **Xanthones with growth inhibition against HeLa cells from Garcinia xipshuanbannaensis**. *Phytochemistry* 2008, **69**(11):2187-2192.
160. Zhou L, Chan WK, Xu N, Xiao K, Luo H, Luo KQ, Chang DC: **Tanshinone IIA, an isolated compound from Salvia miltiorrhiza Bunge, induces apoptosis in HeLa cells through mitotic arrest**. *Life sciences* 2008, **83**(11-12):394-403.
161. Huang SX, Feng C, Zhou Y, Xu G, Han QB, Qiao CF, Chang DC, Luo KQ, Xu HX: **Bioassay-guided isolation of xanthones and polycyclic prenylated acylphloroglucinols from Garcinia oblongifolia**. *Journal of natural products* 2009, **72**(1):130-135.
162. Han QB, Zhou Y, Feng C, Xu G, Huang SX, Li SL, Qiao CF, Song JZ, Chang DC, Luo KQ *et al*: **Bioassay guided discovery of apoptosis inducers from gamboge by high-speed counter-current chromatography and high-pressure liquid chromatography/electrospray ionization quadrupole time-of-flight mass spectrometry**. *Journal of chromatography B, Analytical technologies in the biomedical and life sciences* 2009, **877**(4):401-407.
163. Gao XM, Yu T, Lai FS, Zhou Y, Liu X, Qiao CF, Song JZ, Chen SL, Luo KQ, Xu HX: **Identification and evaluation of apoptotic compounds from Garcinia paucinervis**. *Bioorganic & medicinal chemistry* 2010, **18**(14):4957-4964.
164. Gao XM, Yu T, Cui MZ, Pu JX, Du X, Han QB, Hu QF, Liu TC, Luo KQ, Xu HX: **Identification and evaluation of apoptotic compounds from Garcinia oligantha**. *Bioorganic & medicinal chemistry letters* 2012, **22**(6):2350-2353.
165. Liu X, Yu T, Gao XM, Zhou Y, Qiao CF, Peng Y, Chen SL, Luo KQ, Xu HX: **Apoptotic effects of polyprenylated benzoylphloroglucinol derivatives from the twigs of Garcinia multiflora**. *Journal of natural products* 2010, **73**(8):1355-1359.
166. Han QB, Yu T, Lai F, Zhou Y, Feng C, Wang WN, Fu XH, Lau CB, Luo KQ, Xu HX *et al*: **Quick identification of apoptosis inducer from Isodon eriocalyx by a drug discovery platform composed of analytical high-speed counter-current chromatography and the fluorescence-based caspase-3 biosensor detection**. *Talanta* 2010, **82**(4):1521-1527.
167. Tian HL, Yu T, Xu NN, Feng C, Zhou LY, Luo HW, Chang DC, Le XF, Luo KQ: **A novel compound modified from tanshinone inhibits tumor growth in vivo via activation of the intrinsic apoptotic pathway**. *Cancer letters* 2010, **297**(1):18-30.
168. Feng C, Zhou LY, Yu T, Xu G, Tian HL, Xu JJ, Xu HX, Luo KQ: **A new anticancer compound, oblongifolin C, inhibits tumor growth and promotes apoptosis in HeLa cells through Bax activation**. *International journal of cancer Journal international du cancer* 2012, **131**(6):1445-1454.
169. Yu T, Zhou Z, Mu Y, de Lima Lopes G, Luo KQ: **A novel anti-cancer agent, acetyltanshinone IIA, inhibits oestrogen receptor positive breast cancer cell growth by down-regulating the oestrogen receptor**. *Cancer letters* 2014, **346**(1):94-103.

ATTENTION: The Singapore Copyright Act applies to the use of this document. Nanyang Technological University Library

170. Zhu X, Fu A, Luo KQ: **A high-throughput fluorescence resonance energy transfer (FRET)-based endothelial cell apoptosis assay and its application for screening vascular disrupting agents**. *Biochemical and biophysical research communications* 2012, **418**(4):641-646.
171. Chiew GG, Fu A, Low KP, Luo KQ: **Physical supports from liver cancer cells are essential for differentiation and remodeling of endothelial cells in a HepG2-HUVEC co-culture model**. *Scientific reports* 2015, **5**:10801.
172. Chin LK, Yu JQ, Fu Y, Yu T, Liu AQ, Luo KQ: **Production of reactive oxygen species in endothelial cells under different pulsatile shear stresses and glucose concentrations**. *Lab on a chip* 2011, **11**(11):1856-1863.
173. Yu JQ, Liu XF, Chin LK, Liu AQ, Luo KQ: **Study of endothelial cell apoptosis using fluorescence resonance energy transfer (FRET) biosensor cell line with hemodynamic microfluidic chip system**. *Lab on a chip* 2013, **13**(14):2693-2700.
174. Liu XF, Yu JQ, Dalan R, Liu AQ, Luo KQ: **Biological factors in plasma from diabetes mellitus patients enhance hyperglycaemia and pulsatile shear stress-induced endothelial cell apoptosis**. *Integrative biology : quantitative biosciences from nano to macro* 2014, **6**(5):511-522.
175. Holohan C, Van Schaeybroeck S, Longley DB, Johnston PG: **Cancer drug resistance: an evolving paradigm**. *Nature reviews Cancer* 2013, **13**(10):714-726.
176. Gonzalez-Angulo AM, Morales-Vasquez F, Hortobagyi GN: **Overview of resistance to systemic therapy in patients with breast cancer**. *Advances in experimental medicine and biology* 2007, **608**:1-22.
177. Longley DB, Johnston PG: **Molecular mechanisms of drug resistance**. *The Journal of pathology* 2005, **205**(2):275-292.
178. Swanton C: **Intratumor heterogeneity: evolution through space and time**. *Cancer research* 2012, **72**(19):4875-4882.
179. Valent P, Bonnet D, De Maria R, Lapidot T, Copland M, Melo JV, Chomienne C, Ishikawa F, Schuringa JJ, Stassi G *et al*: **Cancer stem cell definitions and terminology: the devil is in the details**. *Nature reviews Cancer* 2012, **12**(11):767-775.
180. Chang G, Roth CB: **Structure of MsbA from E. coli: a homolog of the multidrug resistance ATP binding cassette (ABC) transporters**. *Science* 2001, **293**(5536):1793-1800.
181. Thomas H, Coley HM: **Overcoming multidrug resistance in cancer: an update on the clinical strategy of inhibiting p-glycoprotein**. *Cancer control : journal of the Moffitt Cancer Center* 2003, **10**(2):159-165.
182. Meijer C, Mulder NH, Timmer-Bosscha H, Sluiter WJ, Meersma GJ, de Vries EG: **Relationship of cellular glutathione to the cytotoxicity and resistance of seven platinum compounds**. *Cancer research* 1992, **52**(24):6885-6889.
183. Manolitsas TP, Englefield P, Eccles DM, Campbell IG: **No association of a 306-bp insertion polymorphism in the progesterone receptor gene with ovarian and breast cancer**. *British journal of cancer* 1997, **75**(9):1398-1399.
184. Hinds M, Deisseroth K, Mayes J, Altschuler E, Jansen R, Ledley FD, Zwelling LA: **Identification of a point mutation in the topoisomerase II gene from a human leukemia cell line containing an amsacrine-resistant form of topoisomerase II**. *Cancer research* 1991, **51**(17):4729-4731.

ATTENTION: The Singapore Copyright Act applies to the use of this document. Nanyang Technological University Library

185. Sarkar S, Faller DV: **T-oligos inhibit growth and induce apoptosis in human ovarian cancer cells**. *Oligonucleotides* 2011, **21**(1):47-53.
186. Karran P: **Mechanisms of tolerance to DNA damaging therapeutic drugs**. *Carcinogenesis* 2001, **22**(12):1931-1937.
187. Miki Y, Swensen J, Shattuck-Eidens D, Futreal PA, Harshman K, Tavtigian S, Liu Q, Cochran C, Bennett LM, Ding W *et al*: **A strong candidate for the breast and ovarian cancer susceptibility gene BRCA1**. *Science* 1994, **266**(5182):66-71.
188. Wooster R, Bignell G, Lancaster J, Swift S, Seal S, Mangion J, Collins N, Gregory S, Gumbs C, Micklem G: **Identification of the breast cancer susceptibility gene BRCA2**. *Nature* 1995, **378**(6559):789-792.
189. Dhillon KK, Swisher EM, Taniguchi T: **Secondary mutations of BRCA1/2 and drug resistance**. *Cancer science* 2011, **102**(4):663-669.
190. Apel K, Hirt H: **Reactive oxygen species: metabolism, oxidative stress, and signal transduction**. *Annual review of plant biology* 2004, **55**:373-399.
191. Waris G, Ahsan H: **Reactive oxygen species: role in the development of cancer and various chronic conditions**. *J Carcinog* 2006, **5**:14.
192. Schumacker PT: **Reactive oxygen species in cancer: a dance with the devil**. *Cancer Cell* 2015, **27**(2):156-157.
193. Watson J: **Oxidants, antioxidants and the current incurability of metastatic cancers**. *Open Biol*, **3**(1):120144.
194. Ray PD, Huang BW, Tsuji Y: **Reactive oxygen species (ROS) homeostasis and redox regulation in cellular signaling**. *Cell Signal* 2012, **24**(5):981-990.
195. Liou GY, Storz P: **Reactive oxygen species in cancer**. *Free Radic Res* 2010, **44**(5):479-496.
196. Crompton M: **The mitochondrial permeability transition pore and its role in cell death**. *Biochem J* 1999, **341 (Pt 2)**:233-249.
197. Storz P: **Reactive oxygen species-mediated mitochondria-to-nucleus signaling: a key to aging and radical-caused diseases**. *Sci STKE* 2006, **2006**(332):re3.
198. McCord JM, Fridovich I: **Superoxide dismutase. An enzymic function for erythrocuprein (hemocuprein)**. *The Journal of biological chemistry* 1969, **244**(22):6049-6055.
199. Bienert GP, Moller AL, Kristiansen KA, Schulz A, Moller IM, Schjoerring JK, Jahn TP: **Specific aquaporins facilitate the diffusion of hydrogen peroxide across membranes**. *The Journal of biological chemistry* 2007, **282**(2):1183-1192.
200. Dansen TB, Wirtz KW: **The peroxisome in oxidative stress**. *IUBMB Life* 2001, **51**(4):223-230.
201. Ames BN: **Dietary carcinogens and anticarcinogens. Oxygen radicals and degenerative diseases**. *Science* 1983, **221**(4617):1256-1264.
202. Jaiyesimi IA, Buzdar AU, Hortobagyi G: **Inflammatory breast cancer: a review**. *Journal of clinical oncology : official journal of the American Society of Clinical Oncology* 1992, **10**(6):1014-1024.
203. Esposito LA, Melov S, Panov A, Cottrell BA, Wallace DC: **Mitochondrial disease in mouse results in increased oxidative stress**. *Proceedings of the National Academy of Sciences of the United States of America* 1999, **96**(9):4820-4825.

ATTENTION: The Singapore Copyright Act applies to the use of this document. Nanyang Technological University Library

204. Bendayan M, Reddy JK: **Immunocytochemical localization of catalase and heat-labile enoyl-CoA hydratase in the livers of normal and peroxisome proliferator-treated rats**. *Lab Invest* 1982, **47**(4):364-369.
205. Holley AK, Dhar SK, Xu Y, St Clair DK: **Manganese superoxide dismutase: beyond life and death**. *Amino Acids* 2010, **42**(1):139-158.
206. Abe Y, Okazaki T: **Purification and properties of the manganese superoxide dismutase from the liver of bullfrog, Rana catesbeiana**. *Arch Biochem Biophys* 1987, **253**(1):241-248.
207. Borrelli A, Schiattarella A, Bonelli P, Tuccillo FM, Buonaguro FM, Mancini A: **The functional role of MnSOD as a biomarker of human diseases and therapeutic potential of a new isoform of a human recombinant MnSOD**. *Biomed Res Int* 2014, **2014**:476789.
208. Buettner GR, Ng CF, Wang M, Rodgers VG, Schafer FQ: **A new paradigm: manganese superoxide dismutase influences the production of H2O2 in cells and thereby their biological state**. *Free Radic Biol Med* 2006, **41**(8):1338-1350.
209. Keller JN, Kindy MS, Holtsberg FW, St Clair DK, Yen HC, Germeyer A, Steiner SM, Bruce-Keller AJ, Hutchins JB, Mattson MP: **Mitochondrial manganese superoxide dismutase prevents neural apoptosis and reduces ischemic brain injury: suppression of peroxynitrite production, lipid peroxidation, and mitochondrial dysfunction**. *J Neurosci* 1998, **18**(2):687-697.
210. Minotti G, Menna P, Salvatorelli E, Cairo G, Gianni L: **Anthracyclines: molecular advances and pharmacologic developments in antitumor activity and cardiotoxicity**. *Pharmacol Rev* 2004, **56**(2):185-229.
211. Doroshow JH: **Anthracycline antibiotic-stimulated superoxide, hydrogen peroxide, and hydroxyl radical production by NADH dehydrogenase**. *Cancer research* 1983, **43**(10):4543-4551.
212. Marcillat O, Zhang Y, Davies KJ: **Oxidative and non-oxidative mechanisms in the inactivation of cardiac mitochondrial electron transport chain components by doxorubicin**. *Biochem J* 1989, **259**(1):181-189.
213. Kotamraju S, Chitambar CR, Kalivendi SV, Joseph J, Kalyanaraman B: **Transferrin receptor-dependent iron uptake is responsible for doxorubicin-mediated apoptosis in endothelial cells: role of oxidant-induced iron signaling in apoptosis**. *The Journal of biological chemistry* 2002, **277**(19):17179-17187.
214. Minotti G, Ronchi R, Salvatorelli E, Menna P, Cairo G: **Doxorubicin irreversibly inactivates iron regulatory proteins 1 and 2 in cardiomyocytes: evidence for distinct metabolic pathways and implications for iron-mediated cardiotoxicity of antitumor therapy**. *Cancer research* 2001, **61**(23):8422-8428.
215. Halliwell B: **Superoxide-dependent formation of hydroxyl radicals in the presence of iron chelates: is it a mechanism for hydroxyl radical production in biochemical systems?** *FEBS Lett* 1978, **92**(2):321-326.
216. Veal EA, Day AM, Morgan BA: **Hydrogen peroxide sensing and signaling**. *Molecular cell* 2007, **26**(1):1-14.
217. Wang M, Kirk JS, Venkataraman S, Domann FE, Zhang HJ, Schafer FQ, Flanagan SW, Weydert CJ, Spitz DR, Buettner GR *et al*: **Manganese**

ATTENTION: The Singapore Copyright Act applies to the use of this document. Nanyang Technological University Library

superoxide dismutase suppresses hypoxic induction of hypoxia-inducible factor-1alpha and vascular endothelial growth factor. *Oncogene* 2005, **24**(55):8154-8166.

218. Zhao Y, Xue Y, Oberley TD, Kiningham KK, Lin SM, Yen HC, Majima H, Hines J, St Clair D: **Overexpression of manganese superoxide dismutase suppresses tumor formation by modulation of activator protein-1 signaling in a multistage skin carcinogenesis model**. *Cancer research* 2001, **61**(16):6082-6088.
219. Hempel N, Carrico PM, Melendez JA: **Manganese superoxide dismutase (Sod2) and redox-control of signaling events that drive metastasis**. *Anti-cancer agents in medicinal chemistry* 2011, **11**(2):191-201.
220. Behrend L, Mohr A, Dick T, Zwacka RM: **Manganese superoxide dismutase induces p53-dependent senescence in colorectal cancer cells**. *Molecular and cellular biology* 2005, **25**(17):7758-7769.
221. Oberley LW, Buettner GR: **Role of superoxide dismutase in cancer: a review**. *Cancer research* 1979, **39**(4):1141-1149.
222. Oberley LW, Oberley TD, Buettner GR: **Cell differentiation, aging and cancer: the possible roles of superoxide and superoxide dismutases**. *Medical hypotheses* 1980, **6**(3):249-268.
223. Church SL, Grant JW, Ridnour LA, Oberley LW, Swanson PE, Meltzer PS, Trent JM: **Increased manganese superoxide dismutase expression suppresses the malignant phenotype of human melanoma cells**. *Proceedings of the National Academy of Sciences of the United States of America* 1993, **90**(7):3113-3117.
224. Li JJ, Oberley LW, St Clair DK, Ridnour LA, Oberley TD: **Phenotypic changes induced in human breast cancer cells by overexpression of manganese-containing superoxide dismutase**. *Oncogene* 1995, **10**(10):1989-2000.
225. Van Remmen H, Ikeno Y, Hamilton M, Pahlavani M, Wolf N, Thorpe SR, Alderson NL, Baynes JW, Epstein CJ, Huang TT *et al*: **Life-long reduction in MnSOD activity results in increased DNA damage and higher incidence of cancer but does not accelerate aging**. *Physiological genomics* 2003, **16**(1):29-37.
226. Malafa M, Margenthaler J, Webb B, Neitzel L, Christophersen M: **MnSOD expression is increased in metastatic gastric cancer**. *The Journal of surgical research* 2000, **88**(2):130-134.
227. Toh Y, Kuninaka S, Oshiro T, Ikeda Y, Nakashima H, Baba H, Kohnoe S, Okamura T, Mori M, Sugimachi K: **Overexpression of manganese superoxide dismutase mRNA may correlate with aggressiveness in gastric and colorectal adenocarcinomas**. *International journal of oncology* 2000, **17**(1):107-112.
228. Tsanou E, Ioachim E, Briasoulis E, Damala K, Charchanti A, Karavasilis V, Pavlidis N, Agnantis NJ: **Immunohistochemical expression of superoxide dismutase (MnSOD) anti-oxidant enzyme in invasive breast carcinoma**. *Histology and histopathology* 2004, **19**(3):807-813.
229. Miriyala S, Spasojevic I, Tovmasyan A, Salvemini D, Vujaskovic Z, St Clair D, Batinic-Haberle I: **Manganese superoxide dismutase, MnSOD and its mimics**. *Biochimica et biophysica acta* 2012, **1822**(5):794-814.

ATTENTION: The Singapore Copyright Act applies to the use of this document. Nanyang Technological University Library

230. Wan XS, Devalaraja MN, St Clair DK: **Molecular structure and organization of the human manganese superoxide dismutase gene**. *DNA and cell biology* 1994, **13**(11):1127-1136.
231. Xu Y, Porntadavity S, St Clair DK: **Transcriptional regulation of the human manganese superoxide dismutase gene: the role of specificity protein 1 (Sp1) and activating protein-2 (AP-2)**. *Biochem J* 2002, **362**(Pt 2):401-412.
232. Dhar SK, Xu Y, Chen Y, St Clair DK: **Specificity protein 1-dependent p53-mediated suppression of human manganese superoxide dismutase gene expression**. *The Journal of biological chemistry* 2006, **281**(31):21698-21709.
233. Xu Y, Kiningham KK, Devalaraja MN, Yeh CC, Majima H, Kasarskis EJ, St Clair DK: **An intronic NF-kappaB element is essential for induction of the human manganese superoxide dismutase gene by tumor necrosis factor-alpha and interleukin-1beta**. *DNA and cell biology* 1999, **18**(9):709-722.
234. Dhar SK, Lynn BC, Daosukho C, St Clair DK: **Identification of nucleophosmin as an NF-kappaB co-activator for the induction of the human SOD2 gene**. *The Journal of biological chemistry* 2004, **279**(27):28209-28219.
235. Xu Y, Krishnan A, Wan XS, Majima H, Yeh CC, Ludewig G, Kasarskis EJ, St Clair DK: **Mutations in the promoter reveal a cause for the reduced expression of the human manganese superoxide dismutase gene in cancer cells**. *Oncogene* 1999, **18**(1):93-102.
236. Xu Y, Fang F, Dhar SK, St Clair WH, Kasarskis EJ, St Clair DK: **The role of a single-stranded nucleotide loop in transcriptional regulation of the human sod2 gene**. *The Journal of biological chemistry* 2007, **282**(22):15981-15994.
237. Xu Y, Fang F, Dhar SK, Bosch A, St Clair WH, Kasarskis EJ, St Clair DK: **Mutations in the SOD2 promoter reveal a molecular basis for an activating protein 2-dependent dysregulation of manganese superoxide dismutase expression in cancer cells**. *Mol Cancer Res* 2008, **6**(12):1881-1893.
238. Miao L, St Clair DK: **Regulation of superoxide dismutase genes: implications in disease**. *Free Radic Biol Med* 2009, **47**(4):344-356.
239. Huang Y, He T, Domann FE: **Decreased expression of manganese superoxide dismutase in transformed cells is associated with increased cytosine methylation of the SOD2 gene**. *DNA and cell biology* 1999, **18**(8):643-652.
240. Hodge DR, Peng B, Pompeia C, Thomas S, Cho E, Clausen PA, Marquez VE, Farrar WL: **Epigenetic silencing of manganese superoxide dismutase (SOD-2) in KAS 6/1 human multiple myeloma cells increases cell proliferation**. *Cancer Biol Ther* 2005, **4**(5):585-592.
241. Hurt EM, Thomas SB, Peng B, Farrar WL: **Molecular consequences of SOD2 expression in epigenetically silenced pancreatic carcinoma cell lines**. *British journal of cancer* 2007, **97**(8):1116-1123.
242. Maehara K, Uekawa N, Isobe K: **Effects of histone acetylation on transcriptional regulation of manganese superoxide dismutase gene**. *Biochemical and biophysical research communications* 2002, **295**(1):187-192.
243. Hitchler MJ, Oberley LW, Domann FE: **Epigenetic silencing of SOD2 by histone modifications in human breast cancer cells**. *Free Radic Biol Med* 2008, **45**(11):1573-1580.

ATTENTION: The Singapore Copyright Act applies to the use of this document. Nanyang Technological University Library

244. Patel M, Day BJ: **Metalloporphyrin class of therapeutic catalytic antioxidants**. *Trends Pharmacol Sci* 1999, **20**(9):359-364.
245. Faulkner KM, Liochev SI, Fridovich I: **Stable Mn(III) porphyrins mimic superoxide dismutase in vitro and substitute for it in vivo**. *The Journal of biological chemistry* 1994, **269**(38):23471-23476.
246. Tumurkhuu G, Koide N, Dagvadorj J, Hassan F, Islam S, Naiki Y, Mori I, Yoshida T, Yokochi T: **MnTBAP, a synthetic metalloporphyrin, inhibits production of tumor necrosis factor-alpha in lipopolysaccharide-stimulated RAW 264.7 macrophages cells via inhibiting oxidative stress-mediating p38 and SAPK/JNK signaling**. *FEMS Immunol Med Microbiol* 2007, **49**(2):304-311.
247. Malassagne B, Ferret PJ, Hammoud R, Tulliez M, Bedda S, Trebeden H, Jaffray P, Calmus Y, Weill B, Batteux F: **The superoxide dismutase mimetic MnTBAP prevents Fas-induced acute liver failure in the mouse**. *Gastroenterology* 2001, **121**(6):1451-1459.
248. Luanpitpong S, Chanvorachote P, Nimmannit U, Leonard SS, Stehlik C, Wang L, Rojanasakul Y: **Mitochondrial superoxide mediates doxorubicin-induced keratinocyte apoptosis through oxidative modification of ERK and Bcl-2 ubiquitination**. *Biochem Pharmacol* 2012, **83**(12):1643-1654.
249. Konorev EA, Kotamraju S, Zhao H, Kalivendi S, Joseph J, Kalyanaraman B: **Paradoxical effects of metalloporphyrins on doxorubicin-induced apoptosis: scavenging of reactive oxygen species versus induction of heme oxygenase-1**. *Free Radic Biol Med* 2002, **33**(7):988.
250. Pan H, Shen K, Wang X, Meng H, Wang C, Jin B: **Protective effect of metalloporphyrins against cisplatin-induced kidney injury in mice**. *PLoS One* 2014, **9**(1):e86057.
251. Huang P, Feng L, Oldham EA, Keating MJ, Plunkett W: **Superoxide dismutase as a target for the selective killing of cancer cells**. *Nature* 2000, **407**(6802):390-395.
252. Pribluda VS, Gubish ER, Jr., Lavallee TM, Treston A, Swartz GM, Green SJ: **2-Methoxyestradiol: an endogenous antiangiogenic and antiproliferative drug candidate**. *Cancer metastasis reviews* 2000, **19**(1-2):173-179.
253. Schumacher G, Neuhaus P: **The physiological estrogen metabolite 2-methoxyestradiol reduces tumor growth and induces apoptosis in human solid tumors**. *J Cancer Res Clin Oncol* 2001, **127**(7):405-410.
254. Basini G, Santini SE, Grasselli F: **2-Methoxyestradiol inhibits superoxide anion generation while it enhances superoxide dismutase activity in swine granulosa cells**. *Annals of the New York Academy of Sciences* 2006, **1091**:34-40.
255. Lakhani NJ, Sarkar MA, Venitz J, Figg WD: **2-Methoxyestradiol, a promising anticancer agent**. *Pharmacotherapy* 2003, **23**(2):165-172.
256. Tevaarwerk AJ, Holen KD, Alberti DB, Sidor C, Arnott J, Quon C, Wilding G, Liu G: **Phase I trial of 2-methoxyestradiol NanoCrystal dispersion in advanced solid malignancies**. *Clinical cancer research : an official journal of the American Association for Cancer Research* 2009, **15**(4):1460-1465.
257. Harrison MR, Hahn NM, Pili R, Oh WK, Hammers H, Sweeney C, Kim K, Perlman S, Arnott J, Sidor C *et al*: **A phase II study of 2-methoxyestradiol (2ME2) NanoCrystal(R) dispersion (NCD) in patients with taxane-**

ATTENTION: The Singapore Copyright Act applies to the use of this document. Nanyang Technological University Library

refractory, metastatic castrate-resistant prostate cancer (CRPC). *Invest New Drugs* 2011, **29**(6):1465-1474.

258. Sweeney C, Liu G, Yiannoutsos C, Kolesar J, Horvath D, Staab MJ, Fife K, Armstrong V, Treston A, Sidor C *et al*: **A phase II multicenter, randomized, double-blind, safety trial assessing the pharmacokinetics, pharmacodynamics, and efficacy of oral 2-methoxyestradiol capsules in hormone-refractory prostate cancer**. *Clinical cancer research : an official journal of the American Association for Cancer Research* 2005, **11**(18):6625-6633.
259. Mooberry SL: **New insights into 2-methoxyestradiol, a promising antiangiogenic and antitumor agent**. *Curr Opin Oncol* 2003, **15**(6):425-430.
260. Mabjeesh NJ, Escuin D, LaVallee TM, Pribluda VS, Swartz GM, Johnson MS, Willard MT, Zhong H, Simons JW, Giannakakou P: **2ME2 inhibits tumor growth and angiogenesis by disrupting microtubules and dysregulating HIF**. *Cancer Cell* 2003, **3**(4):363-375.
261. Lambert C, Apel K, Biesalski HK, Frank J: **2-methoxyestradiol induces caspase-independent, mitochondria-centered apoptosis in DS-sarcoma cells**. *International journal of cancer Journal international du cancer* 2004, **108**(4):493-501.
262. Golab J, Nowis D, Skrzycki M, Czeczot H, Baranczyk-Kuzma A, Wilczynski GM, Makowski M, Mroz P, Kozar K, Kaminski R *et al*: **Antitumor effects of photodynamic therapy are potentiated by 2-methoxyestradiol. A superoxide dismutase inhibitor**. *The Journal of biological chemistry* 2003, **278**(1):407-414.
263. Li W, Wang H, Lei C, Ying T, Tan X: **Manganese superoxide dismutase from human pathogen Clostridium difficile**. *Amino Acids* 2015, **47**(5):987-995.
264. Chen Y, Azad MB, Gibson SB: **Superoxide is the major reactive oxygen species regulating autophagy**. *Cell Death Differ* 2009, **16**(7):1040-1052.
265. Fulda S, Galluzzi L, Kroemer G: **Targeting mitochondria for cancer therapy**. *Nature reviews Drug discovery* 2010, **9**(6):447-464.
266. Ting CM, Lee YM, Wong CK, Wong AS, Lung HL, Lung ML, Lo KW, Wong RN, Mak NK: **2-Methoxyestradiol induces endoreduplication through the induction of mitochondrial oxidative stress and the activation of MAPK signaling pathways**. *Biochem Pharmacol* 2010, **79**(6):825-841.
267. Matthews EE, Schmiege SJ, Cook PF, Sousa KH: **Breast cancer and symptom clusters during radiotherapy**. *Cancer nursing* 2012, **35**(2):E1-11.
268. Kimmel CB, Ballard WW, Kimmel SR, Ullmann B, Schilling TF: **Stages of embryonic development of the zebrafish**. *Dev Dyn* 1995, **203**(3):253-310.
269. Eshita Y, Ji R, Onishi M, Runtuwene L, Noguchi K: **Supramolecular Targeting of B16F10 Melanoma Cells With Nanoparticles Consisting of a DEAE-Dextran-MMA Copolymer-Paclitaxel Complex**. In.: vivo; 2012.
270. Chiang AC, Massague J: **Molecular basis of metastasis**. *The New England journal of medicine* 2008, **359**(26):2814-2823.
271. Bos PD, Nguyen DX, Massague J: **Modeling metastasis in the mouse**. *Current opinion in pharmacology* 2010, **10**(5):571-577.
272. McClatchey AI: **Modeling metastasis in the mouse**. *Oncogene* 1999, **18**(38):5334-5339.

ATTENTION: The Singapore Copyright Act applies to the use of this document. Nanyang Technological University Library

273. Arora A, Scholar EM: **Role of tyrosine kinase inhibitors in cancer therapy**. *J Pharmacol Exp Ther* 2005, **315**(3):971-979.
274. Ellis PM, Morzycki W, Melosky B, Butts C, Hirsh V, Krasnoshtein F, Murray N, Shepherd FA, Soulieres D, Tsao MS *et al*: **The role of the epidermal growth factor receptor tyrosine kinase inhibitors as therapy for advanced, metastatic, and recurrent non-small-cell lung cancer: a Canadian national consensus statement**. *Curr Oncol* 2009, **16**(1):27-48.
275. Fidler IJ, Nicolson GL: **Organ selectivity for implantation survival and growth of B16 melanoma variant tumor lines**. *Journal of the National Cancer Institute* 1976, **57**(5):1199-1202.
276. Ali S, Champagne DL, Spaink HP, Richardson MK: **Zebrafish embryos and larvae: a new generation of disease models and drug screens**. *Birth Defects Res C Embryo Today* 2011, **93**(2):115-133.
277. MacRae CA, Peterson RT: **Zebrafish as tools for drug discovery**. *Nature reviews Drug discovery* 2015, **14**(10):721-731.
278. Weiss L, Nannmark U, Johansson BR, Bagge U: **Lethal deformation of cancer cells in the microcirculation: a potential rate regulator of hematogenous metastasis**. *International journal of cancer Journal international du cancer* 1992, **50**(1):103-107.
279. Yu L, Li HZ, Lu SM, Liu WW, Li JF, Wang HB, Xu W: **Alteration in TWIST expression: possible role in paclitaxel-induced apoptosis in human laryngeal carcinoma Hep-2 cell line**. *Croatian medical journal* 2009, **50**(6):536-542.
280. Mehlen P, Puisieux A: **Metastasis: a question of life or death**. *Nat Rev Cancer* 2006, **6**(6):449-458.
281. Wirtz D, Konstantopoulos K, Searson PC: **The physics of cancer: the role of physical interactions and mechanical forces in metastasis**. *Nat Rev Cancer* 2011, **11**(7):512-522.
282. Liotta LA, Kohn E: **Anoikis: cancer and the homeless cell**. *Nature* 2004, **430**(7003):973-974.
283. Steeg PS: **Tumor metastasis: mechanistic insights and clinical challenges**. *Nat Med* 2006, **12**(8):895-904.
284. Jakobisiak M, Lasek W, Golab J: **Natural mechanisms protecting against cancer**. *Immunol Lett* 2003, **90**(2-3):103-122.
285. Fidler IJ: **Metastasis: quantitative analysis of distribution and fate of tumor embolilabeled with 125 I-5-iodo-2'-deoxyuridine**. *J Natl Cancer Inst* 1970, **45**(4):773-782.
286. Fidler IJ, Gersten DM, Riggs CW: **Relationship of host immune status to tumor cell arrest, distribution, and survival in experimental metastasis**. *Cancer* 1977, **40**(1):46-55.
287. Koop S, MacDonald IC, Luzzi K, Schmidt EE, Morris VL, Grattan M, Khokha R, Chambers AF, Groom AC: **Fate of melanoma cells entering the microcirculation: over 80% survive and extravasate**. *Cancer Res* 1995, **55**(12):2520-2523.
288. Luzzi KJ, MacDonald IC, Schmidt EE, Kerkvliet N, Morris VL, Chambers AF, Groom AC: **Multistep nature of metastatic inefficiency: dormancy of solitary cells after successful extravasation and limited survival of early micrometastases**. *The American journal of pathology* 1998, **153**(3):865-873.

ATTENTION: The Singapore Copyright Act applies to the use of this document. Nanyang Technological University Library

289. Brooks DE: **The biorheology of tumor cells**. In: *Biorheology*. vol. 21, 1984/01/01 edn; 1984: 85-91.
290. Barnes JM, Nauseef JT, Henry MD: **Resistance to fluid shear stress is a conserved biophysical property of malignant cells**. *PLoS One* 2012, **7**(12):e50973.
291. Budihardjo I, Oliver H, Lutter M, Luo X, Wang X: **Biochemical pathways of caspase activation during apoptosis**. *Annual review of cell and developmental biology* 1999, **15**:269-290.
292. Heim R, Tsien RY: **Engineering green fluorescent protein for improved brightness, longer wavelengths and fluorescence resonance energy transfer**. *Curr Biol* 1996, **6**(2):178-182.
293. Tian H, Ip L, Luo H, Chang DC, Luo KQ: **A high throughput drug screen based on fluorescence resonance energy transfer (FRET) for anticancer activity of compounds from herbal medicine**. *Br J Pharmacol* 2007, **150**(3):321-334.
294. Rouhi P, Jensen LD, Cao Z, Hosaka K, Lanne T, Wahlberg E, Steffensen JF, Cao Y: **Hypoxia-induced metastasis model in embryonic zebrafish**. *Nat Protoc* 2010, **5**(12):1911-1918.
295. Turitto VT: **Blood viscosity, mass transport, and thrombogenesis**. *Progress in hemostasis and thrombosis* 1982, **6**:139-177.
296. Reneman RS, Hoeks AP: **Wall shear stress as measured in vivo: consequences for the design of the arterial system**. *Medical & biological engineering & computing* 2008, **46**(5):499-507.
297. Deeble DJ, Parsons BJ, Phillips GO: **Evidence for the addition of the superoxide anion to the anti-oxidant n-propyl gallate in aqueous solution**. *Free Radic Res Commun* 1987, **2**(4-6):351-358.
298. Deeble DJ, Parsons BJ, Phillips GO, Schuchmann HP, Von Sonntag C: **Superoxide radical reactions in aqueous solutions of pyrogallol and n-propyl gallate: the involvement of phenoxyl radicals. A pulse radiolysis study**. *Int J Radiat Biol* 1988, **54**(2):179-193.
299. Salvemini D, Riley DP, Cuzzocrea S: **SOD mimetics are coming of age**. *Nature reviews Drug discovery* 2002, **1**(5):367-374.
300. Fidler IJ: **Metastasis: guantitative analysis of distribution and fate of tumor embolilabeled with 125 I-5-iodo-2'-deoxyuridine**. *Journal of the National Cancer Institute* 1970, **45**(4):773-782.
301. Hanahan D, Weinberg RA: **Hallmarks of cancer: the next generation**. *Cell*, **144**(5):646-674.
302. Chishima T, Miyagi Y, Wang X, Yamaoka H, Shimada H, Moossa AR, Hoffman RM: **Cancer invasion and micrometastasis visualized in live tissue by green fluorescent protein expression**. *Cancer research* 1997, **57**(10):2042-2047.
303. Yamamoto N, Jiang P, Yang M, Xu M, Yamauchi K, Tsuchiya H, Tomita K, Wahl GM, Moossa AR, Hoffman RM: **Cellular dynamics visualized in live cells in vitro and in vivo by differential dual-color nuclear-cytoplasmic fluorescent-protein expression**. *Cancer research* 2004, **64**(12):4251-4256.
304. Yamauchi K, Yang M, Jiang P, Yamamoto N, Xu M, Amoh Y, Tsuji K, Bouvet M, Tsuchiya H, Tomita K *et al*: **Real-time in vivo dual-color imaging of**

ATTENTION: The Singapore Copyright Act applies to the use of this document. Nanyang Technological University Library

intracapillary cancer cell and nucleus deformation and migration. *Cancer research* 2005, **65**(10):4246-4252.

305. Hoffman RM: **The multiple uses of fluorescent proteins to visualize cancer in vivo**. *Nature reviews Cancer* 2005, **5**(10):796-806.
306. Kimura H, Lee C, Hayashi K, Yamauchi K, Yamamoto N, Tsuchiya H, Tomita K, Bouvet M, Hoffman RM: **UV light killing efficacy of fluorescent protein-expressing cancer cells in vitro and in vivo**. *J Cell Biochem* 2010, **110**(6):1439-1446.
307. Kimura H, Hayashi K, Yamauchi K, Yamamoto N, Tsuchiya H, Tomita K, Kishimoto H, Bouvet M, Hoffman RM: **Real-time imaging of single cancer-cell dynamics of lung metastasis**. *J Cell Biochem* 2010, **109**(1):58-64.
308. Lee SL, Rouhi P, Dahl Jensen L, Zhang D, Ji H, Hauptmann G, Ingham P, Cao Y: **Hypoxia-induced pathological angiogenesis mediates tumor cell dissemination, invasion, and metastasis in a zebrafish tumor model**. *Proceedings of the National Academy of Sciences of the United States of America* 2009, **106**(46):19485-19490.
309. Mitchell MJ, King MR: **Fluid Shear Stress Sensitizes Cancer Cells to Receptor-Mediated Apoptosis via Trimeric Death Receptors**. *New journal of physics* 2013, **15**:015008.
310. Egan K, Cooke N, Kenny D: **Living in shear: platelets protect cancer cells from shear induced damage**. *Clinical & experimental metastasis* 2014, **31**(6):697-704.
311. Mehes G, Witt A, Kubista E, Ambros PF: **Circulating breast cancer cells are frequently apoptotic**. *The American journal of pathology* 2001, **159**(1):17-20.
312. Spiliotaki M, Mavroudis D, Kapranou K, Markomanolaki H, Kallergi G, Koinis F, Kalbakis K, Georgoulias V, Agelaki S: **Evaluation of proliferation and apoptosis markers in circulating tumor cells of women with early breast cancer who are candidates for tumor dormancy**. *Breast cancer research : BCR* 2014, **16**(6):485.
313. Gourlay CW, Ayscough KR: **The actin cytoskeleton: a key regulator of apoptosis and ageing?** *Nature reviews Molecular cell biology* 2005, **6**(7):583-589.
314. Tsujimoto Y, Shimizu S: **Role of the mitochondrial membrane permeability transition in cell death**. *Apoptosis* 2007, **12**(5):835-840.
315. Morris PG, McArthur HL, Hudis CA: **Therapeutic options for metastatic breast cancer**. *Expert opinion on pharmacotherapy* 2009, **10**(6):967-981.
316. Cooke VG, LeBleu VS, Keskin D, Khan Z, O'Connell JT, Teng Y, Duncan MB, Xie L, Maeda G, Vong S *et al*: **Pericyte depletion results in hypoxia-associated epithelial-to-mesenchymal transition and metastasis mediated by met signaling pathway**. *Cancer cell* 2012, **21**(1):66-81.
317. Weitz J, Kienle P, Lacroix J, Willeke F, Benner A, Lehnert T, Herfarth C, von Knebel Doeberitz M: **Dissemination of tumor cells in patients undergoing surgery for colorectal cancer**. *Clinical cancer research : an official journal of the American Association for Cancer Research* 1998, **4**(2):343-348.
318. Mehlen P, Puisieux A: **Metastasis: a question of life or death**. *Nature reviews Cancer* 2006, **6**(6):449-458.
319. Malek AM, Alper SL, Izumo S: **Hemodynamic shear stress and its role in atherosclerosis**. *Jama* 1999, **282**(21):2035-2042.

ATTENTION: The Singapore Copyright Act applies to the use of this document. Nanyang Technological University Library

320. Carey LA, Dees EC, Sawyer L, Gatti L, Moore DT, Collichio F, Ollila DW, Sartor CI, Graham ML, Perou CM: **The triple negative paradox: primary tumor chemosensitivity of breast cancer subtypes**. *Clinical cancer research : an official journal of the American Association for Cancer Research* 2007, **13**(8):2329-2334.
321. Persidis A: **Cancer multidrug resistance**. *Nature biotechnology* 1999, **17**(1):94-95.
322. Luo D, Cheng SC, Xie H, Xie Y: **Effects of Bcl-2 and Bcl-XL protein levels on chemoresistance of hepatoblastoma HepG2 cell line**. *Biochemistry and cell biology = Biochimie et biologie cellulaire* 2000, **78**(2):119-126.
323. Williams J, Lucas PC, Griffith KA, Choi M, Fogoros S, Hu YY, Liu JR: **Expression of Bcl-xL in ovarian carcinoma is associated with chemoresistance and recurrent disease**. *Gynecologic oncology* 2005, **96**(2):287-295.
324. Sledge GW, Neuberg D, Bernardo P, Ingle JN, Martino S, Rowinsky EK, Wood WC: **Phase III trial of doxorubicin, paclitaxel, and the combination of doxorubicin and paclitaxel as front-line chemotherapy for metastatic breast cancer: an intergroup trial (E1193)**. *Journal of clinical oncology : official journal of the American Society of Clinical Oncology* 2003, **21**(4):588-592.
325. Tsang WP, Chau SP, Kong SK, Fung KP, Kwok TT: **Reactive oxygen species mediate doxorubicin induced p53-independent apoptosis**. *Life sciences* 2003, **73**(16):2047-2058.
326. Feinstein E, Canaani E, Weiner LM: **Dependence of nucleic acid degradation on in situ free-radical production by adriamycin**. *Biochemistry* 1993, **32**(48):13156-13161.
327. Holley AK, Dhar SK, Xu Y, St Clair DK: **Manganese superoxide dismutase: beyond life and death**. *Amino acids* 2012, **42**(1):139-158.
328. Hirose K, Longo DL, Oppenheim JJ, Matsushima K: **Overexpression of mitochondrial manganese superoxide dismutase promotes the survival of tumor cells exposed to interleukin-1, tumor necrosis factor, selected anticancer drugs, and ionizing radiation**. *FASEB J* 1993, **7**(2):361-368.
329. Manna SK, Zhang HJ, Yan T, Oberley LW, Aggarwal BB: **Overexpression of manganese superoxide dismutase suppresses tumor necrosis factor-induced apoptosis and activation of nuclear transcription factor-kappaB and activated protein-1**. *The Journal of biological chemistry* 1998, **273**(21):13245-13254.
330. Kamarajugadda S, Cai Q, Chen H, Nayak S, Zhu J, He M, Jin Y, Zhang Y, Ai L, Martin SS *et al*: **Manganese superoxide dismutase promotes anoikis resistance and tumor metastasis**. *Cell Death Dis* 2013, **4**:e504.
331. Holliday DL, Speirs V: **Choosing the right cell line for breast cancer research**. *Breast cancer research : BCR* 2011, **13**(4):215.
332. Chandel NS, Maltepe E, Goldwasser E, Mathieu CE, Simon MC, Schumacker PT: **Mitochondrial reactive oxygen species trigger hypoxia-induced transcription**. *Proceedings of the National Academy of Sciences of the United States of America* 1998, **95**(20):11715-11720.
333. Chandel NS, McClintock DS, Feliciano CE, Wood TM, Melendez JA, Rodriguez AM, Schumacker PT: **Reactive oxygen species generated at**

ATTENTION: The Singapore Copyright Act applies to the use of this document. Nanyang Technological University Library

mitochondrial complex III stabilize hypoxia-inducible factor-1alpha during hypoxia: a mechanism of O2 sensing. *The Journal of biological chemistry* 2000, **275**(33):25130-25138.

334. Li AE, Ito H, Rovira, II, Kim KS, Takeda K, Yu ZY, Ferrans VJ, Finkel T: **A role for reactive oxygen species in endothelial cell anoikis**. *Circ Res* 1999, **85**(4):304-310.
335. Chiu JJ, Wung BS, Shyy JY, Hsieh HJ, Wang DL: **Reactive oxygen species are involved in shear stress-induced intercellular adhesion molecule-1 expression in endothelial cells**. *Arterioscler Thromb Vasc Biol* 1997, **17**(12):3570-3577.
336. Matlung HL, Bakker EN, VanBavel E: **Shear stress, reactive oxygen species, and arterial structure and function**. *Antioxidants & redox signaling* 2009, **11**(7):1699-1709.
337. Fiaschi T, Chiarugi P: **Oxidative stress, tumor microenvironment, and metabolic reprogramming: a diabolic liaison**. *International journal of cell biology*, **2012**:762825.
338. Venkataraman S, Jiang X, Weydert C, Zhang Y, Zhang HJ, Goswami PC, Ritchie JM, Oberley LW, Buettner GR: **Manganese superoxide dismutase overexpression inhibits the growth of androgen-independent prostate cancer cells**. *Oncogene* 2005, **24**(1):77-89.
339. Malafa M, Margenthaler J, Webb B, Neitzel L, Christophersen M: **MnSOD expression is increased in metastatic gastric cancer**. *J Surg Res* 2000, **88**(2):130-134.
340. Kattan Z, Minig V, Leroy P, Dauca M, Becuwe P: **Role of manganese superoxide dismutase on growth and invasive properties of human estrogen-independent breast cancer cells**. *Breast Cancer Res Treat* 2008, **108**(2):203-215.
341. Piotrowska H, Kucinska M, Murias M: **Expression of CYP1A1, CYP1B1 and MnSOD in a panel of human cancer cell lines**. *Mol Cell Biochem* 2013, **383**(1-2):95-102.
342. Marusyk A, Almendro V, Polyak K: **Intra-tumour heterogeneity: a looking glass for cancer?** *Nature reviews Cancer* 2012, **12**(5):323-334.
343. Zhong W, Oberley LW, Oberley TD, St Clair DK: **Suppression of the malignant phenotype of human glioma cells by overexpression of manganese superoxide dismutase**. *Oncogene* 1997, **14**(4):481-490.
344. Weydert C, Roling B, Liu J, Hinkhouse MM, Ritchie JM, Oberley LW, Cullen JJ: **Suppression of the malignant phenotype in human pancreatic cancer cells by the overexpression of manganese superoxide dismutase**. *Molecular cancer therapeutics* 2003, **2**(4):361-369.
345. Oberley LW: **Mechanism of the tumor suppressive effect of MnSOD overexpression**. *Biomedicine & pharmacotherapy = Biomedecine & pharmacotherapie* 2005, **59**(4):143-148.
346. Hart PC, Mao M, de Abreu AL, Ansenberger-Fricano K, Ekoue DN, Ganini D, Kajdacsy-Balla A, Diamond AM, Minshall RD, Consolaro ME *et al*: **MnSOD upregulation sustains the Warburg effect via mitochondrial ROS and AMPK-dependent signalling in cancer**. *Nature communications* 2015, **6**:6053.

ATTENTION: The Singapore Copyright Act applies to the use of this document. Nanyang Technological University Library

347. Kolkman A, Dirksen EH, Slijper M, Heck AJ: **Double standards in quantitative proteomics: direct comparative assessment of difference in gel electrophoresis and metabolic stable isotope labeling**. *Mol Cell Proteomics* 2005, **4**(3):255-266.
348. Wu WW, Wang G, Baek SJ, Shen RF: **Comparative study of three proteomic quantitative methods, DIGE, cICAT, and iTRAQ, using 2D gel- or LC-MALDI TOF/TOF**. *J Proteome Res* 2006, **5**(3):651-658.
349. Mendez MG, Kojima S, Goldman RD: **Vimentin induces changes in cell shape, motility, and adhesion during the epithelial to mesenchymal transition**. *FASEB J* 2010, **24**(6):1838-1851.
350. Sutoh Yoneyama M, Hatakeyama S, Habuchi T, Inoue T, Nakamura T, Funyu T, Wiche G, Ohyama C, Tsuboi S: **Vimentin intermediate filament and plectin provide a scaffold for invadopodia, facilitating cancer cell invasion and extravasation for metastasis**. *Eur J Cell Biol* 2014, **93**(4):157-169.
351. Li H, Li Y, Liu D, Sun H, Su D, Yang F, Liu J: **Extracellular HSP70/HSP70-PCs promote epithelial-mesenchymal transition of hepatocarcinoma cells**. *PLoS One* 2013, **8**(12):e84759.
352. Fu J, Yang QY, Sai K, Chen FR, Pang JC, Ng HK, Kwan AL, Chen ZP: **TGM2 inhibition attenuates ID1 expression in CD44-high glioma-initiating cells**. *Neuro Oncol* 2013, **15**(10):1353-1365.
353. Savagner P: **The epithelial-mesenchymal transition (EMT) phenomenon**. *Annals of oncology : official journal of the European Society for Medical Oncology / ESMO* 2010, **21 Suppl 7**:vii89-92.
354. Wellberg EA, Rudolph MC, Lewis AS, Padilla-Just N, Jedlicka P, Anderson SM: **Modulation of tumor fatty acids, through overexpression or loss of thyroid hormone responsive protein spot 14 is associated with altered growth and metastasis**. *Breast cancer research : BCR* 2014, **16**(6):481.
355. Alur M, Nguyen MM, Eggener SE, Jiang F, Dadras SS, Stern J, Kimm S, Roehl K, Kozlowski J, Pins M *et al*: **Suppressive roles of calreticulin in prostate cancer growth and metastasis**. *The American journal of pathology* 2009, **175**(2):882-890.
356. Wang N, Stamenovic D: **Contribution of intermediate filaments to cell stiffness, stiffening, and growth**. *American journal of physiology Cell physiology* 2000, **279**(1):C188-194.
357. Tang HL, Lung HL, Wu KC, Le AH, Tang HM, Fung MC: **Vimentin supports mitochondrial morphology and organization**. *Biochem J* 2008, **410**(1):141-146.
358. Chernoivanenko IS, Matveeva EA, Gelfand VI, Goldman RD, Minin AA: **Mitochondrial membrane potential is regulated by vimentin intermediate filaments**. *FASEB J* 2015, **29**(3):820-827.
359. Veigel D, Wagner R, Stubiger G, Wuczkowski M, Filipits M, Horvat R, Benhamu B, Lopez-Rodriguez ML, Leisser A, Valent P *et al*: **Fatty acid synthase is a metabolic marker of cell proliferation rather than malignancy in ovarian cancer and its precursor cells**. *International journal of cancer Journal international du cancer* 2015, **136**(9):2078-2090.
360. Matsuyama Y, Suzuki M, Arima C, Huang QM, Tomida S, Takeuchi T, Sugiyama R, Itoh Y, Yatabe Y, Goto H *et al*: **Proteasomal non-catalytic subunit PSMD2 as a potential therapeutic target in association with**

ATTENTION: The Singapore Copyright Act applies to the use of this document. Nanyang Technological University Library

various clinicopathologic features in lung adenocarcinomas. *Mol Carcinog* 2011, **50**(4):301-309.

361. Israelsen WJ, Massachusetts Institute of Technology. Department of Biology.: **The role of pyruvate kinase regulation in tumor growth and metabolism**; 2014.
362. Wong N, De Melo J, Tang D: **PKM2, a Central Point of Regulation in Cancer Metabolism**. *International journal of cell biology* 2013, **2013**:242513.
363. Ai L, Kim WJ, Demircan B, Dyer LM, Bray KJ, Skehan RR, Massoll NA, Brown KD: **The transglutaminase 2 gene (TGM2), a potential molecular marker for chemotherapeutic drug sensitivity, is epigenetically silenced in breast cancer**. *Carcinogenesis* 2008, **29**(3):510-518.
364. Tsukamoto N, Chen J, Yoshida A: **Enhanced expressions of glucose-6-phosphate dehydrogenase and cytosolic aldehyde dehydrogenase and elevation of reduced glutathione level in cyclophosphamide-resistant human leukemia cells**. *Blood Cells Mol Dis* 1998, **24**(2):231-238.
365. Zeller C, Dai W, Steele NL, Siddiq A, Walley AJ, Wilhelm-Benartzi CS, Rizzo S, van der Zee A, Plumb JA, Brown R: **Candidate DNA methylation drivers of acquired cisplatin resistance in ovarian cancer identified by methylome and expression profiling**. *Oncogene* 2012, **31**(42):4567-4576.
366. Zagryazhskaya A, Surova O, Akbar NS, Allavena G, Gyuraszova K, Zborovskaya IB, Tchevkina EM, Zhivotovsky B: **Tudor staphylococcal nuclease drives chemoresistance of non-small cell lung carcinoma cells by regulating S100A11**. *Oncotarget* 2015, **6**(14):12156-12173.